

Vanadium and Chromium Complexes Supported by Sterically Demanding Ligands. Studies
Relevant to the Reduction of Dinitrogen to Ammonia

by

Nathan Christopher Smythe

B.Sc. in Chemistry
University of California, Berkeley
May, 2001

Submitted to the Department of Chemistry
in Partial Fulfillment of the Requirements
for the Degree of

DOCTOR OF PHILOSOPHY

at the

MASSACHUSETTS INSTITUTE OF TECHNOLOGY

September, 2006

© Massachusetts Institute of Technology, 2006
All rights reserved.

Signature of Author _____
Department of Chemistry
July 14, 2006

Certified by _____
Richard R. Schrock
Thesis Supervisor

Accepted by _____
Robert W. Field
Chairman, Departmental Committee on Graduate Students

This doctoral thesis has been examined by a committee of the Department of Chemistry as follows:

Professor Richard R. Schrock _____
Thesis Supervisor

Professor Christopher C. Cummins _____
Committee Chairman

Professor Daniel G. Nocera _____

Vanadium and Chromium Complexes Supported by Sterically Demanding Ligands. Studies Relevant to the Reduction of Dinitrogen to Ammonia

by

Nathan Christopher Smythe

Submitted to the Department of Chemistry, September 2006,
in Partial Fulfillment of the Requirements
for the Degree of Doctor of Philosophy in Chemistry

ABSTRACT

Chapter 1

Using the $[\text{HIPTN}_3\text{N}]^{3-}$ ligand ($[\text{HIPTN}_3\text{N}]^{3-} = [(\text{HIPTNCH}_2\text{CH}_2)_3\text{N}]^{3-}$; **HIPT** = 3,5-(2,4,6-*i*-Pr₃C₆H₂)₂C₆H₃ = HexalsoPropylTerphenyl), green paramagnetic $[\text{HIPTN}_3\text{N}]\text{V}(\text{THF})$ (**1**) can be prepared from $\text{VCl}_3(\text{THF})_3$. Reduction of **1** with potassium graphite in ethereal solvents yields a highly sensitive red solution identified as containing paramagnetic $\{[\text{HIPTN}_3\text{N}]\text{VN}_2\}^-$ (**2**) *via* infrared spectroscopy. **1** also reacts with ammonia to form bright green paramagnetic $[\text{HIPTN}_3\text{N}]\text{V}(\text{NH}_3)$ (**5**), 2-methylaziridine to form red diamagnetic $[\text{HIPTN}_3\text{N}]\text{V}=\text{NH}$ (**7**), azidotrimethylsilane to form orange diamagnetic $[\text{HIPTN}_3\text{N}]\text{V}=\text{N}(\text{SiMe}_3)$ (**9**), propylene oxide to form purple diamagnetic $[\text{HIPTN}_3\text{N}]\text{V}=\text{O}$ (**11**), elemental sulfur to form dark green diamagnetic $[\text{HIPTN}_3\text{N}]\text{V}=\text{S}$ (**10**), and carbon monoxide to form red-gold $[\text{HIPTN}_3\text{N}]\text{V}(\text{CO})$ (**12**). X-Ray crystal structures were obtained for **1**, **5**, and the decomposition product $[\text{HIPTN}_3\text{N}]\text{VH}$. **5** could be converted to **7** by oxidation/deprotonation using $[\text{FeCp}_2]\text{OTf}/(\text{Me}_3\text{Si})_2\text{NLi}$. The anionic nitride " $[\text{HIPTN}_3\text{N}]\text{V}\equiv\text{N}$ " could not be obtained through deprotonation of **7**, removal of the $-\text{SiMe}_3$ group from **9**, or the reaction of **1** with azides. Addition of potassium graphite to **5** resulted in decomposition rather than the formation of **2**. Under the catalytic conditions used for the $[\text{HIPTN}_3\text{N}]\text{Mo}$ system, **1** produced no ammonia, while **2** and **7** yielded 0.2 and 0.78 equivalents respectively.

Chapter 2

Four dianionic diamidoamine-donor based ligands were synthesized. Two were based on a pyridine donor arm $[2-(\text{C}_5\text{H}_4\text{N})\text{CH}_2\text{N}(\text{CH}_2\text{CH}_2\text{NHIPT})_2]^{2-}$ ($[\text{Pyrl}]^{2-}$) and $[2-(6\text{-MeC}_5\text{H}_3\text{N})\text{CH}_2\text{N}(\text{CH}_2\text{CH}_2\text{NHIPT})_2]^{2-}$ ($[\text{Myrl}]^{2-}$), one was based on an oxygen donor arm $[(3,5\text{-Me}_2\text{C}_6\text{H}_3)\text{OCH}_2\text{CH}_2\text{N}(\text{CH}_2\text{CH}_2\text{NHIPT})_2]^{2-}$ ($[\text{NNO}]^{2-}$), and one was based on a sulfur donor arm $[(3,5\text{-Me}_2\text{C}_6\text{H}_3)\text{SCH}_2\text{CH}_2\text{N}(\text{CH}_2\text{CH}_2\text{NHIPT})_2]^{2-}$ ($[\text{NNS}]^{2-}$) where **HIPT** = 3,5-(2,4,6-*i*-Pr₃C₆H₂)₂C₆H₃. The reaction between $\text{H}_2[\text{Pyrl}]$ with $\text{VCl}_3(\text{THF})_3$ yielded an unstable orange product believed to be dimeric. Using $\text{H}_2[\text{Myrl}]$ yielded a stable product that on reduction with potassium graphite generated what is believed to be a dimeric, bridging dinitrogen complex, which was not catalytically active under the conditions used for the $[\text{HIPTN}_3\text{N}]\text{Mo}$ system. The reaction between $\text{VCl}_3(\text{THF})_3$ and $\text{H}_2[\text{NNO}]$ yielded $\{[\text{NNO}]\text{VCl}\}_2$ (**32**), which underwent

ligand decomposition upon reduction with potassium graphite (**33**) or attempted alkylation with di-neopentyl magnesium (**34**). Ligand decomposition was also observed in the reaction of $H_2[NNS]$ with $VCl_3(THF)_3$ (**35**). X-Ray crystal structures were obtained for **32**, **33**, **34**, and **35**.

Chapter 3

Red-black $[HIPTN_3N]Cr$ (**1**) can be prepared from $CrCl_3$ ($[HIPTN_3N]^{3-} = [(HIPTNCH_2CH_2)_3N]^{3-}$, while green-black $[HIPTN_3N]Cr(THF)$ (**2**) can be prepared from $CrCl_3(THF)_3$ where **HIPT** = 3,5-(2,4,6-*i*-Pr₃C₆H₂)₂C₆H₃ = HexaIsoPropylTerphenyl). Reduction of {**1|2**} (which means either **1** or **2**) with potassium graphite in diethyl ether at room temperature yields $[HIPTN_3N]CrK$ (**3**) as a yellow-orange powder. There is no evidence that dinitrogen is incorporated into **1**, **2**, or **3**. Compounds that can be prepared readily from {**1|2**} include red $[HIPTN_3N]CrCO$ (**4**), blood-red $[HIPTN_3N]CrNO$ (**6**), and purple $[HIPTN_3N]CrCl$ (**7**, upon oxidation of {**1|2**} with AgCl). The dichroic (purple/green) Cr(VI) nitride, $[HIPTN_3N]CrN$ (**8**) was prepared from Bu_4NN_3 and **7**. X-ray studies have been carried out on **4**, **6**, and **7**, and on two co-crystallized compounds, **7** and $[HIPTN_3N]CrN_3$ (65:35) and $[HIPTN_3N]CrN_3$ and **8** (50:50). Exposure of a degassed solution of {**1|2**} to an atmosphere of ammonia does not yield " $[HIPTN_3N]Cr(NH_3)$ " as a stable and well-behaved species analogous to $[HIPTN_3N](NH_3)$. An attempt to reduce dinitrogen under conditions described for the catalytic reduction of dinitrogen by $[HIPTN_3N]Mo$ compounds with **8** yielded a substoichiometric amount (0.8 equiv) of ammonia, which suggests that some ammonia is formed from the nitride, but none is formed from dinitrogen.

Chapter 4

TRAP ($P(CH_2CH_2NH_2)_3$), a phosphine containing analogue to **TREN** ($N(CH_2CH_2NH_2)_3$) was synthesized from PH_3 , but suitable conditions for arylation of the amine arms could not be found. Using the "pre-arylated" arm $BrCH_2CH_2N(BOC)HIPT$ (BOC = *tert*-butoxycarbonyl; **HIPT** = 3,5-(2,4,6-*i*-Pr₃C₆H₂)₂C₆H₃) in the reaction with PH_3 resulted in the isolation of $H_2PCH_2CH_2N(BOC)HIPT$, but further substitution was unsuccessful. **HIPTBr** could be converted to **HIPTNH₂** using benzophenone imine and a *rac*-BINAP (2,2'-*bis*(diphenylphosphino)-1,1'-binaphthyl) supported Pd catalyst in preparation for DCC (dicyclohexylcarbodiimide) mediated coupling to *tris*-(3-propylcarboxylic acid)phosphine.

Thesis Supervisor:

Prof. Richard R. Schrock

Title:

Frederick G. Keyes Professor of Chemistry

Table of contents

Title Page.....	1
Signature Page.....	2
Abstract.....	3
Table of Contents.....	5
List of Abbreviations.....	7
List of Compounds.....	10
List of Figures.....	13
List of Schemes.....	17
List of Tables.....	18
General Introduction.....	20
CHAPTER 1.....	26
1.1 INTRODUCTION.....	27
1.2 SYNTHESIS AND PROPERTIES OF METAL COMPLEXES.....	28
1.2.1 $[\text{HIPTN}_3\text{N}]V(\text{THF})$	28
1.2.2 $\{[\text{HIPTN}_3\text{N}]V\text{N}_2\}^+$	29
1.2.3 $[\text{HIPTN}_3\text{N}]V(\text{NH}_3)$	35
1.2.4 $[\text{HIPTN}_3\text{N}]V=\text{NH}$	35
1.2.5 $[\text{HIPTN}_3\text{N}]V=\text{N}(\text{SiMe}_3)$	38
1.2.6 $[\text{HIPTN}_3\text{N}]V=\text{S}$	39
1.2.7 $[\text{HIPTN}_3\text{N}]V=\text{O}$	39
1.2.8 Other Reactions.....	40
1.3 X-RAY DISCUSSION.....	41
1.4 EVALUATION OF CATALYTIC ACTIVITY.....	45
1.5 COMPARISON OF ^{51}V NMR SHIFTS.....	46
1.6 CONCLUSIONS.....	46
1.7 EXPERIMENTAL DETAILS.....	47
1.8 REFERENCES.....	53
CHAPTER 2.....	55
2.1 INTRODUCTION.....	56
2.2 LIGAND SYNTHESSES.....	57
2.2.1 Pyridine Based Donor Arm.....	57
2.2.2 Chalcogenide Donor Arms.....	59
2.3 OTHER LIGANDS.....	62
2.3.1 Amine Donor.....	62
2.3.2 Phosphine Donor.....	64
2.4 VANADIUM COMPLEXES OF $\text{H}_2[\text{NNO}]$ AND $\text{H}_2[\text{NNS}]$	65
2.4.1 $\{[\text{NNO}]V\text{Cl}\}_2$	65
2.4.2 Reaction of $\{[\text{NNO}]V\text{Cl}\}_2$ with Np_2Mg	66
2.4.3 Reduction of $\{[\text{NNO}]V\text{Cl}\}_2$ with KC_8	68
2.4.4 Reaction of $\text{H}_2[\text{NNS}]$ with $V\text{Cl}_3(\text{THF})_3$	69
2.5 PYRIDYL BASED LIGANDS.....	71
2.5.1 Reaction of $\text{H}_2[\text{Pyrl}]$ with $V\text{Cl}_3(\text{THF})_3$	71
2.5.2 $\{[\text{Myrl}]V\text{Cl}\}_2$	71
2.6 OTHER APPROACHES.....	74

2.6.1	<i>A Carbene Ligand</i>	74
2.6.2	<i>Tethered Ligand</i>	74
2.7	CONCLUSIONS	75
2.8	EXPERIMENTAL DETAILS	75
2.9	REFERENCES	85
CHAPTER 3.....		87
3.1	INTRODUCTION	88
3.2	RESULTS	88
3.2.1	<i>Syntheses of [HIPTN₃N]Cr Complexes</i>	88
3.3	X-RAY STUDIES	98
3.4	ATTEMPTS TO PREPARE AN AMMONIA COMPLEX AND TO REDUCE DINITROGEN	102
3.5	DISCUSSION AND CONCLUSIONS	102
3.6	EXPERIMENTAL DETAILS	104
3.7	REFERENCES	108
CHAPTER 4.....		110
4.1	INTRODUCTION	111
4.2	TRIS-(2-AMINOETHYL)PHOSPHINE (TRAP)	112
4.2.1	<i>Phosphine Arm</i>	118
4.3	AN ARYL PHOSPHINE BACKBONE	122
4.4	TRIS-(2-AMINOPROPYL)PHOSPHINE (TAPP)	124
4.4.1	<i>tris-(2-cyanoethyl)phosphine</i>	125
4.4.2	<i>Synthesis of HIPTNH₂</i>	126
4.5	CONCLUSIONS	129
4.6	EXPERIMENTAL DETAILS	129
4.7	REFERENCES	135
APPENDIX A.....		136
Acknowledgements		205
Curriculum Vitae		206

List of abbreviations

Anal.	analysis
Ar	aryl
b	broad
BINAP	2,2'- <i>bis</i> (diphenylphosphino)-1,1'-binaphthyl
BM	Bohr magneton
BOC	<i>tert</i> -butoxycarbonyl, Me ₃ CO(CO)-
<i>n</i> -Bu	<i>n</i> -butyl, -CH ₂ CH ₂ CH ₂ CH ₃
<i>t</i> -Bu	<i>tert</i> -butyl, -CMe ₃
Calcd.	calculated
Cp	(C ₅ H ₅) ⁻
Cp*	(C ₅ Me ₅) ⁻
d	doublet
dba	dibenzylideneacetone
deg, (°)	degree(s)
Δ	change, difference
DME	1,2-dimethoxyethane
DMF	<i>N,N</i> -dimethylformamide
dppe	<i>bis</i> (diphenylphosphino)ethane
ESI	electrospray ionization
Et	ethyl, -CH ₂ CH ₃
η ^x	hapticity of x
fw	formula weight (g/mol)
g	grams
GoF	Goodness of Fit
HIPT	hexaisopropylterphenyl
Hz	hertz
J	coupling constant in Hertz
m	multiplet(s)

Me	methyl, -CH ₃
Mes	mesityl, 2,4,6-trimethylphenyl
MS	mass spectrometry
μ	bridging
μ _B	Bohr magneton
μ _{eff}	effective magnetic moment
mol	mole(s)
Myrl	2-(6-MeC ₅ H ₅ N)CH ₂ CH ₂ N(CH ₂ CH ₂ NHHIPT) ₂
NMR	nuclear magnetic resonance
N(Phth)	phthalimide
N ₂ N	ethylenediamine
NNO	(3,5-Me ₂ PhOCH ₂ CH ₂)N(CH ₂ CH ₂ NHHIPT) ₂
NNS	(3,5-Me ₂ PhSCH ₂ CH ₂)N(CH ₂ CH ₂ NHHIPT) ₂
Np	neopentyl, -CH ₂ C(CH ₃) ₃
OTf	triflate, trifluoromethanesulfonate, [F ₃ CSO ₃] ⁻
PG	protecting group
Ph	phenyl
ppm	parts per million
Pyrl	2-(C ₅ H ₅ N)CH ₂ CH ₂ N(CH ₂ CH ₂ NHHIPT) ₂
<i>i</i> -Pr	<i>iso</i> -propyl, -CHMe ₂
q	quartet
<i>rac</i>	racemic
RT	room temperature
s	singlet
sept	septet
t	triplet
TAPP	<i>tris</i> -(3-aminopropyl)phosphine
TBDMS	<i>tert</i> -butyldimethylsilyl, <i>t</i> -BuMe ₂ Si-
THF	tetrahydrofuran
TLC	thin layer chromatography

TMEDA	<i>N,N,N',N'</i> -tetramethylethylenediamine
TRAP	<i>tris</i> -(2-aminoethyl)phosphine
TREN, N ₃ N	<i>tris</i> -(2-aminoethyl)amine
Trip	2,4,6-triisopropylphenyl, 2,4,6- <i>i</i> -PrC ₆ H ₂
Ts, Tosyl	<i>para</i> -toluenesulfonate, [(4-MeC ₆ H ₄)SO ₂] ⁺
X-Phos	2-(Dicyclohexylphosphino)-2',4',6'-tri- <i>i</i> -propyl-1,1'-biphenyl
δ	chemical shift downfield from tetramethylsilane (¹ H), 85% H ₃ PO ₄ in water (³¹ P), or VOCl ₃ (⁵¹ V) in ppm

List of compounds

Chapter 1

- 1 [HIPTN₃N]V(THF)
- 2 {[HIPTN₃N]VN₂}K
- 3 {[HIPTN₃N]VN₂}18-crown-6(K)
- 4 {[HIPTN₃N]V¹⁵N₂}K
- 5 [HIPTN₃N]V(NH₃)
- 6 [HIPTN₃N]V(¹⁵NH₃)
- 7 [HIPTN₃N]V=NH
- 8 [HIPTN₃N]V=¹⁵NH
- 9 [HIPTN₃N]V=N(SiMe₃)
- 10 [HIPTN₃N]V=S
- 11 [HIPTN₃N]V=O
- 12 [HIPTN₃N]V(CO)
- 13 [HIPTN₃N]V(¹³CO)

Chapter 2

- 14 H₂[HIPTN₂N]CH₂CH₂NH-*i*-Pr
- 15 N1-(2-aminoethyl)-N1-((pyridin-2-yl)methyl)ethane-1,2-diamine
- 16 H₂[Pyrl]
- 17 N1-(2-aminoethyl)-N1-((6-methylpyridin-2-yl)methyl)ethane-1,2-diamine
- 18 H₂[Myrl]
- 19 2-(3,5-dimethylphenoxy)acetonitrile
- 20 2-(3,5-dimethylphenoxy)ethanamine
- 21 3,5-dimethylphenoxyethyl-*bis*-(ethylphthalimide)amine
- 22 N1-(2-(3,5-dimethylphenoxy)ethyl)-N1-(2-aminoethyl)ethane-1,2-diamine
- 23 H₂[NNO]
- 24 2-(3,5-dimethylphenylthio)acetonitrile

- 25 2-(3,5-dimethylphenylthio)ethanamine
 26 3,5-dimethylphenylthioethyl-*bis*(ethylphthalimide)amine
 27 *N*1-(2-(3,5-dimethylphenylthio)ethyl)-*N*1-(2-aminoethyl)ethane-1,2-diamine
 28 $\text{H}_2[\text{NNS}]$
 29 $\{[\text{PyrI}]\text{VCl}\}_2$
 30 $\{[\text{MyrI}]\text{VCl}\}_2$
 31 $\{[\text{MyrI}]\text{VN}\}_2$
 32 $\{[\text{NNO}]\text{VCl}\}_2$
 33 Reduction of $\{[\text{NNO}]\text{VCl}\}_2$
 34 Reaction of $\{[\text{NNO}]\text{VCl}\}_2$ with Np_2Mg
 35 Reaction of $\text{H}_2[\text{NNS}]$ with $\text{VCl}_3(\text{THF})_3$

Chapter 3

- 36 $[\text{HIPTN}_3\text{N}]\text{Cr}$
 37 $[\text{HIPTN}_3\text{N}]\text{Cr}(\text{THF})$
 38 $[\text{HIPTN}_3\text{N}]\text{CrK}$
 39 $[\text{HIPTN}_3\text{N}]\text{Cr}(\text{CO})$
 40 $\{[\text{HIPTN}_3\text{N}]\text{Cr}(\text{CO})\}\text{K}$
 41 $[\text{HIPTN}_3\text{N}]\text{Cr}(\text{NO})$
 42 $[\text{HIPTN}_3\text{N}]\text{CrCl}$
 43 $[\text{HIPTN}_3\text{N}]\text{Cr}\equiv\text{N}$

Chapter 4

- 44 *tris*-(2-aminoethyl)phosphine•3HCl
 45 *tris*-(2-aminoethyl)phosphine
 46 $\text{O}=\text{P}(\text{CH}_2\text{CH}_2\text{NH}_2)$
 47 (*t*-BuMe₂Si)OCH₂CH₂N(H)**HIPT**
 48 (*t*-BuMe₂Si)OCH₂CH₂N(BOC)**HIPT**
 49 HOCH₂CH₂N(BOC)**HIPT**

- 50 $\text{BrCH}_2\text{CH}_2\text{N}(\text{BOC})\mathbf{HIPT}$
- 51 $\text{H}_2\text{PCH}_2\text{CH}_2\text{N}(\text{BOC})\mathbf{HIPT}$
- 52 *p*-tolylaniline(**HIPT**)
- 53 *tris*(2-cyanoethyl)phosphine
- 54 **HIPT**(benzophenoneimine)
- 55 **HIPTNH**₂

List of Figures

Introduction

Figure I.1: First stable dinitrogen metal complex	21
Figure I.2: Chatt complexes	22
Figure I.3: TREN backbone	22
Figure I.4: POV-Ray rendering of $\{[para(t-Bu)C_6H_4N_3N]Mo\}(\mu-N_2)$	23
Figure I.5: TREN substituent progression	23
Figure I.6: Example $[HIPTN_3N]Mo$ complex, $[HIPTN_3N]MoN_2$	24
Figure I.7: Step-wise Chatt type dinitrogen reduction cycle	24
Figure I.8: POV-Ray rendering of the $[HIPTN_3N]MoN_2$	25

Chapter 1

Figure 1.1: Adaptation of the $[HIPTN_3N]Mo$ cycle to a potential vanadium cycle.	28
Figure 1.2: ORTEP diagram of $[HIPTN_3N]V(THF)$	30
Figure 1.3: Solution IR spectrum of $\{[HIPTN_3N]VN_2\}K$	31
Figure 1.4: Solution IR spectrum of $\{[HIPTN_3N]V^{15}N_2\}K$	32
Figure 1.5: Solution IR spectra of $\{[HIPTN_3N]VN_2\}K$ and $\{[HIPTN_3N]VN_2\}18-Crown-6(K)$	33
Figure 1.6: ORTEP diagram of $[HIPTN_3N]VH$	34
Figure 1.7: ORTEP diagram of $[HIPTN_3N]V(NH_3)$	35
Figure 1.8: 1H and ^{51}V NMR spectra (C_6D_6) of $[HIPTN_3N]V=NH$	36
Figure 1.9: Solution IR spectra of $[HIPTN_3N]V=NH$ and $[HIPTN_3N]V=^{15}NH$	37
Figure 1.10: 1H and ^{51}V NMR spectra of $[HIPTN_3N]V=N(SiMe_3)$	38
Figure 1.11: 1H and ^{51}V NMR spectra of $[HIPTN_3N]V=S$	39
Figure 1.12: 1H and ^{51}V NMR spectra of $[HIPTN_3N]V=O$	40
Figure 1.13: Comparison of V-N(amine) bond lengths	45
Figure 1.14: Reaction summary of $[HIPTN_3N]V$ complexes.	47

Chapter 2

Figure 2.1: Ideal diamidoamine-donor ligand	56
Figure 2.2: Modified dinitrogen reduction scheme for vanadium using a dianionic ligand.....	56
Figure 2.3: Pyridine-based dianionic ligand.	57
Figure 2.4: ¹ H NMR spectrum of H ₂ [Pyrl].	58
Figure 2.5: ¹ H NMR spectrum of H ₂ [Myrl].	59
Figure 2.6: ¹ H NMR spectrum of H ₂ [NNO].	61
Figure 2.7: Targeted amine and phosphine donor ligands.....	62
Figure 2.8: ¹ H NMR spectrum of H ₂ [HIPTN₂N]CH ₂ CH ₂ NH- <i>i</i> -Pr	63
Figure 2.9: ORTEP diagram of {[NNO]VCl} ₂	66
Figure 2.10: ORTEP diagram of the reaction product of {[NNO]VCl} ₂ with Np ₂ Mg	67
Figure 2.11: ORTEP diagram of the reduction product of {[NNO]VCl} ₂	68
Figure 2.12: ORTEP diagram of the reaction of H ₂ [NNS] with VCl ₃ (THF) ₃	70
Figure 2.13: ORTEP of the core structure of 35	69
Figure 2.14: Possible decomposition path for {[Pyrl]VCl} ₂	71
Figure 2.15: Reduction product of {[Myrl]VCl} ₂ under N ₂ and ¹⁵ N ₂	72
Figure 2.16: Difference spectrum between reduction products of {[Myrl]VCl} ₂ under N ₂ and ¹⁵ N ₂	73
Figure 2.17: Possible core structures of {[Myrl]VCl} ₂ and its reduction product.....	73
Figure 2.18: Pyridyl vs. Carbene comparison.....	74
Figure 2.19: Diagram of a hypothetical tethered ligand.	74

Chapter 3

Figure 3.1: Solution IR spectra of [HIPTN₃N]Cr and [HIPTN₃N]Cr(THF).....	90
Figure 3.2: ORTEP diagram of [HIPTN₃N]CrCO.....	91
Figure 3.3: ¹ H NMR spectrum of {[HIPTN₃N]CrCO} 18-Crown-6(K).....	92
Figure 3.4: ORTEP diagram of [HIPTN₃N]CrNO.....	93

Figure 3.5: ^1H NMR spectrum of $[\text{HIPTN}_3\text{N}]\text{CrNO}$.	93
Figure 3.6: ORTEP diagram of $[\text{HIPTN}_3\text{N}]\text{CrCl}$	94
Figure 3.7: ORTEP diagram of $[\text{HIPTN}_3\text{N}]\text{CrCl}/[\text{HIPTN}_3\text{N}]\text{CrN}_3$	95
Figure 3.8: ORTEP diagram of $[\text{HIPTN}_3\text{N}]\text{CrN}/[\text{HIPTN}_3\text{N}]\text{CrN}_3$	95
Figure 3.9: ^1H NMR spectrum of $[\text{HIPTN}_3\text{N}]\text{CrN}$.	96
Figure 3.10: UV/Vis spectra of $[\text{HIPTN}_3\text{N}]\text{CrN}$.	97
Figure 3.11: Calculation of metal displacement from the <i>tris</i> -amide plane.	100

Chapter 4

Figure 4.1: Reaction apparatus for PH_3 alkylation.	114
Figure 4.2: ^{31}P spectrum of HPR_2 and H_2PR	115
Figure 4.3: ^1H NMR spectrum of TRAP	116
Figure 4.4: $^{31}\text{P}\{^1\text{H}\}$ and ^{31}P NMR spectra of TRAP	116
Figure 4.5: $^{31}\text{P}\{^1\text{H}\}$ and ^{31}P NMR spectra of $\text{O}=\text{P}(\text{CH}_2\text{CH}_2\text{NH}_2)_3$	117
Figure 4.6: Ligand for Cu mediated aryl halide coupling.	117
Figure 4.7: Ligand arm for PH_3 .	118
Figure 4.8: $(t\text{-BuMe}_2\text{Si})\text{OCH}_2\text{CH}_2\text{NH}(\text{BOC})$.	119
Figure 4.9: ^1H NMR spectrum of 50 .	120
Figure 4.10: ^1H NMR spectrum of $\text{H}_2\text{PCH}_2\text{CH}_2\text{N}(\text{BOC})\text{HIPT}$	121
Figure 4.11: $^{31}\text{P}\{^1\text{H}\}$ and ^{31}P NMR spectra of $\text{H}_2\text{PCH}_2\text{CH}_2\text{N}(\text{BOC})\text{HIPT}$	122
Figure 4.12: ^{31}P NMR spectrum of the reaction of 51 with K metal.	123
Figure 4.13: Comparison of Fryzuk system and the simplified HIPT system.	124
Figure 4.14: Reaction apparatus for the synthesis of <i>tris</i> -(cyanoethyl)phosphine.	126
Figure 4.15: ^{31}P NMR spectrum of the <i>mono</i> -, <i>bis</i> -, and <i>tris</i> -substituted PH_3 .	127
Figure 4.16: ^1H NMR spectrum of HIPTNH ₂ .	128

Appendix A

Figure A.1: Full ORTEP diagram of $[\text{HIPTN}_3\text{N}]\text{V}(\text{THF})$	138
Figure A.2: Labeling scheme for $[\text{HIPTN}_3\text{N}]\text{V}(\text{THF})$	139
Figure A.3: Full ORTEP diagram of $[\text{HIPTN}_3\text{N}]\text{VH}$	144
Figure A.4: ORTEP labeling scheme for $[\text{HIPTN}_3\text{N}]\text{VH}$	145
Figure A.5: Full ORTEP of $[\text{HIPTN}_3\text{N}]\text{V}(\text{NH}_3)$	148
Figure A.6: ORTEP labeling scheme for $[\text{HIPTN}_3\text{N}]\text{V}(\text{NH}_3)$	149
Figure A.7: Full ORTEP of $\{[\text{NNO}]\text{VCl}\}_2$	154
Figure A.8: ORTEP labeling scheme for $\{[\text{NNO}]\text{VCl}\}_2$	155
Figure A.9: Full ORTEP of the reduction product of $\{[\text{NNO}]\text{VCl}\}_2$	161
Figure A.10: ORTEP labeling scheme for 33	162
Figure A.11: Full ORTEP of $\{[\text{NNO}]\text{VO}\}_2$	166
Figure A.12: ORTEP labeling scheme for $\{[\text{NNO}]\text{VO}\}_2$	167
Figure A.13: Full ORTEP of 35	171
Figure A.14: ORTEP labeling scheme for 35	172
Figure A.15: Full ORTEP of $[\text{HIPTN}_3\text{N}]\text{CrCO}$	176
Figure A.16: ORTEP labeling scheme for $[\text{HIPTN}_3\text{N}]\text{CrCO}$	177
Figure A.17: Full ORTEP of $[\text{HIPTN}_3\text{N}]\text{CrNO}$	182
Figure A.18: ORTEP labeling scheme for $[\text{HIPTN}_3\text{N}]\text{CrNO}$	183
Figure A.19: Full ORTEP of $[\text{HIPTN}_3\text{N}]\text{CrCl}$	188
Figure A.20: ORTEP labeling scheme for $[\text{HIPTN}_3\text{N}]\text{CrCl}$	189
Figure A.21: Full ORTEP of $[\text{HIPTN}_3\text{N}]\text{CrCl} / [\text{HIPTN}_3\text{N}]\text{CrN}_3$	194
Figure A.22: ORTEP labeling scheme for $[\text{HIPTN}_3\text{N}]\text{CrCl} / [\text{HIPTN}_3\text{N}]\text{CrN}_3$	195
Figure A.23: Full ORTEP of $[\text{HIPTN}_3\text{N}]\text{CrN} / [\text{HIPTN}_3\text{N}]\text{CrN}_3$	200
Figure A.24: ORTEP labeling scheme for $[\text{HIPTN}_3\text{N}]\text{CrN} / [\text{HIPTN}_3\text{N}]\text{CrN}_3$	201

List of Schemes

Chapter 1

Scheme 1.1: Pathway to $[\text{HIPTN}_3\text{N}]\text{VH}$ from $\{[\text{HIPTN}_3\text{N}]\text{VN}_2\}^-$	33
---	----

Chapter 2

Scheme 2.1: Two published routes to the pyridyl ligand scaffold.....	57
Scheme 2.2: Reaction scheme for $\text{H}_2[\text{NNO}]$ and $\text{H}_2[\text{NNS}]$	60
Scheme 2.3: Anticipated route to a diamidoaminophosphine ligand.	64

Chapter 3

Scheme 3.1: Reaction summary of $[\text{HIPTN}_3\text{N}]\text{Cr}$ and $[\text{HIPTN}_3\text{N}]\text{Cr}(\text{THF})$	102
---	-----

Chapter 4

Scheme 4.1: Proposed scheme for the synthesis of arylated TRAP	111
Scheme 4.2: Simplified synthesis of TRAP •3HCl.....	113
Scheme 4.3: Synthetic scheme for $\text{BrCH}_2\text{CH}_2\text{N}(\text{BOC})\text{HIPT}$	119
Scheme 4.4: Fryzuk synthesis of a phosphine donor ligand.....	123
Scheme 4.5: Reaction scheme for a propyl backbone ligand.	124
Scheme 4.6: Synthesis of HIPTNH ₂ from HIPTBr	128

List of tables

Chapter 1

Table 1.1: Structural Solution Parameters for [HIPTN ₃ N]V Complexes	42
Table 1.2: Structural parameters for selected triamidoamine complexes	44
Table 1.3: Core symmetry and HIPT group torsion angles in [HIPTN ₃ N]V complexes.....	43
Table 1.4: ⁵¹ V NMR shifts of analogous [Me ₃ SiN ₃ N]V and [HIPTN ₃ N]V complexes	46

Chapter 2

Table 2.1: Selected bond lengths and angles for {[NNO]VCl} ₂	65
Table 2.2: Selected bond lengths and angles for 34	67
Table 2.3: Selected bond lengths and angles for 33	69
Table 2.4: Selected bond lengths and angles related to the [NNS]V core	70

Chapter 3

Table 3.1: X-Ray structure solution parameters and selected ligand core parameters.	99
Table 3.2: Selected structural data relevant to the apical ligand.....	101

Chapter 4

Table A.1: Crystal data and structure refinement for [HIPTN ₃ N]V(THF).....	137
Table A.2: Atomic coordinates and equivalent isotropic displacement parameters for [HIPTN ₃ N]V(THF).....	140
Table A.3: Crystal data and structure refinement for [HIPTN ₃ N]VH	143
Table A.4: Atomic coordinates and equivalent isotropic displacement parameters for [HIPTN ₃ N]VH	146
Table A.5: Crystal data and structure refinement for [HIPTN ₃ N]V(NH ₃)	147
Table A.6: Atomic coordinates and equivalent isotropic displacement parameters for [HIPTN ₃ N]V(NH ₃)	150

Table A.7: Crystal data and structure refinement for $\{[\text{NNO}]\text{VCl}\}_2$	153
Table A.8: Atomic coordinates and equivalent isotropic displacement parameters for $\{[\text{NNO}]\text{VCl}\}_2$	156
Table A.9: Crystal data and structure refinement for the $\{[\text{NNO}]\text{VCl}\}_2$ reduction product.....	160
Table A.10: Atomic coordinates and equivalent isotropic displacement parameters for 33	163
Table A.11: Crystal data and structure refinement for $\{[\text{NNO}]\text{VO}\}_2$	165
Table A.12: Atomic coordinates and equivalent isotropic displacement parameters for $\{[\text{NNO}]\text{VO}\}_2$	168
Table A.13: Crystal data and structure refinement for 35	170
Table A.14: Atomic coordinates and equivalent isotropic displacement parameters for 35	173
Table A.15: Crystal data and structure refinement for $[\text{HIPTN}_3\text{N}]\text{CrCO}$	175
Table A.16: Atomic coordinates and equivalent isotropic displacement parameters for $[\text{HIPTN}_3\text{N}]\text{CrCO}$	178
Table A.17: Crystal data and structure refinement for $[\text{HIPTN}_3\text{N}]\text{CrNO}$	181
Table A.18: Atomic coordinates and equivalent isotropic displacement parameters for $[\text{HIPTN}_3\text{N}]\text{CrNO}$	184
Table A.19: Crystal data and structure refinement for $[\text{HIPTN}_3\text{N}]\text{CrCl}$	187
Table A.20: Atomic coordinates and equivalent isotropic displacement parameters for $[\text{HIPTN}_3\text{N}]\text{CrCl}$	190
Table A.21: Crystal data and structure refinement for $[\text{HIPTN}_3\text{N}]\text{CrCl} / [\text{HIPTN}_3\text{N}]\text{CrN}_3$. ..	193
Table A.22: Atomic coordinates and equivalent isotropic displacement parameters for $[\text{HIPTN}_3\text{N}]\text{CrCl} / [\text{HIPTN}_3\text{N}]\text{CrN}_3$	196
Table A.23: Crystal data and structure refinement for $[\text{HIPTN}_3\text{N}]\text{CrN} / [\text{HIPTN}_3\text{N}]\text{CrN}_3$	199
Table A.24: Atomic coordinates and equivalent isotropic displacement parameters for $[\text{HIPTN}_3\text{N}]\text{CrN} / [\text{HIPTN}_3\text{N}]\text{CrN}_3$	202

General Introduction

Ammonia is an important biologically accessible source of nitrogen, which is produced from dinitrogen both in nature by the nitrogenase enzymes, and industrially *via* the Haber-Bosch process in quantities on the order of 10^8 tons per year.^{1,2} While the nitrogenases perform this transformation at ambient temperature and pressure using protons and electrons, the Haber-Bosch process requires high temperatures (*ca.* 400 °C) and pressures (*ca.* 200 atm) to react dinitrogen and dihydrogen directly over an iron-based catalyst. This process is both energy intensive and, as a heterogeneous surface reaction, difficult to study. This has made the pursuit of a catalyst capable of supporting the conversion of dinitrogen to ammonia at room temperature and pressure a long-running research goal.^{2,3,4,5} With the isolation of the first stable dinitrogen complex, $[(\text{NH}_3)_5\text{RuN}_2]^{2+}$ (Figure I.1), in 1965 by Allen and Senoff,⁶ attention was brought to the possibility of a synthetic catalyst being able to convert dinitrogen to ammonia at ambient temperature and pressure. They showed that a single metal center could be used to activate dinitrogen, a molecule that was and continues to be used largely as an inert gas.

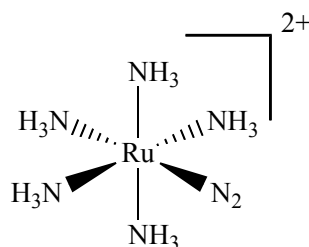


Figure I.1: First stable dinitrogen metal complex.

Chatt was able to expand upon this result by using phosphine supported molybdenum and tungsten complexes (Figure I.2) to stoichiometrically generate ammonia from dinitrogen.⁷ This was accomplished by using various acids as a proton source and the metal itself as the electron source, with the oxidation state changing from (0) to (VI) through the reaction. Although catalytic activity was never obtained, it was the first example of ammonia formation from a well-defined dinitrogen precursor. In the intervening years there have been many reports of dinitrogen containing complexes^{2,3,4,5} and even some catalytic ammonia formation,⁸ but not in a well-defined manner using an isolable catalyst.

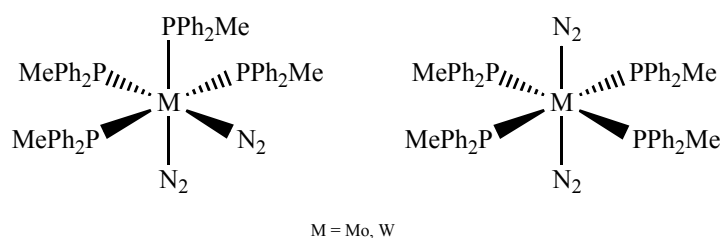


Figure I.2: Chatt complexes.

Our approach to this chemistry began with the belief that dimeric dinitrogen bridged complexes are a thermodynamic sink. Thus we were (and are) interested in monomeric complexes where dinitrogen is bound end-on. In this bonding mode, dinitrogen acts as a σ -donor/ π -acceptor ligand similar to carbon monoxide. Metal complexes supported by a triamidoamine (**TREN**, N_3N) base have orbitals of approximately d_{xz} , d_{yz} (E set) and d_{z^2} (A_1 set) ideally situated for metal-ligand multiple bonds (Figure I.3).⁹

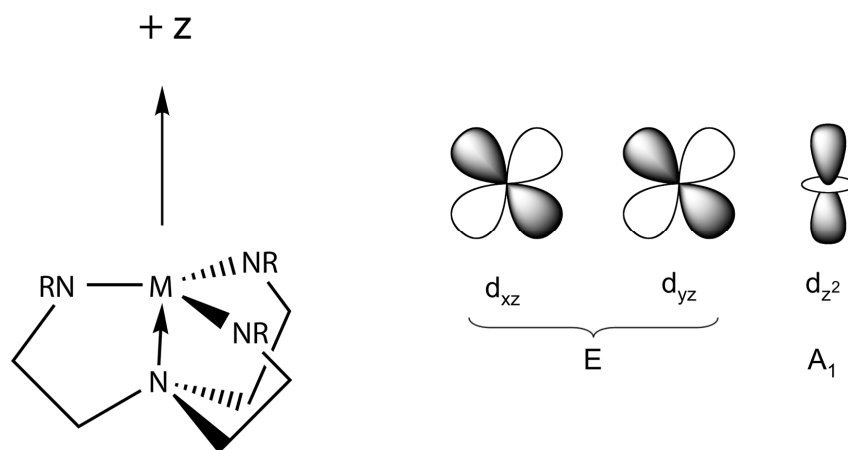


Figure I.3: TREN backbone.

Early work using the silylated **TREN** derivative $[\text{Me}_3\text{SiN}_3\text{N}]^{3-}$ on molybdenum yielded bridging dinitrogen complexes, and ligand decomposition through Si-N bond activation.⁹ Moving to arylated **TREN** derivatives, which were accessible *via* Pd catalyzed C-N bond formation,¹⁰ yielded complexes that were stable towards ligand decomposition, but were still dimeric. It was observed in the crystal structure of $\{[para-(t\text{-BuPh})\text{N}_3\text{N}]\text{Mo}\}_2(\mu\text{-N}_2)$ ¹¹ (Figure I.4) that the *tert*-butyl groups were interstitially oriented.

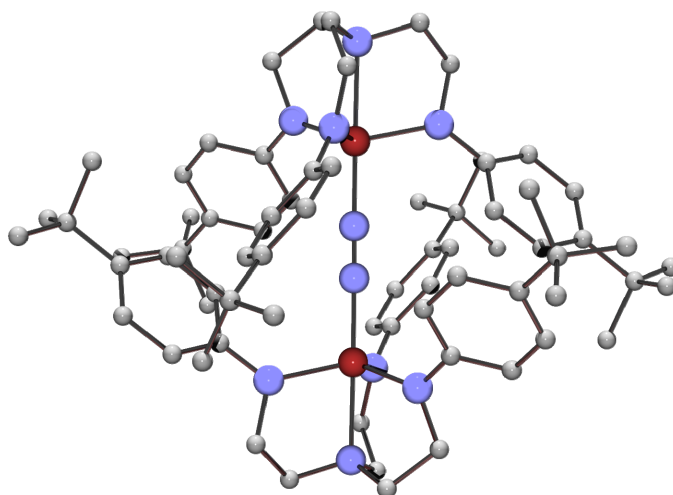


Figure I.4: POV-Ray rendering of the $\{[para(t-Bu)C_6H_4N_3N]Mo\}(\mu-N_2)$ crystal structure. Hydrogen atoms have been omitted for clarity.

This arrangement suggested that bulkier aryl groups would sterically prevent dimer formation. In pursuit of this, a *meta*-terphenyl based ligand $[3,5-(C_6H_5)_2C_6H_3N_3N]^{3-}$ was synthesized.¹⁰ Although molybdenum complexes containing this ligand were very insoluble, electrochemical measurements, which indicated that the dinitrogen containing derivative was reduced reversibly, suggested that no $\mu-N_2$ dimer was formed.¹¹

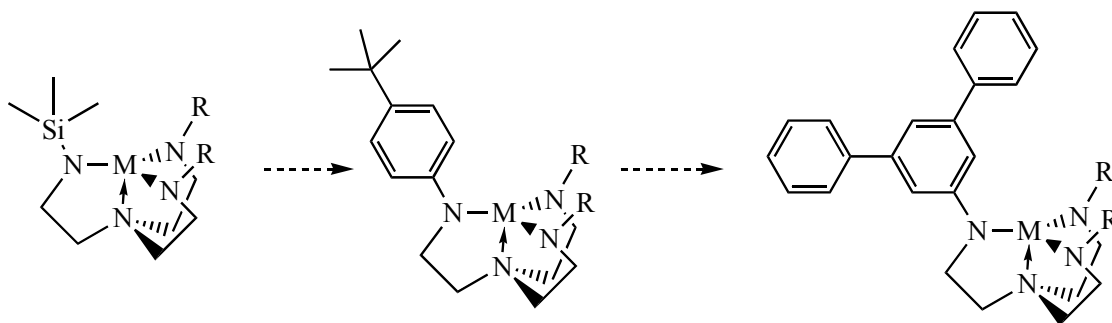


Figure I.5: TREN substituent progression.

In order to increase solubility, the hexaisopropylterphenyl $(3,5-(2,4,6-i-Pr_3C_6H_2)_2C_6H_3)$, **HIPT** based ligand was introduced (Figure I.6).^{12,13} Using the $[HIPTN_3N]Mo$ scaffold, various intermediates along a Chatt-like reduction cycle (Figure I.7) were isolated including paramagnetic $[HIPTN_3N]Mo(N_2)$ (Figure I.8), diamagnetic $\{[HIPTN_3N]Mo(N_2)\}^-$, diamagnetic $[HIPTN_3N]Mo-N=N-H$, diamagnetic $\{[HIPTN_3N]Mo=N-NH_2\}BAR^4$, diamagnetic

$[\text{HIPTN}_3\text{N}]\text{Mo}\equiv\text{N}$, diamagnetic $\{[\text{HIPTN}_3\text{N}]\text{Mo}=\text{NH}\}\text{BAR}'_4$, paramagnetic $\{[\text{HIPTN}_3\text{N}]\text{Mo}(\text{NH}_3)\}\text{BAR}'_4$, and paramagnetic $[\text{HIPTN}_3\text{N}]\text{Mo}(\text{NH}_3)$. It was further shown that several of these complexes were capable of supporting the catalytic conversion of dinitrogen to ammonia at room temperature and pressure upon the addition of protons and electrons.^{14,15} Thus, these molybdenum complexes were the first well-defined single molecule catalysts for the conversion of dinitrogen to ammonia at room temperature and pressure.

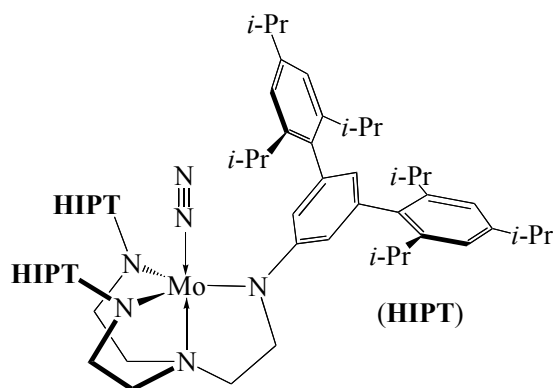


Figure I.6: Example $[\text{HIPTN}_3\text{N}]\text{Mo}$ complex, $[\text{HIPTN}_3\text{N}]\text{MoN}_2$.

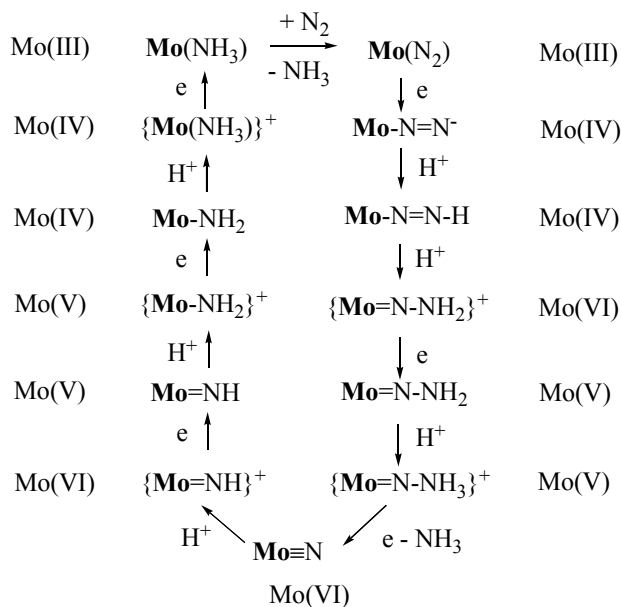


Figure I.7: Step-wise Chatt type dinitrogen reduction cycle.

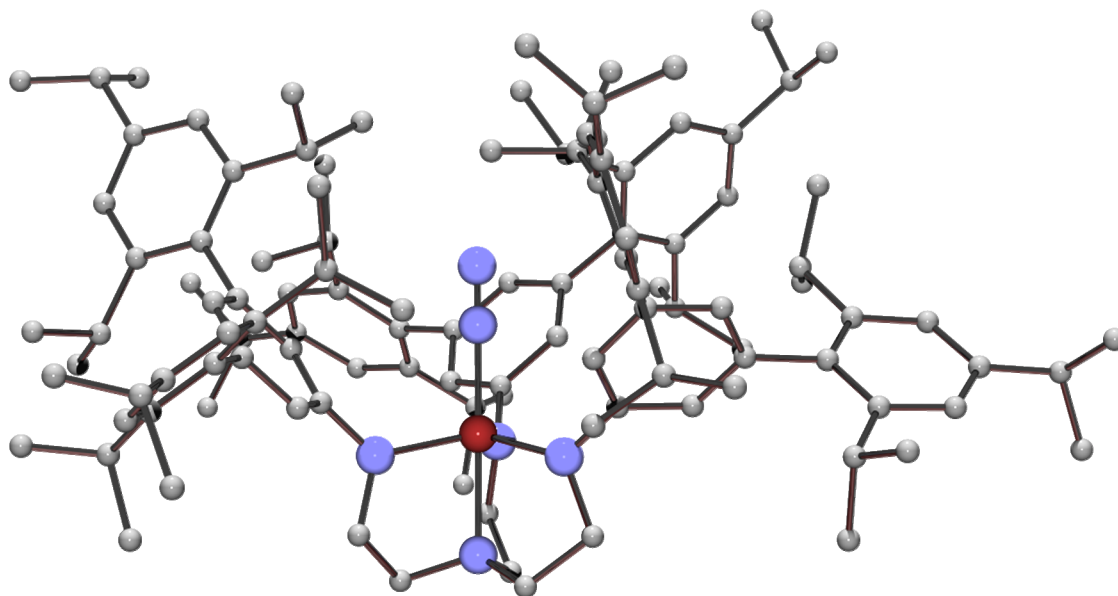


Figure I.8: POV-Ray rendering of the [HIPTN₃N]MoN₂ crystal structure. Hydrogen atoms omitted for clarity.

References

- ¹ Travis, T. *Chemistry and Industry* **1993**, 581.
- ² Fryzuk, M. D.; Johnson, S. A. *Coord. Chem. Rev.* **2000**, 200-202, 379.
- ³ Chatt, J.; Dilworth, J. R.; Richards, R. L. *Chem. Rev.* **1978**, 78, 589.
- ⁴ Gambarotta, S. *J. Organomet. Chem.* **1995**, 500, 117.
- ⁵ Hidai, M.; Mizobe, Y. *Chem. Rev.* **1995**, 95, 1115.
- ⁶ Allen, A. D.; Senoff, C. V. *J. Chem. Soc., Chem. Commun.* **1965**, 621.
- ⁷ Chatt, J.; Pearman, A. J.; Richards, R. L. *J. Chem. Soc., Dalton Trans.* **1977**, 1852.
- ⁸ Bazhenova, T. A.; Shilov, A. E. *Coord. Chem. Rev.* **1995**, 144, 69.
- ⁹ Schrock, R. R. *Acc. Chem. Res.* **1997**, 30, 9.
- ¹⁰ Greco, G. E.; Schrock, R. R. *Inorg. Chem.* **2001**, 40, 3850.
- ¹¹ Greco, G. E.; Schrock, R. R. *Inorg. Chem.* **2001**, 40, 3861.
- ¹² Yandulov, D. V.; Schrock, R. R. *J. Am. Chem. Soc.* **2002**, 124, 6252.
- ¹³ Yandulov, D. V.; Schrock, R. R.; Rheingold, A. L.; Ceccarelli, C.; Davis, W. M. *Inorg. Chem.* **2003**, 42, 796.
- ¹⁴ Yandulov, D.; Schrock, R. R. *Science* **2003**, 301, 76.
- ¹⁵ Schrock, R. R. *Acc. Chem. Res.* **2005**, 38, 955.

Chapter 1

Vanadium Complexes Supported by a Sterically Demanding Triamidoamine Ligand with a Focus on Species Relevant to Dinitrogen Reduction and Reactivity.

1.1 Introduction

In addition to the more studied Mo-Fe nitrogenase, V-Fe and Fe-Fe nitrogenases form when molybdenum (V-Fe) or molybdenum and vanadium (Fe-Fe) are not available. Unlike the Mo-Fe nitrogenase, the V-Fe and Fe-Fe nitrogenases have not been structurally characterized, although it is believed that they adopt similar, but distinct, structures.¹ The efficiency of these enzymes follows the order Mo-Fe > V-Fe > Fe-Fe, where the less efficient the enzyme, the greater the percentage of hydrogen produced during catalysis.^{2,3} Although our goal is not to create bio-mimetic systems,⁴ that nature has found a way to use these metals to realize the conversion of dinitrogen to ammonia under mild conditions indicates that they are likely candidates for us to explore. Given our success with molybdenum in the [HIPTN₃N]Mo system, we took interest in the possibility of a [HIPTN₃N]V system supporting the reduction of dinitrogen to ammonia.

Triamidoamine based vanadium complexes have been synthesized with the [MeN₃N]³⁻,⁵ [C₆F₅N₃N]³⁻,^{6,7} [Me₃SiN₃N]³⁻,^{8,9} and {[*t*-BuMe₂SiN₃N]³⁻}¹⁰ ligands, but the studies did not focus on chemistry related to dinitrogen reduction. With the [C₆F₅N₃N]³⁻, [Me₃SiN₃N]³⁻, and [*t*-BuMe₂SiN₃N]³⁻ ligands, unsubstituted V(III) complexes were formed with no evidence of dinitrogen activation. In retrospect, this may not be surprising given that a perusal of V(III) dinitrogen complexes shows that the few of which we are aware are dimeric with dinitrogen acting as a bridging ligand.^{11,12,13,14,15} This, coupled with the lack of observed dinitrogen complexation by [Me₃SiN₃N]V and [*t*-BuMe₂SiN₃N]V, implies that a single V(III) center may not be reducing enough to activate dinitrogen and suggests that a V(II) complex may be required to activate dinitrogen. Although work with [C₆F₅N₃N]V, [Me₃SiN₃N]V, and [*t*-BuMe₂SiN₃N]V complexes did not demonstrate dinitrogen activation, they did demonstrate bonding with weak σ donors (THF, MeCN) and the imide (=NH, =N(SiMe₃), =Npy) functionality. Along with the similar *tris*-anilide vanadium nitride systems reported by Cummins,¹⁶ these complexes demonstrated support for the different types of bonding required for the various intermediates in a potential dinitrogen reduction cycle (Figure 1.1).

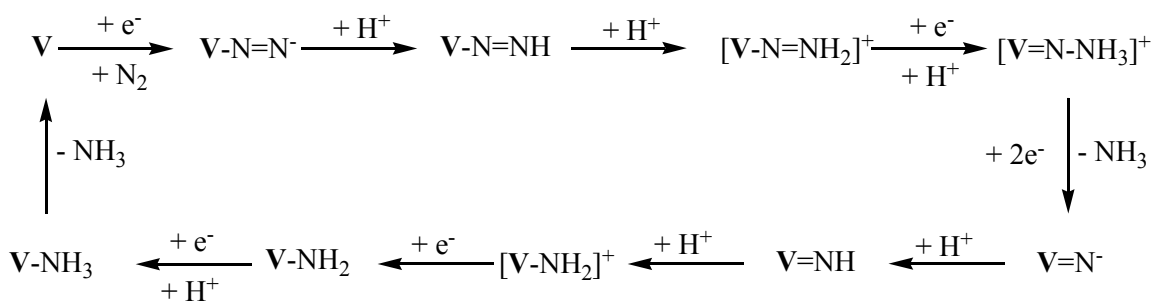


Figure 1.1: Adaptation of the [HIPTN₃N]Mo cycle to a potential vanadium cycle.

1.2 Synthesis and Properties of Metal Complexes

1.2.1 [HIPTN₃N]V(THF)

The reaction of H₃[HIPTN₃N] with VCl₃(THF)₃ proceeds analogously to that of MoCl₄(THF)₂ with H₃[HIPTN₃N].^{17,18} A violet adduct is formed upon mixing H₃[HIPTN₃N] and VCl₃(THF)₃ in THF, which turns dark green upon addition of (Me₃Si)₂NLi. Although [HIPTN₃N]V(THF) is quite soluble in organic solvents, it readily crystallized from a supersaturated pentane solution at low temperature (*ca.* -35 °C), and is not quick to redissolve, allowing isolation in good yield (generally 70-80%). This is notable as complexes containing the [HIPTN₃N]³⁻ ligand are generally quite soluble and can be difficult to isolate. In solution and upon crystallization, the solid is bright lime green, but darkens to a dark army green upon loss of the solvent of crystallization. This color change is not the result of the loss of THF as the bright lime green color returns upon re-solvation in solvents such as pentane or toluene. [HIPTN₃N]V(THF) tends to crystallize as flakes, but a crystal suitable for single crystal x-ray diffraction was obtained from a supersaturated heptane solution at room by slowly concentrating the solution stepwise (Figure 1.2).

While [HIPTN₃N]V(THF) appears to be quite stable at room temperature, it exemplifies the difference between stability and reactivity. It has been successfully stored for months (room temperature) and over a year (*ca.* -35 °C) without decomposition under N₂ in a well-sealed container. However, [HIPTN₃N]V(THF) will react with even trace amounts (not detectable using Et₃Al) of oxygen to give a purple complex (subtly different from the violet solution obtained upon addition of H₃[HIPTN₃N] to VCl₃(THF)₃). This necessitates that two guidelines

are observed when working with this complex: (1) That the desired quantity is quickly weighed and placed in a sealed container (it is possible to watch the remaining residue on the weighing boat turn purple within minutes, which extends to the bulk material if it is left exposed to the box atmosphere). (2) That either small quantities are synthesized at a time or that larger quantities are kept in multiple containers as, over time, the atmosphere exchange from opening and closing the container result in visible decomposition. The stability of $[\text{HIPTN}_3\text{N}]\text{V}(\text{THF})$ does not extend to higher temperatures. Starting at *ca.* 60 °C, visible decomposition to a black solid begins to occur. This is attributed to ring opening of the coordinated THF molecule.¹⁹ This black product is quite soluble even in Me_4Si , making attempts to isolate and identify this product unsuccessful. Thus, during isolation, the complex was always dried at room temperature and attempts at obtaining the THF free complex by heating *in vacuo* were unsuccessful.

$[\text{HIPTN}_3\text{N}]\text{V}(\text{THF})$ is most closely analogous to $[\text{C}_6\text{F}_5\text{N}_3\text{N}]\text{V}(\text{THF})$.⁶ $[\text{Me}_3\text{SiN}_3\text{N}]\text{V}$ does not appear to bind THF, though it does bind stronger σ donors such as acetonitrile.⁹ The entrance into the vanadium chemistry of the $[\text{Me}_3\text{SiN}_3\text{N}]^{3-}$ and $[\text{HIPTN}_3\text{N}]^{3-}$ ligands is also different. Using $\text{VCl}_3(\text{THF})_3$ was not found to be viable with the former,⁹ while $\text{VCl}_4(\text{DME})$ was not found to be viable with the latter. Even on a multi-gram scale, attempting to synthesize " $[\text{HIPTN}_3\text{N}]\text{VCl}$ " using $\text{VCl}_4(\text{DME})$ in a manner analogous to the synthesis of $[\text{HIPTN}_3\text{N}]\text{V}(\text{THF})$ results in an extremely soluble violet material that could not be crystallized.

1.2.2 $\{[\text{HIPTN}_3\text{N}]\text{VN}_2\}^-$

Addition of potassium graphite or sodium naphthalenide to a green THF or DME solution of $[\text{HIPTN}_3\text{N}]\text{V}(\text{THF})$ results in the immediate formation of a bright red solution. Potassium graphite is the preferred reductant as graphite is easily removed *via* filtration. The reduction product is quite reactive, attacking Teflon on contact. With wet solvents or prolonged contact with Teflon, the solution turns from red to brown. Attempts to grow single crystals of $\{[\text{HIPTN}_3\text{N}]\text{VN}_2\}^- \text{K}$ have been complicated by its apparent tendency to decompose. Green solid that is presumably $[\text{HIPTN}_3\text{N}]\text{V}(\text{THF})$ will solidify preferentially. In two cases for which red crystals were obtained from reduction in the presence of 18-Crown-6, the collected data could not be resolved for the apical pocket. Lowering the data collection temperature from -80 °C to 100 K resulted in cracking of the crystal, which is indicative of a change in morphology. An

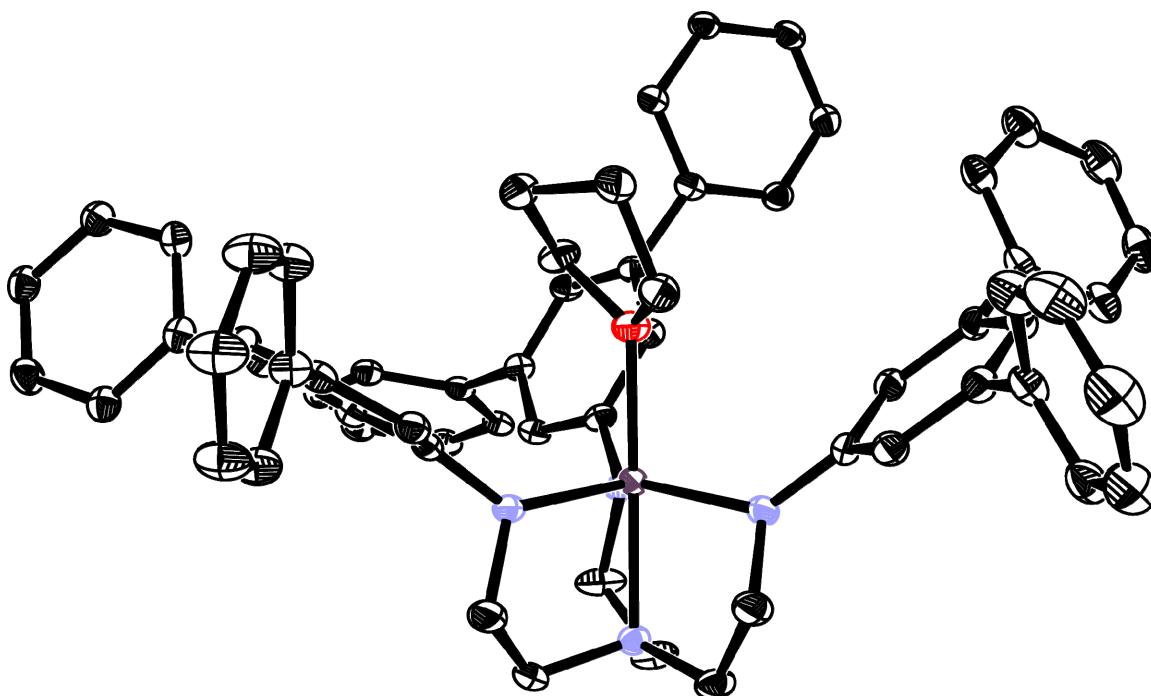


Figure 1.2: ORTEP diagram of $[\text{HIPTN}_3\text{N}]\text{V}(\text{THF})$ with thermal ellipsoids at 50% probability. Hydrogen atoms, solvent (heptane), and isopropyl groups removed for clarity.

apical nitrogen was found bound to vanadium, but there was undefined electron density in the apical position and no evidence of potassium or 18-Crown-6. This may be due to co-crystallization with possible decomposition products such as $[\text{HIPTN}_3\text{N}]\text{VH}$ and/or $[\text{HIPTN}_3\text{N}]\text{V}=\text{NH}$. If this is the case, then decomposition is occurring during crystallization rather than data collection as it would be expected that crystallinity would be lost during decomposition. While it initially seems attractive to assign $[\text{HIPTN}_3\text{N}]\text{V}=\text{NH}$ as the decomposition product due to the vanadium-nitrogen bond and undefined electron density, based on the lack of ammonia from $\{[\text{HIPTN}_3\text{N}]\text{VN}_2\}\text{K}$ vs. $[\text{HIPTN}_3\text{N}]\text{V}=\text{NH}$ (Section 1.4), this seems unlikely. Additionally, decomposition to $[\text{HIPTN}_3\text{N}]\text{VH}$ (Figure 1.6) has precedent in $[\text{HIPTN}_3\text{N}]\text{MoNNH}/[\text{HIPTN}_3\text{N}]\text{MoH}$ decomposition/co-crystallization.¹⁸ No signal was found in the attempted X-band EPR spectrum of $\{[\text{HIPTN}_3\text{N}]\text{VN}_2\}$ 18-Crown-6(K).

In THF or DME, $\{[\text{HIPTN}_3\text{N}]\text{VN}_2\}\text{K}$ shows an IR stretch consistent with monomeric end-on dinitrogen ($\nu_{\text{NN}}(\text{N}_2) = 1883 \text{ cm}^{-1}$, Figure 1.3; $\nu_{\text{NN}}(^{15}\text{N}_2) = 1821 \text{ cm}^{-1}$, Figure 1.4). This compares well with the dinitrogen stretches in the phosphine supported vanadium(I-) complexes reported by Rehder²⁰ ($\nu_{\text{NN}}(\text{N}_2) = 1706 \text{ cm}^{-1} - 1833 \text{ cm}^{-1}$), amongst which the monomeric end-on

geometry has been crystallographically determined in the case of *trans*-[(dppe)₂V(N₂)₂]Na(THF).²¹ Thus, it appears that {[HIPTN₃N]VN₂}⁻ is the first example of a monomeric vanadium dinitrogen complex supported by an amide ligand. Exchange of coordinated dinitrogen appears to be rapid as seen by the presence of {[HIPTN₃N]VN₂}⁻ in the {[HIPTN₃N]V¹⁵N₂}⁻ infrared spectrum. In the time it takes to filter the reaction mixture and obtain the spectrum (*ca.* 10 min.), an approximately 1:1 mixture of {[HIPTN₃N]VN₂}⁻ : {[HIPTN₃N]V¹⁵N₂}⁻ was observed (Figure 1.4). Upon sitting under an atmosphere of N₂ for a day, the ¹⁵N₂ resonance was completely converted to that of N₂, further confirming the ligation of dinitrogen. The mechanism of this exchange is unknown and is too rapid for us to collect kinetic data using on-hand apparatus.

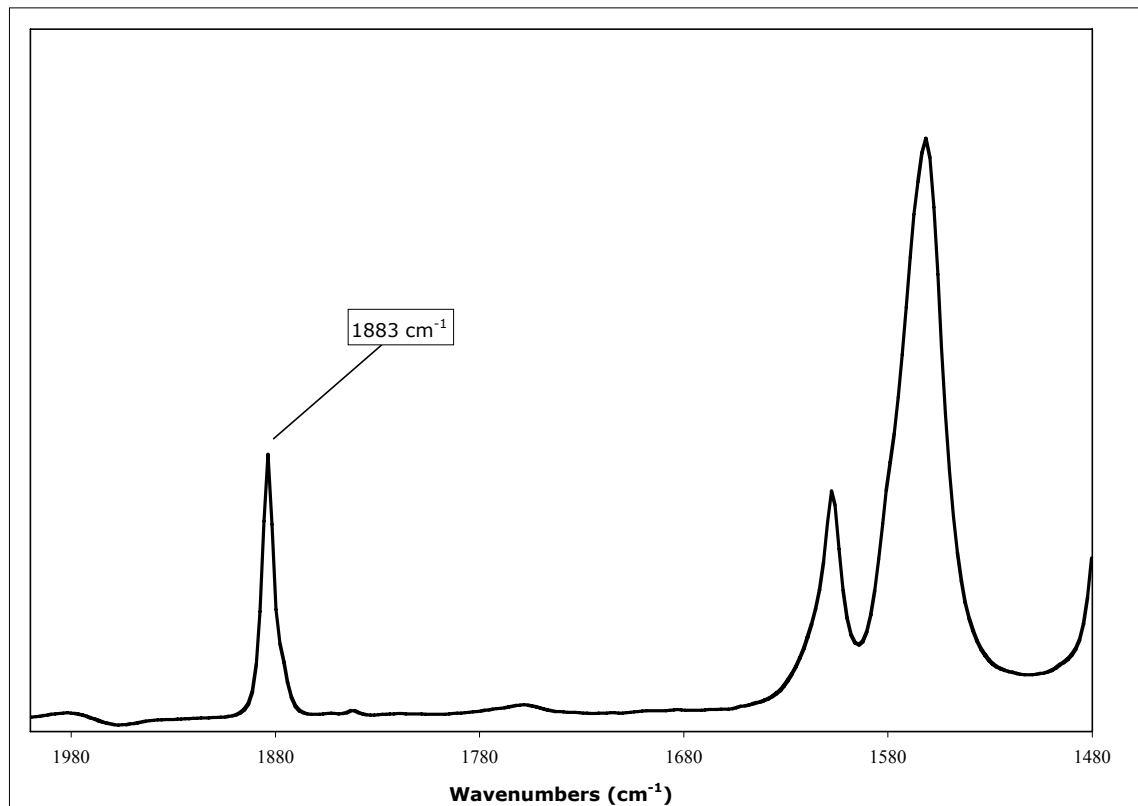


Figure 1.3: Solution IR spectrum (THF, solvent subtracted) of {[HIPTN₃N]VN₂}K.

Variation of the dinitrogen infrared stretch with the degree of solvation (THF) was observed in {[HIPTN₃N]MoN₂}MgCl•xTHF,¹⁸ and a similar dependence was also found in {[HIPTN₃N]VN₂}K. In coordinating solvents such as THF, the K⁺ ion is encapsulated by

solvent and does not strongly interact with the N_2 substrate. This can be seen in the solution spectrum of $\{[\text{HIPTN}_3\text{N}]\text{VN}_2\}\text{K}$ in C_6D_6 (very weak resonance at 1843 cm^{-1}) and of $\{[\text{HIPTN}_3\text{N}]\text{VN}_2\}18\text{-Crown-6(K)}$ in THF ($\nu_{\text{NN}}(\text{N}_2) = 1884\text{ cm}^{-1}$) and C_6D_6 ($\nu_{\text{NN}}(\text{N}_2) = 1882\text{ cm}^{-1}$) The dinitrogen stretches of $\{[\text{HIPTN}_3\text{N}]\text{VN}_2\}\text{K}$ in C_6D_6 are expected to be weak based on the aforementioned molybdenum study, and indeed there is a very

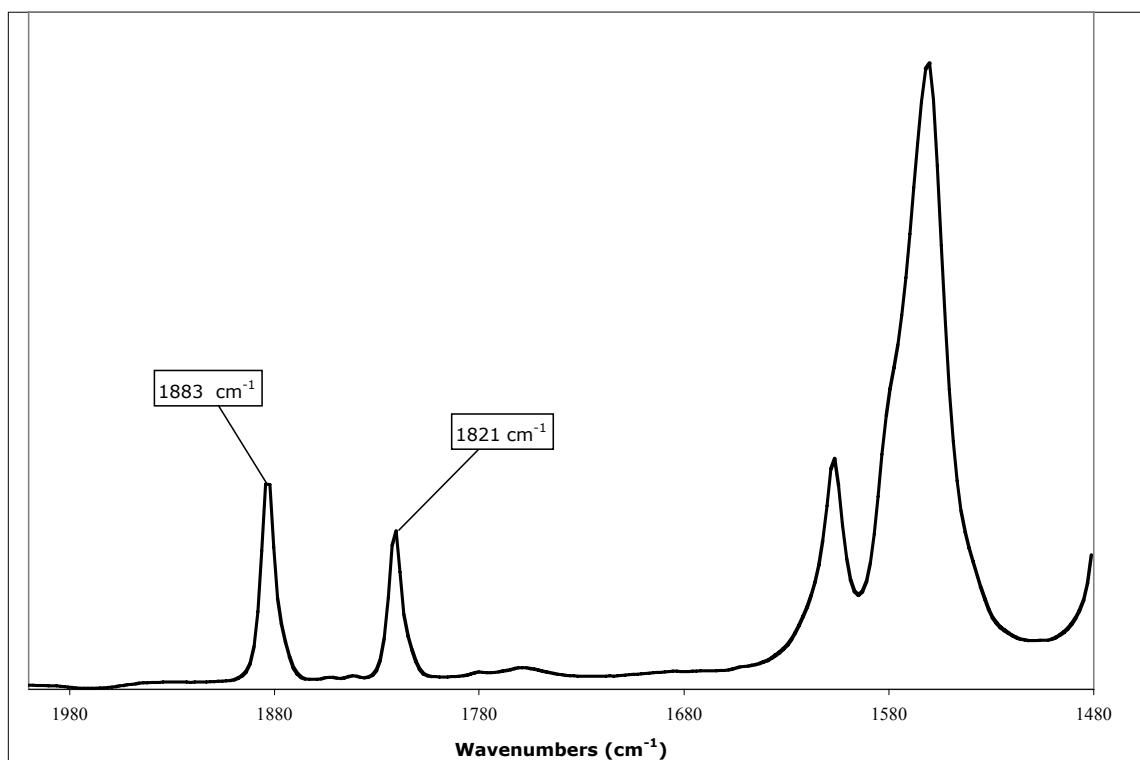
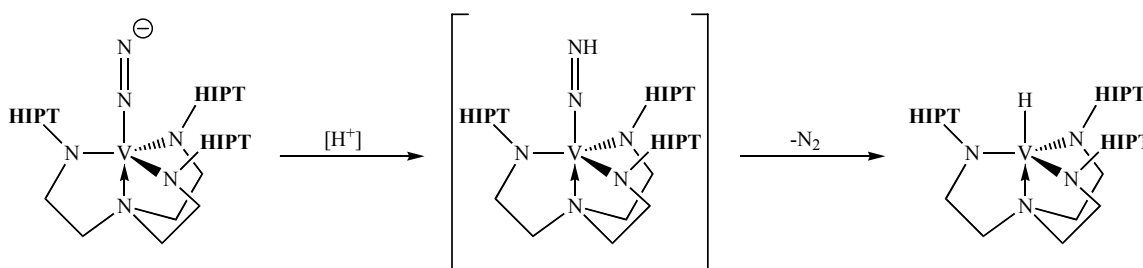


Figure 1.4: Solution IR spectrum (THF, solvent subtracted) of $\{[\text{HIPTN}_3\text{N}]\text{V}^{15}\text{N}_2\}\text{K}$.

weak resonance at 1843 cm^{-1} (Figure 1.5, dashed line). The addition of 18-Crown-6 to $\{[\text{HIPTN}_3\text{N}]\text{VN}_2\}\text{K}$ results in the appearance to a stretch at 1882 cm^{-1} (Figure 1.5) which demonstrates that K^+ is being pulled out of the coordination sphere of the N_2 substituent. Addition of one equivalent of 18-Crown-6 to a THF solution of $\{[\text{HIPTN}_3\text{N}]\text{VN}_2\}\text{K}$ does not result in any change in the observed stretch, showing that, in the absence of 18-Crown-6, THF is acting as an effective encapsulating agent. Attempting encapsulation with 2,2,2-Cyptand resulted in decomposition as shown by the loss of the N_2 stretch in THF.



Scheme 1.1: Pathway to $[\text{HIPTN}_3\text{N}]\text{VH}$ from $\{[\text{HIPTN}_3\text{N}]\text{VN}_2\}^-$.

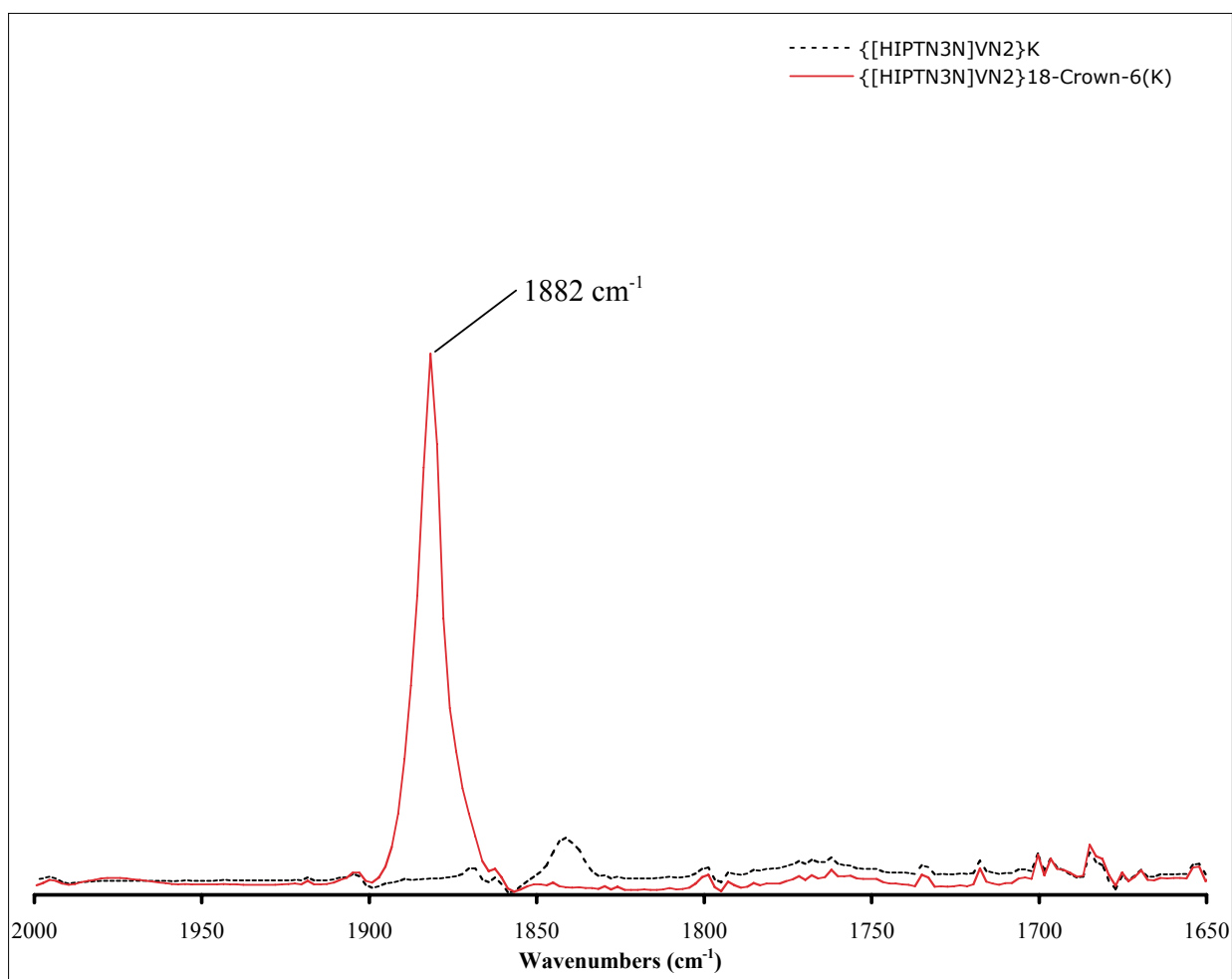


Figure 1.5: Solution IR spectra (C_6D_6 , solvent subtracted) of $\{[\text{HIPTN}_3\text{N}]\text{VN}_2\}\text{K}$ (Black, dashed line) and $\{[\text{HIPTN}_3\text{N}]\text{VN}_2\}$ 18-Crown-6(K) (Red, solid).

Using $\text{VCl}_2(\text{TMEDA})_2$ as a V(II) source for directly synthesizing $\{[\text{HIPTN}_3\text{N}]\text{VN}_2\}^-$ from $\text{H}_3[\text{HIPTN}_3\text{N}]$ (dissolution of $\text{H}_3[\text{HIPTN}_3\text{N}]$ and 3 equiv. $(\text{Me}_3\text{Si})_2\text{NLi}$ in Et_2O , followed

by addition of $\text{VCl}_2(\text{TMEDA})_2$ resulted in a light brown solution that did not display a dinitrogen stretch and which yielded crystals identified as $[\text{HIPTN}_3\text{N}]\text{VH}$ *via* x-ray diffraction (Figure 1.6). The room temperature solution EPR spectrum in benzene displayed eight peaks, which is consistent with a d^1 species where the electron is coupled to the $I = 7/2$ ^{51}V nucleus (99.8% natural abundance). Interestingly, if this reaction is done in THF, $[\text{HIPTN}_3\text{N}]\text{V}(\text{THF})$ is obtained as evidenced by the crystallization of a green product. Although the formation of $[\text{HIPTN}_3\text{N}]\text{VH}$ from $\text{VCl}_2(\text{TMEDA})_2$ is not a clean reaction, it demonstrates the feasibility of $\{[\text{HIPTN}_3\text{N}]\text{VN}_2\}^-/\text{K}^+ / [\text{HIPTN}_3\text{N}]\text{VH}$ co-crystallization and the sensitivity of $\{[\text{HIPTN}_3\text{N}]\text{VN}_2\}^-$ to even very weak acids ($(\text{Me}_3\text{Si})_2\text{NH}$).

Attempts to protonate $\{[\text{HIPTN}_3\text{N}]\text{VN}_2\}^-$ with $[2,6\text{-lutidinium}]\text{BAR}_f'$ or $\text{H}(\text{Et}_2\text{O})\text{BAR}_f'$ in benzene or THF resulted in unidentified mixtures. Addition of Me_3SiCl to a benzene solution of $\{[\text{HIPTN}_3\text{N}]\text{VN}_2\}^-$ also yielded a complex mixture and loss of the dinitrogen IR stretch. A component of this mixture was $[\text{HIPTN}_3\text{N}]\text{VH}$ as suggested by *via* x-ray crystallography. However, the data was not sufficient for full refinement and only connectivity was obtained.

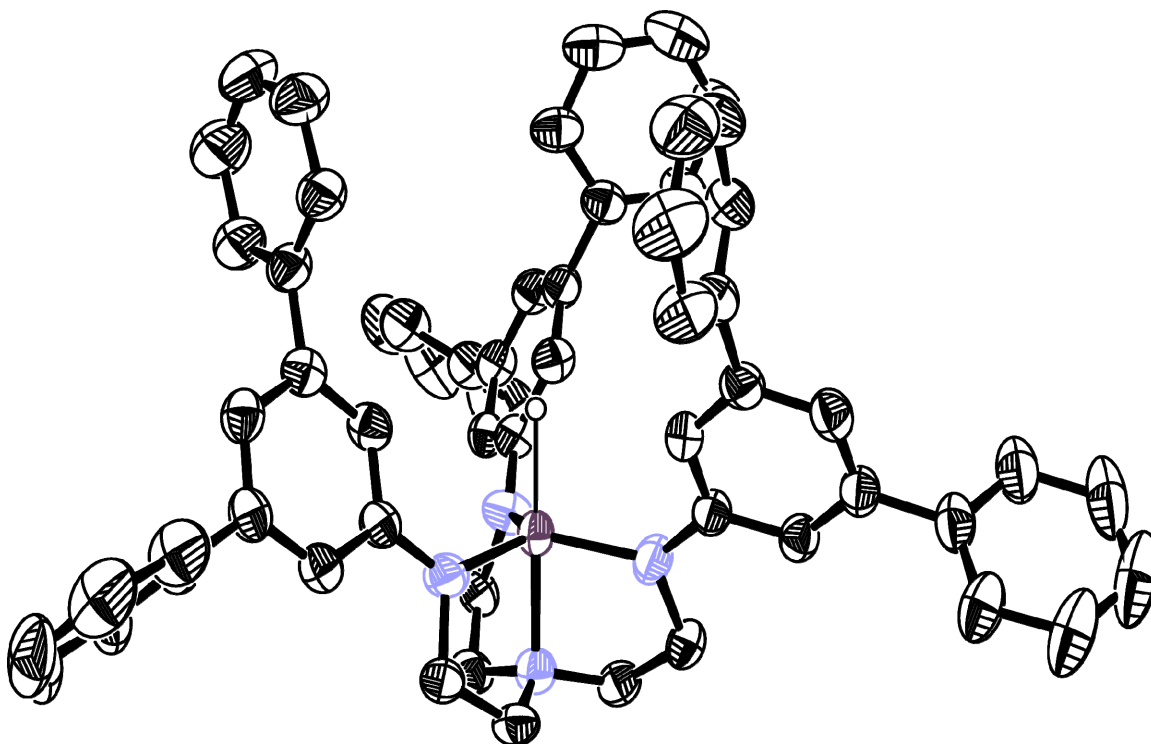


Figure 1.6: ORTEP diagram of $[\text{HIPTN}_3\text{N}]\text{VH}$ with thermal ellipsoids at 50% probability. Isopropyl groups, solvent (heptane), and non-hydride hydrogen atoms removed for clarity.

1.2.3 [HIPTN₃N]V(NH₃)

Exposure of a degassed pentane or toluene solution of [HIPTN₃N]V(THF) to NH₃ results in an immediate lightening of color to bright green and the appearance of an N-H stretch (C₆D₆, $\nu_{\text{NH}}(\text{NH}_3) = 3358 \text{ cm}^{-1}$, $\nu_{\text{NH}}(^{15}\text{NH}_3) = 3359 \text{ cm}^{-1}$). [HIPTN₃N]V(NH₃) is much more soluble than the parent complex, and is best crystallized from hexamethyldisiloxane. A crystal suitable for x-ray diffraction was obtained from a super-saturated heptane solution (Figure 1.7). [HIPTN₃N]V(NH₃) is also more temperature sensitive than [HIPTN₃N]V(THF). It is not stable at room temperature over a period of months, as evidenced by the formation of black solid which can be washed away with Me₄Si. It was also found that dinitrogen did not replace ammonia upon reduction of [HIPTN₃N]V(NH₃) with potassium graphite. Instead, [HIPTN₃N]V(NH₃) decomposed to unidentified black material.

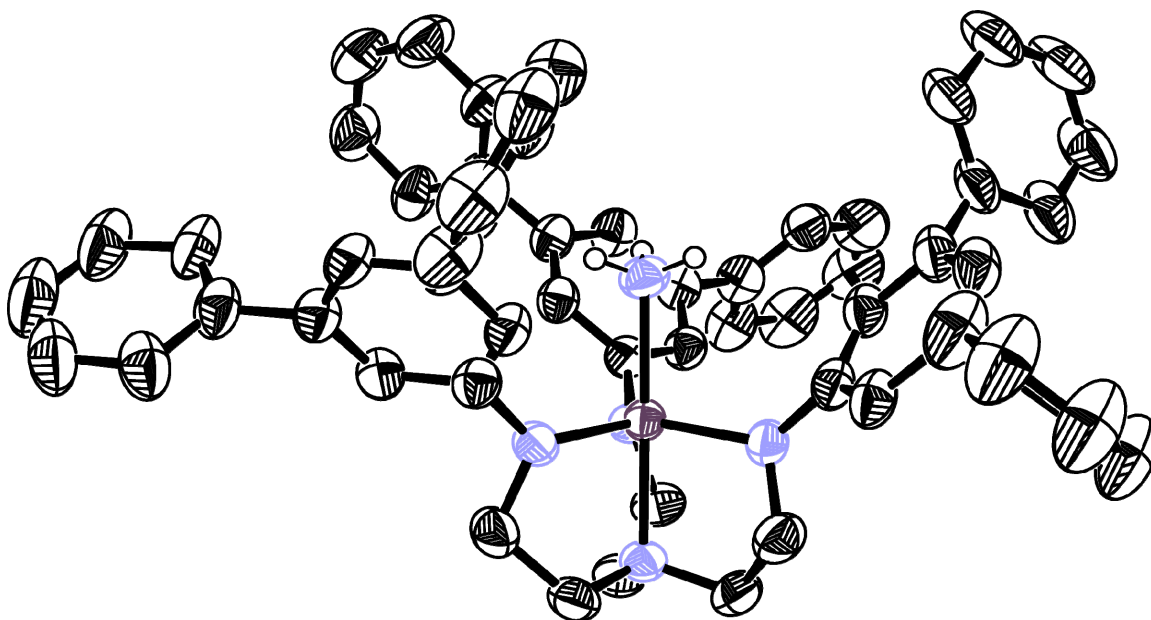


Figure 1.7: ORTEP diagram of [HIPTN₃N]V(NH₃) with thermal ellipsoids at 50% probability. Isopropyl groups, solvent (heptane) and non-ammonia hydrogen atoms removed for clarity.

1.2.4 [HIPTN₃N]V=NH

The addition of 2-methylaziridine to a toluene solution of [HIPTN₃N]V(THF) at room temperature resulted in a red solution containing a paramagnetic complex. In contrast to the synthesis of [Me₃SiN₃N]V=NH which proceeds at room temperature,⁹ the intermediate product remains paramagnetic even after 12 hours. Upon heating, there is no noticeable color change,

but a diamagnetic product is formed that can be easily crystallized from pentane as large blocks. X-ray crystallography demonstrated connectivity consistent with $[\text{HIPTN}_3\text{N}]\text{V}=\text{NH}$, but the data could not be refined satisfactorily. $[\text{HIPTN}_3\text{N}]\text{V}=\text{NH}$ displays sharp ^1H NMR resonances and a broad ^{51}V NMR peak ($\delta = -334$ ppm, 2365 Hz wide at half-height). No detectable coupling to the imido nitrogen in the ^{51}V NMR spectra of $[\text{HIPTN}_3\text{N}]\text{V}=\text{NH}$ or $[\text{HIPTN}_3\text{N}]\text{V}=\text{}^{15}\text{NH}$ was found. With a report of a ^{51}V - ^{14}N coupling constant 115 Hz,²² the observed ^{51}V NMR peak is likely too broad to show coupling to the imido nitrogen. As was the case for $[\text{Me}_3\text{SiN}_3\text{N}]\text{V}=\text{NH}$, the imido proton could not be found in the room temperature ^1H NMR spectrum presumably due to coupling to the $I = 7/2$ ^{51}V nucleus.⁹ It has been shown using π -tropyliumvanadium(-I) tricarbonyl that increasing the viscosity of a solution can decrease the ^{51}V quadrupolar coupling, allowing increased resolution of the ^1H NMR spectrum.²³ However, attempting to resolve the imido proton by decreasing the temperature of a toluene solution of $[\text{HIPTN}_3\text{N}]\text{V}=\text{NH}$ to -80 °C in 10 °C increments failed to yield a resonance assignable to it.

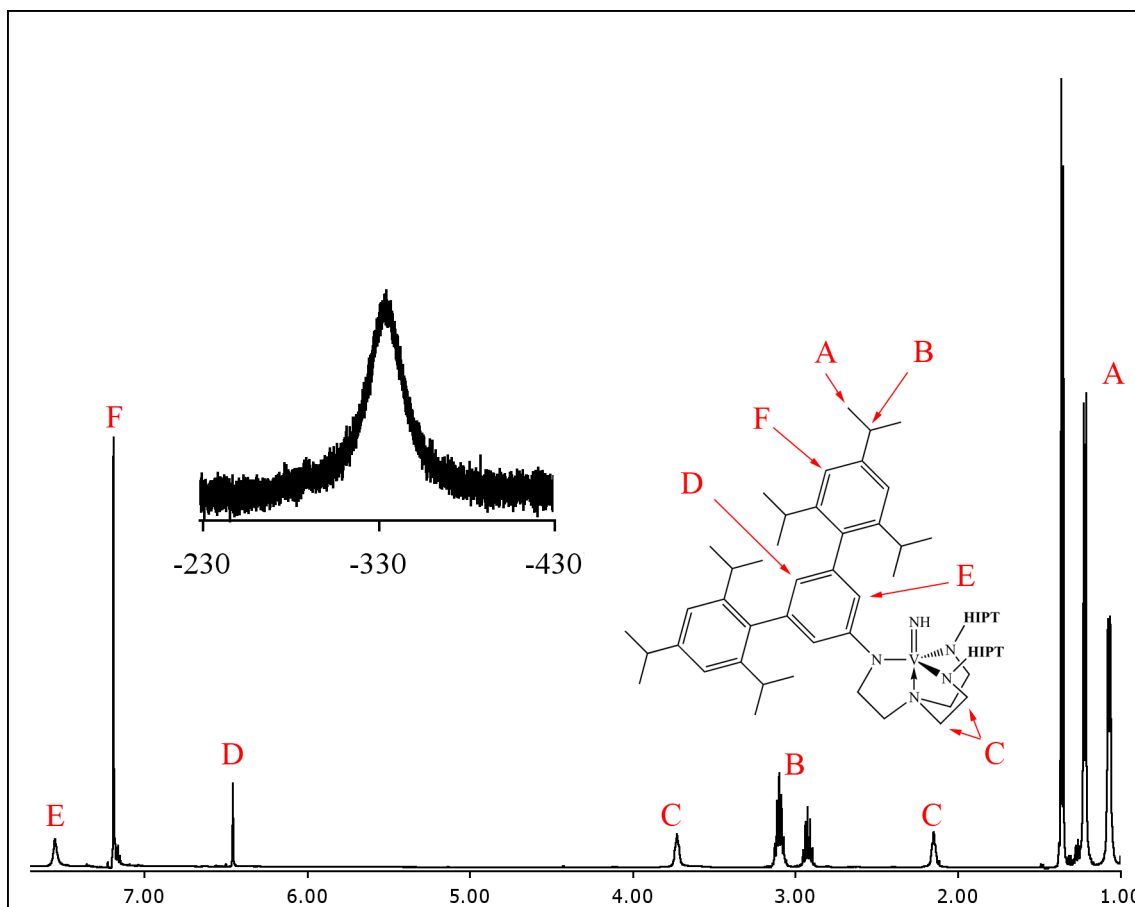


Figure 1.8: ^1H and ^{51}V NMR (inset) spectra (C_6D_6) of $[\text{HIPTN}_3\text{N}]\text{V}=\text{NH}$.

Addition of two equivalents of $(\text{Me}_3\text{Si})_2\text{NLi}$ to $[\text{HIPTN}_3\text{N}]\text{V}(\text{NH}_3)$ followed by two equivalents of $[\text{FeCp}_2]\text{OTf}$ converts the ammonia adduct to $[\text{HIPTN}_3\text{N}]\text{V}=\text{NH}$, allowing assignment of the N-H stretch in the infrared spectrum (C_6D_6 , $\nu_{\text{NH}}(\text{NH}) = 3360 \text{ cm}^{-1}$, $\nu_{\text{NH}}(^{15}\text{NH}) = 3351 \text{ cm}^{-1}$). This is a functional analogue of the conversion of $\{[\text{TerN}_3\text{N}]\text{Mo}(\text{NH}_3)\}^+$ (**Ter** = terphenyl) complexes to $\{[\text{TerN}_3\text{N}]\text{Mo}\equiv\text{N}$ using $[\text{FeCp}_2]\text{PF}_6$ and triethylamine.²⁸ The conversion of $[\text{HIPTN}_3\text{N}]\text{V}(\text{NH}_3)$ to $[\text{HIPTN}_3\text{N}]\text{V}=\text{NH}$ is quite facile, occurring even without the addition of a base. Presumably in this scenario, the coordinated ligand acts as the base generating free ligand. Addition of even one equivalent of $[\text{FeCp}_2]\text{OTf}$ results in the formation of $[\text{HIPTN}_3\text{N}]\text{V}=\text{NH}$ as the only identifiable product. Like the analogous $[\text{N}_3\text{N}]\text{Mo}\equiv\text{N}$ complexes and $[\text{Me}_3\text{SiN}_3\text{N}]\text{V}=\text{NH}$, $[\text{HIPTN}_3\text{N}]\text{V}=\text{NH}$, as a d^0 metal complex, is not susceptible to oxidation and is thus relatively stable in air.

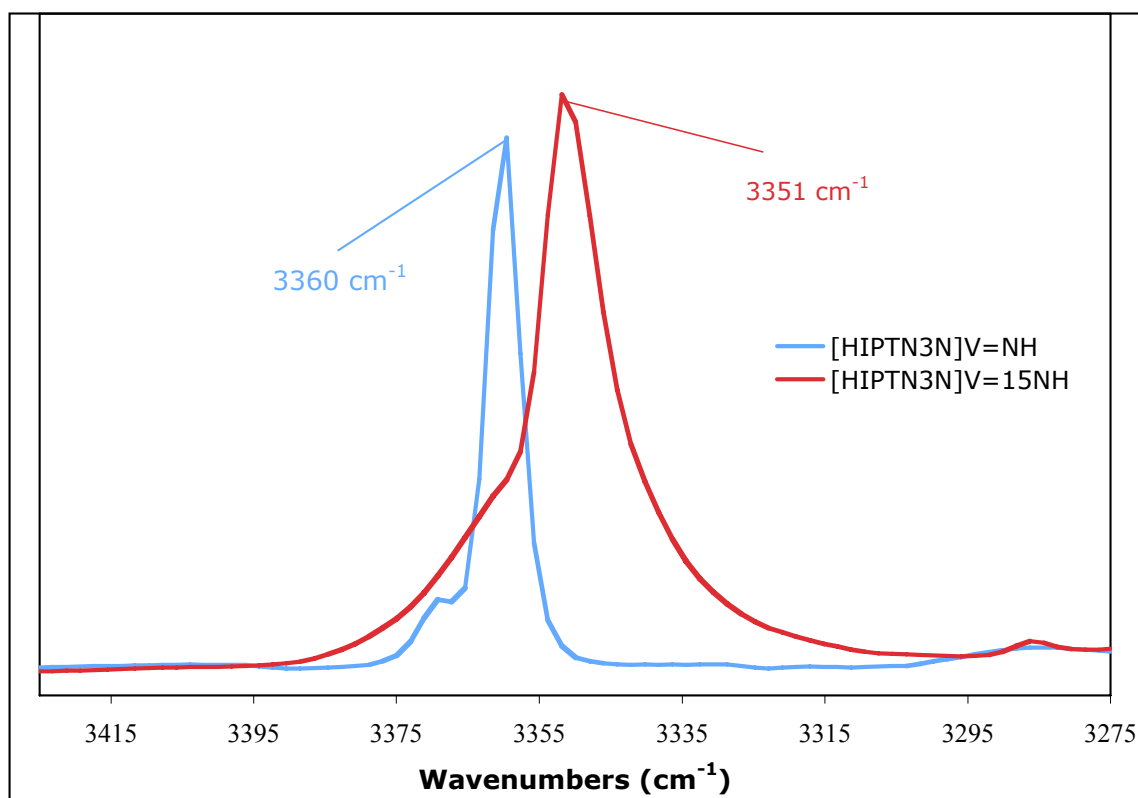


Figure 1.9: Solution IR spectra (C_6D_6 , solvent subtracted) of $[\text{HIPTN}_3\text{N}]\text{V}=\text{NH}$ (blue) and $[\text{HIPTN}_3\text{N}]\text{V}=\text{NH}$ (red).

1.2.5 [HIPTN₃N]V=N(SiMe₃)

Treatment of [HIPTN₃N]V(THF) with (Me₃Si)₃N₃ in benzene or toluene affords orange [HIPTN₃N]V=N(SiMe₃) in varying yield depending on the temperature to which and the length of time that the reaction mixture is heated. Although quantitative optimization was not undertaken, longer heating times result in decomposition to unidentified product(s) and, over long enough periods, inability to isolate any [HIPTN₃N]V=N(SiMe₃). The ¹H NMR spectrum (Figure 1.10) is typical of a diamagnetic complex with sharp resonances ($\delta(\text{Me}_3\text{SiN}) = -0.12$ ppm), and a broad ⁵¹V NMR resonance ($\delta = -276.31$ ppm, 1326 Hz wide at half-height). The Me₃Si resonance is shifted upfield slightly from that of [Me₃SiN₃N]V=N(SiMe₃) ($\delta = 0.55$ ppm).⁹

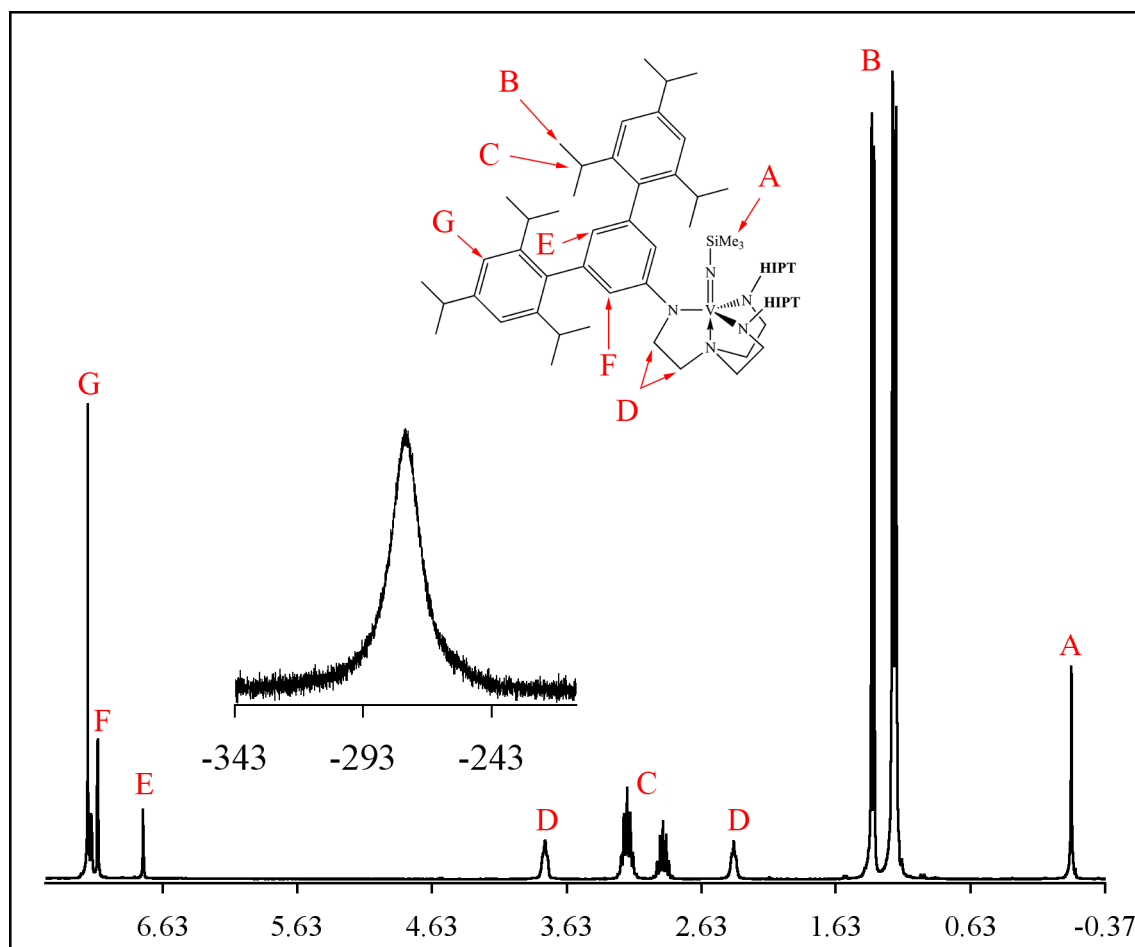


Figure 1.10: ¹H and ⁵¹V (inset) NMR spectra (C₆D₆) of [HIPTN₃N]V=N(SiMe₃).

1.2.6 [HIPTN₃N]V=S

Unlike other analogous reactions of the [HIPTN₃N]V and [Me₃SiN₃N]V fragments, the generation of [HIPTN₃N]V=S from elemental sulfur does not require heating. Simple addition of S₈ to a stirring pentane solution of [HIPTN₃N]V(THF) yields [HIPTN₃N]V=S as a dark green product which displays a well-defined ¹H NMR spectrum (Figure 1.11) and a sharp ⁵¹V NMR resonance ($\delta = 756$ ppm, 30 Hz wide at half-height). Even after crystallization, a second small (*ca.* 2-3% by integration) ⁵¹V resonance can be observed ($\delta(^{51}\text{V}) = 754$ ppm). Although it is tempting to assign this resonance to a by-product not removed by crystallization, it is curious that the same phenomenon is observed in [HIPTN₃N]V=O which is obtained using different methodology (Section 1.2.7).

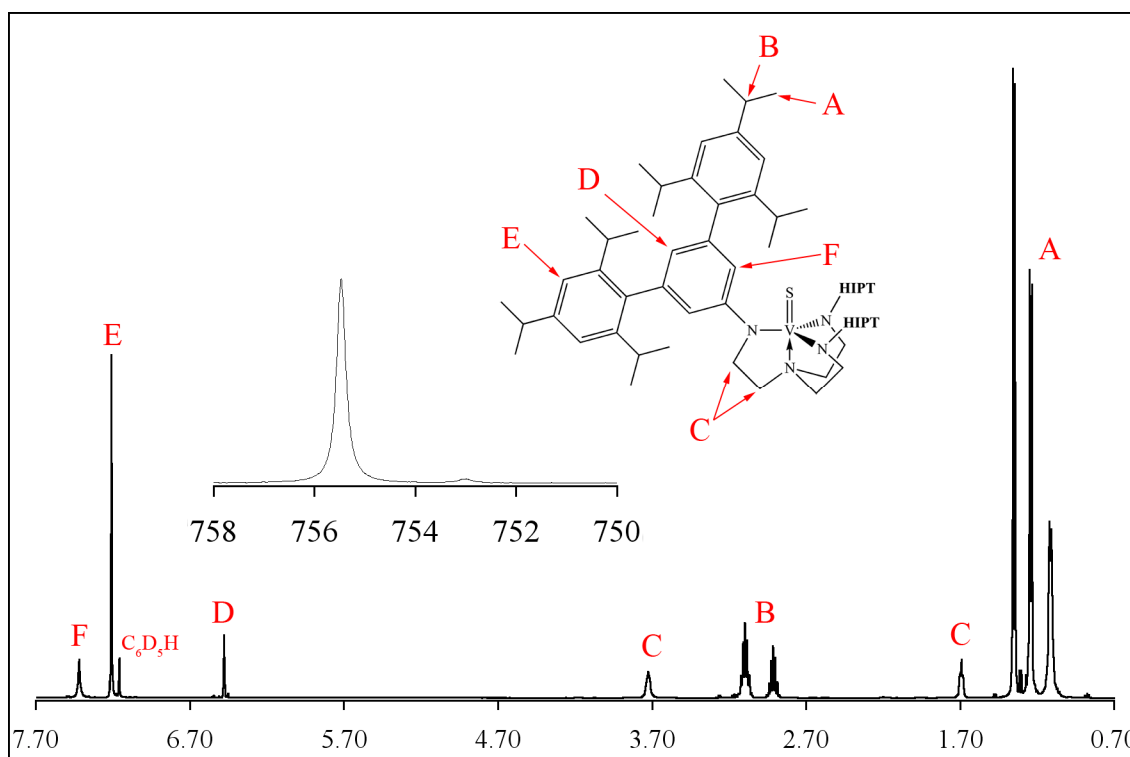


Figure 1.11: ¹H and ⁵¹V (inset) NMR spectra (C₆D₆) of [HIPTN₃N]V=S.

1.2.7 [HIPTN₃N]V=O

Similar to the reaction of [HIPTN₃N]V(THF) with 2-methylaziridine (Section 1.2.4), upon addition of propylene oxide to a toluene solution of [HIPTN₃N]V(THF) the color of the solution immediately turns purple, but the solution does not contain a diamagnetic product.

Heating at 80 °C was required to isolate purple $[\text{HIPTN}_3\text{N}]\text{V}=\text{O}$ as a microcrystalline powder from pentane ($\delta(^{51}\text{V}) = -116$ ppm, 785 Hz wide at half-height). A small impurity is present in the ^{51}V NMR spectrum ($\delta(^{51}\text{V}) = -69$ ppm), even in the spectrum of re-crystallized material (Figure 1.12). Given the similar observation with $[\text{HIPTN}_3\text{N}]\text{V}=\text{S}$ (Section 1.2.6), and the different synthetic routes to $[\text{HIPTN}_3\text{N}]\text{V}=\text{S}$ and $[\text{HIPTN}_3\text{N}]\text{V}=\text{O}$, this may be the result of an inherent impurity. Variable temperature ^{51}V NMR spectra of $[\text{HIPTN}_3\text{N}]\text{V}=\text{O}$ and $[\text{HIPTN}_3\text{N}]\text{V}=\text{S}$ from -20 °C to 80 °C taken in 10 °C increments show that the smaller second ^{51}V NMR resonance remains fairly constant at *ca.* 1-3% until -20 °C, where it disappears. An attempt to synthesize $[\text{HIPTN}_3\text{N}]\text{V}=\text{O}$ from $\text{Cl}_3\text{V}=\text{O}$, as in the synthesis of $[\text{C}_6\text{F}_5\text{N}_3\text{N}]\text{V}=\text{O}$,⁶ yielded multiple products by ^{51}V NMR and was abandoned in favor of the propylene oxide route.

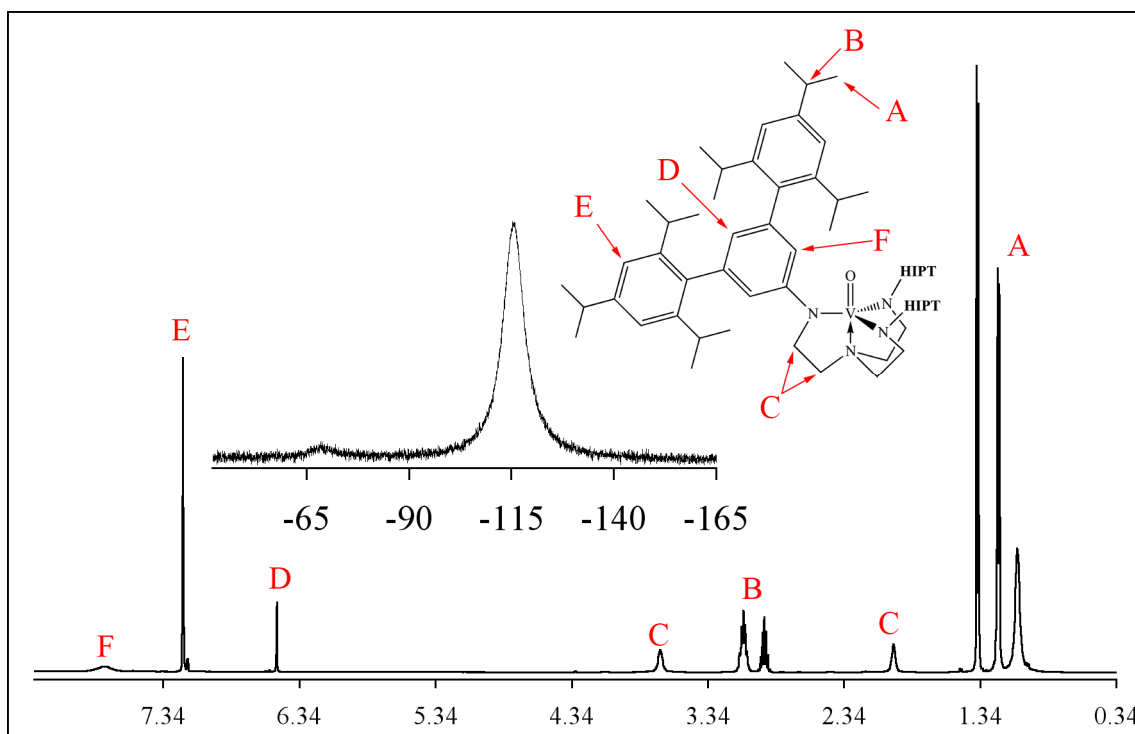


Figure 1.12: ^1H and ^{51}V (inset) NMR spectra (C_6D_6) of $[\text{HIPTN}_3\text{N}]\text{V}=\text{O}$.

1.2.8 Other Reactions

Although $[\text{HIPTN}_3\text{N}]\text{V}=\text{NH}$ is readily accessible, the anionic vanadium nitride ($\{[\text{HIPTN}_3\text{N}]\text{V}\equiv\text{N}\}^-$) has proved elusive. Addition of NaN_3 to a THF solution of $[\text{HIPTN}_3\text{N}]\text{V}(\text{THF})$ (*cf.* the synthesis of the *tris*-anilide complexes $\{[\text{Ar}(\text{R})\text{N}]\text{VN}\}\text{Na}$ ($\text{Ar} = 3,5-$

$\text{Me}_2\text{C}_6\text{H}_3$; R = Ad, *t*-Bu) by Cummins¹⁶) does not result in any reaction. Heating a toluene or DME solution of $[\text{HIPTN}_3\text{N}]\text{V}(\text{THF})$ with NaN_3 at 65-70 °C over *ca.* 12 hours yields a paramagnetic orange product that displays an IR stretch ($\nu = 2124 \text{ cm}^{-1}$) which suggests an azide complex based on the $[\text{Me}_3\text{SiN}_3\text{N}]\text{VN}_3$ azide stretch ($\nu_{\text{azide}} = 2088 \text{ cm}^{-1}$).⁹ Addition of 15-Crown-5 to this reaction results in a dark yellow solid that is insoluble in pentane. However, the product is paramagnetic, showing that loss of N_2 from the azide substituent does not occur. Addition of (*n*-Bu₄N)N₃ to a solution of $[\text{HIPTN}_3\text{N}]\text{V}(\text{THF})$ in toluene at room temperature results in a dark, dirty yellow product that is again paramagnetic, while heating the reaction at temperatures of up to 140 °C results in a red paramagnetic solution. Although the product obtained at room temperature does contain a hint of some diamagnetic component, nothing was successfully isolated. Attempting to deprotonate $[\text{HIPTN}_3\text{N}]\text{V}=\text{NH}$ with $(\text{Me}_3\text{Si})_2\text{NLi}$ or (*i*-Pr)NHLi does not result in any reaction, while the use of *n*-BuLi results in unidentified decomposition. Attempting to remove the (Me₃Si-) group from $[\text{HIPTN}_3\text{N}]\text{V}=\text{N}(\text{SiMe}_3)$ using (*i*-Pr)NHLi as used by Gambarotta in the synthesis of $[(\text{Ph}_2\text{N})_3\text{VN}]\text{Na}(\text{THF})_3$ ¹⁹ resulted in no reaction at room temperature and decomposition upon heating. A similar result was observed with the use of (*n*-Bu₄N)F in an attempt to take advantage of the strong Si-F bond. It is possible that an explanation for this inability to form $\{[\text{HIPTN}_3\text{N}]\text{V}\equiv\text{N}\}^-$ may be found in the observation that $[\text{Me}_3\text{SiN}_3\text{N}]\text{V}=\text{NH}$ is found as an impurity in the synthesis of $[\text{Me}_3\text{SiN}_3\text{N}]\text{V}(\text{N}_3)$.

Addition of MeCN to a solution of $[\text{HIPTN}_3\text{N}]\text{V}(\text{THF})$ results in an immediate color change to bright green similar to what is observed with $[\text{Me}_3\text{SiN}_3\text{N}]\text{V}$. Exposure of a degassed pentane solution of $[\text{HIPTN}_3\text{N}]\text{V}(\text{THF})$ to an atmosphere of CO (a stronger σ donor π acceptor type ligand than N_2) yields a red-gold solution of $[\text{HIPTN}_3\text{N}]\text{V}(\text{CO})$ ($\nu_{\text{CO}}(\text{CO}) = 2076 \text{ cm}^{-1}$, $\nu_{\text{CO}}(^{13}\text{CO}) = 2030 \text{ cm}^{-1}$, $\nu_{\text{CO}}(^{13}\text{C}^{18}\text{O}) = 1980 \text{ cm}^{-1}$). This shows that $[\text{HIPTN}_3\text{N}]\text{V}(\text{III})$ is capable of binding a σ donor/ π acceptor type ligands, but that V(III) is not reducing enough to bind dinitrogen.

1.3 X-Ray Discussion

Three crystal structures were obtained of $[\text{HIPTN}_3\text{N}]\text{V}$ complexes and the structural parameters are given in Table 1.1. Selected structural parameters related to the triamidoamine

	V(THF)	V(NH ₃)	V-H
Formula	C ₁₃₂ H ₁₉₉ N ₄ OV	C ₁₂₁ H ₁₇₈ N ₅ V	C ₁₂₁ H ₁₇₆ N ₄ V
fw (g/mol)	1908.89	1753.62	1737.60
Temperature (K)	100(2)	193(2)	194(2)
Space Group	P $\bar{1}$	Cc	R $\bar{3}c$
a (Å)	17.7727(6)	16.1153(4)	21.0178(7)
b (Å)	18.3700(7)	39.7548(11)	21.0178(7)
c (Å)	21.2032(9)	18.0197(5)	98.698(6)
α (°)	113.9930(10)	90	90
β (°)	99.8920(10)	93.0540(10)	90
γ (°)	96.5660(10)	90	120
GoF	1.043	1.015	1.783
R [I>2σ(I)] (%)	R ₁ = 7.0 wR ₂ = 17.6	R ₁ = 5.8 wR ₂ = 14.5	R ₁ = 9.9 wR ₂ = 26.4
R (all data) (%)	R ₁ = 10.7 wR ₂ = 20.1	R ₁ = 7.7 wR ₂ = 15.9	R ₁ = 13.0 wR ₂ = 27.7

Table 1.1: Structural Solution Parameters for [HIPTN₃N]V Complexes.

core for the structurally characterized [HIPTN₃N]V complexes ([HIPTN₃N]V(THF), [HIPTN₃N]V(NH₃), and [HIPTN₃N]VH) along with selected other triamidoamine based vanadium complexes ([C₆F₅N₃N]V(MeCN),⁶ [*t*-BuMe₂N₃N]V,¹⁰ [C₆F₅N₃N]V,⁷ [C₆F₅N₃N]V(THF),⁶ [Me₃SiN₃N]VCl,⁸ [MeN₃N]V=O,⁵ [Me₃SiN₃N]V=Npy,²⁴ and [Me₃SiN₃N]V=NH)⁹ can be found in Table 1.3. Within the [HIPT]V group, there does not appear to be a simple correlation between oxidation state and N(amine)-V bond distance. There does appear to be, however, a correlation between the apical substituent (or lack thereof) and the N(amine)-V bond distance with [C₆F₅N₃N]V (2.08 Å) and [*t*-BuMe₂N₃N]V (2.08 Å), and [C₆F₅N₃N]V(THF) (2.13 Å) and [HIPTN₃N]V(THF) (2.16 Å). Taking the displacement from the plane of the amido nitrogens (taken as an average of the distance calculated by (N(amide)-V)•cos(N(amide)-V-N(amine)) over the three amide nitrogens) into account (Figure 1.13) leads to a more constant distance ($\Delta = 0.3$ Å vs. $\Delta = 0.1$ Å) considering the variation in ligand. This is even more pronounced across complexes containing the same ligand (HIPT: $\Delta = 0.08$ Å vs. $\Delta = 0.04$ Å; Me₃Si: $\Delta = 0.13$ Å vs. $\Delta = 0.05$ Å) except for the [C₆F₅N₃N]V for which there isn't much

of a change ($\Delta = 0.07 \text{ \AA}$ vs. $\Delta = 0.06 \text{ \AA}$), but for which the distance is already fairly constant. The average V-N(amide) bond lengths do not show a significant difference between variations in oxidation state, ligand, or apical substituent (**HIPT**: 1.950 \AA , $\sigma = 0.006 \text{ \AA}$; **C₆F₅**: 1.948 \AA , $\sigma = 0.007 \text{ \AA}$; **Me₃Si**: 1.90 \AA , $\sigma = 0.02 \text{ \AA}$; **t-BuMe₂**: 1.930 \AA ; **Me**: 1.895 \AA).

While the **HIPT** substituent is quite sterically encumbering, it is capable of rotation in response to steric pressure. This property, coupled with the flexibility of the triamidoamine backbone, allows complexes employing the $[\text{HIPTN}_3\text{N}]^{3-}$ ligand to accommodate apical ligands that might not otherwise be able to fit in the protected pocket (Table 1.2). $[\text{HIPTN}_3\text{N}]\text{VH}$ contains the smallest substituent and is rigorously 3-fold symmetric. With $[\text{HIPTN}_3\text{N}]\text{VH}$, as the smallest, containing **HIPT** groups that are nearly vertical. Moving to the more encumbering NH_3 ligand, probably as much due to the increased V-N(apical) bond length (2.16 \AA vs. 1.64 \AA in $[\text{Me}_3\text{SiN}_3\text{N}]\text{V}=\text{NH}$) as the size increase, results in tilting of the **HIPT** groups to *ca.* 60° off of vertical while maintaining an approximately C_3 symmetric backbone. The much larger THF molecule in $[\text{HIPTN}_3\text{N}]\text{V}(\text{THF})$ results in significant tilting and deviation from C_3 symmetry. The **HIPT** group under the bent THF molecule is nearly horizontal (81.0°), while the other two are tilted *ca.* 50° from vertical, for which the triamidoamine base opens up to accommodate.

	V(THF)	V(NH ₃)	V-H
N(amide ₁)-V-N(amide ₂) (°)	123.82(8)	118.19(3)	120
N(amide ₂)-V-N(amide ₃) (°)	115.95(8)	118.43(3)	—
N(amide ₃)-V-N(amide ₁) (°)	114.39(8)	118.67(3)	—
Torsion Angle 1 (°)	128.3	119.4	7.0
Torsion Angle 2 (°)	50.6	123.3	—
Torsion Angle 3 (°)	81.0	117.8	—

Table 1.2: Core symmetry and **HIPT** group torsion angles in $[\text{HIPTN}_3\text{N}]\text{V}$ complexes.

Ligand	C ₆ F ₅	<i>t</i> -BuMe ₂	C ₆ F ₅	C ₆ F ₅	C ₆ F ₅	THF	THF	THF	NH ₃	Cl	H	O	NPY	Me ₃ Si	Me ₃ Si
Apical Substituent (X)	MeCN	—	—	—	—	THF	THF	THF	NH ₃	Cl	H	O	NPY	Me ₃ Si	Me ₃ Si
Space Group	R3	P $\bar{1}$	R $\bar{3}$	R $\bar{3}$	R $\bar{3}$	P2 ₁ /n	P $\bar{1}$	P $\bar{1}$	Cc	P2 ₁ /a	R $\bar{3}$ c	R3c	Pna2 ₁	P2 ₁ /n	P2 ₁ /n
Oxidation State	3+	3+	3+	3+	3+	3+	3+	3+	3+	4+	4+	5+	5+	5+	5+
Color	Lime Green	Green	Bright Green	Bright Green	Green	Green	Green	Green	Bright Green	Blue-black	Orange-brown	Red	Red-black	Yellow	Yellow
V-N(amine) (Å)	2.149	2.084	2.079(6)	2.132(3)	2.1627(18)	2.1486(7)	2.1627(18)	2.1627(18)	2.1486(7)	2.238	2.087(4)	2.320	2.364	2.241	2.241
V-N(amide) (Å)	1.940	1.930 $\sigma = 0.004$	1.947(4)	1.957 $\sigma = 0.009$	1.95 $\sigma = 0.03$	1.955 $\sigma = 0.002$	1.95 $\sigma = 0.03$	1.95 $\sigma = 0.03$	1.955 $\sigma = 0.002$	1.884 $\sigma = 0.006$	1.942(3)	1.895	1.897 $\sigma = 0.001$	1.921 $\sigma = 0.004$	1.921 $\sigma = 0.004$
V-X(apical) (Å)	1.599	—	—	2.152(3)	2.1399(15)	2.1623(8)	2.152(3)	2.1399(15)	2.1623(8)	2.279	1.857	1.599	1.693	1.638	1.638
Plane Displacement (Å)	0.23	0.16 $\sigma = 0.01$	0.22	0.261 $\sigma = 0.002$	0.27 $\sigma = 0.02$	0.25 $\sigma = 0.01$	0.261 $\sigma = 0.002$	0.27 $\sigma = 0.02$	0.25 $\sigma = 0.01$	0.31 $\sigma = 0.02$	0.23	0.40	0.40 $\sigma = 0.02$	0.33 $\sigma = 0.02$	0.33 $\sigma = 0.02$
X(apical)-V-N(amine) (°)	180	—	—	169.74(11)	171.42(6)	179.43(3)	169.74(11)	171.42(6)	179.43(3)	179.32	180	180	177.28	177.71	177.71
X(apical)-V-N(amide) (°)	96.9	—	—	98 $\sigma = 7$	98 $\sigma = 6$	97.3 $\sigma = 0.5$	98 $\sigma = 7$	98 $\sigma = 6$	97.3 $\sigma = 0.5$	99.5 $\sigma = 0.4$	—	102.1	102 $\sigma = 1$	100 $\sigma = 1$	100 $\sigma = 1$

Table 1.3: Structural parameters for selected triamidoamine complexes.

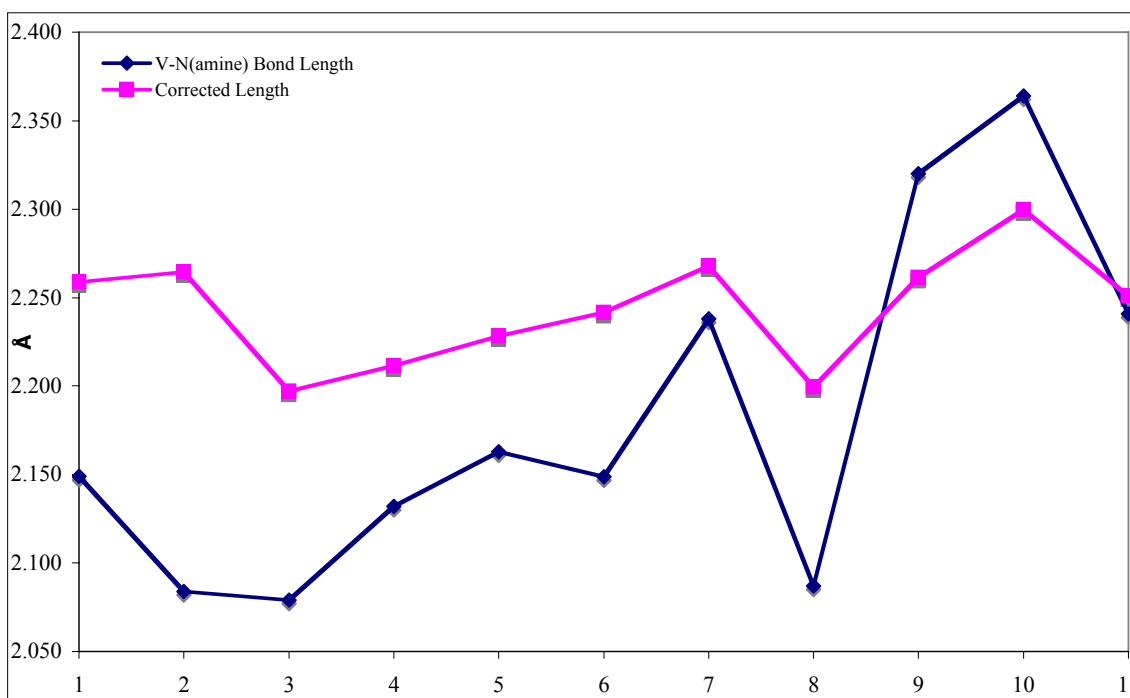


Figure 1.13: Comparison of V-N(amine) bond lengths before and after plane displacement correction.

1.4 Evaluation of Catalytic Activity

Three complexes along a potential dinitrogen reduction cycle have been independently synthesized, namely ($\{[\text{HIPTN}_3\text{N}]\text{VN}_2\}^-$, $[\text{HIPTN}_3\text{N}]\text{V}=\text{NH}$, and $[\text{HIPTN}_3\text{N}]\text{V}(\text{NH}_3)$). The conversion of $[\text{HIPTN}_3\text{N}]\text{V}(\text{NH}_3)$ to $[\text{HIPTN}_3\text{N}]\text{V}=\text{NH}$ (Section 1.2.4) was observed, which by microscopic reversibility implies that conversion of $[\text{HIPTN}_3\text{N}]\text{V}=\text{NH}$ to $[\text{HIPTN}_3\text{N}]\text{V}(\text{NH}_3)$ is possible. Therefore, catalytic activity of various $[\text{HIPTN}_3\text{N}]\text{V}$ complexes was evaluated by the use of $(\text{Cp}^*)_2\text{Cr}$ as the reducing agent and 2,6-lutidinium BAR_4' as the acid source. Catalytic experiments were performed using $[\text{HIPTN}_3\text{N}]\text{V}(\text{THF})$,²⁵ $\{[\text{HIPTN}_3\text{N}]\text{VN}_2\}^-$,²⁶ and $[\text{HIPTN}_3\text{N}]\text{V}=\text{NH}$ ²⁶ in the manner described for the $[\text{HIPTN}_3\text{N}]\text{Mo}$ complexes²⁷ and variations thereof.²⁸ Although catalytic activity was not expected on the basis of decomposition observed upon addition of potassium graphite to $[\text{HIPTN}_3\text{N}]\text{V}(\text{NH}_3)$ (Section 1.2.3), we were still interested in whether any ammonia could be generated from these systems. No ammonia was generated by $[\text{HIPTN}_3\text{N}]\text{V}(\text{THF})$, while $\{[\text{HIPTN}_3\text{N}]\text{VN}_2\}^-$ and $[\text{HIPTN}_3\text{N}]\text{V}=\text{NH}$ yielded 0.2 and 0.78 equivalents respectively; none of which was from gaseous ammonia. These yields

imply that no ammonia is being generated from atmospheric dinitrogen. The lack of ammonia from $[\text{HIPTN}_3\text{N}]\text{V}(\text{THF})$ is not surprising given that $(\text{Cp}^*)_2\text{Cr}$ is not a strong enough reducing agent to form $\{[\text{HIPTN}_3\text{N}]\text{VN}_2\}^-$. The low amount of ammonia produced by $\{[\text{HIPTN}_3\text{N}]\text{VN}_2\}^-$ is probably due, at least in part, to the highly sensitive nature of this complex, with a decomposition pathway that may be thought of as analogous to the generation of $[\text{HIPTN}_3\text{N}]\text{VH}$ when trying to synthesize $\{[\text{HIPTN}_3\text{N}]\text{VN}_2\}^-$ directly from V(II) and the decomposition of $[\text{HIPTN}_3\text{N}]\text{Mo-N}=\text{NH}$ to $[\text{HIPTN}_3\text{N}]\text{MoH}$. The most surprising result was the less than one equivalent of ammonia from $[\text{HIPTN}_3\text{N}]\text{V}=\text{NH}$ given the facile conversion of $[\text{HIPTN}_3\text{N}]\text{V}(\text{NH}_3)$ to $[\text{HIPTN}_3\text{N}]\text{V}=\text{NH}$. This result may be ascribable to $[\text{HIPTN}_3\text{N}]\text{V}(\text{NH}_3)$ decomposition upon reduction with potassium graphite.

1.5 Comparison of ^{51}V NMR shifts

	$[\text{Me}_3\text{SiN}_3\text{N}]^9$	$[\text{HIPTN}_3\text{N}]$
V=S	621 ppm	756 ppm
V=NH	252 ppm	-334 ppm
V=N(SiMe ₃)	~ -80 ppm	-276 ppm
V=O	-173 ppm	-115 ppm

Table 1.4: ^{51}V NMR shifts (C_6D_6) of analogous $[\text{Me}_3\text{SiN}_3\text{N}]\text{V}$ and $[\text{HIPTN}_3\text{N}]\text{V}$ complexes.

1.6 Conclusions

Using the $[\text{HIPTN}_3\text{N}]^{3-}$ ligand, a variety of vanadium containing complexes were synthesized: $[\text{HIPTN}_3\text{N}]\text{V}(\text{THF})$, $[\text{HIPTN}_3\text{N}]\text{V}=\text{N}(\text{SiMe}_3)$, $[\text{HIPTN}_3\text{N}]\text{V}=\text{S}$, $[\text{HIPTN}_3\text{N}]=\text{O}$, and $[\text{HIPTN}_3\text{N}]\text{V}(\text{CO})$. Three complexes ($\{[\text{HIPTN}_3\text{N}]\text{VN}_2\}^-$, $[\text{HIPTN}_3\text{N}]\text{V}=\text{NH}$, and $[\text{HIPTN}_3\text{N}]\text{V}(\text{NH}_3)$) are relevant to dinitrogen reduction. While the chemistry of vanadium complexes containing this ligand is largely tractable and well-behaved, neither catalytic nor stoichiometric reduction of dinitrogen to ammonia was observed. We propose that there are four problems with the $[\text{HIPTN}_3\text{N}]\text{V}$ system. (1) the large reduction potential needed to form $\{[\text{HIPTN}_3\text{N}]\text{VN}_2\}^-$; (2) the sensitivity of $\{[\text{HIPTN}_3\text{N}]\text{VN}_2\}^-$ to oxidation/decomposition; (3) the difficulty in forming " $[\text{HIPTN}_3\text{N}]\text{VN}$ "; (4) and decomposition of $[\text{HIPTN}_3\text{N}]\text{V}(\text{NH}_3)$ on reduction. We see the solution to these problems being the use of a dianionic diamidoamine donor type ligand which would yield a system more electronically similar to $[\text{HIPTN}_3\text{N}]\text{Mo}$.

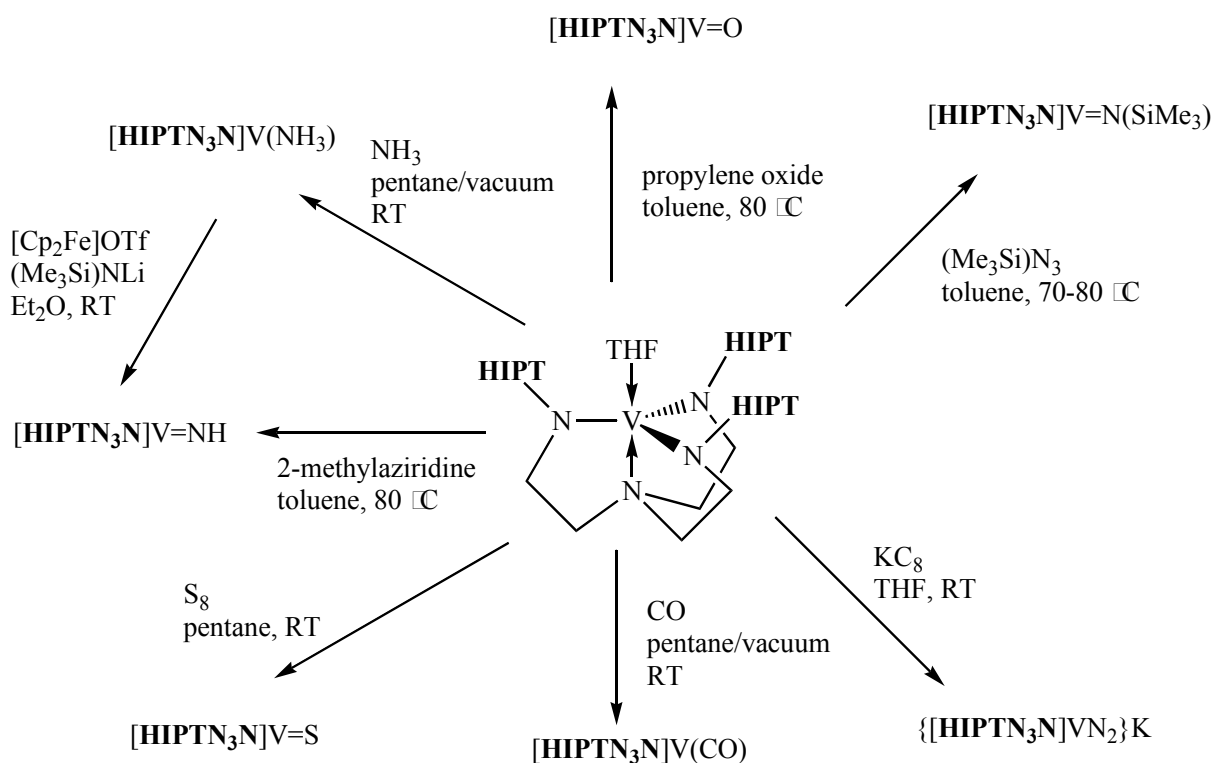


Figure 1.14: Reaction summary of $[\text{HIPTN}_3\text{N}]\text{V}$ complexes.

1.7 Experimental Details

General. All experiments involving air and/or moisture sensitive complexes or reactions were performed under nitrogen in a Vacuum Atmospheres drybox or using standard Schlenk techniques with glassware stored in an oven at $\sim 190\text{ }^\circ\text{C}$ for at least 12 hours prior to use. Pentane was washed with $\text{HNO}_3/\text{H}_2\text{SO}_4$ (5:95 by volume), sodium bicarbonate, and water, dried over CaCl_2 , and then sparged with nitrogen and passed through an alumina column followed by storage over $\text{Na}/\text{benzophenone}$ and vacuum transfer prior to use. Dry and deoxygenated benzene was purchased from Aldrich and passed through Q5 and alumina columns. Heptane, benzene- d_6 and toluene- d_8 were dried over $\text{Na}/\text{benzophenone}$ then degassed (freeze-pump-thaw) and vacuum transferred prior to use. THF, diethyl ether and toluene were pre-dried by passage through an alumina column followed by storage over $\text{Na}/\text{benzophenone}$. They were degassed (freeze-pump-thaw) and vacuum transferred prior to use. All solvents were stored over 4 \AA molecular sieves in a drybox after transfer.

VCl₃ (Strem), CO (Aldrich, passed through dry ice/acetone), ¹³CO (Matheson, passed through dry ice/acetone), NH₃ (BOC, condensed onto Na sand), ¹⁵NH₃ (Cambridge Isotope labs, condensed onto Na sand), ¹⁵N₂ (Cambridge Isotope Labs), (TMS)₂NLi (Aldrich, sublimed), 2-methylaziridine (Aldrich, vacuum transferred and stored at *ca.* -40 °C), (TMS)N₃ (Acros Organics), propylene oxide (Aldrich), 18-Crown-6 (Aldrich, dried *in vacuo*), 15-Crown-5 (Acros Organics, degassed and stored over 4Å molecular sieves) were purchased as used as received or purified as indicated.

H₃[HIPTN₃N],^{18,29,30} VCl₃(THF)₃,^{31,32} VCl₂(TMEDA)₂,^{33,34,35} [FeCp₂]OTf,³⁶ and (*n*-Bu₄N)N₃³⁷ were synthesized *via* literature procedures. Potassium graphite was synthesized by stirring a 1:8 mixture of potassium:graphite under partial vacuum for 2 hours using a glass stirbar at *ca.* 200 °C.

¹H NMR spectra were obtained on a Varian Mercury (300 MHz) or Inova (500 MHz) spectrometer and were referenced to the residual protio-solvent peak. ⁵¹V NMR spectra were obtained on a Varian Inova (131.5 MHz) spectrometer outfitted with an broadband probe and externally referenced to a commercial sample of VOCl₃ ($\delta(^{51}\text{V}) = 0$ ppm). Infrared spectra were obtained on a Nicolet Avatar 360 FT-IR spectrometer using a demountable liquid cell (0.2 mm Teflon or lead spacer with KBr plates). UV/Vis spectra were obtained on a Hewlett-Packard 8452A Diode Array Spectrophotometer equipped with a Hewlett Packard 89090A Peltier temperature control accessory with the solvent contribution manually subtracted using a standard background. Magnetic measurements (Evans method^{38,39}) employed the shift of the toluene methyl group. The sample was dissolved in a 4:1 (by volume) mixture of C₆D₆:toluene and a concentric sealed capillary filled with toluene was added. Elemental Analyses were performed by H. Kolbe Microanalytics Laboratory, Mülheim an der Ruhr, Germany.

Structural data for [HIPTN₃N]V(THF) was collected at 100 K using graphite-monochromated Mo K α radiation ($\lambda = 0.71073$ Å) and a Bruker-AXS Smart Apex CCD detector. All other structural data was collected at -80 °C using a CCD area detector. The structures were solved using SHELXS⁴⁰ and refined against F² on all data by full-matrix least squares with SHELXL-97.⁴¹ All non-hydrogen atoms were refined anisotropically, while hydrogen atoms were placed at calculated positions and refined using a riding model. ORTEP diagrams were generated using ORTEP-3.⁴² The structure solutions for [HIPTN₃N]V(THF)

(05099), [HIPTN₃N]V(NH₃) (03316) and [HIPTN₃N]VH (04123) can be found on <http://www.reciprocalnet.org> using the number in parentheses.

Refinement of the [HIPTN₃N]V(NH₃) structure did not converge well, and required damping. As a result, the calculated uncertainties are underrated. The ammonia hydrogens could be found in a Fourier difference map and refined semi-freely with distance restraints.

The hydride hydrogen in [HIPTN₃N]VH could be found in the difference Fourier map.

[HIPTN₃N]V(THF) (1). VCl₃(THF)₃ (1.17 g, 3.14 mmol) and H₃[HIPTN₃N] (5.00 g, 3.15 mmol) were added to a 100 mL flask equipped with a 0-8 Teflon valve *via* a solid addition funnel followed by THF (*ca.* 50 mL). The flask was sealed and the resulting purple adduct was allowed to stir for 1 hour. (TMS)₂NLi (1.53 g, 9.16 mmol) was then added, resulting in a dark green solution within minutes. After further stirring for an hour, the THF was removed *in vacuo* to minimum pressure (*ca.* 5-10 mTorr) at room temperature. The resulting solid was taken up in pentane and filtered through celite to remove LiCl. The filtrate was concentrated and the product obtained as a lime green solid through crystallization at *ca.* -35 °C. This solid was again dried at room temperature *in vacuo* to minimum pressure to yield lime green solid (4.6 g, 86 %). Substituting (Me₃Si)₂NK for (Me₃Si)₂NLi gave the same product (2.4 g, 45 %). UV/Vis λ_{max} (nm), ϵ (M⁻¹•cm⁻¹): heptane (260 (sh), 6.6 x 10⁴; 306, 1.9 x 10⁴; 350 (sh), 1.1 x 10⁴; 404 (sh), 5.8 x 10³); μ_{eff} = 2.51, 2.54, 2.55 BM, ; Anal. Calcd. for C₁₁₈H₁₆₇N₄VO: C, 79.95; H, 7.85; N, 2.28; Cl, 0.00. Found: C, 80.11; H, 7.92; N, 2.25; Cl, 0.00.

{[HIPTN₃N]VN₂}K (2). [HIPTN₃N]V(THF) (300 mg, 0.176 mmol) and KC₈ (37.5 mg, 0.277 mmol) were added to a 20 mL scintillation vial along with a glass-coated stir-bar and 5 - 10 mL of solvent (typically THF, but also DME, diethyl ether, benzene, or toluene). Using ethereal solvents, the solution turns red within minutes (overnight in the case of toluene or benzene) and was filtered through glass wool in a pipet to remove the graphite and excess KC₈. The solvent was removed *in vacuo* to afford red solid that was used without further purification. IR(THF) cm⁻¹ 1883 (ν_{NN}).

{[HIPTN₃N]VN₂}18-crown-6(K) (3). [HIPTN₃N]V(THF) (300 mg, 0.176 mmol), KC₈ (38.1 mg, 0.282 mmol), and 18-crown-6 (49.8 mg, 0.188 mmol) were added to a 20 mL scintillation vial followed by a glass stirbar and DME (*ca.* 4 mL). The solution turned red immediately and was allowed to stir for 30 minutes. Graphite was removed by filtration through glass wool in a pipet followed by removal of the solvent *in vacuo*. The sample was triturated with pentane and collected on a glass frit to yield **3** quantitatively. IR(C₆D₆) cm⁻¹ 1882 (ν_{NN}); IR(THF) cm⁻¹ 1884 (ν_{NN}); Anal. Calcd. for C₁₂₆H₁₈₃N₆VO₆K: C, 76.90; H, 9.37; N, 4.27. Found: C, 77.08; H, 9.28; N, 4.22.

{[HIPTN₃N]V¹⁵N₂}K (4). [HIPTN₃N]V(THF) (52.0 mg, 30 μmol) and KC₈ (9.4 mg, 70 μmol) were added to a J. Young tube. THF (*ca.* 1.6 - 2 mL) was then added to a second J. Young tube. Both J. Young tubes were connected to a transfer bridge. The solid containing tube was evacuated, and the solvent containing tube was degassed using 5 freeze-pump-thaw cycles. The THF was then vacuum transferred onto the solid, but kept frozen in liquid nitrogen. This tube was attached to a gas transfer bridge and filled with *ca.* 13 equivalents of ¹⁵N₂. The tube was subsequently placed in a dry ice/acetone bath to react with occasional shaking. Once the sample was fully thawed it was allowed to warm to room temperature followed by filtration through glass wool in a pipet. The resultant red solution was used directly for IR measurements. IR(THF) cm⁻¹ 1821 (ν_{NN}).

[HIPTN₃N]V(NH₃) (5). [HIPTN₃N]V(THF) (1.00 g, 0.59 mmol) in a 100 mL solvent bomb type flask equipped with a Teflon valve was dissolved in pentane and exposed to *ca.* 1 atm. of NH₃. The color immediately changed to a lighter shade of green and removal of the volatiles *in vacuo* yields a green solid quantitatively. Crystallization from a supersaturated pentane solution at *ca.* -35 °C yielded green flakes (661 mg, 68 %). UV/Vis λ_{max} (nm), ε (M⁻¹•cm⁻¹): heptane (214, 1.43 x 10⁵; 280, 1.55 x 10⁴; 316, 1.91 x 10⁴; 352, 1.70 x 10⁴); IR(C₆D₆) cm⁻¹ 3358 (ν_{NH}); μ_{eff} = 2.24, 2.22, 2.23 BM; Anal. Calcd. for C₁₁₄H₁₆₂N₅V: C, 82.81; H, 9.88; N, 4.24. Found: C, 82.69; H, 9.76; N, 4.21.

[HIPTN₃N]V(¹⁵NH₃) (6). [HIPTN₃N]V(THF) (500 mg, 0.29 mmol) in a 50 mL solvent bomb type flask equipped with a Teflon valve was dissolved in pentane and exposed to *ca.* 1 atm of ¹⁵NH₃. The color immediately changed to bright green, and the volatiles were removed *in vacuo*. Crystallization from a supersaturated hexamethyldisiloxane solution at *ca.* -35 °C yielded green flakes (402 mg, 83 %). IR(C₆D₆) cm⁻¹ 3349 (ν_{NH}).

[HIPTN₃N]VN_H (7). [HIPTN₃N]V(THF) (500 mg, 0.29 mmol) was dissolved in *ca.* 20 mL of toluene in a 50 mL solvent bomb type flask equipped with a Teflon valve. To this, 2-methylaziridine (41.4 μL, 0.59 mmol) was added and the reaction was left to stir at room temperature for *ca.* 12 hours. The resulting red solution was then heated at 80 °C over 12 hours. The volatiles were removed *in vacuo*, and the resulting solid was crystallized from a supersaturated pentane solution at *ca.* -35 °C to give large dark red blocks (427 mg, 88 %). ¹H NMR (C₆D₆) δ 7.54 (br s, 6H), 7.19 (s, 12H), 6.45 (s, 3H), 3.72 (br t, 6H), 3.09 (sept, J_{HH} = 6.8 Hz, 12H), 2.92 (sept, J_{HH} = 6.8 Hz, 6H), 2.15 (br t, 6H), 1.36 (d, J_{HH} = 6.9 Hz, 36H), 1.22 (d, J_{HH} = 6.8 Hz, 36H), 1.07 (d, J_{HH} = 6.6 Hz, 36H); ⁵¹V NMR (C₆D₆) -334 (br s); UV/Vis λ_{max} (nm), ε (M⁻¹•cm⁻¹): heptane (266, 3.2 x 10⁴; 376, 1.98 x 10⁴; 466, 2.18 x 10⁴); IR(C₆D₆) cm⁻¹ 3360 (ν_{NH}); Anal. Calcd. for C₁₁₄H₁₆₀N₅V: C, 82.91; H, 9.77; N, 4.24. Found: C, 82.74; H, 9.85; N, 4.18.

[HIPTN₃N]V¹⁵N_H (8). [HIPTN₃N]V(¹⁵NH₃) (50 mg, 30 μmol) and (TMS)₂NLi (10 mg, 60 μmol) were dissolved in diethyl ether in a 20 mL scintillation vial. With stirring, [FeCp₂]OTf (20 mg, 60 μmol) was added to immediately give a red solution. The volatiles were removed *in vacuo*. After addition of pentane to the resulting residue and filtration through celite, the sample was dried *in vacuo*. at *ca.* 70 °C and used directly. IR(C₆D₆) cm⁻¹ 3351 (ν_{NH}).

[HIPTN₃N]V=N(SiMe₃) (9). [HIPTN₃N]V(THF) (300 mg, 0.18 mmol) was added to a 50 mL solvent bomb type flask with a Teflon valve and dissolved in *ca.* 10 mL of toluene. (TMS)₃N₃ (47 μL, 0.35 mmol) was added followed by another 1-2 mL of toluene to wash the valve stem of the flask. The reaction was stirred at 70-80 °C over 12 hours to give a red solution. The

volatiles were removed *in vacuo* to give an orange powder that could be re-crystallized from pentane to yield product (30 mg, 10 %). ^1H NMR (C_6D_6) δ 7.19 (s, 12H), 7.11 (d, $J_{\text{HH}} = 1.2$ Hz, 6H), 6.78 (br t, 3H), 3.79 (br t, 6H), 3.18 (sept, $J_{\text{HH}} = 6.7$ Hz, 12H), 2.91 (sept, $J_{\text{HH}} = 6.8$ Hz, 6H), 2.39 (br t, 6H), 1.36 (d, $J_{\text{HH}} = 6.6$ Hz, 36H), 1.20 (d, $J_{\text{HH}} = 6.9$ Hz, 72H), -0.12 (s, 9H); ^{51}V NMR (C_6D_6) δ -276 (br s); UV/Vis λ_{max} (nm), ϵ ($\text{M}^{-1}\cdot\text{cm}^{-1}$): heptane (262 (sh), $3. \times 10^4$; 304, 1.3×10^4 ; 368, 1.0×10^4 ; 456, 1.2×10^4); Anal. Calcd. for $\text{C}_{117}\text{H}_{168}\text{N}_5\text{SiV}$: C, 81.52; H, 9.83; N, 4.06. Found: C, 81.61; H, 9.88; N, 4.05.

[HIPTN₃N]V=S (10). [HIPTN₃N]V(THF) (1.00 g, 0.59 mmol) was added to a 100 mL solvent bomb type flask and dissolved in pentane. While stirring, S₈ (19 mg, 74 μmol) was added. Within minutes the solution turned dark green. Although stirring was continued for 12 hours, no further changes were observed. The reaction mixture was filtered through celite and concentrated *in vacuo*. Crystallization at from the solution at -35 °C yielded product as a microcrystalline green solid (751 mg, 77 %). ^1H NMR (C_6D_6) δ 7.42 (br s, 6H), 7.21 (s, 12H), 6.48 (t, $J_{\text{HH}} = 1.3$ Hz, 3H), 3.73 (br t, 6H), 3.10 (sept, $J_{\text{HH}} = 6.8$ Hz, 12H), 2.92 (sept, $J_{\text{HH}} = 6.9$ Hz, 6H), 1.70 (t, $J_{\text{HH}} = 5.0$ Hz, 6H), 1.35 (d, $J_{\text{HH}} = 6.9$ Hz, 36H), 1.24 (d, $J_{\text{HH}} = 6.9$ Hz, 36H), 1.11 (br d, $J_{\text{HH}} = 6.3$ Hz, 36H); ^{51}V NMR (C_6D_6) δ 755.93 (s); UV/Vis λ_{max} (nm), ϵ ($\text{M}^{-1}\cdot\text{cm}^{-1}$): heptane (260, 4.0×10^4 ; 296, 1.2×10^4 ; 354, 1.2×10^4 ; 414, 1.5×10^4 ; 606, 8.0×10^4); Anal. Calcd. for $\text{C}_{114}\text{H}_{159}\text{N}_4\text{SV}$: C, 82.06; H, 9.61; N, 3.36; S, 1.92. Found: C, 82.15; H, 9.48; N, 3.31; S, 1.97.

[HIPTN₃N]V=O (11). [HIPTN₃N]V(THF) (300 mg, 0.18 mmol) was added to a 25 mL solvent bomb type flask with a Teflon valve, to which was added *ca.* 15 mL of toluene. While the solution was stirring, propylene oxide (25 μL , 0.34 mmol) was added which resulted in an immediate color change to black-violet. The reaction mixture was heated at *ca.* 80 °C for 16 hours and then dried to minimum pressure on a vacuum line. The solid residue was dissolved in pentane and filtered through celite. Crystallization from a supersaturated pentane solution at *ca.* -40 °C yielded [HIPTN₃N]V=O as a purple powder (198 mg, 68%). ^1H NMR (C_6D_6) δ 7.78 (br s, 6H), 7.20 (s, 12H), 6.51 (s, 3H), 3.69 (br s, 6H), 3.08 (sept, $J_{\text{HH}} = 6.7$ Hz, 12H), 2.93 (sept, $J_{\text{HH}} = 6.9$ Hz, 6H), 1.98 (br s, 6H), 1.36 (d, $J_{\text{HH}} = 6.9$ Hz, 36H), 1.21 (d, $J_{\text{HH}} = 6.8$ Hz, 36H), 1.07 (br

s, 36H); ^{51}V NMR (C_6D_6) δ -115 (s); UV/Vis λ_{max} (nm), ϵ ($\text{M}^{-1}\cdot\text{cm}^{-1}$): heptane (264 (sh), 2.4×10^4 ; 288 (sh), 1.7×10^4 ; 412, 1.6×10^4 ; 542, 1.5×10^4); Anal Calcd. for $\text{C}_{114}\text{H}_{159}\text{N}_4\text{OV}$: C, 82.85; H, 9.70; N, 3.39. Found: C, 82.75; H, 9.63; N, 3.35.

[HIPTN₃N]V(CO) (12). A sample of [HIPTN₃N]V(THF) (50 mg, 29 μmol) was added to a 25 mL solvent bomb type flask with a Teflon valve and was dissolved in *ca.* 6-7 mL of pentane. The resulting green solution was degassed once (freeze-pump-thaw) and exposed to 1 atm. of CO. In *ca.* 5 minutes the solution turned red-gold and was allowed to stir for another 30 minutes. The volatiles were then removed *in vacuo* and the resulting residue was taken up in *ca.* 1 mL of heptane and used for IR analysis directly. IR(heptane) cm^{-1} 2076 (ν_{CO}).

[HIPTN₃N]V(^{13}CO) (13). A sample of [HIPTN₃N]V(THF) (50 mg, 29 μmol) was added to a 25 mL solvent bomb type flask with a Teflon valve and was dissolved in *ca.* 6-7 mL of pentane. The resulting green solution was degassed once (freeze-pump-thaw) and exposed to 1 atm. of CO. In *ca.* 5 minutes the solution turned red-gold and was allowed to stir for another 30 minutes. The volatiles were then removed *in vacuo* and the resulting residue was taken up in *ca.* 1 mL of heptane and used for IR analysis directly. IR(heptane) cm^{-1} 2030 (ν_{CO} , ^{13}CO), 1980 (ν_{CO} , $^{13}\text{C}^{18}\text{O}$).

1.8 References

-
- ¹ Einsle, O.; Tezcan, F. A.; Andrade, S. L. A.; Schmid, B.; Yoshida, M.; Howard, J. B.; Rees, D. *C. Science* **2002**, 297, 1696.
 - ² Eady, R. R., *Chem. Rev.* **1996**, 96, 3013.
 - ³ Eady, R. R., *Coord. Chem. Rev.* **2003**, 237, 23.
 - ⁴ MacKay, B. A.; Fryzuk, M. D. *Chem. Rev.* **2004**, 104, 385.
 - ⁵ Plass, W.; Verkade, J. G. *J. Am. Chem. Soc.* **1992**, 114, 2275.
 - ⁶ Nomura, K.; Schrock, R. R.; Davis, W. M. *Inorg. Chem.* **1996**, 35, 3695.
 - ⁷ Rosenberger, C.; Schrock, R. R.; Davis, W. M. *Inorg. Chem.* **1997**, 36, 123.
 - ⁸ Cummins, C. C.; Schrock, R. R.; Davis, W. M. *Organometallics* **1992**, 11, 1452.
 - ⁹ Cummins, C. C.; Schrock, R. R.; Davis, W. M. *Inorg. Chem.* **1994**, 33, 1448.
 - ¹⁰ Cummins, C. C.; Lee, J.; Schrock, R. R. *Angew. Chem., Int. Ed. Engl.* **1992**, 31, 1501.
 - ¹¹ Ferguson, R.; Solari, E.; Floriani, C.; Chiesi-Villa, A.; Rizzoli, C. *Angewandte Chemie* **1993**, 105, 453.

-
- ¹² Buijink, J. K. F.; Meetsma, A.; Teuben, J. H. *Organometallics* **1993**, *12*, 2004.
- ¹³ Song, J.-I.; Berno, P.; Gambarotta, S. *J. Am. Chem. Soc.* **1994**, *116*, 6927.
- ¹⁴ Desmangles, N.; Jenkins, H.; Rupp, K. B.; Gambarotta, S. *Inorg. Chim. Acta* **1996**, *250*, 1.
- ¹⁵ Ferguson, R.; Solari, E.; Floriani, C.; Osella, D.; Ravera, M.; Re, N.; Chiesi-Villa, A.; Rizzoli, C. *J. Am. Chem. Soc.* **1997**, *119*, 10104.
- ¹⁶ Brask, J. K.; Dura-Vila, V.; Diaconescu, P. L.; Cummins, C. C. *Chem. Commun.* **2002**, 902.
- ¹⁷ Yandulov, D. V.; Schrock, R. R. *J. Am. Chem. Soc.* **2002**, *124*, 6252.
- ¹⁸ Yandulov, D. V.; Schrock, R. R.; Rheingold, A. L.; Ceccarelli, C.; Davis, W. M., *Inorg. Chem.* **2003**, *42*, 796.
- ¹⁹ Song, J.-I.; Berno, P.; Gambarotta, S. *J. Am. Chem. Soc.* **1994**, *116*, 6927.
- ²⁰ Gailus, H.; Woitha, C.; Rehder, D. *Journal of the Chemical Society, Dalton Transactions: Inorganic Chemistry* **1994**, 3471.
- ²¹ Rehder, D.; Woitha, C.; Priebisch, W.; Gailus, H. *J. Chem. Soc., Chem. Commun.* **1992**, 364.
- ²² Hayton, T. W.; Daff, P. J.; Legzdins, P.; Rettig, S. J.; Patrick, B. O. *Inorg. Chem.* **2002**, *41*, 4114.
- ²³ Whitesides, G. M.; Mitchell, H. L. *J. Am. Chem. Soc.* **1969**, *91*, 2245.
- ²⁴ Hill, P. L.; Yap, G. P. A.; Rheingold, A. L.; Maata, E. A. *J. Chem. Soc., Chem. Commun.* **1995**, 737.
- ²⁵ Performed by Dmitry Yandulov.
- ²⁶ Performed by Walter Weare.
- ²⁷ Yandulov, D.; Schrock, R. R. *Science* **2003**, *301*, 76.
- ²⁸ Ritleng, V.; Yandulov, D. V.; Weare, W. W.; Schrock, R. R.; Hock, A. S.; Davis, W. M. *J. Am. Chem. Soc.* **2004**, *126*, 6150.
- ²⁹ Yandulov, D. V.; Schrock, R. R., *J. Am. Chem. Soc.* **2002**, *124*, 6252.
- ³⁰ Yandulov, D. V.; Schrock, R. R., *Science* **2003**, *301*, 76.
- ³¹ Manzer *Inorg. Syn.* **1982**, *21*, 135.
- ³² Hawker, P. N.; Timms, P. L. *J. Chem. Soc., Dalton Trans.* **1983**, 1123.
- ³³ Bouma, R. J.; Teuben, J. H.; Beukema, W. R.; Bansemer, R. L.; Huffman, J. C.; Caulton, K. G. *Inorg. Chem.* **1984**, *23*, 2715.
- ³⁴ Smith, P. D.; Martin, J. L.; Huffman, J. C.; Bansemer, R. L.; Caulton, K. G. *Inorg. Chem.* **1985**, *24*, 2997.
- ³⁵ Edema, J. J. H.; Stauthamer, W.; Bolhuis, F. v.; Gambarotta, S.; Smeets, W. J. J.; Spek, A. L. *Inorg. Chem.* **1990**, *29*, 1302.
- ³⁶ Schrock, R. R.; Sturgeooff, L. G.; Sharp, P. R. *Inorg. Chem.* **1983**, *22*, 2801.
- ³⁷ Moss, R. A.; Terpinski, J.; Cox, D. P.; Denney, D. Z.; Krogh-Jespersen, K. *J. Am. Chem. Soc.* **1985**, *107*, 2743.
- ³⁸ Evans, D. F., *J. Chem. Soc.* **1959**, 2003.
- ³⁹ Sur, S. K., *J. Mag. Res.* **1989**, *82*, 169.
- ⁴⁰ Sheldrick, G. M., *Acta Cryst. Sect. A* **1990**, *46*, 467.
- ⁴¹ Sheldrick, G. M. SHELXL 97, Universität Göttingen, Göttingen, Germany, 1997.
- ⁴² Farrugia, L. J., *J. Appl. Cryst.* **1997**, *30*, 565.

Chapter 2

Dianionic Diamidoamine-donor Type Ligands for Vanadium and Evaluation of their Possible Use for the Reduction of Dinitrogen to Ammonia at Vanadium.

2.1 Introduction

In the last chapter it was shown that some vanadium complexes supported by the $[\text{HIPTN}_3\text{N}]^{3-}$ ligand related to a dinitrogen reduction scheme could be synthesized, but that they are not catalytic for the reduction of dinitrogen to ammonia. In the case of $[\text{HIPTN}_3\text{N}]\text{V}=\text{NH}$ and $\{[\text{HIPTN}_3\text{N}]\text{VN}_2\}^-$, however, some ammonia was observed under the catalytic conditions used for the $[\text{HIPTN}_3\text{N}]\text{Mo}$ system. Based on the position of vanadium in the periodic table (Group V) compared to molybdenum (Group VI) it was hypothesized that a dianionic ligand would create an electronically analogous system to the successful molybdenum complexes (Figure 2.2). Ideally, this ligand would remain structurally analogous to $[\text{HIPTN}_3\text{N}]^{3-}$ to preserve steric protection of the metal center (Figure 2.1).

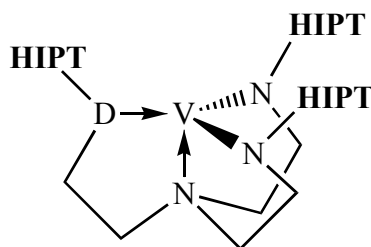


Figure 2.1: Ideal diamidoamine-donor ligand (D = donor atom).

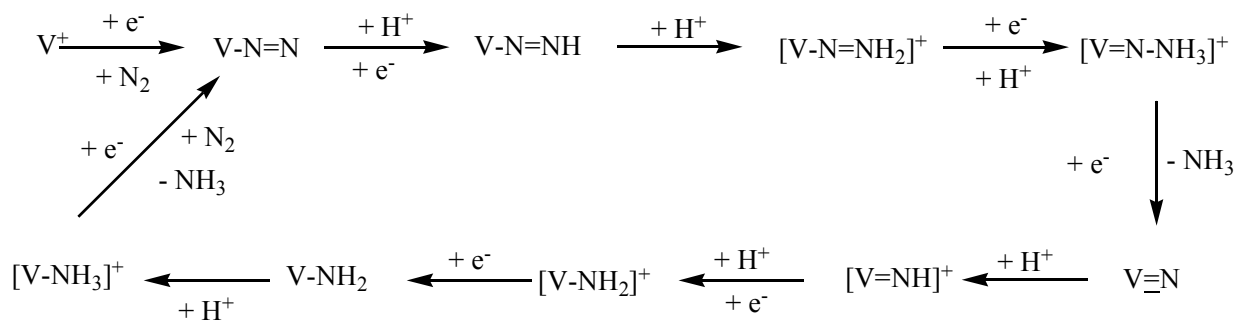


Figure 2.2: Modified dinitrogen reduction scheme for vanadium using a dianionic ligand.

A diamidoamine-donor type ligand using a pyridyl arm as the donor (Figure 2.3) has been reported^{1,2,3} and used to synthesize Group IV and heavier Group V (Nb and Ta) complexes. Although these ligands are not strictly structurally analogous to $[\text{HIPTN}_3\text{N}]^{3-}$, their ideal geometry is similar. Ligands based on a chalcogenide donor were also examined.

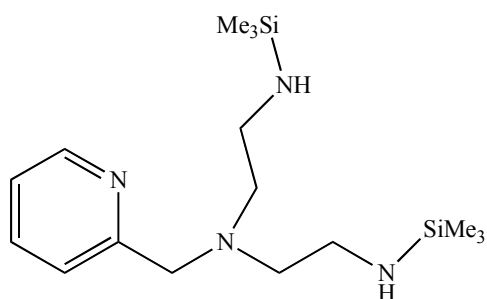
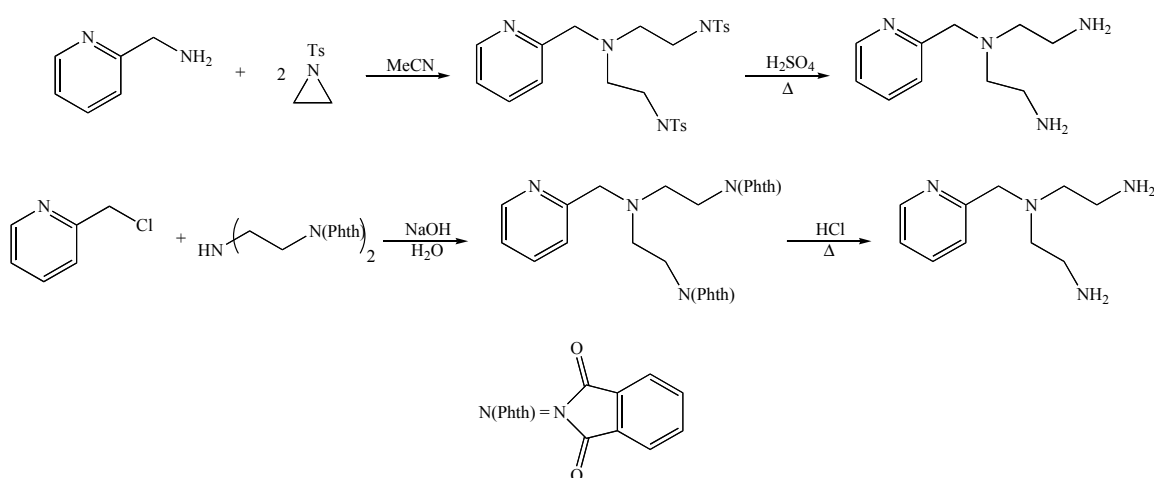


Figure 2.3: Pyridine-based dianionic ligand.^{2,3}

2.2 Ligand Syntheses

2.2.1 Pyridine Based Donor Arm

Two published routes to the pyridine-based ligand scaffold utilize the coupling of diphthaloyldiethylenetriamine with 2-(chloromethyl)pyridine,¹ or the ring-opening of tosyl aziridine by 2-(aminomethyl)pyridine^{2,3} (Scheme 2.1).

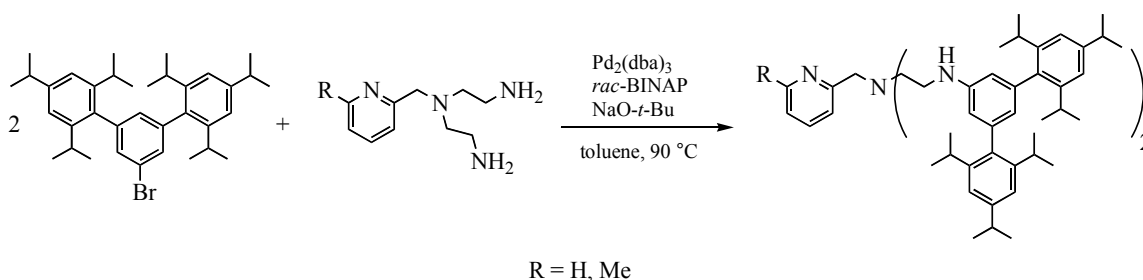


Scheme 2.1: Two published routes to the pyridyl ligand scaffold.

In our hands, attempting to use the tosyl aziridine route led to the formation of what we believe to be polymeric products from the ring-opening of the aziridine and/or formation of pyridinium salts (from which nothing identifiable could be isolated). Therefore we used the 2-(chloromethyl)pyridine route. Protection of diethylenetriamine with phthalic anhydride proceeds exactly as reported,¹ but when done on large scale it is important to add phthalic anhydride in portions to prevent the reaction from becoming too vigorous and to add phthalic anhydride only after the MeOH/diethylenetriamine mixture reaches 60 °C. It is at this temperature that the

reaction appears to begin, and adding the phthalic anhydride before this temperature is reached has the same effect as adding it too quickly. As long as the cautions regarding phthalic anhydride addition are observed, the reaction is quite convenient, and quantities of up to 100 g have been obtained at one time. It should be noted that deprotection in refluxing HCl requires an inert atmosphere (Figure 2.4).

The Buchwald-Hartwig Pd coupling of **HIPTBr** to the pyridyl base using *rac*-BINAP (Equation 2.1, R = H) proceeds smoothly to give the ligand (H_2 [**Pyrl**], Figure 2.4) in moderate yield (66%).



Equation 2.1: Synthesis on H_2 [**Pyrl**] (R = H), and H_2 [**Myrl**] (R = Me).

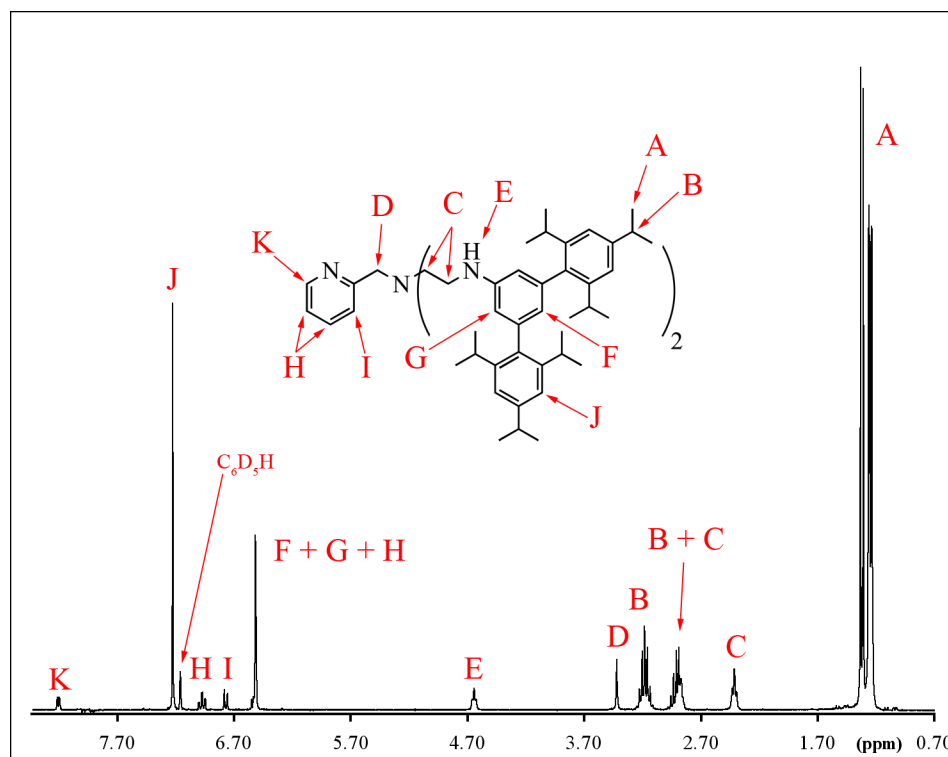


Figure 2.4: 1H NMR spectrum (C_6D_6) of H_2 [**Pyrl**].

Likewise, the derivative where R = Me ($H_2[Myrl]$, Figure 2.5) can be synthesized from the 2-(bromomethyl)-6-methylpyridine. Both $H_2[Pyrl]$ and $H_2[Myrl]$ can be purified *via* chromatography on alumina. When dried, they form a voluminous foam that can be crushed to give each as a powder.

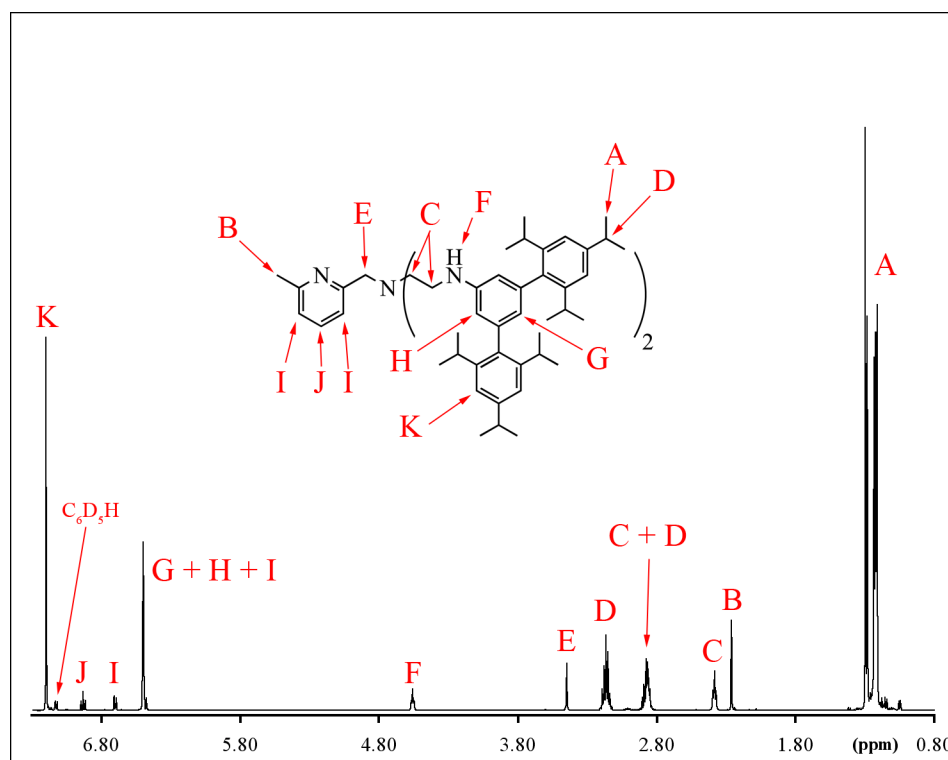
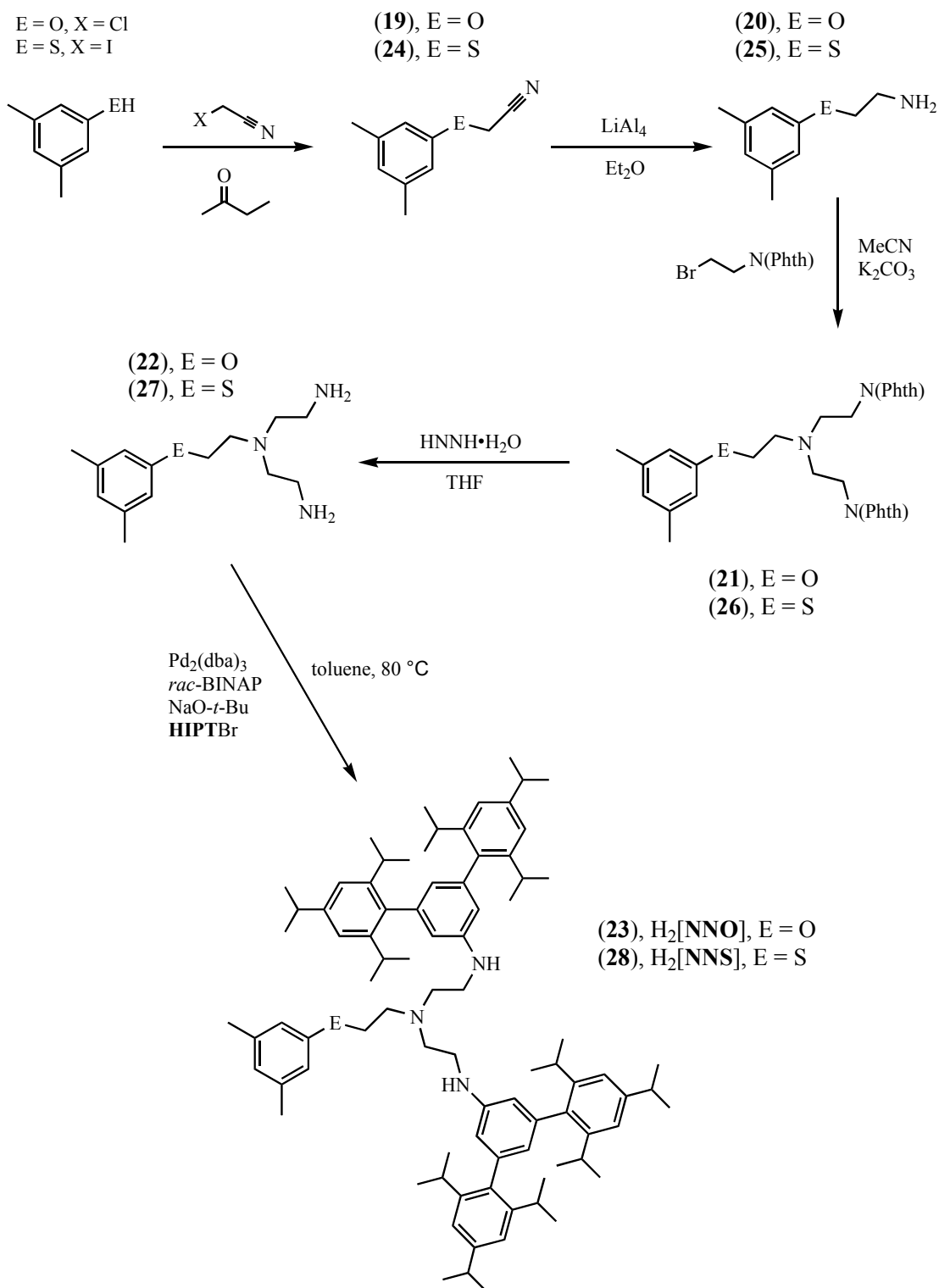


Figure 2.5: 1H NMR spectrum (C_6D_6) of $H_2[Myrl]$.

2.2.2 Chalcogenide Donor Arms

Based on a general method for the reaction of phenols with chloroacetonitrile,⁴ 3,5-dimethylphenol was converted to **19** using chloroacetonitrile in 2-propanone with catalytic KI. Although **19** is a solid, it can be distilled (and must be to cleanly generate **20**) at *ca.* 90-100 °C under vacuum using a bridge without a water jacket so that any material that solidifies in the distillation head during distillation can be melted. Thus, **19** is obtained as a colorless liquid that solidifies upon standing. Reduction of the nitrile moiety in **19** with $LiAlH_4$ in Et_2O gives **20** in moderate yield (50%) as a colorless oil after distillation. Reaction of an acetonitrile solution of **20** with bromoethylphthalimide in the presence of excess K_2CO_3 to yield **21** is the lowest

yielding step (23%) in the synthesis. However, it was the most convenient method found for attaching the remaining two arms. Using two equivalents of chloroacetonitrile gave what is



Scheme 2.2: Reaction scheme for $H_2[NNO]$ and $H_2[NNS]$.

believed to be the *bis*-substitution at the amine of **20**, but the product could not be distilled without decomposition, and acceptable column conditions for its purification were not found. Additionally, attempting to reduce the crude product led to intractable material. Similarly, the reaction of two equivalents of tosyl aziridine with **20** did not yield identifiable material. However, only relatively small amounts of the ligand scaffold are needed given the mass of the **HIPT** substituent, so the bromoethylphthalimide route was sufficient. Finally, deprotection with hydrazine monohydrate in THF yields **22** smoothly without the need for chromatography. Buchwald-Hartwig Pd coupling with **HIPTBr** using *rac*-BINAP, gave H₂[**NNO**] (Figure 2.6) in good yield (76%).

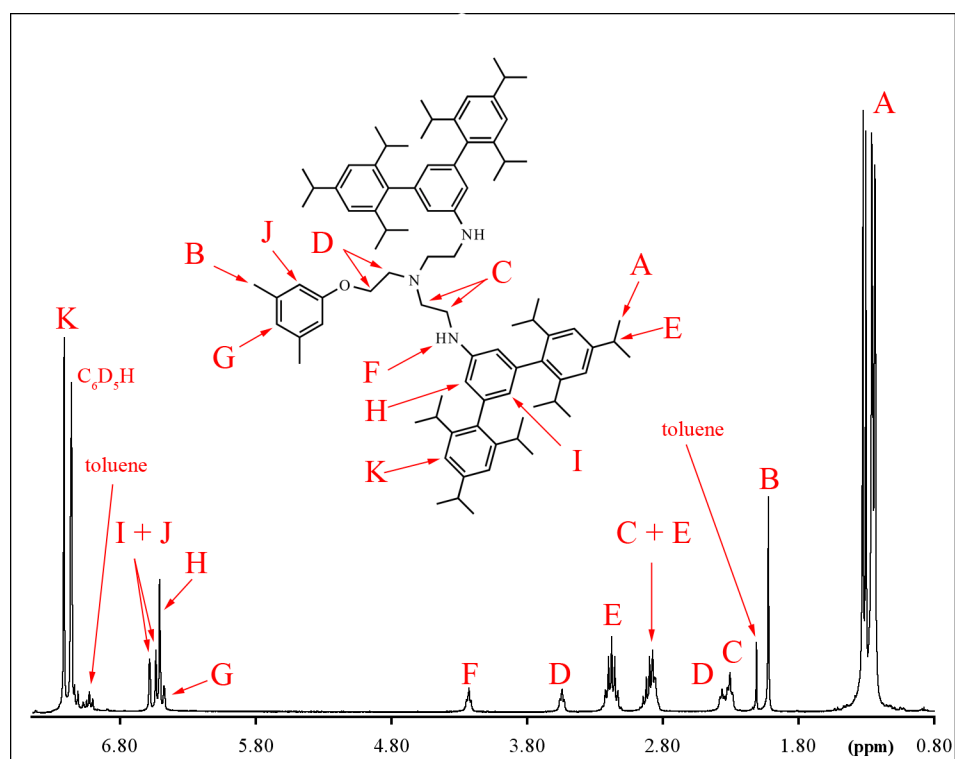


Figure 2.6: ¹H NMR spectrum (C₆D₆) of H₂[**NNO**], residual toluene present.

The synthesis of H₂[**NNS**] (Scheme 2.2) is, for the most part, analogous to that of H₂[**NNO**]. Iodoacetonitrile was used rather than chloroacetonitrile/KI in order to try and more readily generate **24** from the less nucleophilic thiol. **24** was not found to be isolable in pure form, with distillation giving a brown oil which was primarily **24** and 1,2-*bis*(3,5-dimethylphenyl)disulfane in approximately a 3:1 ratio. Significant discoloration occurred during

distillation, indicating decomposition. However, this crude product could be carried through reduction with LiAlH_4 and reaction with bromoethylphthalimide to give **26**, which could be isolated as pure material. **26** behaved completely analogously to the oxo derivative in the subsequent deprotection and Pd coupling steps.

2.3 Other Ligands

Some initial work was also done in pursuit of diamidodiamine and diamidoaminophosphine type ligands (Figure 2.7), but viable routes to these types of ligand scaffolds were not found. Additionally, results with the chalcogenide ($\text{H}_2[\text{NNO}]$ and $\text{H}_2[\text{NNS}]$) and pyridyl ($\text{H}_2[\text{Pyrl}]$) and $\text{H}_2[\text{Myrl}]$) ligands (*vide infra*) indicated a stronger donor is necessary and emphasize the importance of steric protection.

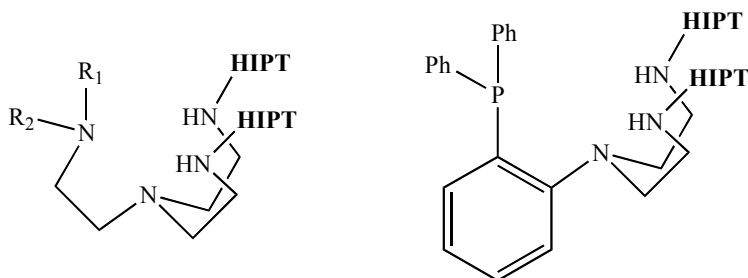
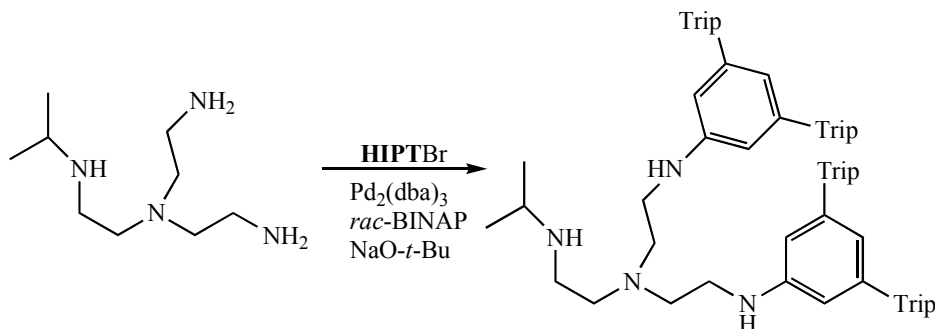


Figure 2.7: Targeted amine and phosphine donor ligands.

2.3.1 Amine Donor

The use of a *mono*-isopropyl substituted **TREN** backbone,⁵ (*i*-Pr**TREN**) allows the synthesis of $\text{H}_2[\text{HIPTN}_2\text{N}]\text{CH}_2\text{CH}_2\text{NH-}i\text{-Pr}$ (**14**, Figure 2.8) *via* Buchwald-Hartwig Pd coupling using 2 equivalents of **HIPTBr** (Equation 2.2).



Equation 2.2: Synthesis of $(\text{HIPTNHCH}_2\text{CH}_2)_2\text{NCH}_2\text{CH}_2\text{NH-}i\text{-Pr}$ (**14**).

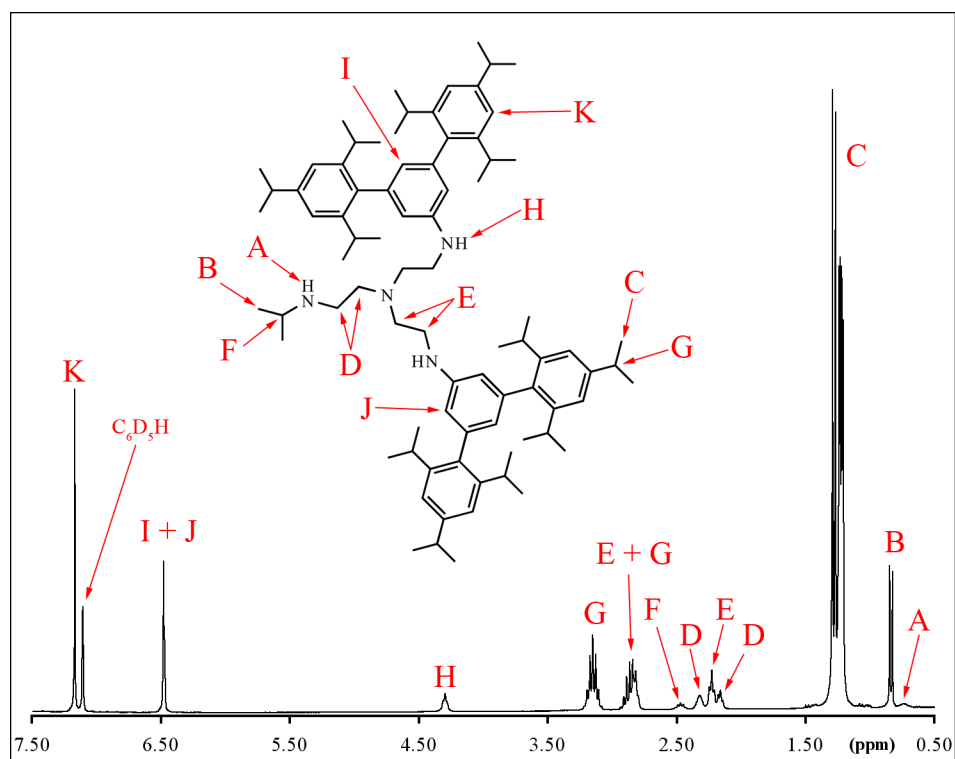


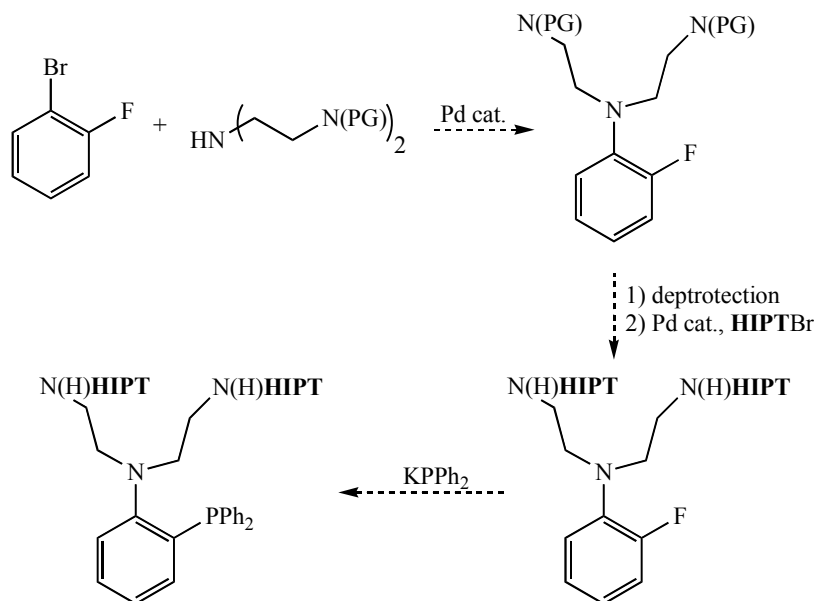
Figure 2.8: ^1H NMR spectrum (C_6D_6) of $\text{H}_2[\text{HIPTN}_2\text{N}]\text{CH}_2\text{CH}_2\text{NH-}i\text{-Pr}$ (**14**).

However, *i*-PrTREN was not found to be a suitable base for the synthesis of a diamidodiamine type ligand. Pd coupling between *i*-PrTREN with three equivalents of HIPTBr did not yield identifiable material, and the Pd coupling between $\text{H}_2[\text{HIPTN}_2\text{N}]\text{CH}_2\text{CH}_2\text{NH-}i\text{-Pr}$ and bromobenzene gave multiple products that could not be separated.

The $(\text{HIPTNHCH}_2\text{CH}_2)_2\text{NCH}_2\text{CH}_2\text{NH}_2$ fragment has proven useful in the synthesis of asymmetric ligands for the study of molybdenum dinitrogen reduction,⁶ but could not be doubly substituted at the primary amine to give a diamidodiamine ligand. Attempting to use 1,5-dibromopentane to create a six-membered heterocycle in a method similar to what has been described^{7,8} resulted in unidentified side reactions, presumably because other intramolecular reactions compete with cyclization. Pd catalyzed coupling with two equivalents of bromobenzene yielded multiple products that could not be separated, which is not surprising given that the Pd catalyzed coupling of bromobenzene to $\text{H}_3[\text{HIPTN}_3\text{N}]$ yielded seven products by TLC.

2.3.2 Phosphine Donor

While the incorporation of a phosphine-based donor is attractive for the incorporation of a ^{31}P spectroscopic handle and the increased donor strength compared to an amine, it complicates ligand synthesis, since phosphine is not expected to be compatible with the Buchwald-Hartwig Pd coupling step required to attach **HIPTBr** to the ligand. One possible route around this was proposed (Scheme 2.3) on the basis of previous work involving addition of KPPh_2 to *N*-(dimethylaminoethyl)-2-fluoroaniline.⁹



Scheme 2.3: Anticipated route to a diamidoaminophosphine ligand.

However, attempting the Pd coupling between 2-fluoro-bromobenzene and diphthaloyldiethylenetriamine resulted in the formation of intractable, insoluble red solid that does not observably react with hydrazine monohydrate. This result was obtained using any combination of Pd ligand (*rac*-BINAP, X-Phos) and solvent (toluene, DME, DMF). On this basis we conclude that the phthalimide group is somehow incompatible with the Pd coupling conditions. Protection of diethylenetriamine with BOC¹⁰ also produced a species incompatible with Pd coupling conditions. Using *rac*-BINAP or X-Phos in toluene, solid begins to appear at *ca.* 70 °C within 1 hour, but ^{19}F NMR of the reaction mixture shows no change in the ^{19}F chemical shift relative to 2-fluorobromobenzene. Continuing heating for 12 hours resulted in a

colorless solution that exhibited no change in ^{19}F NMR shift. That the solution is colorless implies that the Pd catalyst had been deactivated as it is brightly colored.

An initial attempt to use a silyl based protecting group such as 1,2-*bis*(chlorodimethylsilyl)ethane as in the synthesis of 1-(2-chloroethyl)-2,2,5,5-tetramethyl-1,2,5-azadisilolidine,¹¹ resulted in unidentifiable products. It may be possible to use *N*1-(trimethylsilyl)-*N*2-(2-(trimethylsilylamino)ethyl)ethane-1,2-diamine (($\text{Me}_3\text{SiNHCH}_2\text{CH}_2$) $_2\text{NH}$),¹² but this avenue was not explored.

2.4 Vanadium Complexes of $\text{H}_2[\text{NNO}]$ and $\text{H}_2[\text{NNS}]$

2.4.1 $\{[\text{NNO}]\text{VCl}\}_2$

Addition of $\text{VCl}_3(\text{THF})_3$ to a THF solution of $\text{H}_2[\text{NNO}]$ results in a violet adduct that turns red on addition of $(\text{Me}_3\text{Si})_2\text{NLi}$. More so than any of the $[\text{HIPTN}_3\text{N}]\text{V}$ complexes, this complex is extremely soluble, even in Me_4Si . A crystal obtained from a supersaturated $(\text{Me}_3\text{Si})_2\text{O}$ solution showed it to be dimeric with bridging chlorides (Figure 2.9, Table 2.1). The donor arm is not bound to vanadium, but completely unassociated with the core of the complex. Thus, the ligand acts more like a diamidoamine backbone, providing an open face rather than a protected pocket. This is roughly analogous to the diamidoamine ligands used in the synthesis of diamidoamine molybdenum and tungsten complexes.^{13,14,15} The free ethereal arm may account for the solubility of $\{[\text{NNO}]\text{VCl}\}_2$ despite its expected lower solubility based on its dimeric nature.

V(1)-Cl(1)	2.3892(15)	N(201)-V(2)-Cl(2)	127.00(12)
V(1)-Cl(2)	2.4617(14)	N(101)-V(1)-N(102)	81.56(15)
V(2)-Cl(1)	2.4542(14)	N(101)-V(1)-N(103)	81.60(15)
V(2)-Cl(2)	2.3811(15)	N(201)-V(2)-N(202)	81.19(15)
V(1)-N(101)	2.142(4)	N(201)-V(2)-N(203)	87.17(15)
V(1)-N(102)	1.918(4)	N(102)-V(1)-N(103)	116.34(17)
V(1)-N(103)	1.956(4)	N(202)-V(2)-N(203)	117.29(16)
V(2)-N(201)	2.133(4)	V(1)-Cl(1)-V(2)	94.85(5)
V(2)-N(202)	1.926(4)	V(1)-Cl(2)-V(2)	94.86(5)
V(2)-N(203)	1.891(4)	V(1)-N(102)-C(115)-C(120)	2.9
N(101)-V(1)-Cl(1)	88.96(11)	V(1)-N(103)-C(151)-C(152)	14.2
N(101)-V(1)-Cl(2)	171.81(11)	V(2)-N(202)-C(215)-C(216)	165.6
N(201)-V(2)-Cl(1)	107.10(12)	V(2)-V(203)-C(251)-C(252)	149.5

Table 2.1: Selected bond lengths (Å) and angles (°) for $\{[\text{NNO}]\text{VCl}\}_2$. Numbering scheme shown in Figure A.8.

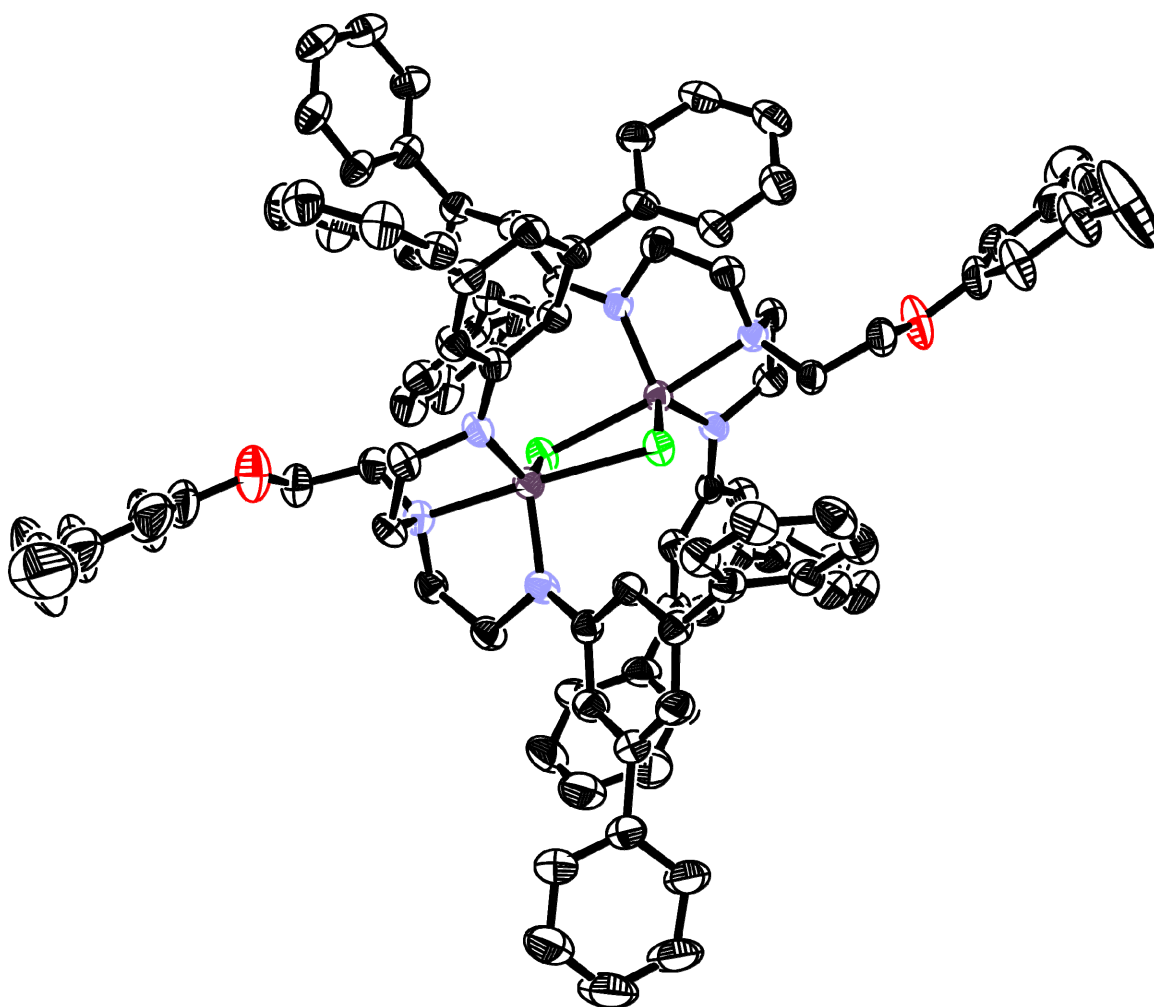


Figure 2.9: ORTEP diagram of $\{[\text{NNO}]\text{VCl}\}_2$ with thermal ellipsoids at 50% probability. Solvent $((\text{Me}_3\text{Si})_2\text{O})$, hydrogen atoms, and isopropyl groups removed for clarity.

2.4.2 Reaction of $\{[\text{NNO}]\text{VCl}\}_2$ with Np_2Mg

An attempt to break up the $\{[\text{NNO}]\text{VCl}\}_2$ dimer by the addition of Np_2Mg to a cold (*ca.* -40 °C) THF solution of $\{[\text{NNO}]\text{VCl}\}_2$ resulted in crystallization of an oxo-bridged dimeric complex (Figure 2.10, Table 2.2). The source of the oxygen is believed to be ligand decomposition based on the results obtained with $\text{H}_2[\text{NNS}]$ (Section 2.4.4). The product is even more soluble than the parent $\{[\text{NNO}]\text{VCl}\}_2$ complex and only a single crystal was obtained from a concentrated sludge. Invoking decomposition of the $[\text{NNO}]^{2-}$ ligand requires that for each oxo-dimer formed, two equivalents of ligand decomposed, and implies that this reaction is, at best, quite messy. Although it is most likely that the oxygen source is not dioxygen, the "side-on"

type bridge indicates that if vanadium complexes containing this ligand were to bind dinitrogen, they might do so in a bridging, side-on fashion which is undesirable in the dinitrogen reduction chemistry we are trying to accomplish.

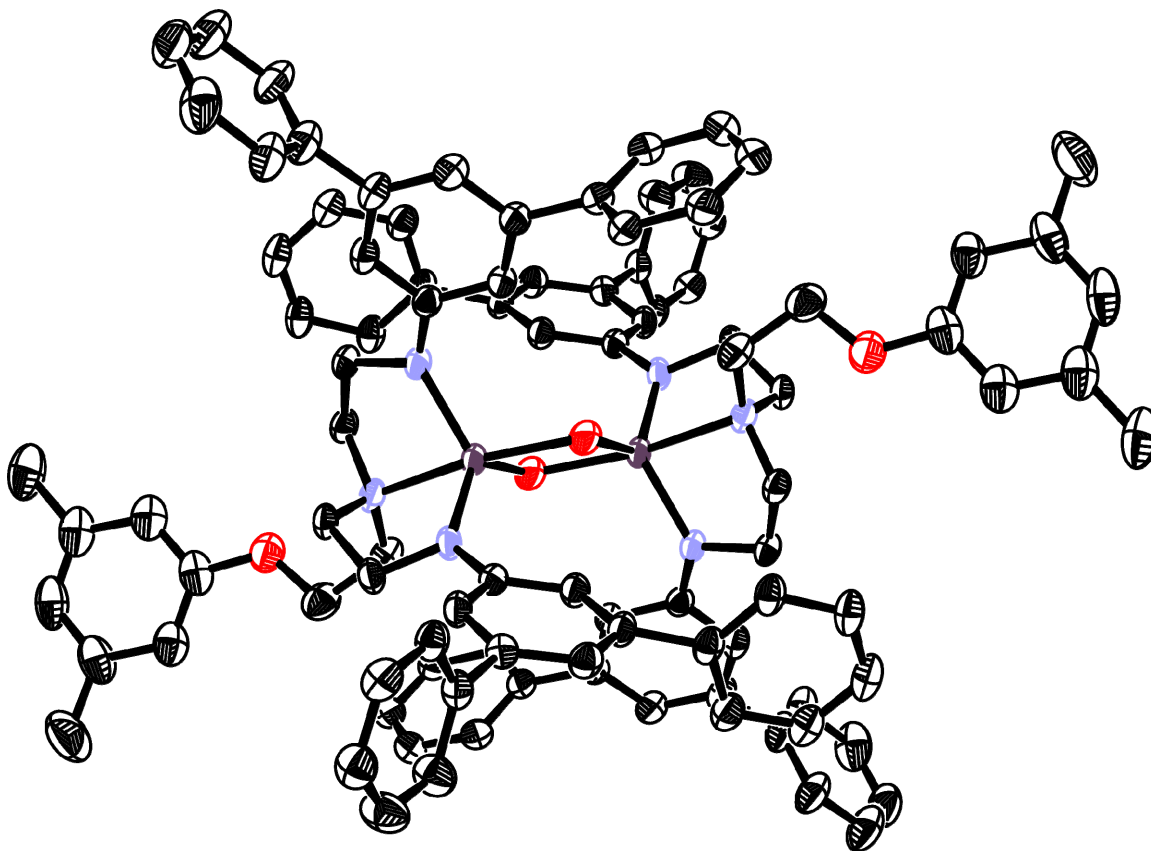


Figure 2.10: ORTEP diagram of the reaction product of $\{[NNO]VCl\}_2$ with Np_2Mg with thermal ellipsoids at 50% probability. Solvent (heptane), hydrogen atoms, and isopropyl groups removed for clarity.

V(1)-O(1)	2.038(3)	O(1)-V(1)-O(1_2)	76.37(13)
V(1)-O(1_2)	2.048(3)	N(4)-V(1)-O(1)	90.82(11)
V(1)-N(1)	1.950(3)	N(4)-V(1)-O(1_2)	166.32(11)
V(1)-N(2)	1.966(3)	N(4)-V(1)-N(1)	82.64(11)
V(1)-N(4)	2.143(3)	N(4)-V(1)-N(2)	82.39(11)
N(1)-V(1)-N(2)	118.38(12)	V(1)-N(1)-C(115)-C(116)	36.6
		V(1)-N(2)-C(215)-C(216)	145.0

Table 2.2: Selected bond lengths (Å) and angles (°) for **34**. Numbering scheme shown in Figure A.12.

2.4.3 Reduction of {[NNO]VCl}₂ with KC₈

The expected dimeric dinitrogen complex was not obtained upon the reduction of {[NNO]VCl}₂ with potassium graphite in benzene or toluene. Instead, *intra*-molecular ligand decomposition was observed in a single crystal grown from heptane (Figure 2.11, Table 2.3). The 3,5-dimethylphenyl group was transferred from oxygen to vanadium, giving a covalent vanadium-oxygen bond with potassium supported oxide bridges.

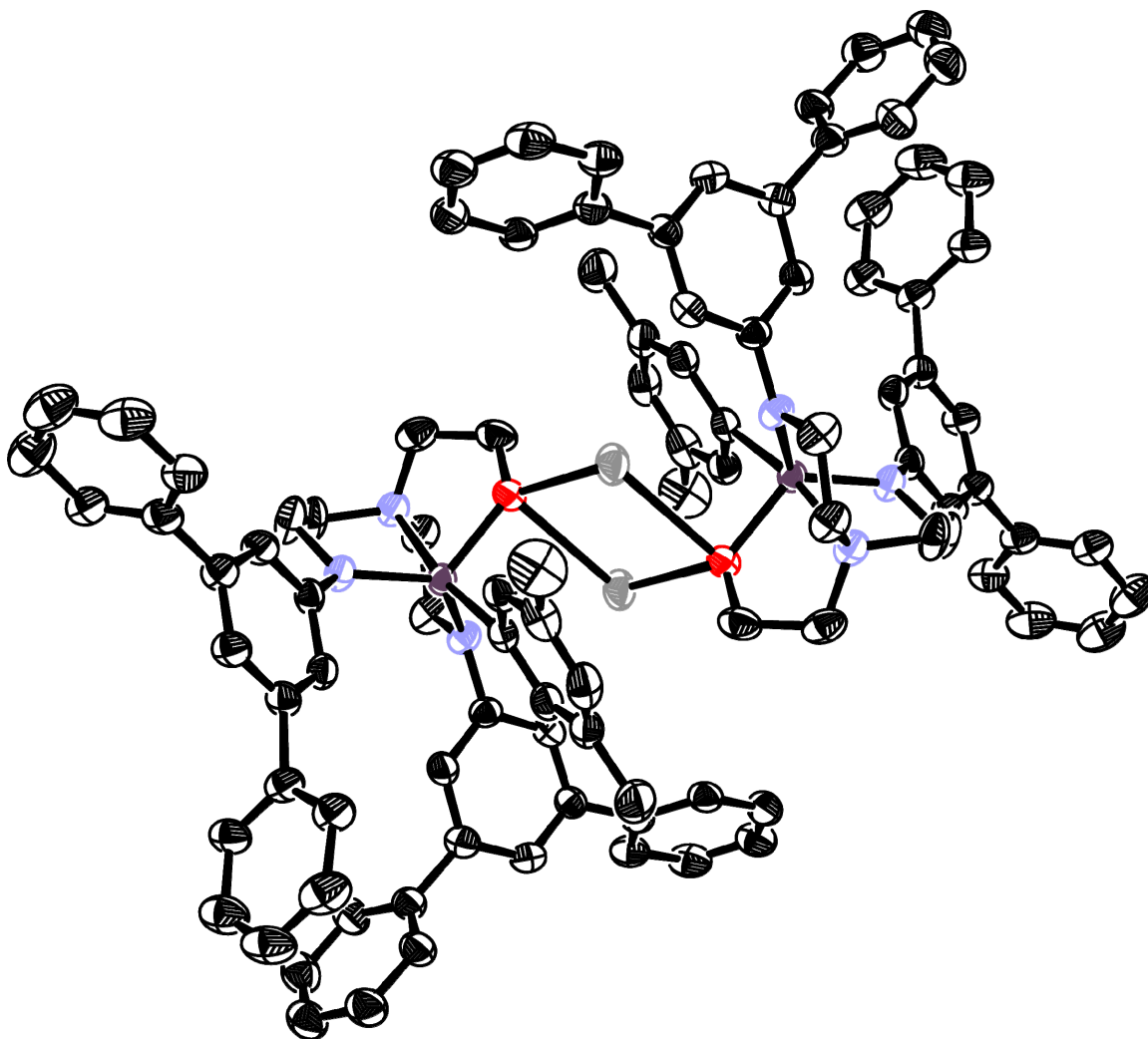


Figure 2.11: ORTEP diagram of the reduction product of {[NNO]VCl}₂ with thermal ellipsoids at 50% probability. Solvent (heptane), hydrogen atoms, and isopropyl groups removed for clarity.

V(1)-N(1)	1.967(3)	O(1)-V(1)-N(2)	110.54(14)
V(1)-N(2)	1.947(4)	N(2)-V(1)-N(1)	122.74(16)
V(1)-N(4)	2.182(4)	N(4)-V(1)-N(1)	82.55(14)
V(1)-O(1)	1.934(3)	N(4)-V(1)-N(2)	80.68(14)
V(1)-C(1)	2.147(5)	N(4)-V(1)-O(1)	81.15(14)
		V(1)-N(1)-C(115)-C(116)	50.3
N(1)-V(1)-O(1)	120.22(14)	V(1)-N(2)-C(215)-C(220)	125.7

Table 2.3: Selected bond lengths (Å) and angles (°) for **33**. Numbering scheme shown in Figure A.10.

2.4.4 Reaction of H₂[NNS] with VCl₃(THF)₃

The reaction of H₂[NNS] with VCl₃(THF)₃ as described in the synthesis of {[NNO]VCl}₂ resulted in a red solution. Like all of the other chalcogenide donor complexes, the product of this reaction is extremely soluble, even in Me₄Si. A single crystal was able to be grown from a concentrated heptane sludge (Figure 2.13, Table 2.4). This crystal showed decomposition of the ligand to create a sulfide bridge, and protonation of one the amide arms to give a amidodiamine ligand scaffold resulted in a distorted pseudo-octahedral complex (Figure 2.12).

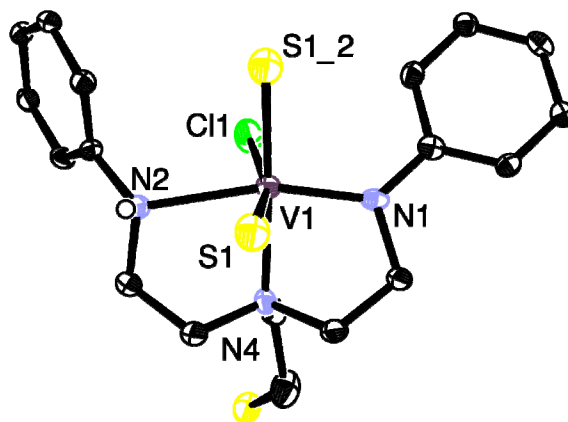


Figure 2.12: ORTEP of the core structure of **35** with thermal ellipsoids at 50% probability.

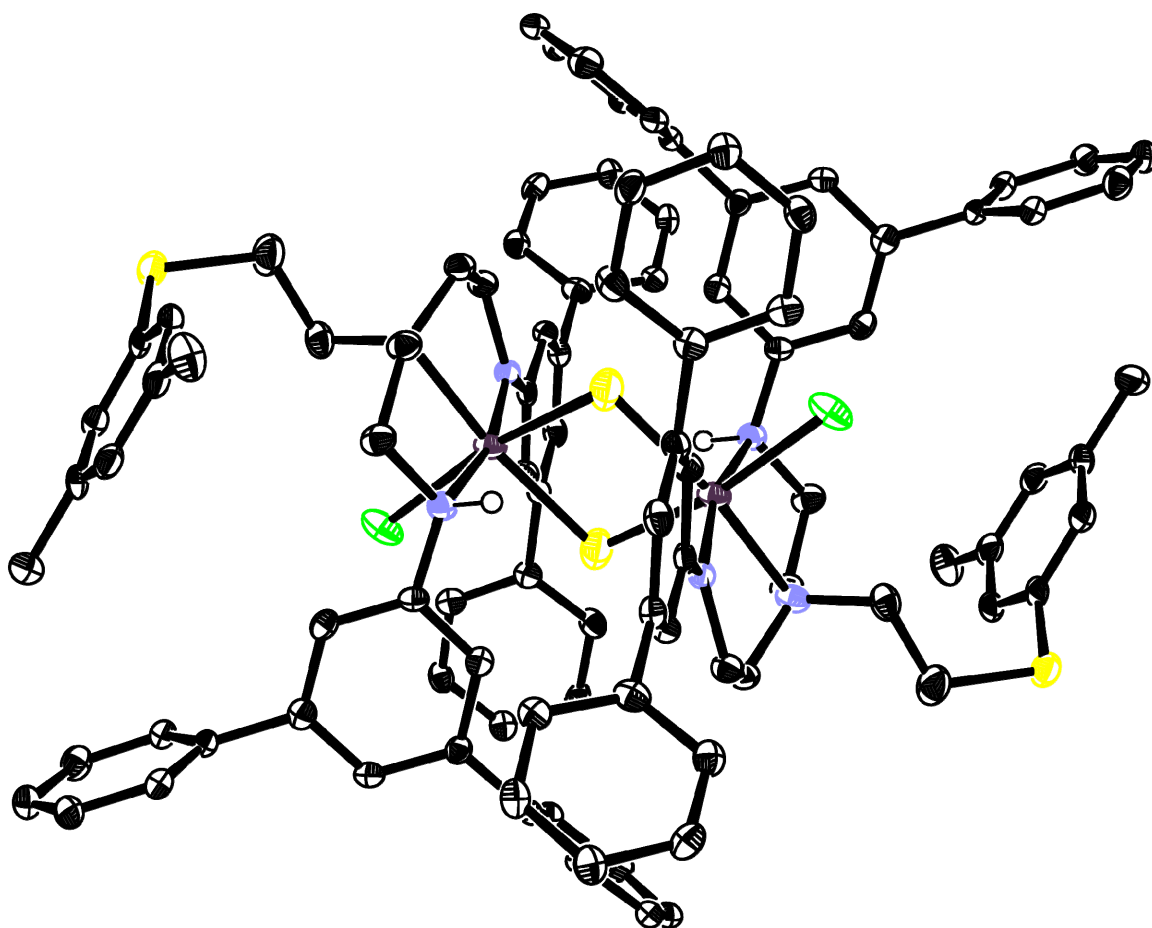


Figure 2.13: ORTEP diagram of the reaction of $\text{H}_2[\text{NNS}]$ with $\text{VCl}_3(\text{THF})_3$ with thermal ellipsoids at 50% probability. Solvent (heptane), non-amine hydrogen atoms, and isopropyl groups removed for clarity.

N(1)-V(1) (Å)	1.923(3)	S(1)-V(1)-N(1) (°)	98.36(9)
N(2)-V(1) (Å)	2.357(3)	N(1)-V(1)-Cl(1) (°)	97.56(9)
N(4)-V(1) (Å)	2.168(3)	Cl(1)-V(1)-N(2) (°)	84.55(8)
Cl(1)-V(1) (Å)	2.3298(12)	N(2)-V(1)-S(1_2) (°)	96.91(8)
S(1)-V(1) (Å)	2.4344(13)	S(1_2)-V(1)-N(1) (°)	99.37(9)
S(1_2)-V(1) (Å)	2.3719(12)	N(1)-V(1)-N(4) (°)	83.40(11)
		N(4)-V(1)-N(2) (°)	80.01(10)
N(2)-V(1)-N(1) (°)	163.41(11)	S(1)-V(1)-S(1_2) (°)	81.04(5)
S(1)-V(1)-Cl(1) (°)	163.83(4)	S(1_2)-V(1)-Cl(1) (°)	93.55(4)
S(1_2)-V(1)-N(4) (°)	169.29(9)	Cl(1)-V(1)-N(4) (°)	96.35(9)
N(2)-V(1)-S(1) (°)	81.01(8)	N(4)-V(1)-S(1) (°)	88.33(9)

Table 2.4: Selected bond lengths (Å) and angles (°) related to the $[\text{NNS}]\text{V}$ core.

2.5 Pyridyl Based Ligands

2.5.1 Reaction of H₂[Pyrl] with VCl₃(THF)₃

The reaction of H₂[Pyrl] with VCl₃(THF)₃ in the same manner as with H₂[NNO] and H₂[NNS] yields an orange solid that is pentane-insoluble. This complex is not stable, even at low temperature (*ca.* -35 °C). The complex turns black over several days, giving a decomposition product that can be washed away with pentane. Based on the insolubility, this complex is believed to be dimeric, {[Pyrl]VCl}₂, with pseudo-octahedral symmetry around the vanadium center, making it structurally analogous to the yttrium and samarium dimers reported by Mountford^{16,17} containing the silylated ligand (Figure 2.3). Unfortunately, crystals suitable for x-ray diffraction have not been forthcoming to confirm this due to the aforementioned decomposition. Operating under the hypothesis that the observed decomposition was occurring at the 6 position on the pyridyl ring, the methylated version of the ligand H₂[Myrl] was synthesized as described (Section 2.2.1).

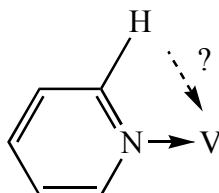


Figure 2.14: Possible decomposition path for {[Pyrl]VCl}₂.

2.5.2 {[Myrl]VCl}₂

Unlike {[Pyrl]VCl}₂, {[Myrl]VCl}₂, synthesized in the same manner as {[Pyrl]VCl}₂, is slightly soluble in pentane. {[Myrl]VCl}₂ is also assigned as a chloride bridged dimer based on its relative insolubility and analogy to the Mountford complexes mentioned in the previous section. Given the VCl₃(THF)₃ starting material, a chloride-bridged dimer is the most logical way to achieve a six-coordinate complex. Suitable crystals for single-crystal x-ray diffraction have remained elusive as only hair-like needles have been obtained. {[Myrl]VCl}₂ is, however, stable which suggests that the instability of {[Pyrl]VCl}₂ is due to the hydrogen atom in the 6 position on the pyridyl group (Figure 2.14). Although we are unaware of reported decomposition of this type, it has been reported that the six position on the pyridyl ring is subject to activation.¹⁶

Attempts to reduce $\{[\text{MyrI}]\text{VCl}\}_2$ with potassium graphite in THF led to decomposition to unidentified material. Performing the reduction in benzene or toluene yielded red powder. This product does not display a dinitrogen stretch in its solution IR spectra (THF or C_6D_6) consistent with a monomeric dinitrogen complex (Figure 2.15). However, the reduction product does appear to incorporate dinitrogen based on the difference spectrum of $\{[\text{MyrI}]\text{VCl}\}_2$ reduced under N_2 and $^{15}\text{N}_2$. The peaks are obscured by ligand modes, but there does appear to be an isotopic shift (Figure 2.15, Figure 2.16). Although end-on bridging is predominant in vanadium dinitrogen complexes,^{18,19,20,21,22,23,24,25,26} η^2 -type geometry is not unprecedented,^{27,28} but it is the result of reductive cleavage of the nitrogen-nitrogen bond. Thus, it is most likely that dinitrogen is bridging in an end-on fashion (Figure 2.17), but in the absence of a crystal structure and without suitable infrared data for comparison, it is impossible for us to determine unambiguously the manner in which dinitrogen is being incorporated. A structure would also be required to determine whether the pyridyl and/or amine donor nitrogens remain bound to vanadium.

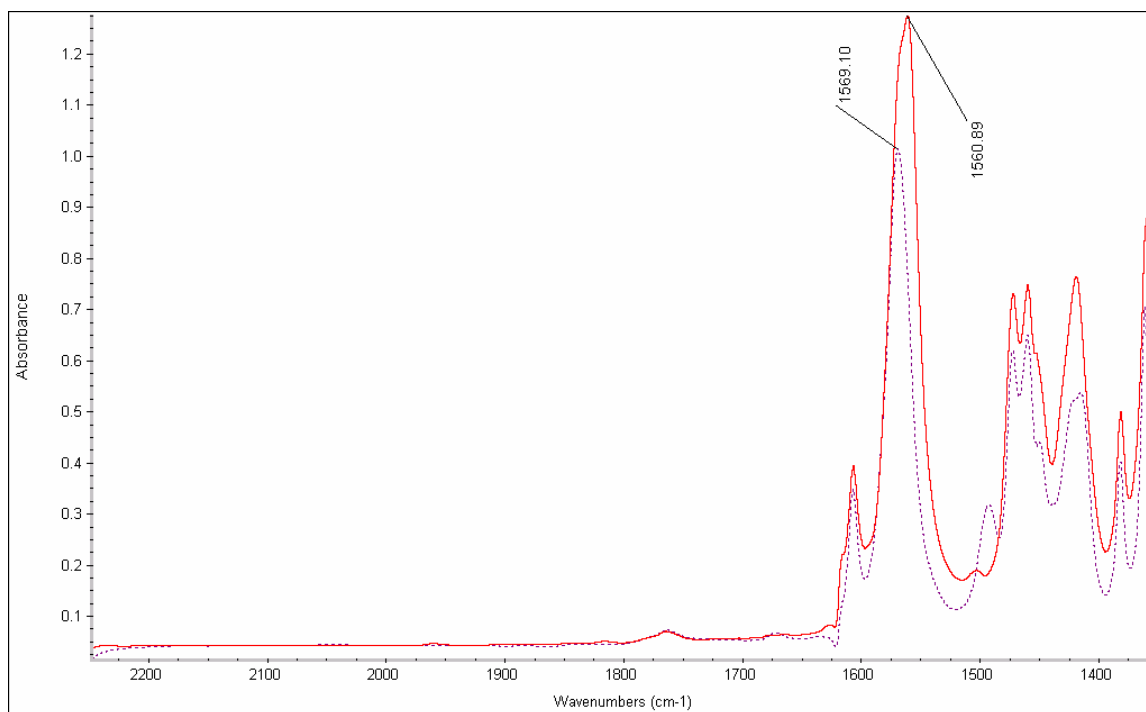


Figure 2.15: Reduction product (C_6D_6 , solvent subtracted) of $\{[\text{MyrI}]\text{VCl}\}_2$ under N_2 (solid, red) and $^{15}\text{N}_2$ (dashed, purple).

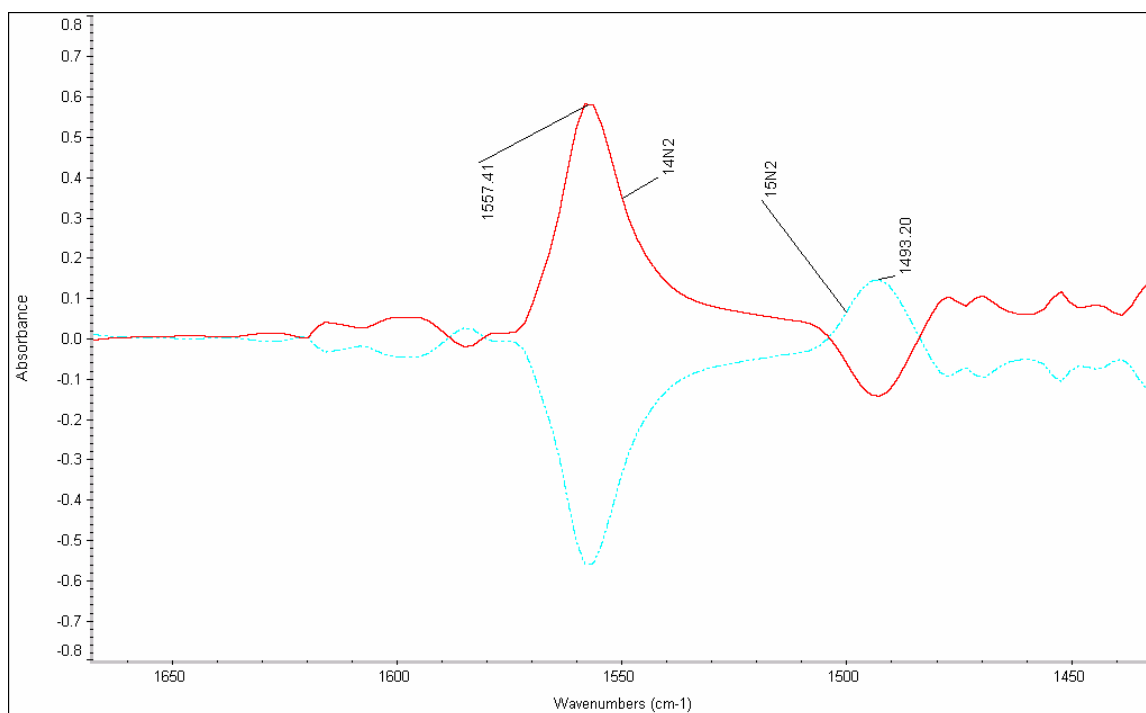


Figure 2.16: Difference spectrum between reduction products of $\{[\text{Myrl}]\text{VCl}_2\}$ under N_2 (solid, red) and $^{15}\text{N}_2$ (dashed, aqua).

A catalytic run using this complex yielded no ammonia⁶ under the $[\text{HIPTN}_3\text{N}]\text{Mo}$ conditions, which we attribute to bridging species being catalytically inactive.

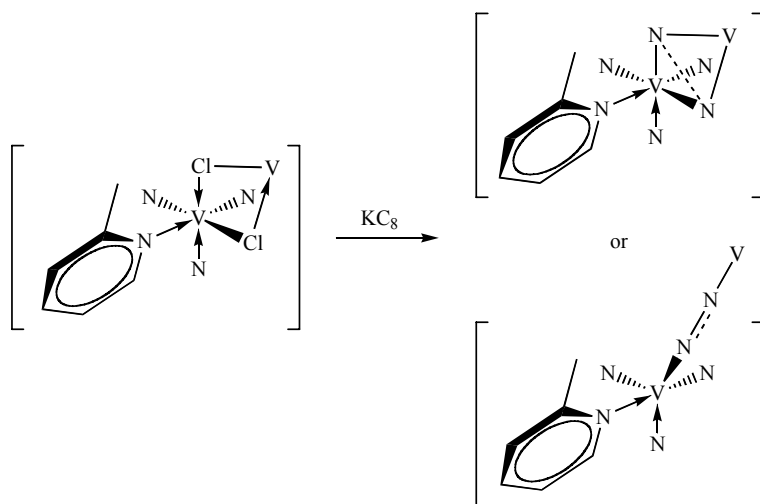


Figure 2.17: Possible core structures of $\{[\text{Myrl}]\text{VCl}_2\}$ and its reduction product.

2.6 Other Approaches

2.6.1 A Carbene Ligand

N-heterocyclic carbenes are strong σ -donors, and as such, are an attractive prospect for a donor that will not dissociate from the metal. Unfortunately, a carbene-based ligand would be expected to be structurally analogous to **Myrl/Pyrl** in its lack of steric protection and that the orientation of any substituent group would be such that it would block the metal center (Figure 2.18).

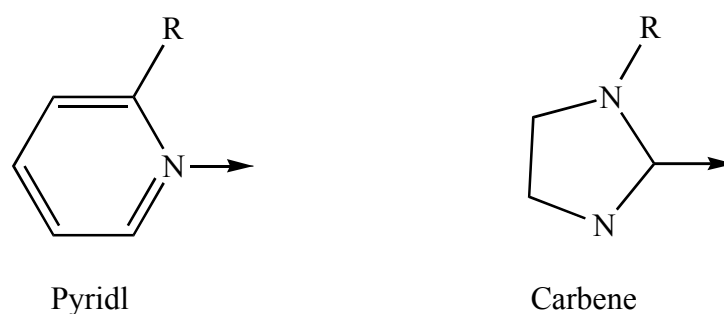


Figure 2.18: Pyridyl vs. Carbene comparison.

2.6.2 Tethered Ligand

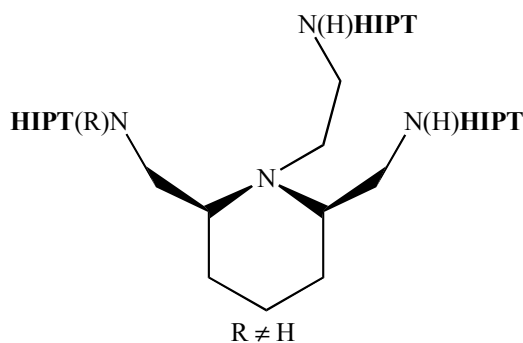


Figure 2.19: Diagram of a hypothetical tethered ligand.

(*2S,6R*)-piperidine-2,6-dicarboxylic acid²⁹ provides a backbone perfectly oriented to prevent dissociation of an amine donor arm (Figure 2.19). However, significant synthetic problems exist in the further development of a suitable ligand from this base. The piperidine ring is subject to ring expansion,^{30,31} and one arm must either be protected or converted into a tertiary amine before the other arms are turned into amines. As these synthetic challenges are significant, we have not seriously pursued a ligand of this type, but a tether would alleviate any

concern about donor dissociation and subsequent dimer formation. It would also retain the protected pocket.

2.7 Conclusions

From the results and structures obtained from the chalcogenide-based ligands $\text{H}_2[\text{NNO}]$ and $\text{H}_2[\text{NNS}]$, it is clear that dimer formation and ligand decomposition are important factors to take into consideration when using chalcogenide-containing ligands. Although the vanadium complexes synthesized with these ligands are not analytically pure, the structures highlight weaknesses of the chalcogenide-based ligands. The donor arm must be strong enough to remain attached to vanadium, and must not be susceptible to cleavage. On the basis of these factors, it is clear that chalcogenide-based ligands are unsuitable for supporting dinitrogen reduction at vanadium in the manner in which we want to use them. Additionally the synthesis of such ligands is not modular, which negates the possibility of accessible ligand variation. Although HIPTOH^{32} is known, indicating that a **HIPT**-based ethereal ligand would be accessible, the lack of steric bulk attached to the donor arm of $\text{H}_2[\text{NNO}]$ is not the major factor in the inability of the ligand to support dinitrogen reduction.

Ligands with an unsubstituted pyridine-based donor arm are also not suitable due to the lack of steric protection. Substitution at the 6 position is not viable for bulky groups as they would directly block the pocket rather than protect it. While substitution at the 5 position may allow protection of the pocket, it is believed that the pyridine nitrogen is too weak of a donor to prevent dissociation and subsequent dimerization.

To realize dinitrogen conversion to ammonia at vanadium, we believe that a ligand which has either a carbene donor arm or an amine arm tethered in some way so that it is forced to remain coordinated to vanadium is required. However, both ligand motifs present significant synthetic challenges that have not yet been overcome.

2.8 Experimental Details

General. All experiments involving air or moisture sensitive complexes or reactions were performed under nitrogen in a Vacuum Atmospheres drybox or using standard Schlenk techniques with glassware stored in an oven at ~ 190 °C for at least 12 hours prior to use.

Pentane was washed with HNO₃/H₂SO₄ (5:95 by volume), sodium bicarbonate, and water, dried over CaCl₂, and then sparged with nitrogen and passed through an alumina column followed by storage over Na/benzophenone and vacuum transfer prior to use. Dry and deoxygenated benzene was purchased from Aldrich and passed through Q5 and alumina columns. Heptane, benzene-*d*₆ and toluene-*d*₈ were dried over Na/benzophenone then degassed (freeze-pump-thaw) and vacuum transferred prior to use. THF, diethyl ether and toluene were pre-dried by passage through an alumina column followed by storage over Na/benzophenone. They were degassed (freeze-pump-thaw) and vacuum transferred prior to use. All solvents were stored over 4 Å molecular sieves in a drybox after transfer.

VCl₃ (Strem), ¹⁵N₂ (Cambridge Isotope Labs), (Me₃Si)₂NLi (Aldrich, sublimed), Pd₂(dba)₃ (Strem), *rac*-BINAP (Strem), NaO-*t*-Bu (Aldrich), diethylenetriamine (Acros, Aldrich), phthalic anhydride (Acros), 2-(chloromethyl)pyridine•HCl (Acros, dissolved in water and filtered through celite), 3,5-dimethylphenol (Acros), chloroacetonitrile (Acros), LiAlH₄ (Aldrich), bromoethylphthalimide (Acros), hydrazine monohydrate (Aldrich), 3,5-dimethylbenzenethiol (Acros), and iodoacetonitrile (Acros) were purchased and used as received or purified as indicated.

HIPTBr,^{33,34,35} VCl₃(THF)₃,^{36,37} N1-(2-aminoethyl)-N1-(2-(isopropylamino)ethyl)ethane-1,2-diamine,⁵ Diphthaloyldiethylenetriamine,¹ and 2-(bromomethyl)-6-methylpyridine³⁸ were synthesized *via* literature procedures. Potassium graphite was synthesized by stirring a 1:8 mixture of potassium:graphite under partial vacuum for 2 hours using a glass stirbar at *ca.* 200 °C.

¹H NMR spectra were obtained on a Varian Mercury (300 MHz) or Inova (500 MHz) spectrometer and were referenced to the residual protio-solvent peak. Infrared spectra were obtained on a Nicolet Avatar 360 FT-IR spectrometer using a demountable liquid cell (0.2 mm Teflon or lead spacer with KBr plates). UV/Vis spectra were obtained on a Hewlett-Packard 8452A Diode Array Spectrophotometer equipped with a Hewlett Packard 89090A Peltier temperature control accessory with the solvent contribution manually subtracted using a standard background. Mass spectrometry data was obtained on a Bruker APEXIV 47 eV FT-ICR-MS (APOLLO ESI source). Magnetic measurements (Evans method^{39,40}) employed the shift of the toluene methyl group. The sample was dissolved in a 4:1 (by volume) mixture of C₆D₆:toluene

and a concentric sealed capillary filled with toluene was added. Elemental Analyses were performed by H. Kolbe Microanalytics Laboratory, Mülheim an der Ruhr, Germany.

Structural data for **34** and **35** were collected at 100 K using graphite-monochromated Mo K α radiation ($\lambda = 0.71073 \text{ \AA}$) and a Bruker-AXS Smart Apex CCD detector. All other structural data was collected at $-80 \text{ }^\circ\text{C}$ using a CCD area detector. The structures were solved using SHELXS⁴¹ and refined against F^2 on all data by full-matrix least squares with SHELXL-97⁴². All non-hydrogen atoms were refined anisotropically, while hydrogen atoms were placed at calculated positions and refined using a riding model. ORTEP diagrams were generated using ORTEP-3.⁴³ The structure solutions for **33** (04130), **34** (05072) and **35** (05085) can be found on <http://www.reciprocalnet.org> using the number in parentheses.

H₂[HIPTN₂N]CH₂CH₂NH-*i*-Pr (14). Pd₂(dba)₃ (12 mg, 13 μmol) and *rac*-BINAP (25 mg, 40 μmol) were added to a 20 mL scintillation vial followed by *ca.* 10 mL of toluene. The mixture was allowed to stir for 3 hours and then filtered through celite into a 100 mL solvent bomb type flask with a 0-8 Teflon valve. To this solution, HIPTBr (1.00 g, 1.78 mmol) and NaO-*t*-Bu (214 mg, 2.23 mmol) were added followed by *N*1-(2-aminoethyl)-*N*1-(2-(isopropylamino)ethyl)ethane-1,2-diamine (168 mg, 0.89 mmol) and toluene to bring the total volume to *ca.* 40 mL. This mixture was then stirred at $80 \text{ }^\circ\text{C}$ for 36 hours. The resulting mixture was filtered through celite and chromatographed on silica gel (washed with *ca.* 15% Et₃N in toluene) using toluene. Drying *in vacuo* yielded a solid that was triturated with MeOH. Collection by filtration of the white solid gave the final product (200 mg, 19%). ¹H NMR (C₆D₆) δ 7.22 (s, 8H), 6.53 (m, 6H), 4.35 (br t, 2H), 3.20 (sept, $J_{\text{HH}} = 6.8 \text{ Hz}$, 8H), 2.91 (m, 8H), 2.52 (quint, $J_{\text{HH}} = 6.17 \text{ Hz}$, 1H), 2.37 (br s, 2H), 2.28 (t, $J_{\text{HH}} = 5.6 \text{ Hz}$, 4H), 2.21 (t, $J_{\text{HH}} = 5.4 \text{ Hz}$, 2H), 1.33 (d, $J_{\text{HH}} = 7.0 \text{ Hz}$, 24H), 1.29 (br d, $J_{\text{HH}} = 3.0 \text{ Hz}$, 24H), 1.27 (br d, $J_{\text{HH}} = 3.0 \text{ Hz}$, 24H), 0.89 (d, $J_{\text{HH}} = 6.2 \text{ Hz}$, 6H) 0.80 (br s, 1H); MS (ESI) Calcd. m/z 1149.9586 ($[\text{M}+\text{H}]^+$), found m/z 1149.9554.

***N*1-(2-aminoethyl)-*N*1-((pyridin-2-yl)methyl)ethane-1,2-diamine (15).** *N,N*-bis(phthalimide)diethylenetriamine (20.0 g, 55.0 mmol) was added to a stirring solution of 200 mL 2.0 M NaOH in water in a 500 mL round bottom flask. The mixture was capped and

allowed to stir (large egg-shaped stirbar) at room temperature until all of the solid dissolved (*ca.* 3-4 hours). 2-(Chloromethyl)pyridine (9.0 g, 55.0 mmol) was weighed out and dissolved in a minimum quantity of water. This was filtered through celite in a glass funnel plugged by glass wool to remove unknown black solid and yield an amber/dark gold solution. The filtrate was then added drop-wise via an addition funnel to the stirring solution. Once addition was complete, the flask was capped and allowed to stir overnight at room temperature. The next day, 2-(chloromethyl)pyridine (4.5 g, 27.5 mmol) was weighed and prepared as before and added to the reaction mixture as before. The reaction was again capped and allowed to stir overnight. The reaction mixture was then extracted with methylene chloride. The water portion was collected, and the solution was concentrated *in vacuo* at *ca.* 40-50 °C. The remaining water was then decanted off the resulting sludge. A 1:1 (by volume) mixture of concentrated aqueous HCl:water (400 mL) was added to the sludge, a condenser attached, and the system put under nitrogen pressure. With vigorous stirring, the solution was heated at *ca.* 90 °C for 24 hours. A copious quantity of white solid was removed by filtering through celite. The remaining solution was cooled in an ice bath and was slowly brought to pH 14 with a saturated NaOH solution. This was concentrated *in vacuo* at *ca.* 40 °C and extracted with Methylene chloride. The Methylene chloride fractions were dried with Na₂SO₄. Distillation of the resulting oil gave a light yellow oil matching previously reported spectroscopic properties (7.68 g, 72 % based on amine). ¹H NMR (CDCl₃) δ 8.41 (q d, J_{HH(d)} = 4.9 Hz, J_{HH(q)} = 0.9 Hz, 1H), 7.54 (d t, J_{HH(t)} = 7.7 Hz, J_{HH(d)} = 1.84 Hz, 1H), 7.33 (d br t, J_{HH(d)} = 7.82 Hz, 1H), 7.03 (m, 1H), 3.65 (s, 2H), 2.66 (t, J_{HH} = 6.1 Hz, 4H), 2.49 (t, J_{HH} = 6.1 Hz, 4H), 1.08 (br s, 4H).

H₂[PyrI] (16). In a glove box, Pd₂(dba)₃ (239 mg, 0.261 mmol) and *rac*-BINAP (487 mg, 0.782 mmol) were added to a 50 mL round bottom flask, to which was added toluene (*ca.* 40 mL). The flask was then capped and heated while stirring to facilitate formation of the catalyst. The mixture was filtered through celite into a 250 mL flask with a side-arm and Teflon valve. To this, NaO-*t*-Bu (4.68 g, 48.7 mmol) and **HIPTBr** (20.0 g, 35.6 mmol) were added. Toluene was then added to bring the total volume to *ca.* 180 mL. With stirring, **15** (3.38g, 17.4 mmol) was added *via* pipette. The flask was sealed and brought outside to be heated at 90 °C for *ca.* 20 hours, after which, TLC showed no more **HIPTBr** present. The mixture was then filtered

through celite to remove NaBr, and the resulting red solution was concentrated and chromatographed on alumina, first with 50:50 (by volume) pentane:toluene then toluene. The appropriate fractions were collected together and the solvent removed *in vacuo* to yield a white foam which was crushed and dried at 80 °C to yield H₂[PyrI] (13.2 g, 66%). ¹H NMR (C₆D₆) δ 8.20 (d, J_{HH} = 4.3 Hz, 1H), 7.23 (s, 8H), 6.97 (d t, J_{HH(t)} = 7.7 Hz, J_{HH(d)} = 1.9 Hz, 1H), 6.77 (d, J_{HH} = 7.9 Hz, 1H), 6.56-6.49 (m, 7H), 4.64 (t, J_{HH} = 4.5 Hz, 2H), 3.42 (s, 2H), 3.18 (sept, J_{HH} = 6.9 Hz, 8H), 2.99-2.83 (m, 8H), 2.42 (t, J_{HH} = 6.0 Hz, 4H), 1.32 (d, J_{HH} = 6.9 Hz, 24H), 1.25 (d d, J_{HH} = 6.9 Hz, J_{HH} = 1.9 Hz, 48H); MS (ESI) Calcd. m/z 1155.9116 ([M+H]⁺), found m/z 1155.9157.

***N*1-(2-aminoethyl)-*N*1-((6-methylpyridin-2-yl)methyl)ethane-1,2-diamine (17).** *N,N*-bis(phthalimide)diethylenetriamine (10.0 g, 27.5 mmol) was added to a stirring solution of 100 mL 2.0 M NaOH in water in a 250 mL round bottom flask. The mixture was capped and allowed to stir (large egg-shaped stirbar) at room temperature until all of the solid dissolved (*ca.* 3-4 hours). 2-(Bromomethyl)-6-methylpyridine (5.12 g, 27.5 mmol) was then added to the stirring solution. Once addition was complete, the flask was capped and allowed to stir overnight at room temperature. The reaction mixture was then extracted with methylene chloride. The water portion was collected, and the solution was concentrated *in vacuo* at *ca.* 40-50 °C. The remaining water was then decanted off the resulting sludge. A 1:1 (by volume) mixture of concentrated aqueous HCl:water (200 mL) was added to the sludge, a condenser attached, and the system put under nitrogen pressure. With vigorous stirring, the solution was heated at *ca.* 90 °C for 24 hours. A copious quantity of white solid was removed by filtering through celite. The remaining solution was cooled in an ice bath and was slowly brought to pH 14 with a saturated NaOH solution. This was concentrated *in vacuo* at *ca.* 40 °C and extracted with Methylene chloride. The Methylene chloride fractions were dried with Na₂SO₄, and the resulting oil was distilled under vacuum (4.7 g, 41%). ¹H NMR (C₆D₆) δ 7.21-7.13 (m, 2H), 6.69-6.58 (m, 1H), 3.27 (s, 2H), 2.56 (t, J_{HH} = 6.1 Hz, 4H), 2.43 (s, 3H), 2.38 (t, J_{HH} = 6.0 Hz, 4H), 0.84 (br s, 4H).

H₂[Myrl] (18). In a glove box, Pd₂(dba)₃ (239 mg, 0.261 mmol) and *rac*-BINAP (487 mg, 0.782 mmol) were added to a 50 mL round bottom flask, to which was added toluene (*ca.* 40 mL). The flask was then capped and heated while stirring to facilitate formation of the catalyst. The mixture was filtered through celite into a 250 mL flask with a side-arm and Teflon valve. To this, NaO-*t*-Bu (4.68 g, 48.7 mmol) and **HIPTBr** (20.0 g, 35.6 mmol) were added. Toluene was then added to bring the total volume to *ca.* 180 mL. With stirring, **17** (3.6, 17.4 mmol) was added *via* pipette. The flask was sealed and brought outside to be heated at 90 °C for *ca.* 20 hours, after which, TLC showed no more **HIPTBr** present. The mixture was then filtered through celite to remove NaBr, and the resulting red solution was concentrated and chromatographed on alumina, first with 50:50 (by volume) pentane:toluene then toluene. The appropriate fractions were collected together and the solvent removed *in vacuo* to yield a white foam which was crushed and dried at 80 °C to yield H₂[**Myrl**] (11 g, 53%). ¹H NMR (C₆D₆) δ 7.23 (m, 8H), 6.96 (t, J_{HH} = 7.6 Hz, 1H), 6.73 (d, J_{HH} = 7.5 Hz, 1H), 6.52-6.47 (m, 7H), 4.59 (t, J_{HH} = 5.1 Hz, 2H), 3.48 (s, 2H), 3.19 (sept, J_{HH} = 6.9 Hz, 8H), 2.96-2.84 (m, 8H), 2.41 (t, J_{HH} = 5.9 Hz, 4H), 2.29 (s, 3H), 1.32 (d, J_{HH} = 6.9 Hz, 24H), 1.28-1.23 (m, 48H); MS (ESI) Calcd. m/z 1169.9273 ([M+H]⁺), found m/z 1169.9312; Calcd. m/z 585.4676 ([M+2H]²⁺), found m/z 585.4691.

2-(3,5-dimethylphenoxy)acetonitrile (19). 3,5-Dimethylphenylphenol (100 g, 0.82 mol) and potassium carbonate (106 g, 0.77 mol) were added to 2-propanone (200 mL). The mixture was brought to reflux and chloroacetonitrile (57.2 mL) in 2-propanone that was stored over KI (500 mg, 3 mmol) over 18 h was added drop wise. After addition, the reaction mixture was refluxed for an additional hour. The residue was then dissolved in diethyl ether and washed with 5% NaOH. The diethyl ether fraction was then dried with Na₂SO₄ and the solvent removed to yield brown solid, which was distilled *in vacuo* (without cooling to prevent solidification in the bridge) into an ice-cooled flask. There was no internal thermometer, but the oil bath was heated to 90-100 °C and the source flask wrapped in foil. The distillate solidified to give a slightly off-white solid upon sitting (105 g, 79%). ¹H NMR (CDCl₃) δ 6.75 (m, 1H), 6.62 (m, 2H), 4.74 (s, 2H), 2.34 (q, J_{HH} = 0.6 Hz, 6H).

2-(3,5-dimethylphenoxy)ethanamine (20). LiAlH₄ (26 g, 0.69 mol) was added to diethyl ether in a 3-neck flask fitted with a condenser, placed under nitrogen, and cooled in an ice bath. **19** (105 g, 0.65 mol) was dissolved in a minimum quantity of diethyl ether and added drop wise. The mixture was refluxed overnight and then quenched with water. The mixture was filtered through celite in a large frit. The filtrate was washed with water, dried with Na₂SO₄ and concentrated. The yellow oil was distilled at 15 mTorr at 75 °C to yield a colorless oil (54 g, 50%). ¹H NMR (CD₂Cl₂) δ 6.60 (m, 1H), 6.54 (m, 2H), 3.92 (t, J_{HH} = 5.2 Hz, 2H), 3.00 (t, J_{HH} = 5.4 Hz, 2H), 2.28 (m, 6H), 1.25 (br s, 2H).

3,5-dimethylphenoxyethyl-bis-(ethylphthalimide)amine (21). **20** (10.0 g, 60.5 mmol), K₂CO₃ (15.9 g, 115 mmol) and bromoethylphthalimide (30.0 g, 118 mmol) were added to MeCN and the mixture was refluxed for 3 days to give a mixture of products as a viscous orange oil. The oil was diluted with Methylene chloride to reduce the viscosity and placed on a large column of silica gel. The column was first eluted with Methylene chloride and then fractions from a 50:50 mixture of EtOAc:Hexane were collected to afford the product as a yellow oil (13.6 g, 23%). ¹H NMR (CDCl₃) δ 7.66 (m, 8H), 6.50 (s, 1H), 6.33 (s, 2H), 3.83 (t, J_{HH} = 5.6 Hz, 2H), 3.76 (t, J_{HH} = 6.3 Hz, 4H), 2.99 (t, J_{HH} = 5.6 Hz, 2H), 2.93 (t, J_{HH} = 6.5 Hz, 4H), 2.22 (s, 6H).

N1-(2-(3,5-dimethylphenoxy)ethyl)-N1-(2-aminoethyl)ethane-1,2-diamine (22). **21** (13.6 g, 26.6 mmol) was diluted with THF and hydrazine monohydrate was added. Refluxing for six hours gave solid that was filtered off. The THF was removed and the residue taken up in Methylene chloride and filtered again. The filtrate was washed with water, dried with Na₂SO₄ and the solvent removed (5.9 g, 88%). ¹H NMR (CDCl₃) δ 6.59 (s, 1H), 6.52 (s, 2H), 4.00 (t, J_{HH} = 5.7 Hz, 2H), 2.88 (t, J_{HH} = 5.7 Hz, 2H), 2.78 (m, 4H), 2.62 (m, 4H), 2.28 (s, 6H), 1.48 (br s, 4H).

H₂[NNO] (23). Pd₂(dba)₃ (239 mg, 0.26 mmol) and *rac*-BINAP (488 mg, 0.78 mmol) were mixed with toluene and heated to form the catalyst. The mixture was filtered to remove Pd black. **HIPTBr** (20.0 g, 35.7 mmol) and NaO-*t*-Bu (4.84 g, 50.4 mmol) were added in a 100 mL flask with a Teflon valve. Upon addition of **22** (4.37 g, 17.4 mmol), the solution turned purple.

The reaction was heated at 80 °C for 24 hours and then chromatographed on silica gel with a 75:25 (by volume) toluene:hexane mixture (16 g, 76%). ¹H NMR (C₆D₆) δ 7.21 (s, 8H), 6.58 (br s, 2H), 6.54 (br t, 2H), 6.51 (br s, 4H), 6.48 (br s, 1H), 4.23 (t, J_{HH} = 5.1 Hz, 2H), 3.55 (t, J_{HH} = 4.8 Hz, 2H), 3.18 (sept, J_{HH} = 6.9 Hz, 8H), 2.98-2.80 (m, 8H), 2.37 (t, J_{HH} = 4.8 Hz, 2H), 2.31 (t, J_{HH} = 5.6 Hz, 4H), 2.02 (s, 6H), 1.32 (d, J_{HH} = 6.9 Hz, 24H), 1.25 (br d, J_{HH} = 6.9 Hz, 48H); MS (ESI) Calcd. m/z 1212.9582 ([M+H]⁺), found m/z 1212.9598; Calcd. m/z 606.9831 ([M+2H]²⁺), found m/z 606.9854.

2-(3,5-dimethylphenylthio)acetonitrile (24). 3,5-Dimethylbenzenethiol (30.5 g, 0.22 mol) and K₂CO₃ (30.4 g, 0.22 mol) were added to 2-propanone (*ca.* 70 mL) along with iodoacetonitrile (15.9 mL, 0.22 mol). The reaction was refluxed for 2 days and worked up as in **19**. Distillation *in vacuo* (15 mTorr) at *ca.* 150 °C gave a *ca.* 3:1 mixture of 3,5-dimethylphenylthioacetonitrile and disulfide as a brown oil which was used directly in the next step without further purification. ¹H NMR (CDCl₃) δ 7.17 (m, 2H), 7.00 (m, 1H), 3.56 (s, 2H), 2.34 (m, 6H). Disulfide: 7.14 (m, 4H), 6.87 (m, 2H), 2.30 (m, 12H).

2-(3,5-dimethylphenylthio)ethanamine (25). LiAlH₄ (8.4 g, 0.22 mol) reduction of **24** was performed as in **20**. Upon solvent removal and distillation, 2-(3,5-dimethylphenylthio)ethanamine was the primary product (1.34 g) and was used without further purification. ¹H NMR (CDCl₃) δ 6.99 (m, 2H), 6.83 (m, 1H), 3.04-2.87 (m, 4H), 2.29 (s, 6H), 1.37 (br s, 2H).

3,5-dimethylphenylthioethyl-bis(ethylphthalimide)amine (26).

Crude **25** (1.3g, 4.86 mmol), K₂CO₃ (1.02 g, 7.40 mmol), and bromoethylphthalimide (3.76 g, 14.8 mmol) were reacted and purified as described in **21**, yielding a white solid (1.6 g, 41%, 1.4% over all steps). ¹H NMR (CDCl₃) 7.78-7.64 (m, 8H), 6.83 (m, 2H), 6.75 (m, 1H), 3.74 (t, J_{HH} = 6.5 Hz, 4H), 2.92-2.79 (m, 8H), 2.26 (s, 6H).

N1-(2-(3,5-dimethylphenylthio)ethyl)-N1-(2-aminoethyl)ethane-1,2-diamine (27). As described in **22**, deprotection of **26** yields **27** as a cloudy, colorless oil (562 mg, 69%). ¹H NMR

(CDCl₃) δ 6.95 (m, 2H), 6.80 (m, 1H), 3.02 (t, $J_{\text{HH}} = 7.0$ Hz, 2H), 2.78-2.69(m, 6H), 2.53 (t, $J_{\text{HH}} = 5.9$ Hz, 4H), 2.28 (q, $J_{\text{HH}} = 0.6$ Hz, 6H), 1.47 (br s, 4H).

H₂[NNS] (28). **27** (0.50 g, 1.87 mmol), **HIPTBr** (2.15 g, 3.84 mmol), NaO-*t*-Bu (0.50 g, 5.20 mmol), Pd₂(dba)₃ (26 mg, 28.4 μ mol), and *rac*-BINAP (52 mg, 83.6 μ mol) were used in a synthesis analogous to **23** to yield H₂[NNS] (1.7g, 73%). ¹H NMR (CDCl₃) δ 7.01 (s, 8H), 6.88 (br s, 2H), 6.73 (br s, 1H), 6.43 (br d, 4H), 6.37 (br t, 2H), 4.46 (br t, 2H), 3.17 (br q, $J_{\text{HH}} = 4.9$ Hz, 4H), 3.05 (t, $J_{\text{HH}} = 6.2$ Hz, 2H), 3.00-2.70 (m, 18H), 2.12 (s, 6H), 1.30 (d, $J_{\text{HH}} = 6.9$ Hz, 24H), 1.11 (d, $J_{\text{HH}} = 6.9$ Hz, 24H), 1.04 (d, $J_{\text{HH}} = 6.9$ Hz, 24H); MS (ESI) Calcd. *m/z* 1228.9354 ([M+H]⁺), found *m/z* 1228.9352.

{[Pyr]VCl}₂ (29). A 100 mL round bottom flask was charged with H₂[Pyr] (5.00 g, 4.33 mmol) and VCl₃(THF)₃ (1.62 g, 4.33 mmol) in a glove box. THF (*ca.* 50 mL) was added and the flask was capped, taped and left stirring for *ca.* 2 hours. To the violet adduct, (Me₃Si)₂NLi (1.45 g, 8.67 mmol) was added, quickly giving a red solution. The flask was again sealed and taped and allowed to stir for *ca.* 1 hour. The flask was then fitted with a Teflon adapter and put under reduced pressure to keep the joint from popping off as the flask was brought out of the box and dried on a Schlenk line at 45 °C. The flask was brought back into the box and the residue was dissolved in benzene. This mixture was filtered through celite and, in the same manner as before, dried on the line. This residue was dissolved in pentane and stirred until a heterogeneous mixture was obtained. The gooey orange solid was collected on a frit and dried at room temperature to afford slightly off-color orange powder (4.2 g, 78%). Anal. Calcd. for C₁₆₄H₂₂₄N₈Cl₂V₂: C, 79.43; H, 9.11; N, 4.52; Cl, 2.82. Found: C, 79.44; H, 9.14; N, 4.39; Cl, 2.88.

{[Myr]VCl}₂ (30). H₂[Myr] (5.00 g, 4.27 mmol) and VCl₃(THF)₃ (1.67 g, 4.47 mmol) were added to a 100 mL solvent bomb type flask with a 0-8 Teflon valve followed by *ca.* 60 mL of THF. The violet solution was allowed to stir for 1 hour and (Me₃Si)₂NLi (1.43 g, 8.55 mmol) to quickly give a reddish solution. This was allowed to stir for another hour and then dried to minimum pressure (*ca.* 5 mTorr) at 40 °C. The residue was taken up in benzene and stirred for

30 min., followed by filtration through celite. The resulting red solution was again dried to minimum pressure at 40 °C. The resulting residue was dissolved in pentane and allowed to stir until a heterogeneous mixture was obtained. The solid was collected on a glass frit and dried *in vacuo* to give a red powder (3.69 g, 69%). UV/Vis λ_{max} (nm), ϵ ($\text{M}^{-1}\cdot\text{cm}^{-1}$): toluene (370, 1.3×10^4); $\mu_{\text{eff}} = 3.69$ BM; Anal. Calcd. for $\text{C}_{166}\text{H}_{228}\text{N}_8\text{Cl}_2\text{V}_2$: C, 79.50; H, 9.17; N, 4.47; Cl, 2.79. Found: C, 79.28; H, 9.06; N, 4.38; Cl, 2.76.

{{[Myrl]VN}₂ (31). {[Myrl]VCl}₂ (1.5 g, 0.60 mmol) and a glass-coated stirbar were added to a 20 mL scintillation vial. KC_8 (178 mg, 1.32 mmol) was then added followed by toluene (*ca.* 15 mL). The vial was capped with a Teflon lined cap, taped and allowed to stir overnight. The resulting mixture was filtered through glass wool to give a red solution which was dried to minimum pressure at room temperature. The resulting residue was taken up in pentane and concentrated to supersaturation and left to crystallize at -40 °C to give a red powder (330 mg, 22%). Anal Calcd. for $\text{C}_{166}\text{H}_{228}\text{N}_{10}\text{V}_2$: C, 80.85; H, 9.33; N, 5.68; Cl, 0.00. Found: C, 80.73, 80.78; H, 9.38, 9.40; N, 5.62, 5.56; Cl, 0.10, 0.08.

{{[NNO]VCl}₂ (32). $\text{H}_2[\text{NNO}]$ (4.00 g, 3.30 mmol) and $\text{VCl}_3(\text{THF})_3$ (1.29 g, 3.47 mmol) were dissolved in THF to give a violet solution. Addition of $(\text{TMS})_2\text{NLi}$ (1.10 g, 6.58 mmol) yielded a red solution. THF was then removed and the product taken up in pentane and filtered. The pentane was then removed to yield a dark orange-red powder in quantitative yield. Anal. Calcd. for $\text{C}_{172}\text{H}_{238}\text{N}_6\text{Cl}_2\text{O}_2\text{V}_2$: C, 79.62; H, 9.25; N, 3.24; Cl, 2.73. Found: C, 72.16, 73.32, 73.38; H, 8.71, 9.75, 9.71; N, 3.39, 2.90, 2.87; Cl, 2.60, 2.39, 2.46 (two independent samples, second two measurements on the same synthetic sample).

Reduction of {[NNO]VCl}₂ (33). {[NNO]VCl}₂ (500 mg, 0.19 mmol) and KC_8 (57 mg, 0.42 mmol) were added to a 20 mL scintillation vial along with a glass-coated stir-bar and *ca.* 10 mL toluene and allowed to stir overnight. The solution was then filtered through glass wool and dried *in vacuo* to minimum pressure (*ca.* 5 mTorr) to give a red solid (180 mg). Anal Calcd. for $\text{C}_{172}\text{H}_{238}\text{N}_6\text{K}_2\text{O}_2\text{V}_2$: C, 79.40; H, 9.22; N, 3.23; Cl, 0.00; K, 3.01. Found: C, 79.20; H, 9.18; N, 3.17; Cl, 0.10; K, 2.94.

Reaction of {[NNO]VCl}₂ with Np₂Mg (34). {[NNO]VCl}₂ (500 mg, 0.19 mmol) and a glass-coated stir-bar were added to a 20 mL scintillation vial followed by THF (*ca.* 10 mL). The vial cooled to *ca.* -40 °C, and, with stirring, Np₂Mg (32 mg, 0.19 mmol) was added. The reaction was allowed to stir for *ca.* 12 hours to give a brown-red solution. The volatiles were removed *in vacuo* and the resulting residue was dissolved in pentane and filtered through celite. After removal of the volatiles, the remaining solid was dissolved in heptane and concentrated to a sludge, from which a single crystal grew.

Reaction of H₂[NNS] with VCl₃(THF)₃ (35). H₂[NNS] (800 mg, 0.65 mmol), VCl₃(THF)₃ (254 mg, 0.68 mmol), and (Me₃Si)₂NLi (218 mg, 1.30 mmol) were used as in the synthesis of {[NNO]VCl}₂. A portion of the resulting red solid (*ca.* 200 mg) was dissolved in heptane and concentrated to a sludge, from which a single crystal grew.

2.9 References

-
- ¹ Cheng, T.-H.; Wang, Y.-M.; Lee, W.-T.; Liu, G.-C. *Polyhedron* **2000**, *19*, 2027.
 - ² Skinner, M. E. G.; Cowhig, D. A.; Mountford, P. *Chem. Commun.* **2000**, 1167.
 - ³ Skinner, M. E. G.; Li, Y.; Mountford, P. *Inorg. Chem.* **2002**, *41*, 1110.
 - ⁴ Djerassi, C.; Scholz, C. R. *J. Am. Chem. Soc.* **1947**, *69*, 1688.
 - ⁵ Kisanga, P. B.; Verkade, J. G. *Tetrahedron* **2001**, *57*, 467.
 - ⁶ Weare, W. W. *Ph.D. Thesis*, MIT **2006**
 - ⁷ Anderson, A. G., Jr.; Harrison, W. F.; Anderson, R. G. *J. Am. Chem. Soc.* **1963**, *85*, 3448.
 - ⁸ Suginome, H.; Yamada, S.; Wang, J. B. *J. Org. Chem.* **1990**, *55*, 2170.
 - ⁹ Lee, W.-Y.; Liang, L.-C. *Dalton Transactions* **2005**, 1952.
 - ¹⁰ Pittelkow, M.; Lewinsky, R.; Christensen, J. B. *Synthesis* **2002**, 2195.
 - ¹¹ Schrock, R. R.; Seidel, S. W.; Schrodi, Y.; Davis, W. M. *Organometallics* **1999**, *18*, 428.
 - ¹² Cloke, F. G. N.; Hitchcock, P. B.; Love, J. B. *J. Chem. Soc., Dalton Trans.* **1995**, 25.
 - ¹³ Cochran, F. V.; Bonitatebus, P. J., Jr.; Schrock, R. R. *Organometallics* **2000**, *19*, 2414.
 - ¹⁴ Cochran, F. V.; Schrock, R. R. *Organometallics* **2001**, *20*, 2127.
 - ¹⁵ Cochran, F. V.; Hock, A. S.; Schrock, R. R. *Organometallics* **2004**, *23*, 665.
 - ¹⁶ Skinner, M. E. G.; Toupance, T.; Cowhig, D. A.; Tyrrell, B. R.; Mountford, P. *Organometallics* **2005**, *24*, 5586.
 - ¹⁷ Bonnet, F.; Hillier, A. C.; Collins, A.; Dubberley, S. R.; Mountford, P. *Dalton Transactions* **2005**, 421.
 - ¹⁸ Edema, J. J. H.; Auke; Meetsma, A.; Gambarotta, S. *J. Am. Chem. Soc.* **1989**, *111*, 6878.
 - ¹⁹ Ferguson, R.; Solari, E.; Floriani, C.; Chiesi-Villa, A.; Rizzoli, C. *Angewandte Chemie* **1993**,

- 105, 453.
- ²⁰ Buijink, J.-K. F.; Meetsma, A.; Teuben, J. H. *Organometallics* **1993**, *12*, 2004.
- ²¹ Berno, P.; Hao, S.; Minhas, R.; Gambarotta, S. *J. Am. Chem. Soc.* **1994**, *116*, 7417.
- ²² Song, J.-I.; Berno, P.; Gambarotta, S. *J. Am. Chem. Soc.* **1994**, *116*, 6927.
- ²³ Desmangles, N.; Jenkins, H.; Rupp, K. B.; Gambarotta, S. *Inorg. Chim. Acta* **1996**, *250*, 1.
- ²⁴ Hao, S.; Berno, P.; Minhas, R. K.; Gambarotta, S. *Inorg. Chim. Acta* **1996**, *244*, 37.
- ²⁵ Ferguson, R.; Solari, E.; Floriani, C.; Osella, D.; Ravera, M.; Re, N.; Chiesi-Villa, A.; Rizzoli, C. *J. Am. Chem. Soc.* **1997**, *119*, 10104.
- ²⁶ Vidyaratne, I.; Gambarotta, S.; Korobkov, I.; Budzelaar, P. H. M. *Inorg. Chem.* **2005**, *44*, 1187.
- ²⁷ Berno, P.; Gambarotta, S. *Angewandte Chemie, International Edition in English* **1995**, *34*, 822.
- ²⁸ Clentsmith, G. K. B.; Bates, V. M. E.; Hitchcock, P. B.; Cloke, F. G. N. *J. Am. Chem. Soc.* **1999**, *121*, 10444.
- ²⁹ Chenevert, R.; Dickman, M. *J. Org. Chem.* **1996**, *61*, 3332.
- ³⁰ Chong, H.-S.; Garmestani, K.; L. Henry Bryant, J.; Brechbiel, M. W. *J. Org. Chem.* **2001**, *66*, 7745.
- ³¹ Chong, H.-s.; Ganguly, B.; Broker, G. A.; Rogers, R. D.; Brechbiel, M. W. *J. Chem. Soc., Perkin Trans. 1* **2002**, 2080.
- ³² Pilyugina, T. S.; Schrock, R. R.; Hock, A. S.; Mueller, P. *Organometallics* **2005**, *24*, 1929.
- ³³ Yandulov, D. V.; Schrock, R. R., *J. Am. Chem. Soc.* **2002**, *124*, 6252.
- ³⁴ Yandulov, D. V.; Schrock, R. R.; Rheingold, A. L.; Ceccarelli, C.; Davis, W. M., *Inorg. Chem.* **2003**, *42*, 796.
- ³⁵ Yandulov, D. V.; Schrock, R. R., *Science* **2003**, *301*, 76.
- ³⁶ Manzer *Inorg. Syn.* **1982**, *21*, 135.
- ³⁷ Hawker, P. N.; Timms, P. L. *J. Chem. Soc., Dalton Trans.* **1983**, 1123.
- ³⁸ Feig, A. L.; Becker, M.; Schindler, S.; Eldik, R. v.; Lippard, S. J. *Inorg. Chem.* **1996**, *35*, 2590.
- ³⁹ Evans, D. F., *J. Chem. Soc.* **1959**, 2003.
- ⁴⁰ Sur, S. K., *J. Mag. Res.* **1989**, *82*, 169.
- ⁴¹ Sheldrick, G. M., *Acta Cryst. Sect. A* **1990**, *46*, 467.
- ⁴² Sheldrick, G. M. SHELXL 97, Universität Göttingen, Göttingen, Germany, 1997.
- ⁴³ Farrugia, L. J., *J. Appl. Cryst.* **1997**, *30*, 565.

Chapter 3

Synthesis of [(HIPTNCH₂CH₂)₃N]Cr Compounds (HIPT = 3,5-(2,4,6-*i*-Pr₃C₆H₂)₂C₆H₃)
and an Evaluation of Chromium for the Reduction of Dinitrogen to Ammonia.

Text from this chapter has appeared in print:

Nathan C. Smythe, Richard R. Schrock, Peter Müller, and Walter W. Weare. "Synthesis of [(HIPTNCH₂CH₂)₃N]Cr Compounds (HIPT = 3,5-(2,4,6-*i*-Pr₃C₆H₂)₂C₆H₃) and an Evaluation of Chromium for the Reduction of Dinitrogen to Ammonia. *Inorganic Chemistry*, In Press.

3.1 Introduction

Many tungsten complexes analogous to the isolated molybdenum catalysts have been prepared and characterized.¹ One important exception is $[\text{HIPTN}_3\text{N}]\text{W}(\text{NH}_3)$, the analog of $[\text{HIPTN}_3\text{N}]\text{Mo}(\text{NH}_3)$, which is known to react with dinitrogen to generate ammonia and $[\text{HIPTN}_3\text{N}]\text{MoN}_2$. Electrochemical reduction of $\{[\text{HIPTN}_3\text{N}]\text{W}(\text{NH}_3)\}[\text{BAr}'_4]$ in 0.1M [*n*-Bu₄N][BAr'₄]/PhF at a glassy carbon electrode reveals an irreversible wave at -2.06 V vs. FeCp₂⁺⁰. In contrast, one electron reduction of $\{[\text{HIPTN}_3\text{N}]\text{Mo}(\text{NH}_3)\}[\text{BAr}'_4]$ is fully reversible both in PhF (0.1M [Bu₄N][BAr'₄]) at a glassy carbon electrode and THF (0.4 M [Bu₄N][PF₆]) at a platinum disk and takes place at $E^{\circ'}([\text{HIPTN}_3\text{N}]\text{Mo}(\text{NH}_3)^{+/0}) = -1.63$ V vs. FeCp₂⁺⁰ in PhF (0.1M [Bu₄N][BAr'₄]). The difference in $[\text{HIPTN}_3\text{N}]\text{M}(\text{NH}_3)^{+/0}$ (M = Mo, W) potentials (~430 mV) suggests that Cr(Cp*)₂ is much too weak a reducing agent to reduce $\{[\text{HIPTN}_3\text{N}]\text{W}(\text{NH}_3)\}[\text{BAr}'_4]$ to any significant degree. The irreversibility of the $\{[\text{HIPTN}_3\text{N}]\text{W}(\text{NH}_3)\}[\text{BAr}'_4]$ reduction suggests that $[\text{HIPTN}_3\text{N}]\text{W}(\text{NH}_3)$ may not be a well-behaved species. In view of these findings it is perhaps not surprising that no ammonia was formed from dinitrogen in attempted catalytic reductions with $[\text{HIPTN}_3\text{N}]\text{W}(\text{N}_2)$.

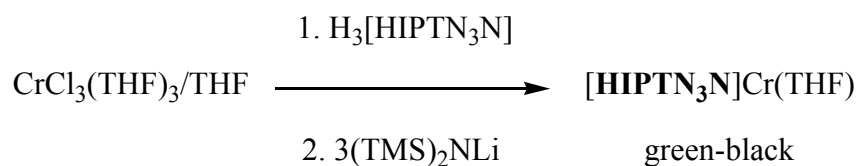
In light of this, we became interested in whether $[\text{HIPTN}_3\text{N}]\text{Cr}$ complexes could be prepared and whether a compound such as $[\text{HIPTN}_3\text{N}]\text{CrN}$ might serve as a catalyst for catalytic reduction of dinitrogen.

3.2 Results

3.2.1 Syntheses of $[\text{HIPTN}_3\text{N}]\text{Cr}$ Complexes

Suitable starting materials for chromium chemistry are CrCl₃ and CrCl₃(THF)₃. $[\text{HIPTN}_3\text{N}]\text{Cr}$ (**36**; $\mu_{\text{eff}} = 3.03$ BM) can be prepared from CrCl₃ and $[\text{HIPTN}_3\text{N}]\text{Cr}(\text{THF})$ (**37**; $\mu_{\text{eff}} = 2.46$ BM) can be prepared from CrCl₃(THF)₃, although no crystals of either **36** or **37** suitable for X-ray studies have been obtained. Both are extraordinarily soluble in organic solvents and difficult to crystallize in general. $[\text{HIPTN}_3\text{N}]\text{Cr}$ is analogous to [*t*-BuMe₂SiN₃N]Cr² and [Me₃SiN₃N]Cr.³

Green-black $[\text{HIPTN}_3\text{N}]\text{Cr}(\text{THF})$ is prepared as shown (Equation 3.1) in a manner that is analogous to the synthesis of $[\text{HIPTN}_3\text{N}]\text{MoCl}$ from $\text{MoCl}_4(\text{THF})_2$. The nature of the adduct that is formed upon stirring $\text{H}_3[\text{HIPTN}_3\text{N}]$ with $\text{CrCl}_3(\text{THF})_3$ in THF for one hour is not known.



Equation 3.1: Synthesis of $[\text{HIPTN}_3\text{N}]\text{Cr}(\text{THF})$.

The synthesis of red-black $[\text{HIPTN}_3\text{N}]\text{Cr}$ consists of generating $\text{Li}_3[\text{HIPTN}_3\text{N}]$ *in situ* from $\text{H}_3[\text{HIPTN}_3\text{N}]$ and three equivalents of $(\text{Me}_3\text{Si})_2\text{NLi}$ in diethyl ether, adding CrCl_3 , and stirring the heterogeneous mixture for two days. $[\text{HIPTN}_3\text{N}]\text{Cr}$ is converted into $[\text{HIPTN}_3\text{N}]\text{Cr}(\text{THF})$ upon addition of THF to a solution of $[\text{HIPTN}_3\text{N}]\text{Cr}$, while application of heat and vacuum to solid $[\text{HIPTN}_3\text{N}]\text{Cr}(\text{THF})$ yields $[\text{HIPTN}_3\text{N}]\text{Cr}$. Interconversion of $[\text{HIPTN}_3\text{N}]\text{Cr}(\text{THF})$ and $[\text{HIPTN}_3\text{N}]\text{Cr}$ in this manner appears to be entirely reversible. The two compounds also appear to react entirely analogously as described below. It should be noted that $[\text{HIPTN}_3\text{N}]\text{Cr}$ and $[\text{HIPTN}_3\text{N}]\text{Cr}(\text{THF})$ show no absorption that can be ascribed to an N_2 stretch in IR spectra in heptane (Figure 3.1). The absorptions shown are ascribed to ligand modes that are comparable to those seen in the $[\text{HIPTN}_3\text{N}]\text{Mo}$ and $[\text{HIPTN}_3\text{N}]\text{W}$ systems.

Reduction of $\{\text{Cr}|\text{Cr}(\text{THF})\}$ (which means either $[\text{HIPTN}_3\text{N}]\text{Cr}$ or $[\text{HIPTN}_3\text{N}]\text{Cr}(\text{THF})$) with potassium graphite in diethyl ether at room temperature yields $[\text{HIPTN}_3\text{N}]\text{CrK}$ ($\mu_{\text{eff}} = 3.74 \text{ BM}$) as a yellow-orange powder. (See Scheme 3.1 for the reactions of $\{\text{Cr}|\text{Cr}(\text{THF})\}$) The solution IR spectrum of $[\text{HIPTN}_3\text{N}]\text{CrK}$ in heptane is identical to the IR spectra for $[\text{HIPTN}_3\text{N}]\text{Cr}$ and $[\text{HIPTN}_3\text{N}]\text{Cr}(\text{THF})$ shown in Figure 3.1, i.e., there is no evidence that dinitrogen is incorporated before or after reduction of Cr(III) to yield " $\{[\text{HIPTN}_3\text{N}]\text{Cr}(\text{N}_2)\}\text{K}$," which would be an analog of various derivatives of $\{[\text{HIPTN}_3\text{N}]\text{Mo}(\text{N}_2)\}^-$. The IR spectra of $\{[\text{HIPTN}_3\text{N}]\text{Mo}(\text{N}_2)\}^-$ derivatives have an absorption for ν_{NN} in the region $1680\text{-}1830 \text{ cm}^{-1}$, depending upon the nature of the metal cation and its degree of solvation.⁴ $[\text{HIPTN}_3\text{N}]\text{CrK}$ is believed to be the potassium salt of the Cr(II) anion with no substituent in the apical pocket except the potassium ion. The potassium ion is likely to be supported through interaction with one or more aryl rings, as observed in a variety of anions

that contain arylated amido ligands in the literature.^{1,5,6,7,8} However, a structure similar to that found in $[\text{Me}_3\text{SiN}_3\text{N}]\text{CrK}(\text{THF})_2$ ⁹ where the alkali metal is supported by two of the amido

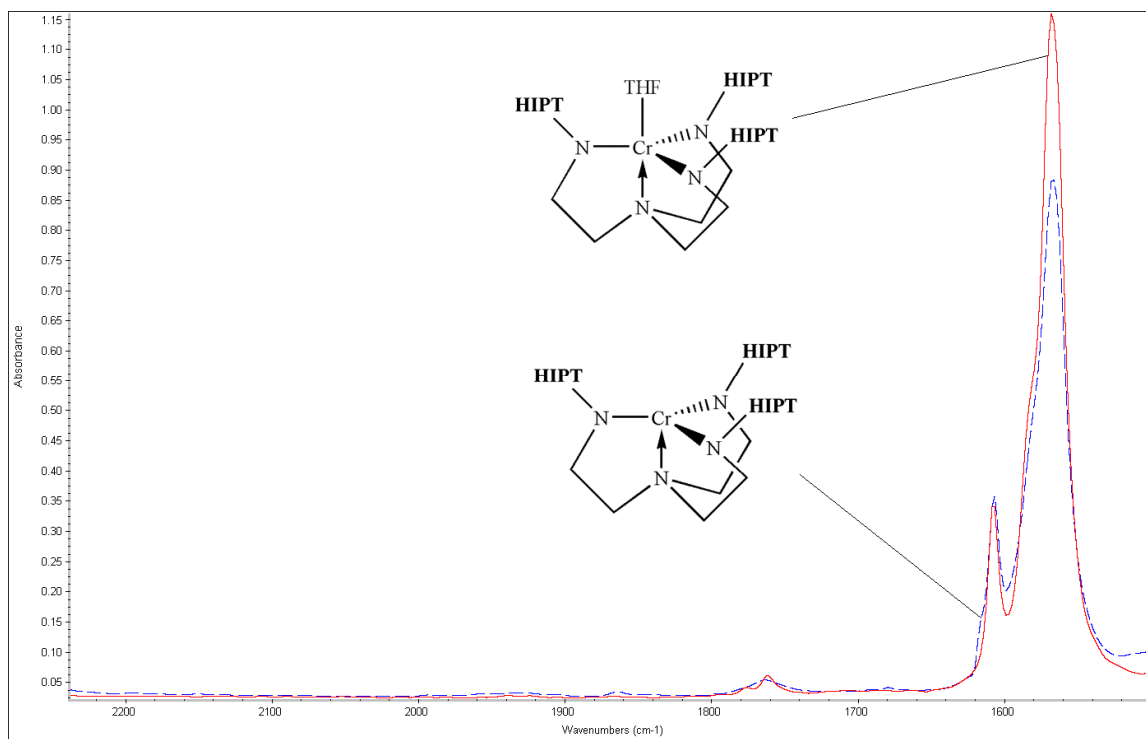


Figure 3.1: Solution IR spectra (heptane, solvent subtracted) of $[\text{HIPTN}_3\text{N}]\text{Cr}$ and $[\text{HIPTN}_3\text{N}]\text{Cr}(\text{THF})$.

nitrogens and THF cannot be ruled out. X-ray quality single crystals of $[\text{HIPTN}_3\text{N}]\text{CrK}$ have not yet been obtained. In an attempt to obtain a more crystalline species 18-crown-6 was added to an ethereal solution of $[\text{HIPTN}_3\text{N}]\text{CrK}$ to yield " $\{[\text{HIPTN}_3\text{N}]\text{Cr}\}18\text{-crown-6(K)}$." This species is only slightly soluble in pentane, which supports our formulation of $[\text{HIPTN}_3\text{N}]\text{CrK}$ as an anionic potassium salt. Unfortunately, attempts to obtain X-ray quality crystals so far have yielded only powder. The formulation of $[\text{HIPTN}_3\text{N}]\text{CrK}$ is further supported by its reaction with CO as discussed below.

Exposure of a degassed solution of $\{\text{Cr}|\text{Cr}(\text{THF})\}$ in pentane to an atmosphere of CO at room temperature yields a red solution, although the reaction requires several minutes to go to completion. IR spectra suggest that the product of this reaction is $[\text{HIPTN}_3\text{N}]\text{CrCO}$. In heptane ν_{CO} is found at 1951 cm^{-1} ; in $[\text{HIPTN}_3\text{N}]\text{Cr}^{13}\text{CO}$ $\nu_{13\text{CO}}$ is found 1907 cm^{-1} and $\nu_{13\text{C}18\text{O}}$ is found at 1862 cm^{-1} . $[\text{HIPTN}_3\text{N}]\text{CrCO}$ was further characterized in an x-ray study of a crystal obtained from heptane at room temperature (Figure 3.2). (All structural studies are discussed together in

Section 3.3) It should be noted that the reaction between $\{\text{Cr}|\text{Cr}(\text{THF})\}$ and CO is not instantaneous, which raises the possibility that $\{\text{Cr}|\text{Cr}(\text{THF})\}$ is a relatively high spin state and that a low spin doublet is required to bind CO. The Evans method was employed to show that $[\text{HIPTN}_3\text{N}]\text{CrCO}$ is a low spin species ($\mu_{\text{eff}} = 1.69 \text{ BM}$). It should be noted that Cummins' chromium *tris*-amide system does not bind CO.¹⁰

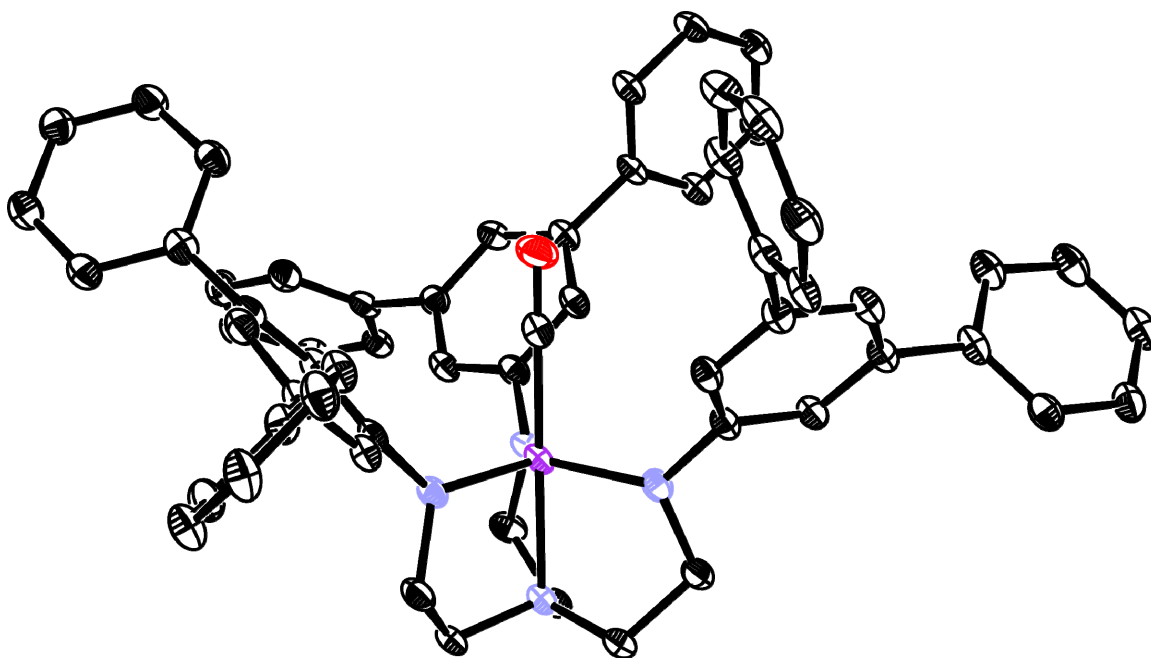


Figure 3.2: ORTEP diagram of $[\text{HIPTN}_3\text{N}]\text{CrCO}$ with thermal ellipsoids at 50% probability. Hydrogen atoms isopropyl groups, and solvent (heptane) removed for clarity.

Reduction of red $[\text{HIPTN}_3\text{N}]\text{CrCO}$ in diethyl ether with potassium graphite quickly yields a green solution of $\{[\text{HIPTN}_3\text{N}]\text{CrCO}\}\text{K}$ (Figure 3.3). IR spectra are consistent with formulation of $\{[\text{HIPTN}_3\text{N}]\text{CrCO}\}\text{K}$ as a reduced carbonyl complex, according to a ν_{CO} stretch at 1711 cm^{-1} and a $\nu_{13\text{CO}}$ stretch at 1670 cm^{-1} . (In $\{[\text{HIPTN}_3\text{N}]\text{MoCO}\}\text{Na}$ the ν_{CO} stretch is found at 1632 cm^{-1} .¹¹) $\{[\text{HIPTN}_3\text{N}]\text{CrCO}\}\text{K}$ also may be prepared by treating $\{[\text{HIPTN}_3\text{N}]\text{Cr}\}\text{K}$ with CO in pentane, consistent with the proposed formulation.

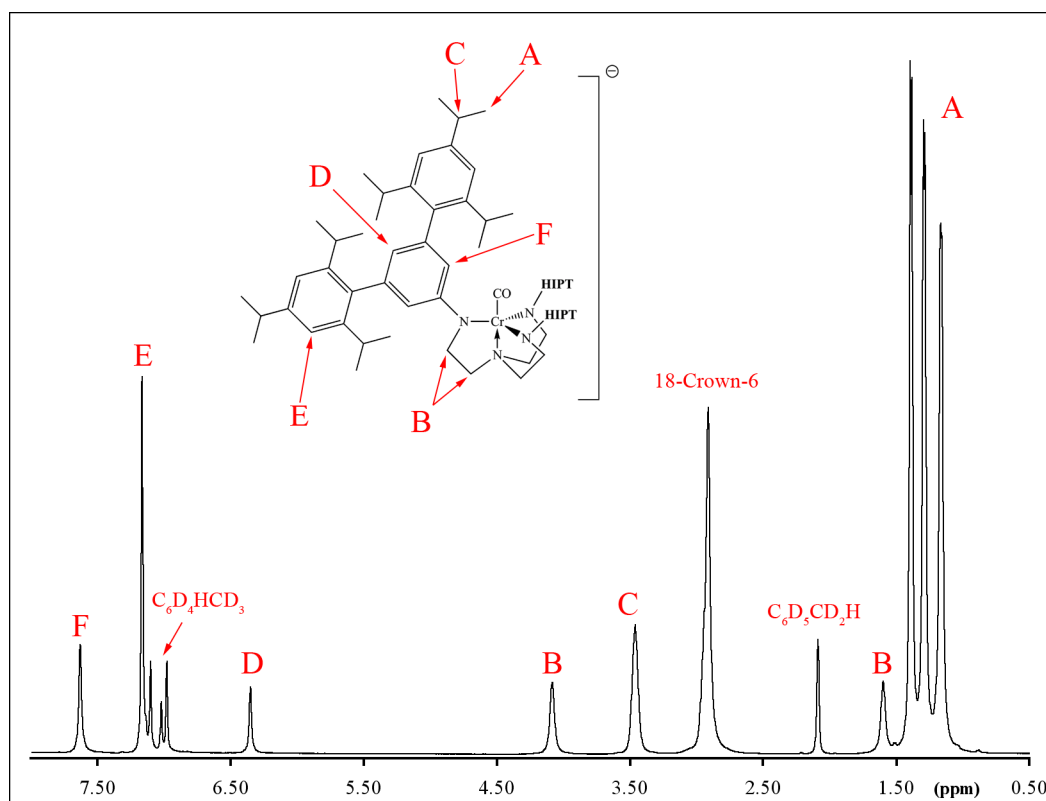


Figure 3.3: ^1H NMR spectrum (toluene- d_8) of $\{[\text{HIPTN}_3\text{N}]\text{CrCO}\}18\text{-Crown-6(K)}$.

The reaction between $\{\text{Cr}|\text{Cr}(\text{THF})\}$ and NO instantly gives a blood-red solution of $[\text{HIPTN}_3\text{N}]\text{CrNO}$. $[\text{HIPTN}_3\text{N}]\text{CrNO}$ has an absorption at 1715 cm^{-1} in its IR spectrum in heptane ascribable to ν_{NO} , and has been further characterized in an X-ray diffraction study (Figure 3.4, and Section 3.3). A ^1H NMR spectrum of $[\text{HIPTN}_3\text{N}]\text{CrNO}$ (Figure 3.5) shows sharp resonances in the normal region typical of a diamagnetic compound. Therefore $[\text{HIPTN}_3\text{N}]\text{CrNO}$ appears to have four electrons in the two orbitals that are employed for back-bonding to NO, namely d_{xz} and d_{yz} (if the z axis is the three-fold axis). Unlike $[\text{HIPTN}_3\text{N}]\text{CrCO}$, $[\text{HIPTN}_3\text{N}]\text{CrNO}$ is not susceptible to reduction by potassium graphite which is consistent with NO acting as a reducing equivalent and chromium existing in the 2^+ oxidation state.

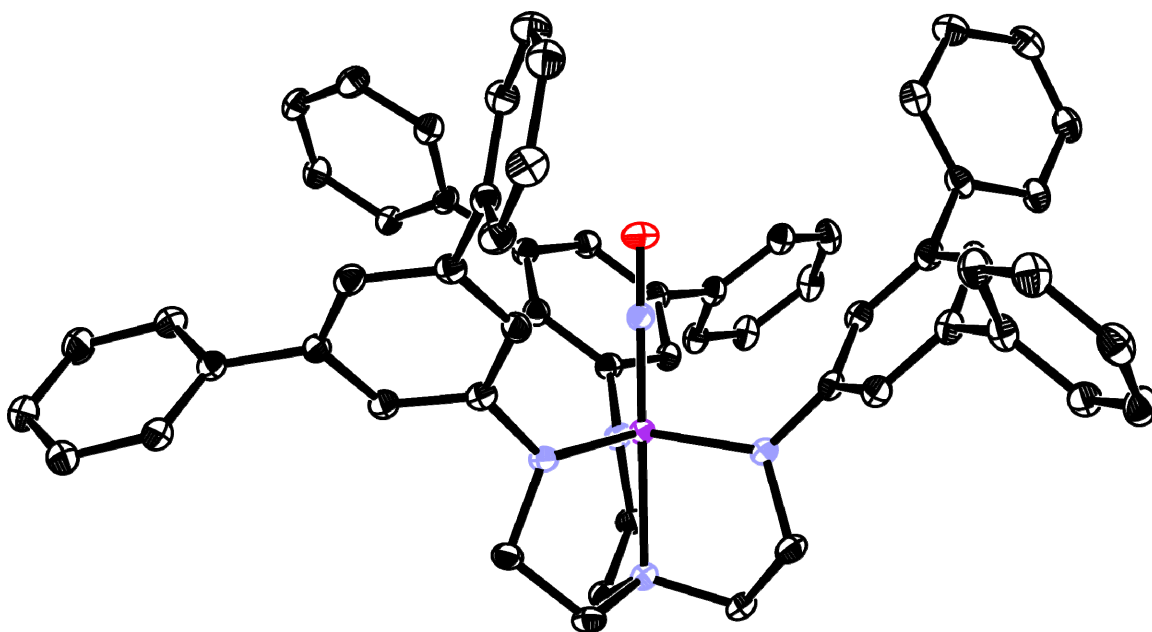


Figure 3.4: ORTEP diagram of [HIPTN₃N]CrNO with thermal ellipsoids at 50% probability. Hydrogen atoms isopropyl groups, and solvent (heptane) removed for clarity.

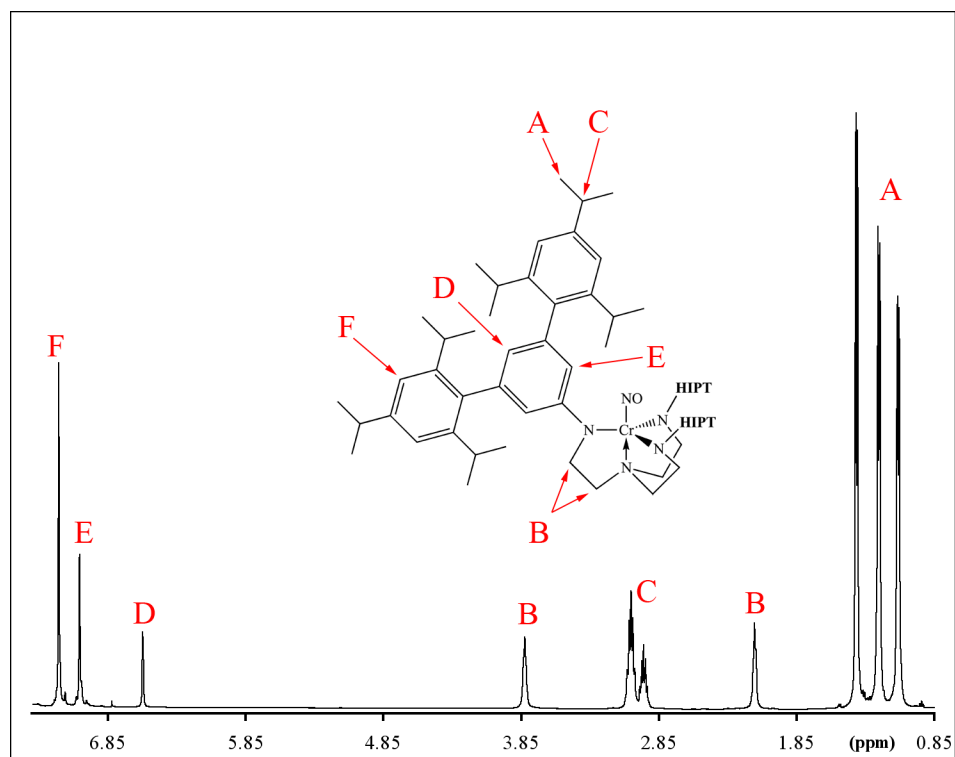


Figure 3.5: ¹H NMR spectrum (C₆D₆) of [HIPTN₃N]CrNO.

Compound $\{\text{Cr}|\text{Cr}(\text{THF})\}$ is oxidized by AgCl in diethyl ether at room temperature over a period of three days in the absence of light to give dark purple $[\text{HIPTN}_3\text{N}]\text{CrCl}$ and silver metal. $[\text{HIPTN}_3\text{N}]\text{CrCl}$ may be crystallized from a saturated pentane solution. Isolated yields of $[\text{HIPTN}_3\text{N}]\text{CrCl}$ vary between 40-65%. Although the yield appears to be higher, according to NMR spectra of solutions of the crude product, little $[\text{HIPTN}_3\text{N}]\text{CrCl}$ can be isolated from what remains after one or two crops have been isolated. A magnetic measurement (Evans method) shows $[\text{HIPTN}_3\text{N}]\text{CrCl}$ to have two unpaired electrons (2.55 BM), consistent with what would be expected of high spin Cr(IV) and what has been observed for the related $[\text{Me}_3\text{SiN}_3\text{N}]\text{CrCl}$ complex (2.6 BM).³ Crystallization of $[\text{HIPTN}_3\text{N}]\text{CrCl}$ from heptane at room temperature yielded crystals suitable for an X-ray structure, as described in section 3.3.

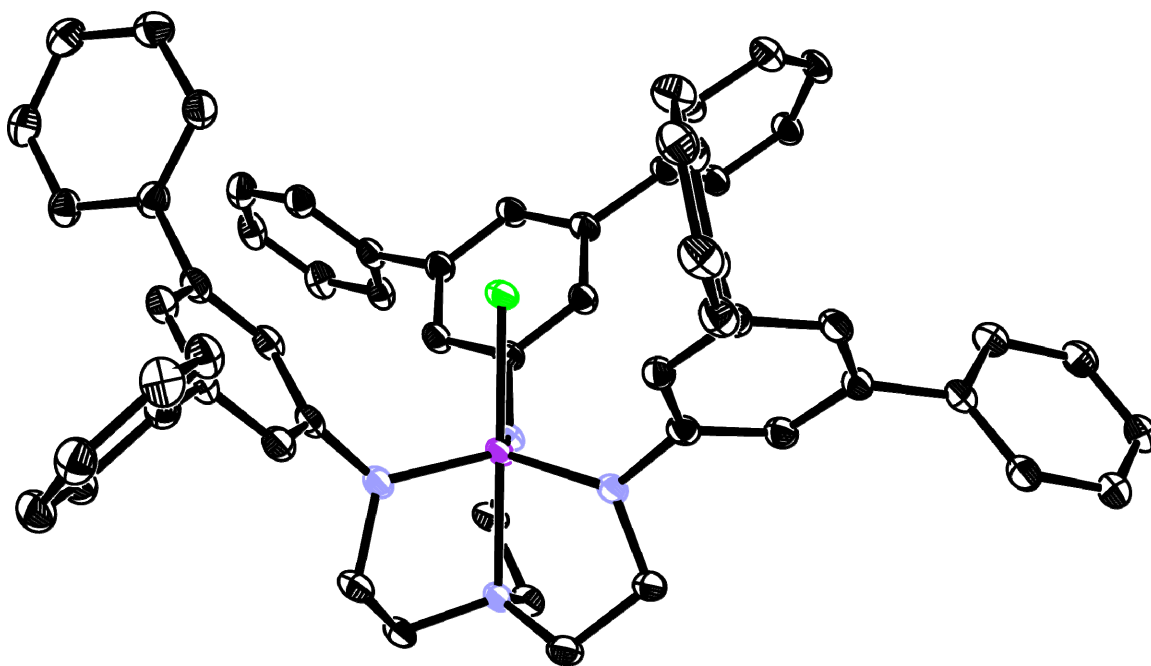


Figure 3.6: ORTEP diagram of $[\text{HIPTN}_3\text{N}]\text{CrCl}$ with thermal ellipsoids at 50% probability. Hydrogen atoms, isopropyl groups, and solvent (heptane) removed for clarity.

The Cr(VI) nitride, $[\text{HIPTN}_3\text{N}]\text{CrN}$ was prepared in 69% yield by heating a solution of $(n\text{-Bu}_4\text{N})\text{N}_3$ and $[\text{HIPTN}_3\text{N}]\text{CrCl}$ in benzene at $\sim 80^\circ\text{C}$ for one week, followed by removing the $(n\text{-Bu}_4\text{N})\text{Cl}$ and excess $(n\text{-Bu}_4\text{N})\text{N}_3$ and then heating the mixture of intermediate $[\text{HIPTN}_3\text{N}]\text{CrN}_3$ and $[\text{HIPTN}_3\text{N}]\text{CrN}$ in toluene to $\sim 110^\circ\text{C}$ for ten days. $[\text{HIPTN}_3\text{N}]\text{CrN}$ is a diamagnetic species with a proton NMR spectrum similar to that of $[\text{HIPTN}_3\text{N}]\text{CrNO}$ (Figure 3.9); it appears to be somewhat stable in air. Crystallization (from heptane) of the product of a

reaction that was carried out in benzene at 80 °C for 3 days was shown in an X-ray study to be a 65:35 mixture of $[\text{HIPTN}_3\text{N}]\text{CrCl}$ and $[\text{HIPTN}_3\text{N}]\text{CrN}_3$ (Figure 3.7, and Section 3.3), while the reaction between $[\text{HIPTN}_3\text{N}]\text{CrCl}$ and $(n\text{-Bu}_4\text{N})\text{N}_3$ in benzene at 100 °C for five days yielded a 50:50 mixture of $[\text{HIPTN}_3\text{N}]\text{CrN}_3$ and $[\text{HIPTN}_3\text{N}]\text{CrN}$, as shown in an X-ray study (Figure 3.8, and Section 3.3). The reaction between $[\text{HIPTN}_3\text{N}]\text{CrCl}$ and $(n\text{-Bu}_4\text{N})\text{N}_3$ in toluene at 120 °C for one week gave a mixture of $[\text{HIPTN}_3\text{N}]\text{CrCl}$ and $[\text{HIPTN}_3\text{N}]\text{CrN}$, according to elemental analysis and IR spectra. We propose that $(n\text{-Bu}_4\text{N})\text{N}_3$ decomposes slowly at 120 °C before it can react with $[\text{HIPTN}_3\text{N}]\text{CrCl}$ to give first $[\text{HIPTN}_3\text{N}]\text{CrN}_3$ and subsequently $[\text{HIPTN}_3\text{N}]\text{CrN}$; this is the reason why the synthesis must be carried out in two stages, as described above. There was little or no reaction between $[\text{HIPTN}_3\text{N}]\text{CrCl}$ and $(\text{Me}_3\text{Si})\text{N}_3$ in benzene at 80 °C or $[\text{HIPTN}_3\text{N}]\text{CrCl}$ and NaN_3 in THF at room temperature. $[\text{HIPTN}_3\text{N}]\text{CrN}$ also could not be prepared by treating $[\text{HIPTN}_3\text{N}]\text{CrNO}$ with *tris*-mesityl vanadium, a method used by Cummins to prepare *tris*-amido chromium nitrides.¹⁰

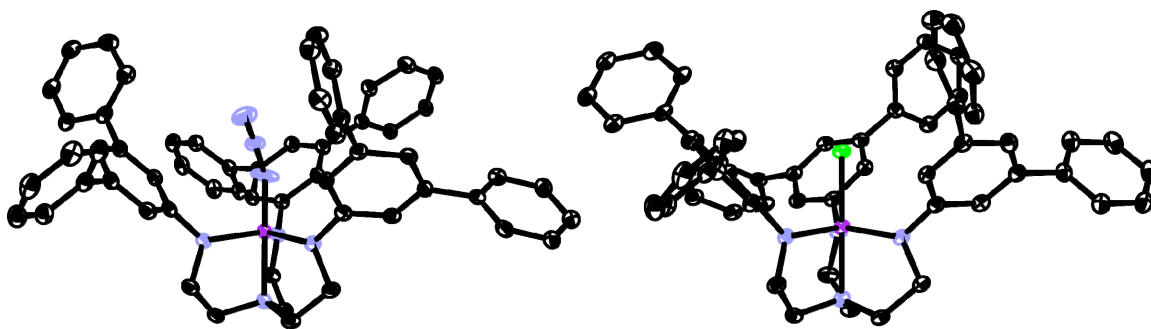


Figure 3.7: ORTEP diagram of $[\text{HIPTN}_3\text{N}]\text{CrCl}/[\text{HIPTN}_3\text{N}]\text{CrN}_3$ (shown as separate diagrams) with thermal ellipsoids at 50% probability. Hydrogen atoms, isopropyl groups, and solvent (heptane) removed for clarity.

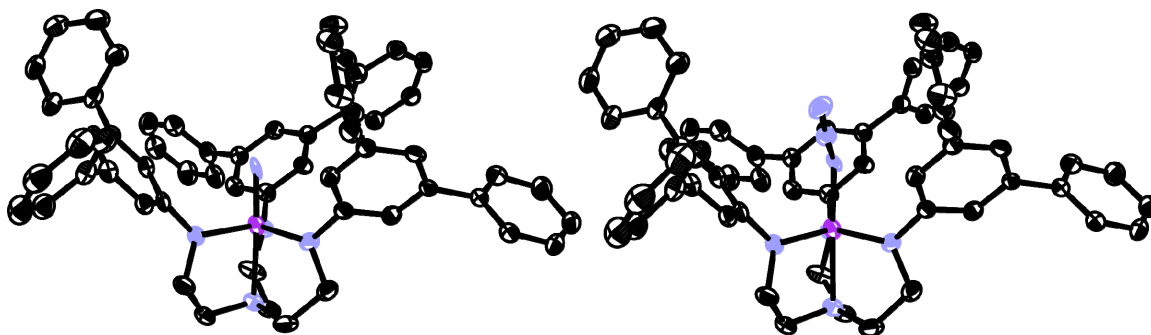


Figure 3.8: ORTEP diagram of $[\text{HIPTN}_3\text{N}]\text{CrN}/[\text{HIPTN}_3\text{N}]\text{CrN}_3$ (shown as separate diagrams) with thermal ellipsoids at 50% probability. Hydrogen atoms, isopropyl groups, and solvent (heptane) removed for clarity.

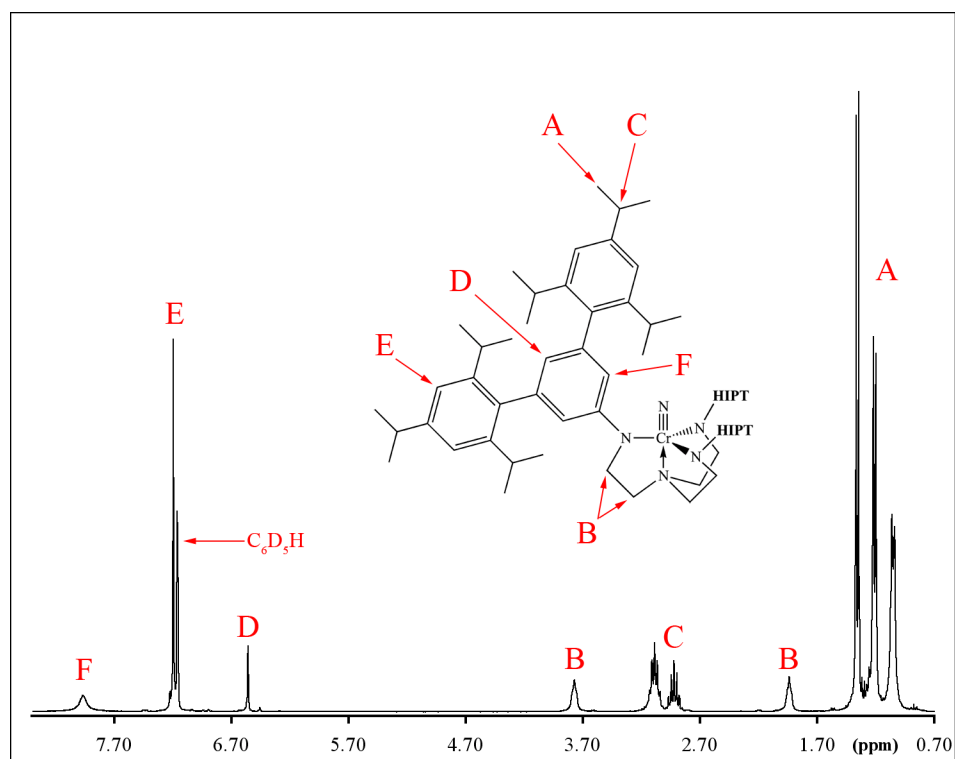


Figure 3.9: ¹H NMR spectrum (C₆D₆) of [HIPTN₃N]CrN.

A striking property of [HIPTN₃N]CrN that complicated its identification is a variation of its color between green and purple in different solvents and at different temperatures (Figure 3.10). For example, at room temperature, a solution of [HIPTN₃N]CrN in benzene is dark green while at 80-90 °C it is dark purple. In contrast, a solution of [HIPTN₃N]CrN in heptane at room temperature is dark purple but turns dark green upon cooling the solution to -35 °C. Upon warming, the solution turns purple again. These color changes are all reversible and adding benzene to a heptane solution of [HIPTN₃N]CrN begins to change the color from dark purple to dark green. UV/Vis spectra of [HIPTN₃N]CrN in benzene and heptane have absorptions that are similar in shape, but at different positions in the two solvents. This solvent/temperature color dependence is illustrated in Figure 3.10. The origin of this behavior is not known. One plausible explanation is that two isomers are present, e.g., the five-coordinate species whose structure has been determined and a *four*-coordinate species in which the central amine donor is not bound to the metal.

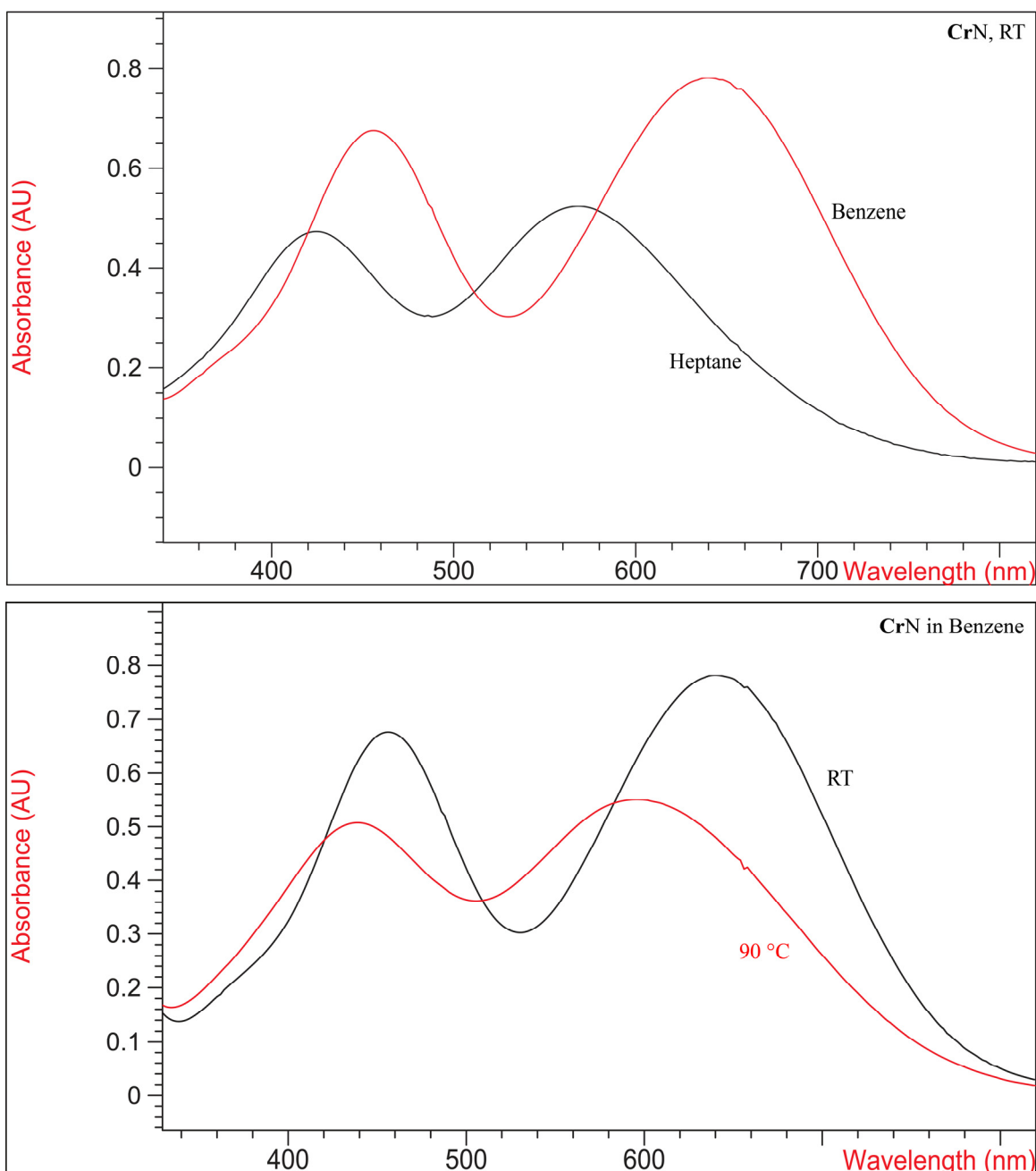


Figure 3.10: UV/Vis spectra of $[\text{HIPTN}_3\text{N}]\text{CrN}$.

The measured magnetic moments of $[\text{HIPTN}_3\text{N}]\text{Cr}$ (3.03 BM), $[\text{HIPTN}_3\text{N}]\text{Cr}(\text{THF})$ (2.46 BM), and $\{[\text{HIPTN}_3\text{N}]\text{Cr}\}\text{K}$ (3.74 BM) are lower than expected based on the spin-only values (3.87 BM for $[\text{HIPTN}_3\text{N}]\text{Cr}$ and $[\text{HIPTN}_3\text{N}]\text{Cr}(\text{THF})$, and 4.90 BM for $\{[\text{HIPTN}_3\text{N}]\text{Cr}\}\text{K}$), which can be explained as a combination of factors. First, it should be emphasized that these are "as isolated" complexes, in contrast to $[\text{HIPTN}_3\text{N}]\text{CrCl}$ and

$[\text{HIPTN}_3\text{N}]\text{CrCO}$ which have been purified by crystallization. An illustration of this can be seen in the magnetic moment of crude $[\text{HIPTN}_3\text{N}]\text{CrCO}$, which was measured to be 1.82 BM compared to the purified complex (1.69 BM). This demonstrates that though the measured moments are undoubtedly different from that of the pure complexes, they are indicative of the order of magnitude. Generating, what is presumed to be a more pure $\{[\text{HIPTN}_3\text{N}]\text{Cr}\}\text{K}$ complex, by the addition of two equivalents of potassium graphite to an ethereal solution or $[\text{HIPTN}_3\text{N}]\text{CrCl}$ yields a moment of 4.16 BM, while doing the reduction in THF (assuming the potassium ion is supported by two molecules as in $\{[\text{Me}_3\text{SiN}_3\text{N}]\text{Cr}\}\text{K}(\text{THF})_2$ (5.1 BM)⁹) yields a moment of 4.06 BM (The question of the quantity of bound THF is not significant on a mass basis as each THF molecule only shifts the moment calculation by about 0.08 BM). These results indicate that the true magnetic moments for $[\text{HIPTN}_3\text{N}]\text{Cr}$, $[\text{HIPTN}_3\text{N}]\text{Cr}(\text{THF})$, and $\{[\text{HIPTN}_3\text{N}]\text{Cr}\}\text{K}$ are in fact below the spin-only value and point to the possibility that the low spin state is more accessible than in chromium complexes supported by $[\text{Me}_3\text{SiN}_3\text{N}]^{3-}$ and $[\text{tBuMe}_2\text{SiN}_3\text{N}]^{3-}$.

3.3 X-ray Studies

Five crystal structures of $[\text{HIPTN}_3\text{N}]^{3-}$ containing chromium complexes have been determined (Table 3.1). Three studies involved pure compounds ($[\text{HIPTN}_3\text{N}]\text{CrCl}$ (Figure 3.6), $[\text{HIPTN}_3\text{N}]\text{CrCO}$ (Figure 3.2), and $[\text{HIPTN}_3\text{N}]\text{CrNO}$ (Figure 3.4)), while two studies involved mixtures of two co-crystallized compounds ($[\text{HIPTN}_3\text{N}]\text{CrCl}$ and $[\text{HIPTN}_3\text{N}]\text{CrN}_3$ (65:35, Figure 3.7) and $[\text{HIPTN}_3\text{N}]\text{CrN}_3$ and $[\text{HIPTN}_3\text{N}]\text{CrN}$ (50:50, Figure 3.8)). All five compounds crystallize in the Cc space group and have almost identical structural parameters. The structures for the $[\text{HIPTN}_3\text{N}]\text{Cr}$ core and the accompanying solvent molecule (heptane) are all identical, ignoring the handedness in this chiral space group, except in the case of the $[\text{HIPTN}_3\text{N}]\text{CrCl}/[\text{HIPTN}_3\text{N}]\text{CrN}_3$ and $[\text{HIPTN}_3\text{N}]\text{CrN}_3/[\text{HIPTN}_3\text{N}]\text{CrN}$ mixtures, which have some ligand disorder in the isopropyl groups. It is clear that separation of any of these compounds from one another through crystallization from heptane will not be possible. Details concerning the solutions of the structures of the compounds in mixtures may be found in the Experimental Section.

	CrCl	CrCO	CrNO	CrN ₃ /CrCl	CrN ₃ /CrN
Formula	C ₁₂₁ H ₁₇₅ ClCr N ₄	C ₁₂₂ H ₁₇₅ CrN ₄ O	C ₁₂₁ H ₁₇₅ CrN ₅ O	C ₁₂₁ H ₁₇₅ Cl _{0.66} CrN ₅	C ₁₂₁ H ₁₇₅ CrN _{5.99}
fw (g/mol)	1773.10	1765.66	1767.66	1775.27	1765.46
Temperature (K)	100(2)	100(2)	100(2)	100(2)	100(2)
Space Group	Cc	Cc	Cc	Cc	Cc
a (Å)	15.7588(8)	15.7406(14)	15.7440(6)	15.7434(6)	15.795(2)
b (Å)	39.997(2)	39.859(4)	39.7549(16)	39.9919(15)	39.976(7)
c (Å)	17.7963(10)	17.7657(17)	17.7703(6)	17.7938(7)	17.856(3)
α (°)	90	90	90	90	90
β (°)	95.501(2)	95.342(3)	95.2400(10)	95.2800(10)	94.499(5)
γ (°)	90	90	90	90	90
GoF	1.029	1.067	1.027	1.037	1.031
R [I>2σ(I)] (%)	R ₁ =4.3, wR ₂ =10.1	R ₁ =6.1, wR ₂ =14.7	R ₁ =4.5, wR ₂ =10.5	R ₁ =5.9, wR ₂ =12.0	R ₁ =5.6, wR ₂ =12.9
R (all data) (%)	R ₁ =5.5, wR ₂ =10.8	R ₁ =8.3, wR ₂ =16.3	R ₁ =5.5, wR ₂ =11.0	R ₁ =8.4, wR ₂ =13.1	R ₁ =7.1, wR ₂ =13.6
Cr-N(x), avg. (Å)	1.886	1.878	1.876	1.885	1.887
Cr-N(donor) (Å)	2.123	2.109	2.132	2.129	2.234
Planar Displacement, avg. (Å)	0.24	0.22	0.25	0.24	0.29
C(x01)-N(x)-Cr, avg (°)	129.6	129.8	128.8	129.3	127.7

Table 3.1: X-Ray structure solution parameters and selected ligand core parameters.

The ligand core of the structures reported here were compared to the available [HIPTN₃N]Mo structures ($\{[\text{HIPTN}_3\text{N}]\text{MoN}_2\}\text{MgBr}(\text{THF})_3$),⁴ [HIPTN₃N]Mo(N₂),⁴

$[\text{HIPTN}_3\text{N}]\text{Mo}\equiv\text{N}$,⁴ $[\text{HIPTN}_3\text{N}]\text{Mo}-\text{N}=\text{NH}$, $[\text{HIPTN}_3\text{N}]\text{Mo}(\text{NH}_3)$,¹² $\{[\text{HIPTN}_3\text{N}]\text{Mo}[2,6\text{-Lutidine}]\}^+$,¹² $\{[\text{HIPTN}_3\text{N}]\text{Mo}=\text{NNH}_2\}\text{BAr}'_4$ ($\text{Ar}' = 3,5\text{-(CF}_3)_2\text{C}_6\text{H}_3$),¹² $\{[\text{HIPTN}_3\text{N}]\text{Mo}(\text{NH}_3)\}\text{BAr}'_4$,⁴ $\{[\text{HIPTN}_3\text{N}]\text{Mo}=\text{NH}\}\text{BAr}'_4$,¹² $[\text{HIPTN}_3\text{N}]\text{Mo}(\eta^2\text{-CH}_2\text{CH}_2)$,¹¹ $[\text{HIPTN}_3\text{N}]\text{Mo}(\text{CH}_2\text{CH}_3)$,¹¹ $\{[\text{HIPTN}_3\text{N}]\text{Mo}(\eta^2\text{-CH}_2\text{CH}_2)\}\text{BAr}'_4$,¹¹ $\{[\text{HIPTN}_3\text{N}]\text{Mo}(\text{THF})\}\text{BPh}_4$,¹³ and $[\text{HIPTN}_3\text{N}]\text{W}$ structures¹ ($\{[\text{HIPTN}_3\text{N}]\text{W}(\text{N}_2)\}\text{K}$, $[\text{HIPTN}_3\text{N}]\text{W}(\text{N}_2)$, $[\text{HIPTN}_3\text{N}]\text{W}-\text{N}=\text{NH}$, $\{[\text{HIPTN}_3\text{N}]\text{W}=\text{NNH}_2\}\text{BAr}'_4$, and $\{[\text{HIPTN}_3\text{N}]\text{W}(\text{NH}_3)\}\text{BAr}'_4$). The displacement of the metal atom from the plane defined by the three ligand amido nitrogens was calculated by using the amido-metal bond length and amido-metal-donor angle and averaging the three results (Figure 3.11).

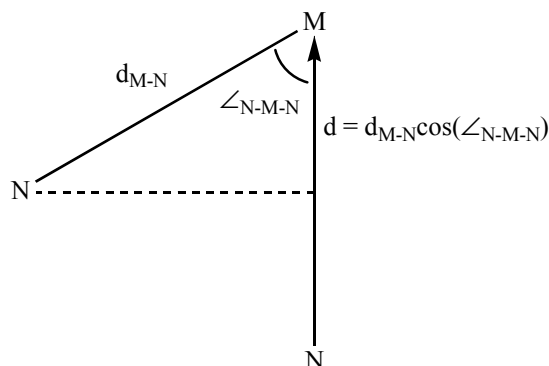


Figure 3.11: Calculation of metal displacement from the *tris*-amido plane.

Although the normality of the M-donor vector to this plane was assumed, the low standard deviations throughout each group of three calculations show that this assumption is reasonable. Average displacements of 0.36 Å ($\sigma = 0.05$ Å) for $[\text{HIPTN}_3\text{N}]\text{Mo}$ and 0.34 Å ($\sigma = 0.03$ Å) for $[\text{HIPTN}_3\text{N}]\text{W}$ are not significantly different. $[\text{HIPTN}_3\text{N}]\text{Cr}$ is slightly different, with parameters 0.25 Å ($\sigma = 0.03$ Å), which translates into chromium being on average ~ 0.1 Å deeper in the protected pocket. This pattern is emulated in the metal-N(amido) bond lengths, with the $[\text{HIPTN}_3\text{N}]\text{Mo}$ and $[\text{HIPTN}_3\text{N}]\text{W}$ averages being identical at 1.98 Å ($\sigma = 0.02$ Å and $\sigma = 0.03$ Å respectively) and $[\text{HIPTN}_3\text{N}]\text{Cr}$ being about 0.1 Å shorter at 1.88 Å ($\sigma = 0.01$ Å). The nitrogen-donor to metal bond shows no significant variation between $[\text{HIPTN}_3\text{N}]\text{Cr}$ (2.16 Å, $\sigma = 0.05$ Å), $[\text{HIPTN}_3\text{N}]\text{Mo}$ (2.23 Å, $\sigma = 0.07$ Å), and $[\text{HIPTN}_3\text{N}]\text{W}$ (2.21 Å, $\sigma = 0.04$ Å). The average C(x01)-N(amido)-metal angle provides some idea of the degree to which the ligand crowds upon the protective pocket; the average angle is the same for $[\text{HIPTN}_3\text{N}]\text{Cr}$ (129°, $\sigma =$

1°), [HIPTN₃N]Mo (129°, $\sigma = 2^\circ$), and [HIPTN₃N]W (129°, $\sigma = 2^\circ$). From these parameters it can be seen that the core structure of [HIPTN₃N]M (M = Cr, Mo, W) complexes varies little down the Group VI triad. The implication is that any difference in reactivity can be ascribed far more to electronic than to steric factors.

	X = Cl ⁻	X = CO	X = NO	X = N ³⁻	X = N ₃ ⁻
Cr-X (Å)	2.2514(5)	1.905(2)	1.6759(13)	1.635(11)	1.717(12) 1.884(9)
X ₁ -X ₂ (Å)	—	1.142(3)	1.1826(17)	—	1.340(14) 1.20(3)
X ₂ -X ₃ (Å)	—	—	—	—	1.192(10) 1.176(7)
N(amine)-Cr-X (°)	179.62(5)	179.39(10)	179.66(7)	176.6(11)	177.2(4) 177.6(10)
Cr-X ₁ -X ₂ (°)	—	179.3(2)	179.58(15)	—	135.0(9) 130(2)
X ₁ -X ₂ -X ₃ (°)	—	—	—	—	176.5(9) 175.3(15)

Table 3.2: Selected structural data relevant to the apical ligand.

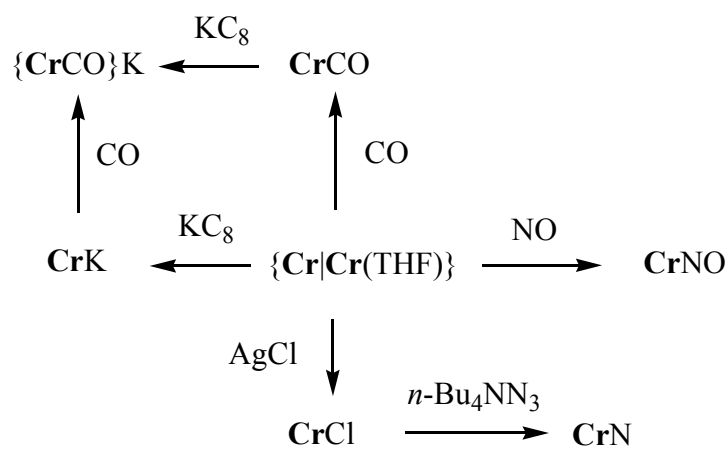
Some bond lengths and angles that involve the ligand in the binding pocket in the five structures are listed in Table 3.2. In the structure of [HIPTN₃N]CrCl, the Cr-Cl bond length is identical to than found in the related [Me₃SiN₃N]CrCl complex,³ and in both cases the N(amine)-Cr-Cl angle is 180°. In both [HIPTN₃N]CrCO and [HIPTN₃N]CrNO the N(amine)-Cr-A (A = C, N) and Cr-A-O angles are close to 180° and the Cr-NO bond in [HIPTN₃N]CrNO is ~0.2 Å shorter than the Cr-CO bond in [HIPTN₃N]CrCO, as might be expected. The Cr-NO and N-O bond lengths in [HIPTN₃N]CrNO and [(Me₃Si)₂N]₃CrNO¹⁴ are identical. The Cr-nitride bond length in [HIPTN₃N]CrN (1.64 Å) is longer than it is in (*i*-Pr₂N)₃CrN¹⁰ (1.54 Å). This slight lengthening is also exhibited when [HIPTN₃N]CrN is compared to other structurally characterized chromium (VI) nitrides.^{15,16,17} However, since the nitride and α -nitrogen of the azide were difficult to separate during refinement of the [HIPTN₃N]CrN/[HIPTN₃N]CrN₃ mixture, this difference should be taken with caution.

3.4 Attempts to prepare an ammonia complex and to reduce dinitrogen

Exposure of a degassed solution of $\{\text{Cr|Cr(THF)}\}$ to an atmosphere of ammonia immediately yields a green solution. This solution turns brown after being stirred overnight. Removal of the solvent from either the green or brown solution yields a bright red solid that does not react with CO to yield $[\text{HIPTN}_3\text{N}]\text{CrCO}$, does not react with AgCl to yield $[\text{HIPTN}_3\text{N}]\text{CrCl}$, and redissolves to yield a red solution. Therefore this red solid cannot be $[\text{HIPTN}_3\text{N}]\text{Cr}$. However, attempts to crystallize the red solid from heptane over a period of days so far have led only to apparent decomposition and formation of a colorless solid. In short, it does not appear that $\{\text{Cr|Cr(THF)}\}$ reacts with ammonia to give " $[\text{HIPTN}_3\text{N}]\text{Cr}(\text{NH}_3)$ " as a stable and well-behaved species analogous to $[\text{HIPTN}_3\text{N}]\text{Mo}(\text{NH}_3)$.

Three experiments were carried out in order to evaluate the viability of reducing dinitrogen to ammonia.¹⁸ A run carried out under conditions described for catalytic reduction of dinitrogen by $[\text{HIPTN}_3\text{N}]\text{Mo}$ compounds with $[\text{HIPTN}_3\text{N}]\text{CrN}$ yielded 0.8 equivalents of ammonia, which suggests that the nitride is reduced to ammonia, but no ammonia is formed from dinitrogen. If $[\text{HIPTN}_3\text{N}]\text{CrN}$ is worked up in a manner analogous to that after an attempted catalytic run, then only 0.1 equivalents of ammonia is obtained. Therefore, much more of the nitride is converted into ammonia under the conditions of an catalytic run. Finally, a run with the 65:35 mixture of $[\text{HIPTN}_3\text{N}]\text{CrCl}$ and $[\text{HIPTN}_3\text{N}]\text{CrN}_3$ yielded 0.3 equivalents of ammonia, consistent with stoichiometric reduction of the azide fraction to ammonia.

3.5 Discussion and Conclusions



Scheme 3.1: Reaction summary of $[\text{HIPTN}_3\text{N}]\text{Cr}$ and $[\text{HIPTN}_3\text{N}]\text{Cr(THF)}$.

We conclude that dinitrogen is not reduced by $[\text{HIPTN}_3\text{N}]\text{Cr}$ compounds under the conditions that are successful for $[\text{HIPTN}_3\text{N}]\text{Mo}$ compounds. We propose that there are at least four problems. First, $[\text{HIPTN}_3\text{N}]\text{Cr}$ is relatively high spin, and dinitrogen, a relatively weakly binding two electron σ -donor/ π -acceptor ligand, cannot bind efficiently to chromium in the quartet state, where there is one electron in each of the three frontier orbitals. Even CO does not bind immediately, although NO, an odd electron ligand, attacks the high spin species readily. Second, Cr(III) is not as good a reducing agent as Mo(III), so any low spin Cr(III) doublet is not captured as efficiently by dinitrogen as the analogous Mo(III) doublet. Third, it is likely that the Cr(III) doublet is not as accessible energetically as the Mo(III) doublet, so little is available to bind dinitrogen. Fourth, it is easier to reduce Cr(III) than Mo(III), so $[\text{HIPTN}_3\text{N}]\text{Cr}$ is reduced to $\{[\text{HIPTN}_3\text{N}]\text{Cr}\}^-$, and $\{[\text{HIPTN}_3\text{N}]\text{Cr}\}^-$ also does not react readily with dinitrogen. Almost certainly there are other problems that prevent reduction of dinitrogen to ammonia, among them the lack of well-behaved chemistry that involves ammonia. Therefore, the prospect of reducing dinitrogen catalytically by $[\text{HIPTN}_3\text{N}]\text{Cr}$ complexes appears slim. If the yield of ammonia from $[\text{HIPTN}_3\text{N}]\text{CrN}$ is taken at face value, even the stoichiometric reduction of $[\text{HIPTN}_3\text{N}]\text{CrN}$ in the presence of a reducing agent and protons is not as efficient as it is for $[\text{HIPTN}_3\text{N}]\text{MoN}$.

We have invoked spin state as a significant problem with respect to binding of dinitrogen to $[\text{HIPTN}_3\text{N}]\text{Cr}$ or $\{[\text{HIPTN}_3\text{N}]\text{Cr}\}^-$. Whether spin state can affect reactivity¹⁹ is a question that has been discussed with greater frequency in the literature in the last ten years.^{20,21,22,23,24} There seems to be agreement that spin state *can* affect reactivity, but the degree to which it does depends greatly upon the particular case being considered. As far as simple addition of an even electron σ -donor/ π -acceptor ligand to a metal is concerned, the more weakly binding the ligand (in terms of its combined σ -donor/ π -acceptor ability) the more spin state can be a determining factor. Conversely, for an odd electron ligand such as NO, the number of unpaired electrons on the metal probably is relatively unimportant. The behavior that we have observed for binding N_2 , CO, and NO to $[\text{HIPTN}_3\text{N}]\text{Cr}$ are consistent with these arguments, i.e., dinitrogen would be considered to be the most weakly binding ligand of the three and the least capable of trapping a $[\text{HIPTN}_3\text{N}]\text{Cr}$ doublet.

3.6 Experimental Details

General. All experiments were conducted under nitrogen in a Vacuum Atmospheres drybox or using standard Schlenk techniques. Glassware was heated at ~ 190 °C for a minimum of 12 hours prior to use. Pentane was washed with $\text{HNO}_3/\text{H}_2\text{SO}_4$ (5/95 v/v), sodium bicarbonate, and water, dried with CaCl_2 , and then sparged with nitrogen and passed through alumina columns followed by vacuum transfer from Na/benzophenone. Dry and deoxygenated benzene was purchased from Aldrich and passed through Q5 and alumina columns. Heptane, benzene- d_6 and toluene- d_8 were dried over Na/benzophenone then degassed (freeze-pump-thaw) and vacuum-transferred prior to use. All other solvents (diethyl ether, THF, toluene) were pre-dried by passing them through an alumina column followed by storage over Na/benzophenone. They were degassed (freeze-pump-thaw) and vacuum-transferred prior to use. Once transferred, all solvents were stored over 4 Å molecular sieves in a drybox.

CrCl_3 (Strem), CO (Aldrich, passed through dry ice/acetone), NO (BOC gases), NH_3 (BOC, condensed onto Na sand), and ^{13}CO (Matheson, passed through dry ice/acetone) were purchased and used as received or purified as indicated. $\text{H}_3[\text{HIPTN}_3\text{N}]^{4,25,26}$ and $\text{CrCl}_3(\text{THF})_3^{27}$ were synthesized *via* literature procedures.

Proton NMR spectra were obtained on a Varian Mercury (300 MHz) or Inova (500 MHz) spectrometer and were referenced to the residual protio-solvent peak. Infrared spectra were obtained on a Nicolet Avatar 360 FT-IR spectrometer using a demountable cell (0.2 mm Teflon spacer and KBr plate). UV/Vis spectra were obtained on a Hewlett-Packard 8452A Diode Array Spectrophotometer equipped with a Hewlett-Packard 89090A Peltier temperature control accessory with the solvent contribution manually subtracted using a standard background. Magnetic measurements (Evans method^{28,29}) employed the shift of the toluene methyl group. The sample was dissolved in toluene- d_8 and a concentric sealed capillary filled with toluene was added. Elemental analyses were performed by H. Kolbe Microanalytics Laboratory, Mülheim an der Ruhr, Germany.

Structural data were collected at 100 K with graphite-monochromated Mo $K\alpha$ radiation ($\lambda = 0.71073$ Å) using a Bruker-AXS Smart Apex CCD detector. The structures were solved using SHELXS³⁰ and refined against F^2 on all data by full-matrix least squares with SHELXL-97.³¹ All non-hydrogen atoms were refined anisotropically, while hydrogen atoms were placed

at calculated positions and refined using a riding model. ORTEP diagrams were created using ORTEP-3.³² Any deviations from this procedure are noted below. Data for all five structures are available at <http://www.reciprocalnet.org/> using the number that follows after each complex. $[\text{HIPTN}_3\text{N}]\text{CrCl}$ (05105), $[\text{HIPTN}_3\text{N}]\text{CrCO}$ (05129) and $[\text{HIPTN}_3\text{N}]\text{CrNO}$ (05137) are isostructural with no disorder, including the solvent (heptane) molecule. The only difference is that $[\text{HIPTN}_3\text{N}]\text{CrNO}$ crystallized as the opposite enantiomer as that found for $[\text{HIPTN}_3\text{N}]\text{CrCO}$ and $[\text{HIPTN}_3\text{N}]\text{CrCl}$.

The unit cell of $[\text{HIPTN}_3\text{N}]\text{CrCl}/[\text{HIPTN}_3\text{N}]\text{CrN}_3$ (05131) is very similar to that of $[\text{HIPTN}_3\text{N}]\text{CrCl}$. Indeed, $[\text{HIPTN}_3\text{N}]\text{CrCl}/[\text{HIPTN}_3\text{N}]\text{CrN}$ is perfectly isostructural to $[\text{HIPTN}_3\text{N}]\text{CrCl}$ (and also to $[\text{HIPTN}_3\text{N}]\text{CrCO}$) and is a mixed crystal, refined as a disorder. It is problematic to refine the 34% nitrogen next to the relatively high electron density of the 67% chlorine. Therefore SIMU and DELU are used for the five critical atoms and ISOR for the nitrogen bound directly to the Cr. Another consequence of the disorder is that the empirical formula has a non-integer value for Cl. This is not true for N, as one third of azide corresponds to one nitrogen atom. However, this is a coincidence and the relative occupancy has been refined freely with the help of a free variable.

The crystal of $[\text{HIPTN}_3\text{N}]\text{CrN}/[\text{HIPTN}_3\text{N}]\text{CrN}_3$ (05167) is a 50:50 mixture (within error of FVAR). The two Cr(1)-N(5) bond distances were refined as a disorder with the help of a free variable and rigid bond restraints.

$[\text{HIPTN}_3\text{N}]\text{Cr}$ (36). $\text{H}_3[\text{HIPTN}_3\text{N}]$ (2 g, 1.26 mmol) and $(\text{Me}_3\text{Si})_2\text{NLi}$ (632 mg, 3.78 mmol) were dissolved in diethyl ether and the solution was stirred at room temperature. In approximately one hour solid began to form. CrCl_3 (199 mg, 1.26 mmol) was added to this solution and the mixture was allowed to stir for two days. The resulting red-black mixture was filtered and the solvent was removed *in vacuo* at $\sim 40^\circ\text{C}$ to give a dark solid: $^1\text{H NMR}$ (C_6D_6) δ -13.05 (br s); $\mu_{\text{eff}} = 3.03$ BM. Anal. Calcd for $\text{C}_{114}\text{H}_{159}\text{N}_4\text{Cr}$: C, 83.62; H, 9.79; N, 3.42; Cl, 0.00. Found: C, 83.47, 83.52; H, 9.66, 9.68; N, 3.34, 3.37; Cl, 0.00.

$[\text{HIPTN}_3\text{N}]\text{Cr}(\text{THF})$ (37). $\text{H}_3[\text{HIPTN}_3\text{N}]$ (6 g, 3.78 mmol) and $\text{CrCl}_3(\text{THF})_3$ (1.42 g, 3.78 mmol) were dissolved in THF and the mixture was stirred for an hour at room temperature to

give a violet colored solution. $(\text{Me}_3\text{Si})_2\text{NLi}$ (1.96 g, 11.7 mmol) was added quickly, which caused the color to change to green-black. After another hour the solvent was removed *in vacuo* at $\sim 40^\circ\text{C}$. The resultant solid was dissolved in pentane and the solution was filtered. The solvent was removed from the filtrate *in vacuo* at $\sim 40^\circ\text{C}$ to give green-black powder; $\mu_{\text{eff}} = 2.46$ BM. Anal. Calcd for $\text{C}_{118}\text{H}_{167}\text{N}_4\text{OCr}$: C, 82.90; H, 9.85, N, 3.28. Found: C, 83.08, 83.12; H, 9.95, 9.98; N, 3.25, 3.21.

[HIPTN₃N]CrK (38). [HIPTN₃N]Cr(THF) (500 mg, 0.29 mmol) was dissolved in diethyl ether in a 20 mL vial. A glass-coated stir bar was added along with KC_8 (47 mg, 0.35 mmol). The mixture was stirred for ~ 12 hours and then filtered. The solvent was removed *in vacuo* to yield a yellow-orange powder. The same results were obtained using [HIPTN₃N]Cr; $\mu_{\text{eff}} = 3.74$ BM. Anal. Calcd for $\text{C}_{114}\text{H}_{159}\text{N}_4\text{CrK}$: C, 81.67; H, 9.56; N, 3.34. Found: C, 81.57, 81.51; H, 9.46, 9.40; N, 3.30, 3.26.

[HIPTN₃N]CrCO (39). [HIPTN₃N]Cr(THF) (500 mg, 0.29 mmol) was dissolved in ~ 20 mL of pentane and the solution was added to a 50 mL solvent bulb which was then attached to a gas-transfer bridge. The solution was cooled in liquid nitrogen and the atmosphere removed. The stainless steel tubing connecting the lecture bottle to the bridge was shaped into a coil that was immersed in CO_2 /acetone. The bulb was pressurized to slightly less than 1 atm with CO and warmed to room temperature. The bulb was closed and the solution was stirred. Within 5-10 minutes the color turned red. The solvent was removed *in vacuo* to give a red solid. X-ray quality crystals were obtained from a saturated heptane solution at room temperature. [HIPTN₃N]Cr can be substituted for [HIPTN₃N]Cr(THF) with the same results. The procedure for preparing the ^{13}C O analog was the same, but on a smaller scale; IR cm^{-1} 1951 (ν_{CO}), 1907 cm^{-1} ($\nu_{^{13}\text{C}\text{O}}$), 1862 ($\nu_{^{13}\text{C}^{18}\text{O}}$); $\mu_{\text{eff}} = 1.69$ BM.

{[HIPTN₃N]CrCO}K (40). [HIPTN₃N]CrCO was reduced as described for the synthesis of {[HIPTN₃N]Cr}K. Alternatively, {[HIPTN₃N]Cr}K was exposed to CO. Both methods yield this green pentane soluble complex quantitatively: ^1H NMR (toluene-*d*₈, 18-crown-6 adduct) δ 7.63 (s, 6H), 7.17 (s, 12H), 6.35 (s, 3H), 4.09 (br s, 6H), 3.46 (br s, 12H), 2.91 (br s, 30H), 1.60

(br s, 6H), 1.39 (d, $J_{\text{HH}} = 6.4$ Hz, 36H), 1.29 (d, $J_{\text{HH}} = 5.8$ Hz, 36H), 1.17 (d, $J_{\text{HH}} = 4.3$ Hz, 36H); IR cm^{-1} 1711 (ν_{CO}), 1671 ($\nu_{13\text{CO}}$). Anal. Calcd for $\text{C}_{115}\text{H}_{159}\text{N}_4\text{OCrK}$: C, 83.76; H, 9.63; N, 3.37. Found: C, 83.66, 83.70; H, 9.51, 9.57; N, 3.44, 3.41.

[HIPTN₃N]CrNO (41). [HIPTN₃N]Cr(THF) (300 mg, 0.18 mmol) was added to a 50 mL solvent bulb and dissolved in ~20 mL of pentane. NO was added as described for the synthesis of [HIPTN₃N]CrCO. The color of the solution turned blood red as soon as it thawed under an atmosphere of NO. The solvent was removed *in vacuo* to give a red solid. X-ray quality crystals were obtained from a supersaturated heptane solution at room temperature. [HIPTN₃N]Cr can be substituted for [HIPTN₃N]Cr(THF) with the same results: ¹H NMR (C_6D_6) δ 7.21 (s, 12H), 7.06 (s, 6H), 6.60 (s, 3H), 3.83 (br t, 6H), 3.05 (sept, $J_{\text{HH}} = 6.7$ Hz, 12H), 2.96 (sept, $J_{\text{HH}} = 6.8$ Hz, 6H), 2.16 (br t, 6H), 1.42 (d, $J_{\text{HH}} = 6.9$ Hz, 36H), 1.26 (d, $J_{\text{HH}} = 6.8$ Hz, 36H), 1.11 (d, $J_{\text{HH}} = 6.7$ Hz, 36H); IR cm^{-1} 1715 (ν_{NO}). Anal. Calcd for $\text{C}_{114}\text{H}_{159}\text{N}_5\text{OCr}$: C, 82.11; H, 9.61; N, 4.20. Found: C, 82.05, 82.00; H, 9.65, 9.69; N, 4.28, 4.25.

[HIPTN₃N]CrCl (42). To a 100 mL round bottom flask covered in electrical tape was added [HIPTN₃N]Cr(THF) (3.00 g, 1.75 mmol) and ~60 mL of diethyl ether. AgCl (251 mg, 1.75 mmol) was added in the dark. The flask was stoppered and covered in electrical tape. The mixture was stirred for three days and filtered to give a purple solution. The solvent was removed *in vacuo* at ~50 °C to give a dark purple solid which could be purified through crystallization from cold pentane. X-ray quality crystals were obtained from a saturated heptane solution at room temperature. The same results are obtained when [HIPTN₃N]Cr is used instead of [HIPTN₃N]Cr(THF): ¹H NMR (toluene-*d*₈) δ 25.58 (br s); UV/Vis λ_{max} (nm), ϵ ($\text{M}^{-1}\text{cm}^{-1}$) heptane (280, 2.7×10^4 ; 372, 1.9×10^4 ; 566, 1.3×10^4); benzene(286, 2.0×10^4 ; 382, 1.5×10^4 ; 472, 7.1×10^3 ; 578, 1.1×10^4); $\mu_{\text{eff}} = 2.55$ BM. Anal. Calcd for $\text{C}_{114}\text{H}_{159}\text{N}_4\text{CrCl}$: C, 81.84; H, 9.58; N, 3.35; Cl, 2.12. Found: C, 81.75, 81.72; H, 9.51, 9.48; N, 3.22, 3.25; Cl, 2.19, 2.16.

[HIPTN₃N]CrN (43). [HIPTN₃N]CrCl (0.974 g, 0.58 mmol) was added to a 100 mL flask with a Teflon valve followed by Bu_4NN_3 (221 mg, 0.78 mmol), a Teflon-coated stir bar, and ~50 mL of benzene, making sure all solid was washed into the flask. The reaction mixture was then

heated at 80 °C for one week with an additional equivalent of (*n*-Bu₄N)N₃ added half-way through. Solvent was removed from the resulting mixture (purplish at 80 °C, green at room temperature) and the resulting solid residue was extracted with pentane. The mixture was filtered through Celite in order to remove (*n*-Bu₄N)Cl and excess (*n*-Bu₄N)N₃. The solvent was removed from the filtrate *in vacuo* and the residue was taken up in toluene (~50 mL) and the solution was then heated at 110 °C for 10 days. The solvent was removed *in vacuo* and the residue was crystallized from saturated pentane solution at -35 to -40 °C to yield a dark purple microcrystalline solid (660 mg, 69%): ¹H NMR (C₆D₆) δ 7.97 (br s, 6H), 7.19 (s, 12H), 6.56 (s, 3H), 3.77 (br t, 6H), 3.09 (sept, J_{HH} = 6.9 Hz, 12H), 2.92 (sept, J_{HH} = 6.9 Hz, 6H), 1.94 (br t, 6H), 1.36 (d, J_{HH} = 6.9 Hz, 36H), 1.21 (d, J_{HH} = 6.9 Hz, 36H), 1.05 (br d, J_{HH} = 6.6 Hz, 36H); UV/Vis λ_{max}(nm), ε (M⁻¹cm⁻¹): heptane (268, 2.9 x 10⁴; 424, 1.6 x 10⁴; 570, 1.8 x 10⁴); benzene (284, 2.7 x 10⁴; 456, 1.9 x 10⁴; 638, 2.2 x 10⁴). Anal. Calcd for C₁₁₄H₁₅₉N₅Cr: C, 82.91; H, 9.70; N, 4.24; Cl, 0.0. Found: C, 82.78, 82.90; H, 9.76, 9.80; N, 4.23, 4.23; Cl, 0.0, 0.0.

3.7 References

-
- ¹ Yandulov, D. V.; Schrock, R. R., *Canad. J. Chem.* **2005**, *83*, 341.
 - ² Cummins, C. C.; Lee, J.; Schrock, R. R.; Davis, W. D., *Angew. Chem. Int. Ed. Engl.* **1992**, *31*, 1501.
 - ³ Schneider, S.; Filippou, A. C., *Inorg. Chem.* **2001**, *40*, 4674.
 - ⁴ Yandulov, D. V.; Schrock, R. R.; Rheingold, A. L.; Ceccarelli, C.; Davis, W. M., *Inorg. Chem.* **2003**, *42*, 796.
 - ⁵ Fickes, M. G.; Odom, A. L.; Cummins, C. C., *Chem. Commun.* **1997**, 1993.
 - ⁶ Peters, J. C.; Odom, A. L.; Cummins, C. C., *Chem. Commun.* **1997**, 1995.
 - ⁷ Greco, J. B.; Peters, J. C.; Baker, T. A.; Davis, W. M.; Cummins, C. C.; Wu, G., *J. Am. Chem. Soc.* **2001**, *123*, 5003.
 - ⁸ Figueroa, J. S.; Cummins, C. C., *Angew. Chem. Int. Ed.* **2004**, *43*, 984.
 - ⁹ Filippou, A. C.; Schneider, S.; Schnakenburg, G., *Inorg. Chem.* **2003**, *42*, 6974.
 - ¹⁰ Odom, A. L.; Cummins, C. C.; Protasiewicz, J. D., *J. Am. Chem. Soc.* **1995**, *117*, 6613.
 - ¹¹ Byrnes, M. J.; Dai, X. L.; Schrock, R. R.; Hock, A. S.; Muller, P., *Organometallics* **2005**, *24*, 4437.
 - ¹² Yandulov, D. V.; Schrock, R. R., *Inorg. Chem.* **2005**, *44*, 1103.
 - ¹³ Weare, W. W.; Dai, X.; Byrnes, M. J.; Chin, J.; Schrock, R. R., *Proc. Nat. Acad. Sci.*, submitted.
 - ¹⁴ Bradley, D. C.; Hursthouse, M. B.; Newing, C. W.; Welch, A. J., *J. Chem. Soc., Chem. Commun.* **1972**, 567.
 - ¹⁵ Chiu, H.-T.; Chen, Y.-P.; Chuang, S.-H.; Jen, J.-S.; Lee, G.-H.; Peng, S.-M., *Chem. Commun.*

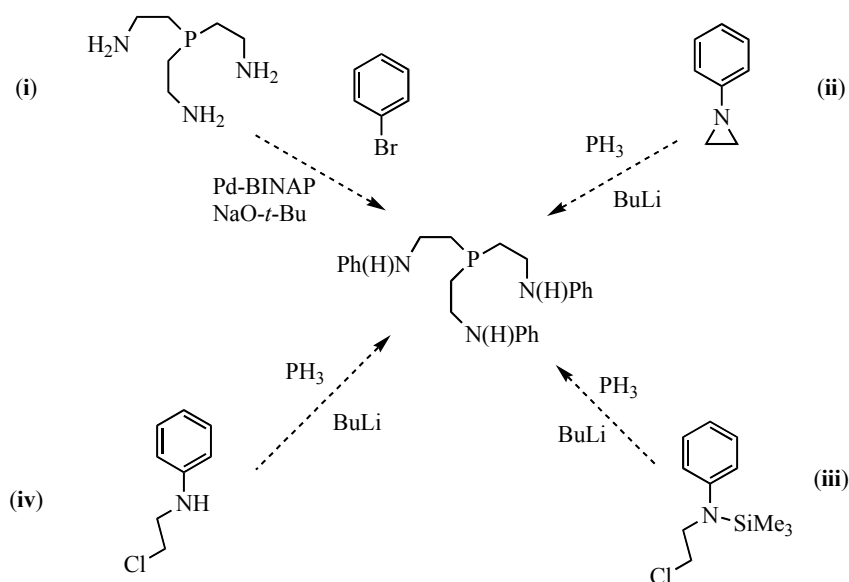
-
- 1996, 139.
- ¹⁶ Odom, A. L.; Cummins, C. *Organometallics* **1996**, *15*, 898.
- ¹⁷ Mindiola, D. J.; Cummins, C. C. *Angew. Chem. Int. Ed.* **1998**, *37*, 945.
- ¹⁸ Performed by Walter Weare.
- ¹⁹ Collman, J. P.; Hegedus, L. S., Principles and Applications of Organotransition Metal Chemistry, University Science Books, Mill Valley, CA, 1980.
- ²⁰ Schrock, R. R.; Shih, K. Y.; Dobbs, D. A.; Davis, W. M., *J. Am. Chem. Soc.* **1995**, *117*, 6609.
- ²¹ Detrich, J. L.; Reinaud, O. M.; Rheingold, A. L.; Theopold, K. H., *J. Am. Chem. Soc.* **1995**, *117*, 11745.
- ²² Harvey, J. N.; Poli, R.; Smith, K. M., *Coord. Chem. Rev.* **2003**, *238*, 347.
- ²³ Cremer, C.; Burger, P., *J. Am. Chem. Soc.* **2003**, *125*, 7664.
- ²⁴ Poli, R., *Chem. Rev.* **1996**, *96*, 2135.
- ²⁵ Yandulov, D. V.; Schrock, R. R., *Science* **2003**, *301*, 76.
- ²⁶ Yandulov, D. V.; Schrock, R. R., *J. Am. Chem. Soc.* **2002**, *124*, 6252.
- ²⁷ Herwig, W.; Zeiss, H. H., *J. Org. Chem.* **1958**, *23*, 1404.
- ²⁸ Evans, D. F., *J. Chem. Soc.* **1959**, 2003.
- ²⁹ Sur, S. K., *J. Mag. Res.* **1989**, *82*, 169.
- ³⁰ Sheldrick, G. M., *Acta Cryst. Sect. A* **1990**, *46*, 467.
- ³¹ Sheldrick, G. M. SHELXL 97, Universität Göttingen, Göttingen, Germany, 1997.
- ³² Farrugia, L. J., *J. Appl. Cryst.* **1997**, *30*, 565.

Chapter 4

Towards a Triamidophosphine Ligand Scaffold for Molybdenum.

4.1 Introduction

Substitution of the central nitrogen atom with phosphorus in *tris*-(2-aminoethyl)amine (**TREN**) is attractive in two respects. (1) Many of the complexes employed in the [HITPN₃N]Mo system are paramagnetic and thus ¹H NMR can be of limited use in identifying minor products. ³¹P NMR spectra are less broadened by paramagnetism in addition to having a wide chemical shift window and there would be only 1 resonance for each complex. (2) The stronger phosphine donor would allow us to probe the effect of the donor on catalytic activity and gain insight into whether the donor atom stays bound throughout the catalytic cycle and of what effect it has on the cycle and the stability/reactivity of the intermediates.



Scheme 4.1: Proposed scheme for the synthesis of arylated **TRAP**.

The syntheses of *tris*-(2-aminoethyl)phosphine•3HCl (**TRAP**•3HCl) and the free base *tris*-(2-aminoethyl)phosphine (**TRAP**, **N₃P**) have been previously described in the group,¹ but as they are unpublished, they are recreated here with slight modifications to the previous procedure. In the course of the previous work with **TRAP**, it was found that H₃[Me₃SiN₃P] is readily accessible from **TRAP**•HCl, Me₃SiCl, and *n*-BuLi in a manner analogous to the synthesis of H₃[Me₃SiN₃N]. However, the molybdenum chemistry of this ligand was not accessible due to decomposition described as the formation of black, pentane insoluble product(s) in the reaction between MoCl₄(THF)₂ and Li₃[Me₃SiN₃P] (generated from BuLi or MeLi). Neither did the

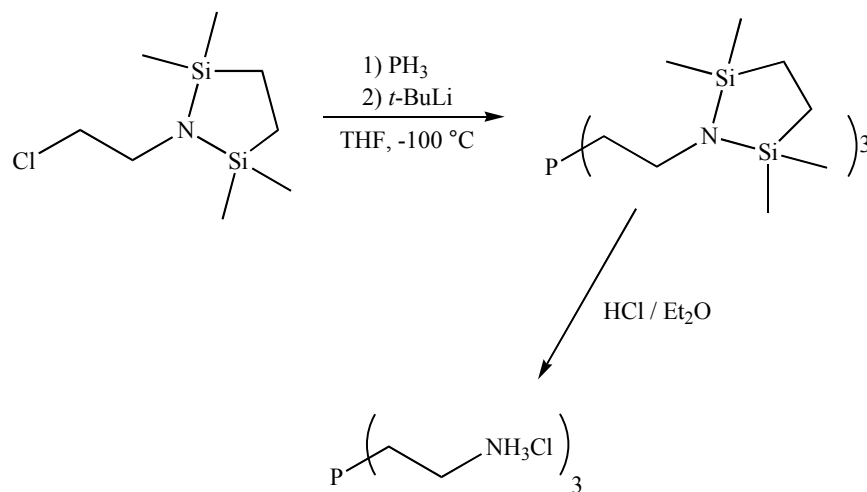
reaction between $\text{H}_3[\text{Me}_3\text{SiN}_3\text{P}]$ and $(\text{Me}_2\text{N})_4\text{Mo}$ at various temperatures between ambient and 90 °C in toluene provide isolable material.

Under the hypothesis that the larger phosphine donor was pushing molybdenum out of the pocket and causing steric interference with the approximately spherical Me_3Si groups, the use of an aryl substituent was also investigated. Four synthetic routes were proposed (Scheme 4.1), but the target phenyl derivative was not obtained. Route (i) yielded unreacted starting materials. Although route (ii) was not experimentally tested, it might be expected that the use of aziridines would suffer the same complications as those encountered in route (iv). Route (iv) proposed the use of an arylated chloroethylamine in a manner similar to that used in the synthesis of **TRAP**. However, it was found though, that the unprotected amine hydrogen was prone to abstraction under the PH_3 condensation conditions leaving a nucleophilic nitrogen competing with phosphide for nucleophilic substitution at chlorine. While steric protection of the amine with 2,6-dimethylphenyl allowed the generation of the *mono*-substituted phosphine complex, even excess butyl lithium did not deprotonate the resultant primary phosphine (as determined by the triplet in the ^1H coupled ^{31}P NMR spectrum). Even if successfully synthesized, a phosphine ligand based on *ortho* substituted aryl groups would be unlikely to bind molybdenum as has been found with *ortho* substituted **TREN** ligands.² Finally, route (iii) was not able to be tested as a successful route to the silylated amine was not found. Attempting to ring-open phenyl aziridine with $(\text{Me}_3\text{Si})\text{Cl}$ led to oligomerization, while reacting *N*-(2-chloroethyl)benzenamine with $(\text{Me}_3\text{Si})\text{Cl}$ in the presence of Et_3N led to the formation of $(\text{Et}_3\text{NH})\text{Cl}$ and an ill-defined tarry precipitate containing unreacted *N*-(2-chloroethyl)benzenamine.

4.2 *tris*-(2-aminoethyl)phosphine (TRAP)

The synthesis of **TRAP** involves the nucleophilic attack of deprotonated PH_3 on 1-(2-chloroethyl)-2,2,5,5-tetramethyl-1,2,5-azadisilolidine. While the reaction is straightforward, it requires the use of PH_3 which means that special handling procedures are needed. PH_3 is a gas with a boiling point of -87.7 °C. Although it has been reported that PH_3 is not itself pyrophoric, it is quite flammable and since P_2H_4 , a highly pyrophoric gas, is inevitably present, PH_3 is effectively a pyrophoric gas and should be treated as such.³ As an illustration of this, if a hose used to transfer PH_3 from the lecture bottle is cut after condensation of PH_3 into the reaction

flask, a flash follows and a loud pop occurs. Removing the regulator from the closed cylinder results in small flames periodically emitting from the regulator. Therefore, when setting up reactions using PH_3 , it is important to make sure that all joints and connections are well secured.



Scheme 4.2: Simplified synthesis of **TRAP•3HCl**.

The reaction apparatus is shown above (Figure 4.1). Excess PH_3 (about twice the stoichiometric amount) is condensed in the graduated sidearm by immersing it in liquid nitrogen and letting the PH_3 flow through the apparatus into a large beaker of water separated from the reaction apparatus by an oil bubbler. The water allows quenching of the uncondensed PH_3 without flames, and the oil bubbler prevents water vapor from entering the reaction. The actual volume is measured by letting the material thaw in a CO_2 /diethyl ether bath (CO_2 /diethyl ether is used as its temperature is $-100\text{ }^\circ\text{C}^4$ which is below the boiling point of PH_3). Once the appropriate volume of PH_3 is condensed, it is frozen with liquid nitrogen and the apparatus is purged with nitrogen for 30 minutes to remove any remaining gaseous PH_3 . Once the apparatus is purged, the solution of 1-(2-chloroethyl)-2,2,5,5-tetramethyl-1,2,5-azadisilolidine in THF can be transferred *via* canula. The solution should be transferred directly into the flask rather than by using the addition funnel to prevent ring-opening of residual THF in the addition funnel when *t*-BuLi is added. The added solution should then be frozen in liquid nitrogen and thawed in a CO_2 /diethyl ether bath to ensure the temperature is at or below $-100\text{ }^\circ\text{C}$ to prevent loss of PH_3 upon mixing. The THF solution is mixed with the condensed PH_3 by tipping the flask back and

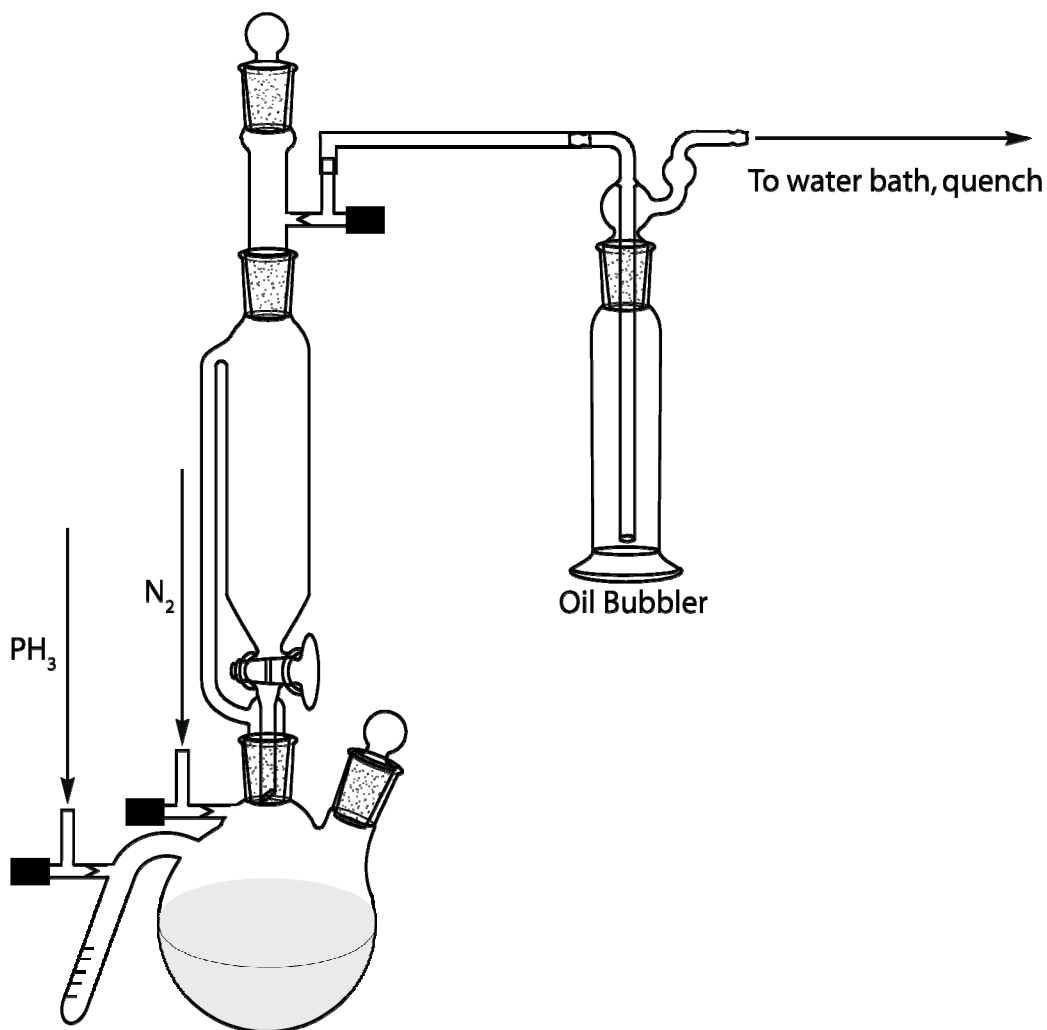


Figure 4.1: Reaction apparatus for PH_3 alkylation.

forth. Based on 1-(2-chloroethyl)-2,2,5,5-tetramethyl-1,2,5-azadisilolidine, one equivalent of *t*-BuLi in pentane (1.7 M) was added drop-wise. The result of the use of excess of PH_3 is a mixture of *mono*- (-151 ppm) and *bis*-substituted phosphine (-84 ppm) as indicated by ^{31}P NMR (Figure 4.2). This crude mixture can be isolated as a viscous orange oil. The usefulness in doing the reaction in two steps is that the tertiary phosphine can be obtained as a pure enough compound for direct use. It is difficult to accurately measure PH_3 , and much easier to weigh the viscous oil and back-calculate the amount of 1-(2-chloroethyl)-2,2,5,5-tetramethyl-1,2,5-azadisilolidine to add from the ratio of *mono* to *bis*-substituted compound as determined by ^{31}P NMR.

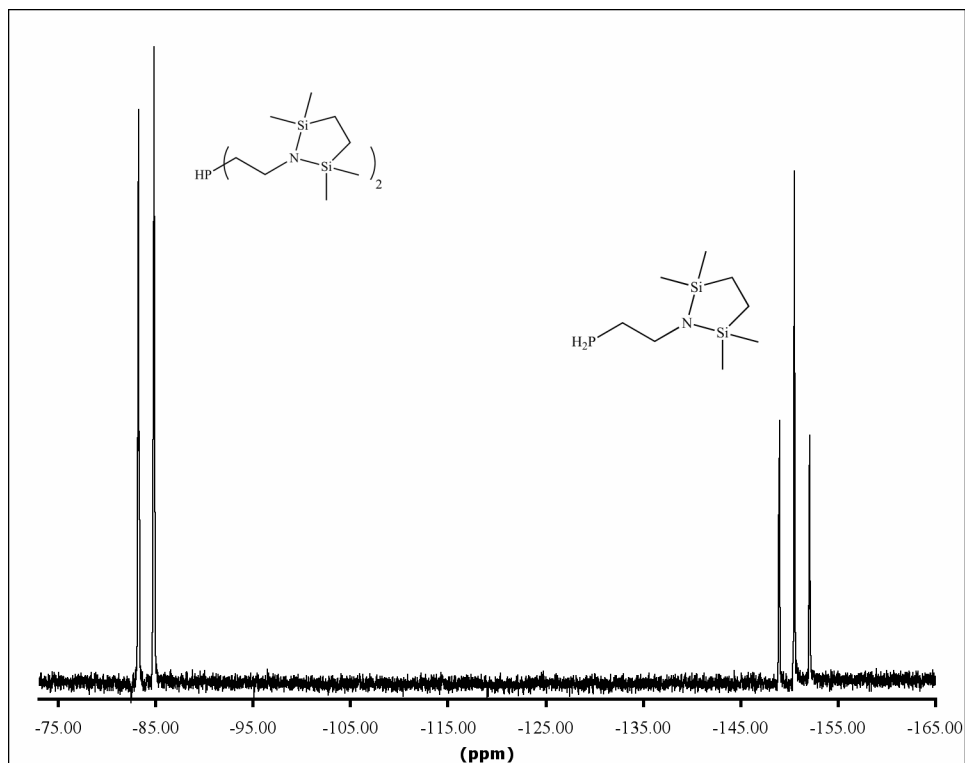


Figure 4.2: ^{31}P spectrum of HPR_2 (doublet) and H_2PR (triplet).

Deprotection of the *tris*-substituted compound with HCl/diethyl ether gives a white solid, identified as **TRAP**•HCl. This solid is only slightly soluble in water, and not soluble in organic solvents. Generation of the free base (Figure 4.3, Figure 4.4) is accomplished by stirring a suspension of powdered NaOH in diethyl ether. This is necessary because **TRAP** is quite soluble in water and cannot be extracted using organic solvents such as diethyl ether or methylene chloride. As an ethereal solution of **TRAP** cools upon removal of solvent, it solidifies and then melts upon warming to give a colorless oil. In previous work,¹ it was found that **TRAP** decomposes on distillation, thus it must be used "as isolated."

Performing Pd coupling on phosphorus containing molecules has been unsuccessful, as might be expected given that the Pd catalysts are supported by phosphine ligands. Using X-PHOS in toluene, DME, or DMF with **HIPTBr** results in no reaction as shown by quantitative recovery of **HIPTBr**. Oxidation of **TRAP** to **OTRAP** (Figure 4.5) by H_2O_2 results in a viscous, water soluble, pungent oil which also does not react under these conditions.

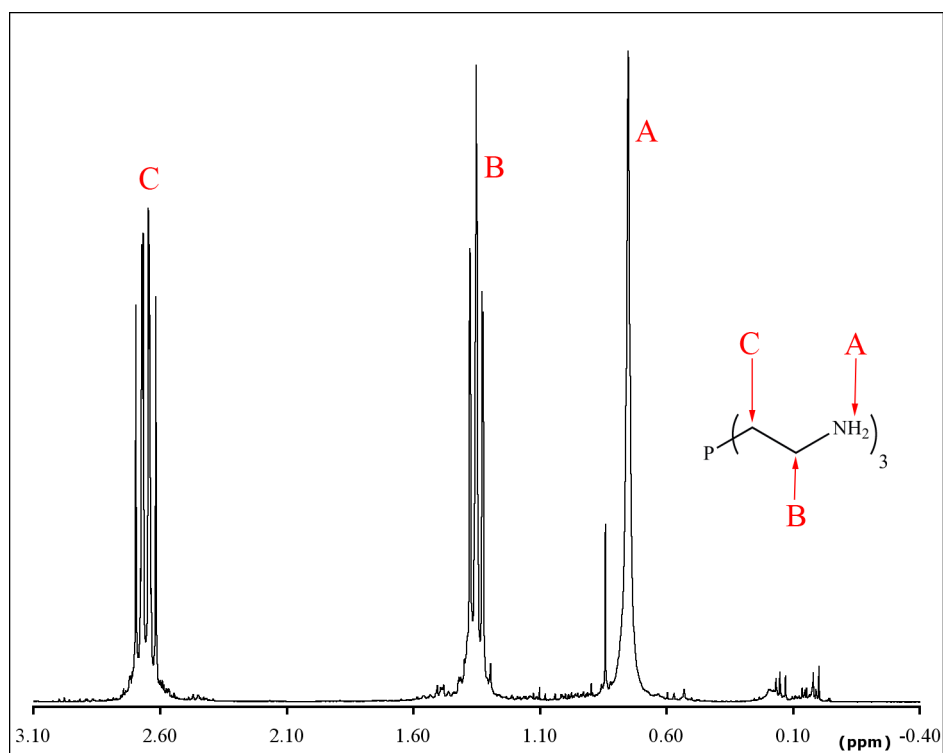


Figure 4.3: ^1H NMR spectrum (C_6D_6) of TRAP.

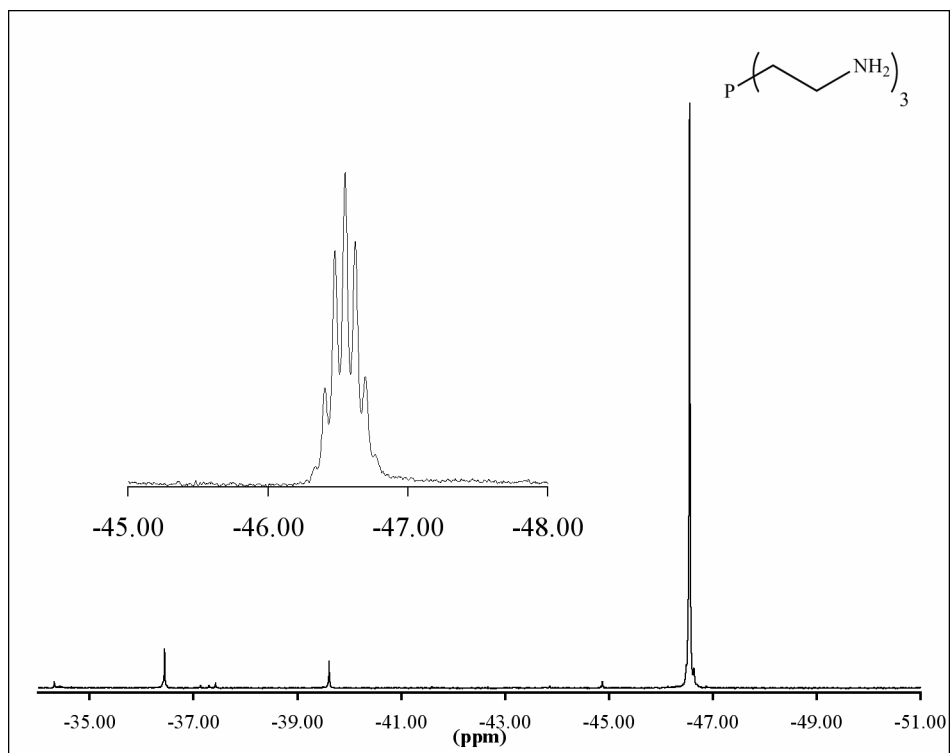


Figure 4.4: $^{31}\text{P}\{^1\text{H}\}$ and ^{31}P (inset) NMR spectra (C_6D_6) of TRAP.

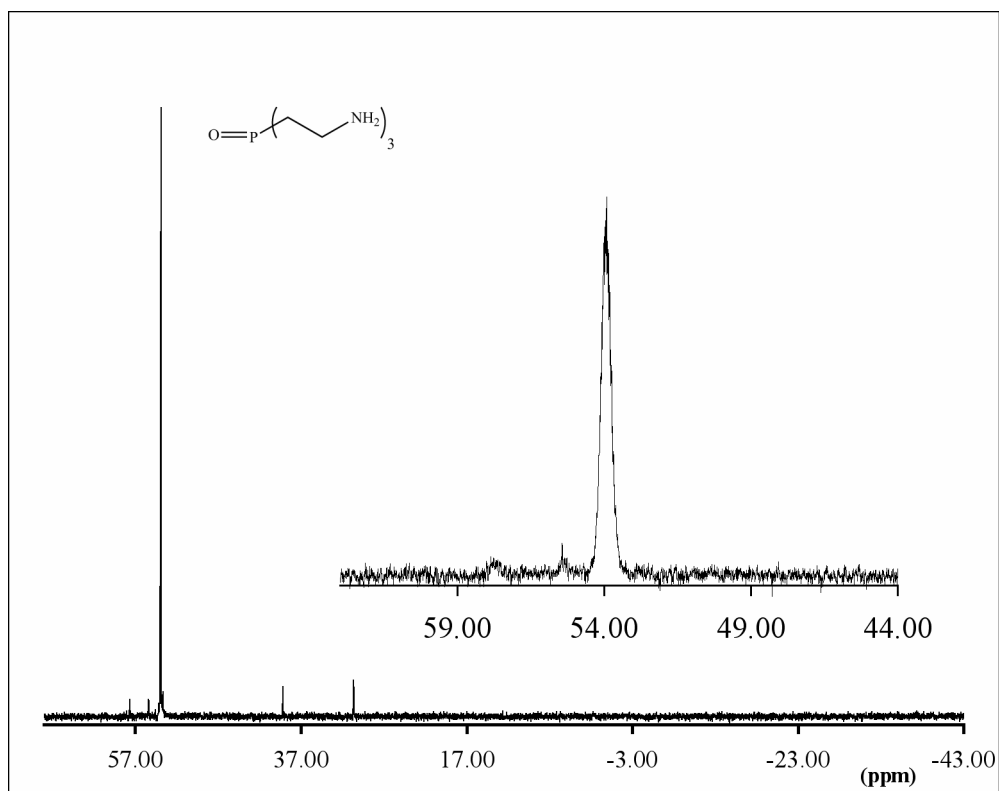


Figure 4.5: $^{31}\text{P}\{^1\text{H}\}$ and ^{31}P (inset) NMR spectra (D_2O) of $\text{O}=\text{P}(\text{CH}_2\text{CH}_2\text{NH}_2)_3$ (**46**).

Cu mediated coupling between **HIPTBr** and **TRAP** or **TRAP**•3HCl was also attempted as has been described by Buchwald.⁵

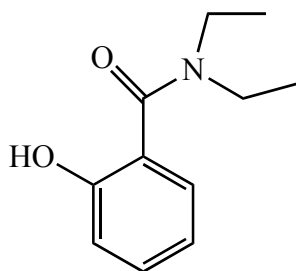


Figure 4.6: Ligand for Cu mediated aryl halide coupling.

A sample ligand (Figure 4.6) for Cu mediated coupling was kindly donated by the Buchwald lab (the compound is no longer commercially available). The standard conditions are 5% CuI, 20% Ligand, 2 equivalents of K_3PO_4 and 0.5 mL DMF per mmol of amine. Due to the molecular weight of **HIPTBr**, the concentration was halved. Attempts were also made using NaO-*t*-Bu as

the base with no difference. Additionally, both the **TRAP**•3HCl and **TRAP** Cu couplings were attempted with negative results. Under all conditions, **HIPTBr** was observed. Strangely, even in the case of the free base (**TRAP**), which is a liquid that is miscible with organic solvents, no ^{31}P NMR resonance is observable in solution.

4.2.1 Phosphine Arm

In light of the unsuccessful attempts at arylation of **TRAP** and the potential difficulty in purification were suitable conditions found, an alternative route was considered. That is, accomplishing the arylation before phosphorus is introduced, in a manner similar to route **iii** (Scheme 4.1), by using an arm already bearing the **HIPT** group instead of the silyl protected arm used in the synthesis of **TRAP**. As was previously established (Scheme 4.1),¹ the amine must be protected to prevent side reactions during alkylation of PH_3 (Figure 4.7).

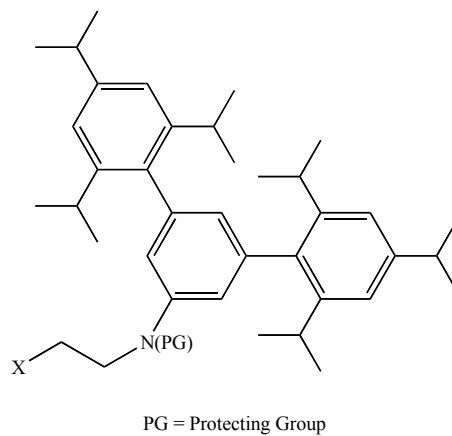
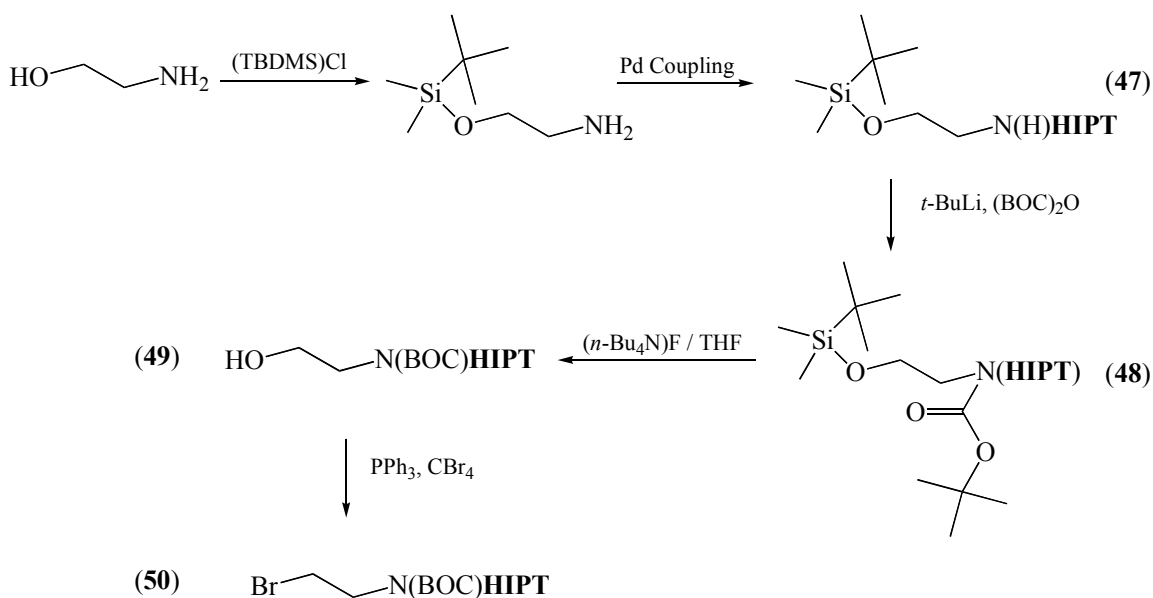


Figure 4.7: Ligand arm for PH_3 .

The synthesis of $(t\text{-BuMe}_2\text{Si})\text{OCH}_2\text{CH}_2\text{NH}_2$ has been published,⁶ and is accomplished by the reaction of $(t\text{-BuMe}_2\text{Si})\text{Cl}$ with ethanolamine in methylene chloride using triethylamine as a base. This protection of the alcohol functionality is necessary as it is incompatible with the Pd catalyzed coupling to **HIPTBr**. The coupling of **HIPTBr** to $(t\text{-BuMe}_2\text{Si})\text{OCH}_2\text{CH}_2\text{NH}_2$ proceeds over 3 hours with a loading of 2.5% $\text{Pd}_2(\text{dba})_3$ and 7.5% X-PHOS in toluene at *ca.* 80 °C using sodium *tert*-butoxide as the base. Purification is accomplished by filtering the reaction mixture through a silica gel plug. Removal of toluene results in a fluffy, slightly yellow foam



Scheme 4.3: Synthetic scheme for $\text{BrCH}_2\text{CH}_2\text{N(BOC)HIPT}$.

that can be ground to yield **47** in powder form. The arylation must be performed before BOC protection of the amine as attempting to arylate the BOC protected amine (Figure 4.8) resulted in quantitative recovery of unreacted **HIPTBr**.

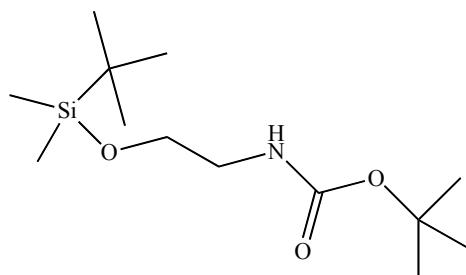
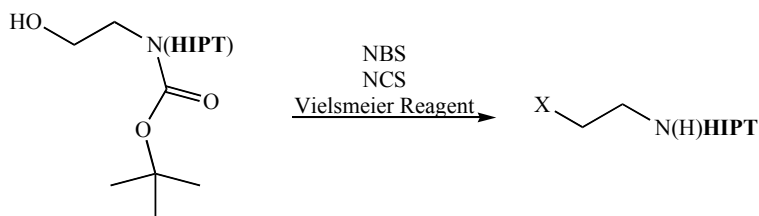


Figure 4.8: $(t\text{-BuMe}_2\text{Si})\text{OCH}_2\text{CH}_2\text{NH(BOC)}$.

Equimolar amounts of **47** and $(\text{BOC})_2\text{O}$ in diethyl ether cooled to *ca.* 0°C yield **48** upon the drop-wise addition of *t*-BuLi. Allowing the solution to warm overnight to room temperature gives a mixture which when filtered gives **48** quantitatively and cleanly. Clean product seems to require the less nucleophilic *t*-BuLi as a small scale test reaction with *n*-BuLi resulted in multiple products. Although amines are generally protected with BOC using a much milder base such as NEt_3 , using BuLi is not unprecedented.⁷ Deprotection of the alcohol is accomplished selectively with $(n\text{-Bu}_4\text{N})\text{F}$ in THF followed by chromatography on silica gel (EtOAc/Hexanes) to give **49**.

Finally, the alcohol can be transformed to a bromide by the use of carbon tetrabromide and triphenyl phosphine to yield **50** (88%). *N*-bromosuccinimide (NBS) was found to be an unsuitable brominating agent as the BOC group was cleaved to give what appeared to be $\text{BrCH}_2\text{CH}_2\text{N(H)HIPT}$ (Equation 4.1), by ^1H NMR, among other unidentified products. The same results were observed when *N*-chlorosuccinimide or the Vilsmeier reagent was used to attempt chlorination (Figure 4.1).



Equation 4.1: Loss of the BOC group during halogenation.

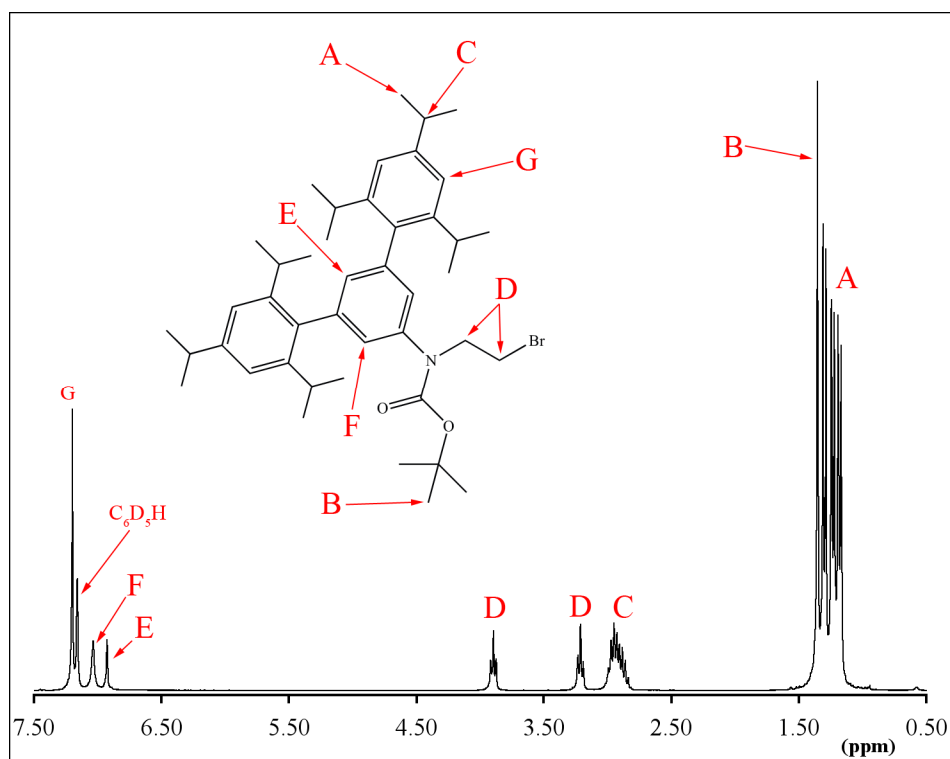
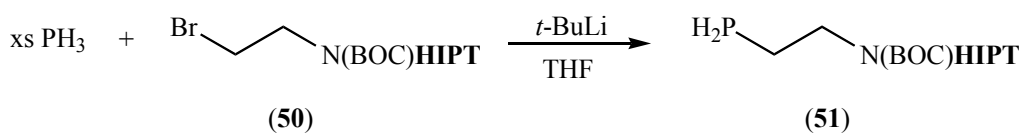


Figure 4.9: ^1H NMR spectrum (C_6D_6) of **50**.

Analogous to the modified synthesis of **TRAP**, excess PH_3 was used to yield the *mono*-substituted phosphine (**51**) in quantitative yield cleanly (Equation 4.2, Figure 4.10, Figure 4.11).



Equation 4.2: Synthesis of $\text{H}_2\text{PCH}_2\text{CH}_2\text{N(BOC)HIPT}$ (51).

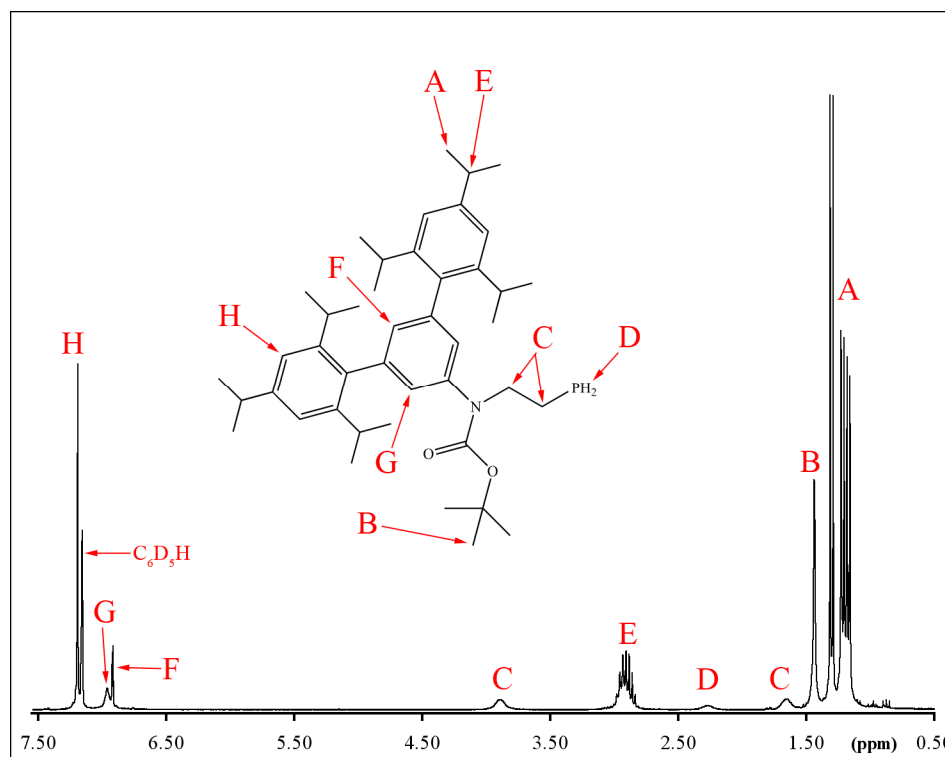


Figure 4.10: ^1H NMR spectrum (C_6D_6) of $\text{H}_2\text{PCH}_2\text{CH}_2\text{N(BOC)HIPT}$ (51).

Unfortunately, further substitution could not be achieved as seen with the 2,6-dimethylphenyl substituted arm (Section 4.1). Attempting to add another equivalent of **50** to **51** using *t*-BuLi or *n*-BuLi as the base resulted in a messy ^1H NMR spectrum and an unchanged ^{31}P spectrum (-150 ppm, triplet). It appears that instead of deprotonating the phosphine, the alkyl lithium reacted with **HIPT** or the BOC protecting group. Thus, for this method to work a more robust protecting group would be required.

Reacting **51** with potassium or potassium hydride in THF at 60 °C for *ca.* 12 hours gives what ^{31}P NMR suggests is the deprotonation of **51** to the potassium salt (Figure 4.12). The ^1H coupled ^{31}P spectrum shows a quantitative downfield shift (-150 ppm to -41 ppm) and a change

from triplet to singlet. Addition of **50** to this product yields unknown material with no change in ^{31}P shift

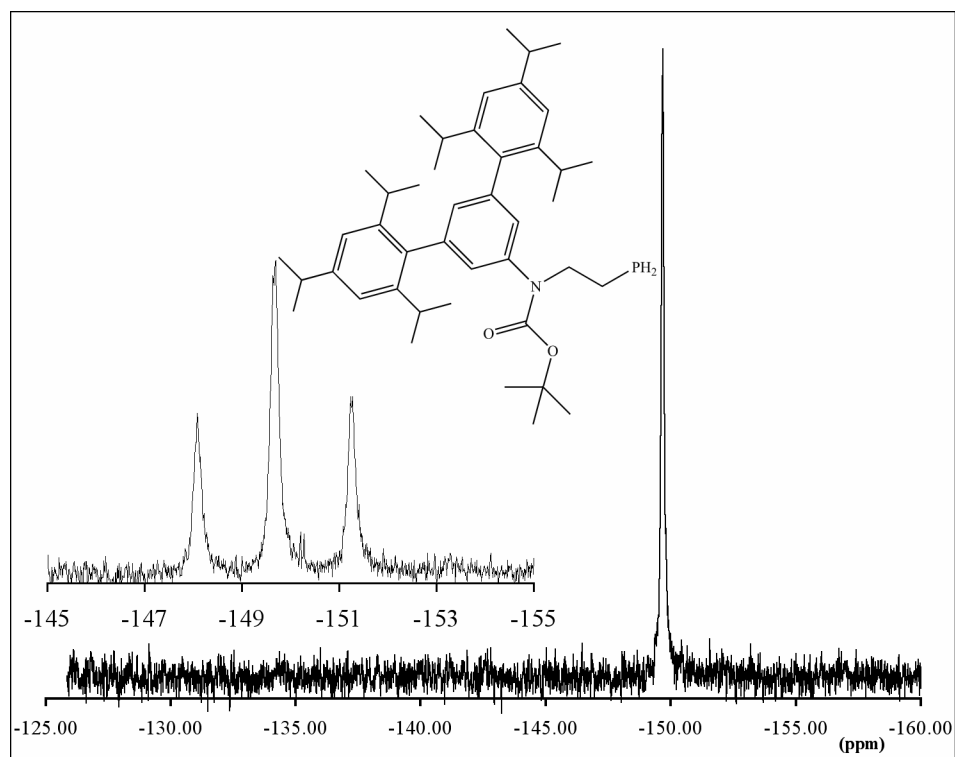


Figure 4.11: $^{31}\text{P}\{^1\text{H}\}$ and ^{31}P (inset) NMR spectra (C_6D_6) of $\text{H}_2\text{PCH}_2\text{CH}_2\text{N}(\text{BOC})\text{HIPT}$ (**51**).

and a messy ^1H NMR. It has been proposed that bromide may not be best for nucleophilic substitution at phosphorus, and that a chloride would be better suited due to radical processes.⁸ Although a chlorinated arm should be accessible using carbon tetrachloride,⁹ it is not likely to yield the tertiary phosphine given the lack of reactivity with the 2,6-dimethylphenyl substituted arm (Section 4.1). A possibility that was not explored was the CsOH promoted alkylation of phosphine.¹⁰

4.3 An Aryl Phosphine Backbone

Another possibility for an N_3P type ligand is to move away from a straight **TREN** analogue through the use of a phenylene rather than ethylene backbone structure in a manner similar to what Fryzuk has done¹¹ (Scheme 4.4), potentially using PCl_3 instead of Cl_2PPh .

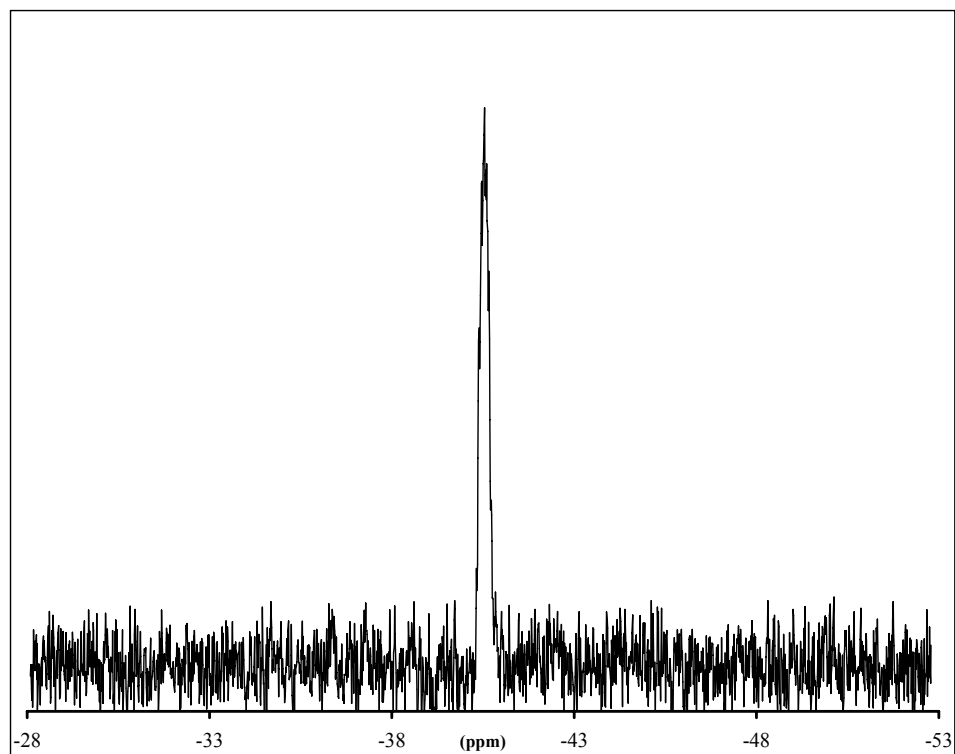
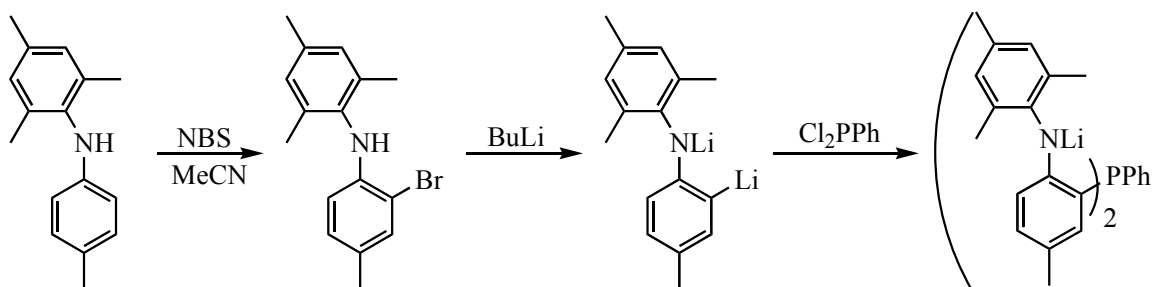
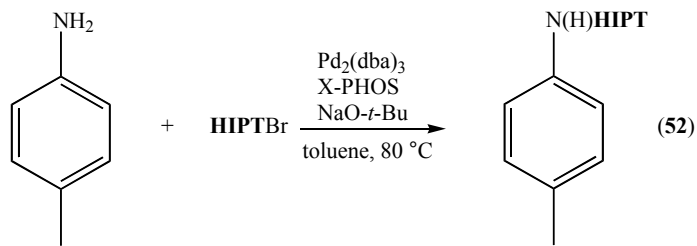


Figure 4.12: ^{31}P NMR spectrum of the reaction of **51** with K metal.



Scheme 4.4: Fryzuk synthesis of a phosphine donor ligand.

The Pd coupling of **HIPTBr** to *p*-tolylaniline (Equation 4.3) proceeds easily to give **52** (97%) without the need for purification besides passage through a silica gel plug.



Equation 4.3: Synthesis of *p*-tolyl(**HIPT**)aniline.

However, where Fryzuk sees nearly quantitative yield, attempting bromination of **52** with *n*-bromosuccinimide under the same conditions yields a mixture of products that were not amenable to separation *via* chromatography. Considering a simplification of **HIPT** to 3,5-dimethylphenyl (Figure 4.13), the reason for this becomes clear.

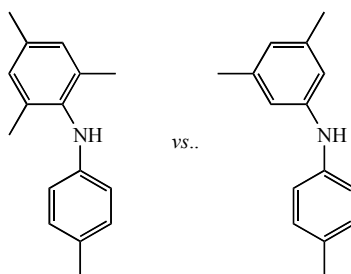
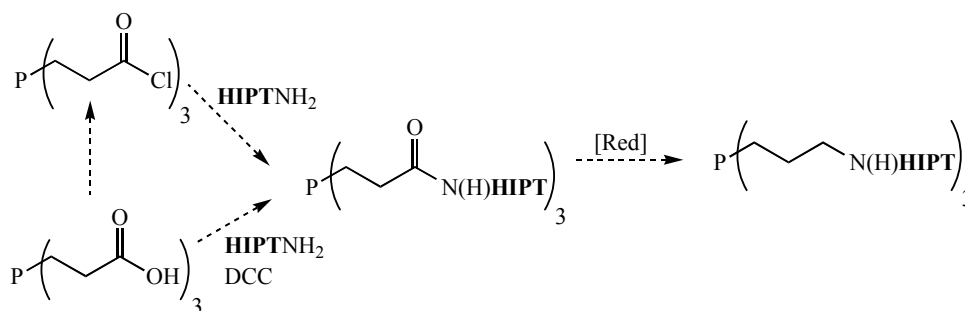


Figure 4.13: Comparison of Fryzuk system and the simplified **HIPT** system.

Unlike the mesityl group in the Fryzuk system, the **HIPT** *ortho* and *para* positions are not protected, so bromination was completely unselective. While increased rigidity would be an interesting avenue to explore, we are unaware of a way to selectively brominate the tolyl *ortho* position.

4.4 *tris*-(2-aminopropyl)phosphine (TAPP)

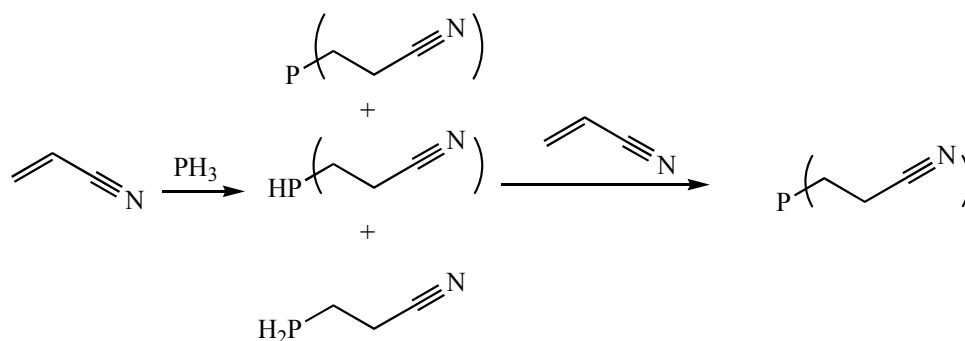
With the difficulties encountered in creating a phosphine ligand with an ethylene backbone, we became interested in the known *tris*-(2-carboxyethyl)phosphine hydrochloride.¹² With this compound, we would be able to incorporate the **HIPT** substituent without the need for Pd by using DCC mediated coupling with **HIPTNH**₂¹³ or by conversion of the carboxylic acid to the acyl chloride and reaction with **HIPTNH**₂ (Scheme 4.5).



Scheme 4.5: Reaction scheme for a propyl backbone ligand.

Although *tris*-(2-carboxyethyl)phosphine hydrochloride and its precursor *tris*-(2-cyanoethyl)phosphine are both commercially available, they are expensive so we looked into their synthesis. The synthesis of *tris*-(2-carboxyethyl)phosphine from *tris*-(2-cyanoethyl)phosphine proceeded exactly as has been described.¹² The only item of note to reinforce is that solid *tris*-(2-carboxyethyl)phosphine is stable enough towards oxidation to allow isolation in air. It is important to prevent oxidation as it is difficult to separate *tris*-(2-carboxyethyl)phosphine from its oxidation product. The synthesis of *tris*-(2-cyanoethyl)phosphine^{14,15} required some modifications to allow for the direct use of PH_3 at one atmosphere rather than PH_3 generated from red phosphorus *in-situ*.

4.4.1 *tris*-(2-cyanoethyl)phosphine



Equation 4.4: Step-wise synthesis of *tris*-(2-cyanoethyl)phosphine (53).

Since the reaction between PH_3 and acrylonitrile is slow even at 0°C , it is not possible to perform this reaction using a measured quantity of PH_3 without using a pressurized vessel. The setup for this reaction is shown in Figure 4.14, and utilizes a gas transfer bridge with a vacuum/pressure gauge attached to the reaction flask. To overcome the need to keep the reaction at pressures no greater than 1 atmosphere, the reaction was done in two steps. By keeping the reaction under an atmosphere of PH_3 , PH_3 is effectively used in excess. It is important to note that the polymerization of acrylonitrile is catalyzed by KOH (as indicated by the solution going from colorless to dark orange). Thus, even though the reaction between PH_3 and acrylonitrile is slow at 0°C , the reaction must be kept cold to prevent as much polymer formation as possible. Also, as both the intended reaction and the polymerization of acrylonitrile are exothermic, lack

of cooling leads to a significant rise in temperature and a potential inability to isolate any of the substituted phosphine. Once the pressure no longer drops over time (hours), an indication

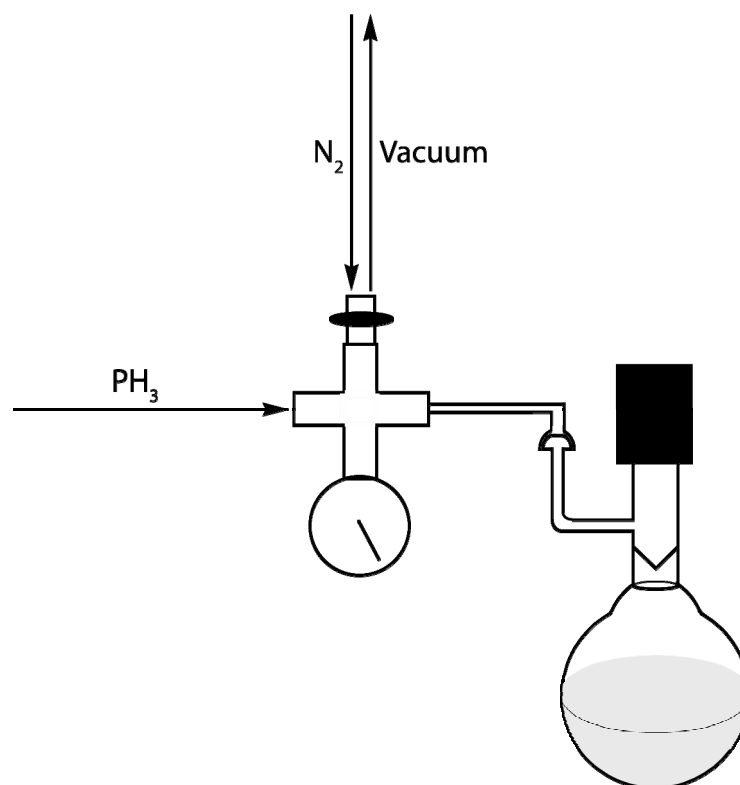


Figure 4.14: Reaction apparatus for the synthesis of *tris*-(cyanoethyl)phosphine.

that no more acrylonitrile is present, the reaction is a mixture of *mono*- (-138 ppm), *bis*- (-71 ppm), and *tris*-cyanoethylphosphine (-23 ppm), the ratio of which can be determined by ^{31}P NMR. Knowing the ratios and the original amount of acrylonitrile (using the assumption that no polymerization occurred), allows calculation of the required amount of acrylonitrile to fully generate the *tris* substituted species. Conveniently, solid *tris*-cyanoethylphosphine is not greatly air sensitive and can be collected by filtration in air with no evidence of oxidation in the ^{31}P NMR spectrum. The brightly colored polymer can be washed away with MeOH to yield a white powder. This is most easily done by trituration.

4.4.2 Synthesis of HIPTNH_2

The conversion of HIPTBr to HIPTNH_2 requires a reagent that can act as an ammonia equivalent since ammonia is not a viable source of the " NH_2 " fragment (Scheme 4.6). Work by

both Buchwald^{16,17} and Hartwig¹⁸ has shown that $(\text{Me}_3\text{Si})_2\text{NLi}$ and benzophenone imine are viable ammonia surrogates which can be readily deprotected. No **HIPTN** $(\text{SiMe}_3)_2$ or **HIPTNH**₂ could

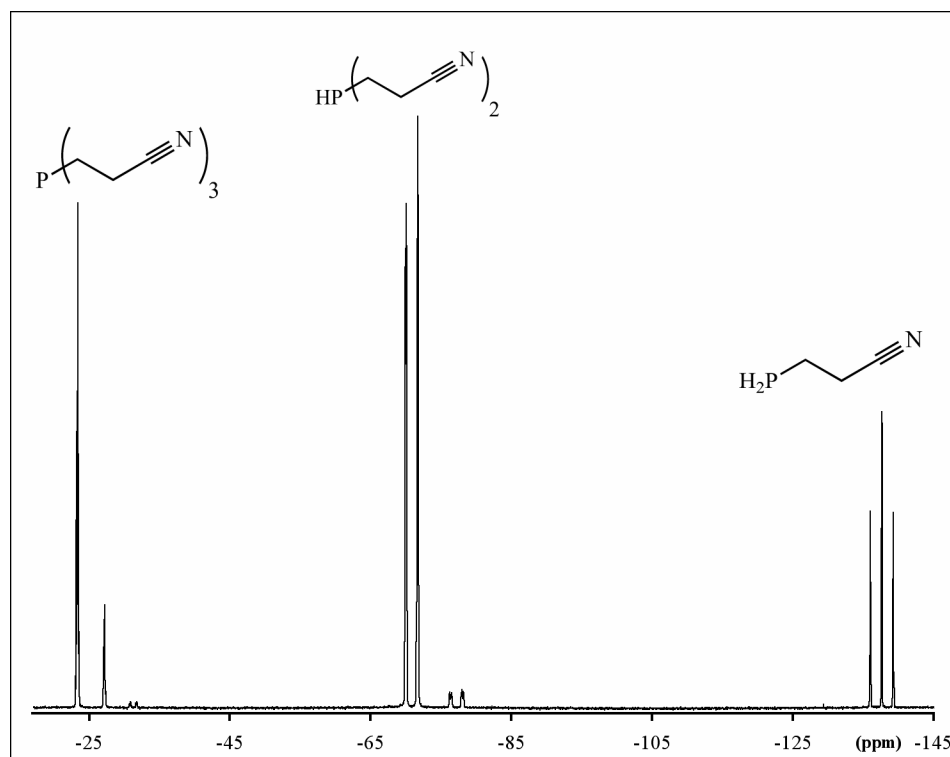
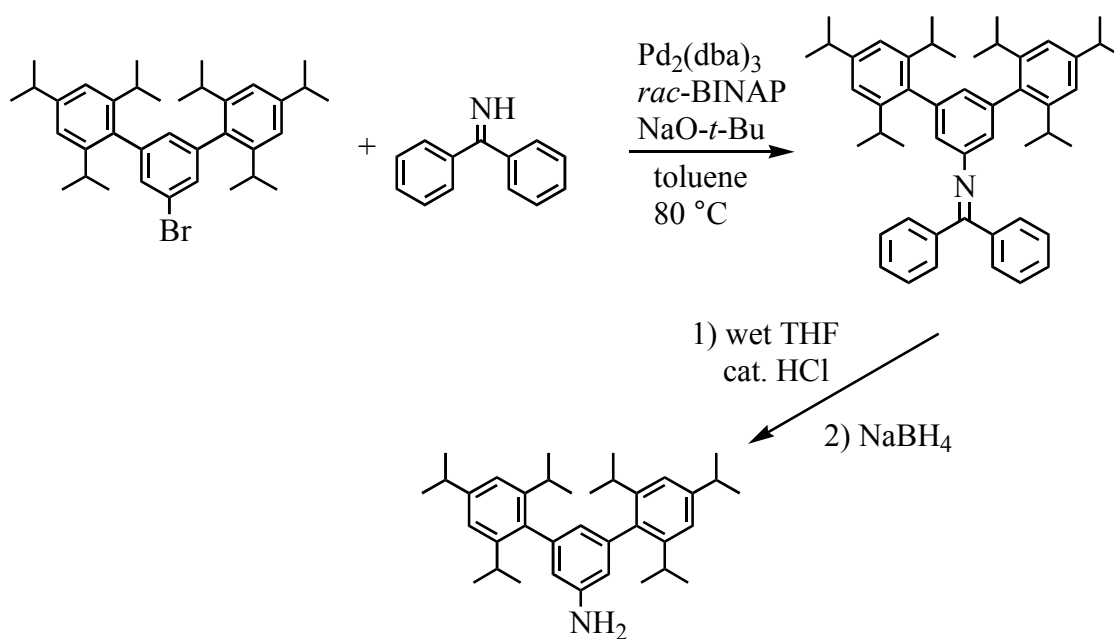


Figure 4.15: ³¹P NMR spectrum (reaction mixture) of the *mono*-, *bis*-, and *tris*-substituted PH_3 .

be isolated from reactions using $(\text{Me}_3\text{Si})_2\text{NLi}$ with any combination of ligand (X-Phos, *rac*-BINAP), solvent (toluene 1,4-dioxane, THF), and temperature (RT, 60 °C, 80°C). Using benzophenone imine yielded the desired product when the ligand was *rac*-BINAP, but not with X-Phos. Deprotection to yield the aniline is accomplished by acid catalyzed generation of benzophenone in wet THF, but isolation by chromatography requires that the benzophenone be oxidized to the corresponding alcohol using NaBH_4 to achieve decent separation on silica gel (Figure 4.16).



Scheme 4.6: Synthesis of **HIPTNH₂ (55)** from **HIPTBr**.

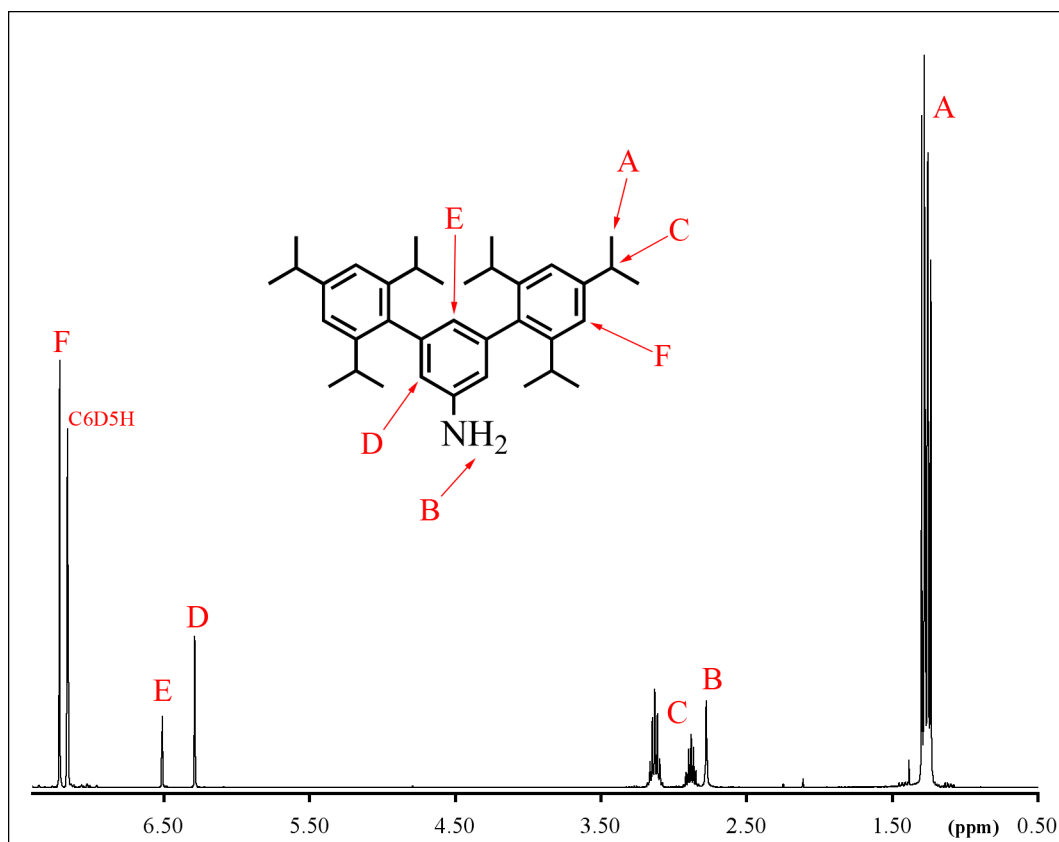


Figure 4.16: ¹H NMR spectrum (C_6D_6) of **HIPTNH₂**.

4.5 Conclusions

The **TRAP** ligand scaffold is accessible, but arylated ligands based on it are not as readily obtained as with its nitrogen containing cousin **TREN**. It may be that an arylated **TRAP**-based ligand would be attainable through the use of pre-formed "arms," but at the very least this would require a protecting group other than BOC to avoid decomposition. This route would also not be modular and would thus not lend itself to exploratory ligand synthesis. We believe that a ligand based on **TAPP** is accessible through the reaction of **HIPTNH₂** with *tris*-(2-carboxyethyl)phosphine or its acylated derivative and plan to continue to pursue this ligand.

4.6 Experimental Details

General. All experiments involving air or moisture sensitive complexes or reactions were performed under nitrogen in a Vacuum Atmospheres drybox or using standard Schlenk techniques with glassware stored in an oven at ~190 °C for at least 12 hours prior to use. Pentane was washed with HNO₃/H₂SO₄ (5:95 by volume), sodium bicarbonate, and water, dried over CaCl₂, and then sparged with nitrogen and passed through an alumina column followed by storage over Na/benzophenone and vacuum transfer prior to use. Dry and deoxygenated benzene was purchased from Aldrich and passed through Q5 and alumina columns. Heptane, benzene-*d*₆ and toluene-*d*₈ were dried over Na/benzophenone then degassed (freeze-pump-thaw) and vacuum transferred prior to use. THF, diethyl ether and toluene were pre-dried by passage through an alumina column followed by storage over Na/benzophenone. They were degassed (freeze-pump-thaw) and vacuum transferred prior to use. All solvents were stored over 4 Å molecular sieves in a drybox after transfer.

Pd₂(dba)₃ (Strem), *rac*-BINAP (Strem), NaO-*t*-Bu (Aldrich), PH₃ (Aldrich), *t*-BuLi (Strem, 1.66 M in pentane), HCl (Anhydrous, BOC gases), H₂O₂ (30 wt. % in water, Aldrich), *tert*-butylchlorodimethylsilane (Aldrich), X-PHOS (Strem), Di-*tert*-butyl dicarbonate ((BOC)₂O, Acros), tetra-*n*-butylammonium fluoride (1 M in THF, Aldrich), CBr₄ (sublimed), PPh₃ (sublimed), *p*-toluidine (Aldrich), acrylonitrile (Aldrich), and NaBH₄ (Strem) were purchased and used as received or purified as indicated.

HIPTBr,^{19,20} 1-(2-chloroethyl)-2,2,5,5-tetramethyl-1,2,5-azadisilolidine,²¹ (*t*-BuMe₂Si)ethanolamine,⁶ Vilsmeier Reagent²² and *tris*-(3-propylcarboxylic acid)phosphine¹² were

synthesized *via* literature procedures. *tris*-(3-propanenitrile)phosphine^{14,15} was synthesized using a modified version of published procedure as detailed below.

¹H NMR spectra were obtained on a Varian Mercury (300 MHz), Bruker Avance (400 MHz) or Inova (500 MHz) spectrometer and were referenced to the residual protio-solvent peak. ³¹P NMR spectra were obtained on a Varian Mercury (121.4 MHz) or Bruker Avance (161.9 MHz) spectrometer and were externally reference to 85% phosphoric acid in H₂O ($\delta(^{31}\text{P}) = 0$ ppm). Mass spectrometry data was obtained on a Bruker APEXIV 47eV FT-ICR-MS (APOLLO ESI source). Elemental Analyses were performed by H. Kolbe Microanalytics Laboratory, Mülheim an der Ruhr, Germany.

***tris*-(2-aminoethyl)phosphine•3HCl (44).** (*NOTE: See discussion for custom apparatus details and handling of PH₃, which will spontaneously ignite on contact with air*)

PH₃ (*ca.* 8 mL) was condensed into the side-arm of the reaction flask and frozen with liquid nitrogen. The reaction apparatus was purged with nitrogen for 30 min, and 1-(2-chloroethyl)-2,2,5,5-tetramethyl-1,2,5-azadisilolidine (60.0 g, 0.27 mol) in THF (*ca.* 200 mL) was added *via* canula. The solution was then frozen with liquid nitrogen and allowed to warm in a CO₂/diethyl ether bath (*ca.* -100 °C). Once the solution was thawed, the PH₃ was thawed in a similar manner. The two liquids were then mixed by tipping the flask back and forth. *t*-BuLi in pentane (1.66 M, 163 mL) was added to the addition funnel, from which it was added drop-wise to the reaction mixture. The reaction was left to warm to room temperature while stirring under nitrogen over *ca.* 12 hours resulting in a heterogeneous mixture. The volatiles were removed *in vacuo* at room temperature, and the resulting residue taken up in pentane and filtered through celite. After removal of pentane a viscous orange oil is obtained which is a mixture of the *mono* and *bis* substituted phosphine by ³¹P NMR (THF) δ *bis*: -84.04 (d q, $J_{\text{HP(d)}} = 194.3$ Hz, $J_{\text{HP(q)}} = 5.3$ Hz), *mono*: -150.52 (t q, $J_{\text{HP(t)}} = 189.2$ Hz, $J_{\text{HP(q)}} = 4.9$ Hz). A portion of this oil (20g, 4:3 *bis:mono*) was added to a Schlenk flask and was dissolved in THF. To this, 1-(2-chloroethyl)-2,2,5,5-tetramethyl-1,2,5-azadisilolidine (23.7 g, 0.107 mol) was added. The reaction mixture was cooled in a CO₂/acetone bath and *t*-BuLi in pentane (1.66 M, 64 mL) was added *via* syringe. The reaction was allowed to warm to room temperature and left stirring over *ca.* 12 hours. The volatiles were removed *in vacuo*, and the resulting residue was taken up in diethyl ether and

filtered through celite. The resulting solution was concentrated and diethyl ether sparged with HCl was added to give a white precipitate (15 g, 82%) that was collected on a medium glass frit. ^1H NMR (D_2O) δ 3.10 (m, 6H), 1.91 (m, 6H); ^{31}P NMR (D_2O) δ -41.91 (m); $^{31}\text{P}\{^1\text{H}\}$ NMR (D_2O) δ -41.89 (s); MS (ESI) Calcd. m/z 164.1311 ($[\text{M}-3\text{HCl}+\text{H}]^+$), found m/z 164.1318; Calcd. m/z 272.0617 ($[\text{M}+\text{H}]^+$), found m/z 272.0611.

tris-(2-aminoethyl)phosphine (45). *tris*-(2-Aminoethyl)phosphine \cdot 3HCl (4.0 g, 15 mmol) was added to a 100 mL solvent bomb type flask with a 0-8 Teflon valve and washed down with diethyl ether (*ca.* 70 mL). Against a counter-flow of nitrogen, powdered NaOH (22 g, 55 mmol) was added in two portions. After vigorous stirring for *ca.* hours, the mixture was filtered through celite. The filtrate was stored over 4 Å molecular sieves for *ca.* 36 hours. The sieves were filtered away and the solvent removed on a rotovap. When cool, the product crystallizes as a white solid, but melts upon warming to give a colorless oil (715 mg, 30%). ^1H NMR (C_6D_6) δ 2.66 (br q, 6H), 1.34 (t, $J_{\text{HH}} = 7.4$ Hz, 6H), 0.71 (br s, 6H); ^{31}P NMR (C_6D_6) δ -46.55 (sept, $J_{\text{HP}} = 8.7$ Hz); $^{31}\text{P}\{^1\text{H}\}$ NMR (C_6D_6) δ -46.49 (s); MS (ESI) Calcd. m/z 186.1131 ($[\text{M}+\text{Na}]^+$), found m/z 186.1137.

tris-(2-aminoethyl)phosphine oxide (46). $\text{P}(\text{CH}_2\text{CH}_2\text{NH}_2)_3$ (300 mg, 1.84 mmol) was added to a 20 mL scintillation vial followed by water (*ca.* 2 mL). H_2O_2 (30 wt. %, 0.5 mL) was added and the vial was swirled, giving an instantaneous exothermic reaction. Another portion of H_2O_2 (30 wt. %, 0.5 mL) was added and the volatiles removed on a rotovap to give a clear viscous oil (265 mg, 80%). ^1H NMR (D_2O) δ 2.86 (m, 6H), 2.03 (m, 6H); ^{31}P NMR (D_2O) δ 53.92 (br m); $^{31}\text{P}\{^1\text{H}\}$ NMR (D_2O) δ 53.91 (s); MS (ESI) Calcd. m/z 180.1260 ($[\text{M}+\text{H}]^+$), found m/z 180.1226.

(*t*-BuMe₂Si)OCH₂CH₂N(H)HIPT (47). $\text{Pd}_2(\text{dba})_3$ (2.14 g, 2.34 mmol) and X-PHOS (2.56 g, 5.37 mmol) were added to a 50 mL round bottom flask, to which *ca.* toluene (40 mL) was added with stirring. After stirring for *ca.* 3 hours the mixture was filtered into a 500 mL solvent bomb with a Teflon valve. To this, NaO-*t*-Bu (9.93 g, 103 mmol), (*t*-BuMe₂Si)OCH₂CH₂NH₂ (10.86 g, 61.9 mmol) that had been stored over sieves after distillation, and HIPTBr (29.0 g, 51.6 mmol)

were added and the solvent level was brought to *ca.* 250 mL. Stirring at *ca.* 80 °C for *ca.* 3-5 hours gives a complete reaction. Filtration followed by concentration and passage through a plug of silica gel (toluene) yields **4** quantitatively after drying *in vacuo*. ¹H NMR (C₆D₆) δ 7.23 (s, 4H), 6.54 (t, J_{HH} = 1.4 Hz, 1H), 6.40 (d, J_{HH} = 1.4 Hz, 2H), 3.86 (t, J_{HH} = 6.1 Hz, 1H), 3.47 (t, J_{HH} = 5.1 Hz, 2H), 3.17 (sept, J_{HH} = 6.8 Hz, 4H), 3.04-2.81 (m, 4H), 1.37-1.23 (m, 36H), 0.92 (s, 9H), 0.01 (s, 6H).

(*t*-BuMe₂Si)OCH₂CH₂N(BOC)HIPT (48). **4** (15.0 g, 22.9 mmol) and (BOC)₂O (4.99 g, 22.9 mmol) were dissolved in diethyl ether (*ca.* 150 mL) in a Schlenk flask. The flask was cooled in an ice bath and *t*-BuLi (13.4 mL) was added drop-wise with stirring. The flask was left to warm overnight (*ca.* 12 hours) to give white precipitate. The mixture was then filtered under N₂ and dried *in vacuo* to give **5** quantitatively. ¹H NMR (C₆D₆) δ 7.19 (s, 4H), 7.11 (br s, 2H), 6.93 (t, J_{HH} = 1.5 Hz, 1H), 3.83 (m, 4H), 2.98 (sept, J_{HH} = 6.9 Hz, 4H), 2.89 (sept, J_{HH} = 6.9 Hz, 2H), 1.39 (s, 9H), 1.30 (d, J_{HH} = 6.9 Hz, 12H), 1.25 (d, J_{HH} = 6.9 Hz, 12H), 1.19 (d, J_{HH} = 6.9 Hz, 12H), 0.90 (s, 9H), 0.02 (s, 6H).

HOCH₂CH₂N(BOC)HIPT (49). **5** (10 g, 13.2 mmol) was taken up in THF, to which was added (TBA)F (1 M in THF, 19.8 mL) at 0 °C with stirring. The solution was allowed to warm to room temperature and Chromatography on silica gel (EtOAc/hexanes) yields **6** (6.8 g, 80%). ¹H NMR (C₆D₆) δ 7.19 (s, 4H), 7.02 (br s, 2H), 6.93 (br s, 1H), 3.78-3.61 (m, 4H), 3.04-2.80 (m, 6H), 2.66 (br s, 1H), 1.35 (s, 9H), 1.31 (d, J_{HH} = 7.2 Hz, 12H), 1.22 (d, J_{HH} = 6.9 Hz, 12H), 1.18 (d, J_{HH} = 6.6 Hz, 12H).

BrCH₂CH₂N(BOC)HIPT (50). **6** (6.8 g, 10.6 mmol) was dissolved in THF (*ca.* 100 mL) and cooled to 0 °C. To this, was added CBr₄ (4.6 g, 13.9 mmol) and PPh₃ (3.6 g, 13.7 mmol). The reaction mixture was allowed to warm to room temperature overnight (*ca.* 12 hours) and chromatographed on silica gel (EtOAc:Hexanes) to give **7** (6.6 g, 88%). ¹H NMR (C₆D₆) δ 7.20 (s, 4H), 7.04 (br s, 2H), 6.93 (br s, 1H), 3.90 (t, J_{HH} = 6.5 Hz, 2H), 3.21 (t, J_{HH} = 6.5 Hz, 2H), 3.07-2.80 (m, 6H), 1.36 (s, 9H), 1.30 (d, J_{HH} = 6.9 Hz, 12H), 1.23 (d, J_{HH} = 6.9 Hz, 12H), 1.18 (d, J_{HH} = 6.9 Hz, 12H); MS (ESI) Calcd. m/z 726.3856 ([M+Na]⁺), found m/z 726.3843.

H₂PCH₂CH₂N(BOC)HIPT (51). Synthetic and apparatus details for using PH₃ are as in the preparation of **1**. In this case excess PH₃ (1.5 – 2 mL) and **7** (3 g, 4.26 mmol) were used along with *t*-BuLi in pentane (1.66 M, 2.6 mL) to ensure *mono*-substitution. ¹H NMR (C₆D₆) δ 7.12 (s, 4H), 6.96 (br s, 2H), 6.92 (t, J_{HH} = 1.4 Hz, 1H), 3.89 (br s, 2H), 3.08-2.78 (m, 6H), 2.27 (br s, 2H), 1.65 (br s, 2H), 1.44 (s, 9H), 1.30 (d, J_{HH} = 6.9 Hz, 12H), 1.22 (d, J_{HH} = 6.9 Hz, 12H), 1.17 (d, J_{HH} = 6.9 Hz, 12H); ³¹P NMR (C₆D₆) δ -149.67 (t, J_{HP} = 191.1 Hz); ³¹P{¹H} NMR (C₆D₆) δ -149.66 (s); MS (ESI) Calcd. m/z 680.4567 ([M+Na]⁺), found m/z 680.4583.

***p*-tolylaniline(HIPT) (52).** Pd₂(dba)₃ (611 mg, 0.67 mmol) and X-PHOS (955 mg, 2.00 mmol) were added to toluene and stirred for *ca.* 3 hours and then filtered. *p*-tolylaniline (3.43 g, 32 mmol), NaO-*t*-Bu (5.13 g, 53.4 mmol), and HIPTBr (15.00 g, 26.7 mmol) and more toluene were added to the filtrate. The reaction mixture was then heated at *ca.* 80 °C for *ca.* 12 hours. Purification consisted of filtration through celite, passage through a plug of silica gel to give a yellow microcrystalline solid (15.2 g, 97%). ¹H NMR (C₆D₆) δ 7.22 (s, 4H), 6.91-6.82 (m, 6H), 6.66 (t, J_{HH} = 1.3 Hz, 1H), 5.09 (br s, 1H), 3.18 (sept, J_{HH} = 6.9 Hz, 4H), 2.89 (sept, J_{HH} = 6.9 Hz, 2H), 2.07 (s, 3H), 1.30 (d, J_{HH} = 6.9 Hz, 12H), 1.27 (d, J_{HH} = 6.9 Hz, 12H), 1.26 (d, J_{HH} = 6.9 Hz, 12H); MS (ESI) Calcd. m/z 588.4564 ([M+H]⁺), found m/z 588.4565.

***tris*-(2-cyanoethyl)phosphine (53).** Acrylonitrile (60 mL, 0.91 mol) in acetonitrile (*ca.* 100 mL) was added to a solvent bomb type flask equipped with a Teflon valve, which was placed in an ice bath and sparged with nitrogen. Keeping the solution cold, a degassed saturated aqueous solution of KOH (*ca.* 10 mL) was transferred into the reaction flask. The reaction flask was then attached to a gas transfer bridge equipped with a vacuum/pressure gauge and put under *ca.* 1 atm of PH₃ pressure. As the pressure decreased, more PH₃ was added until the pressure no longer declined. An aliquot of the reaction mixture was then taken and the ratio of *mono*-, *bis*-, and *tris*-substituted phosphine determined by ³¹P NMR (reaction mixture) δ -23.34 (sept, J_{HP} = 10.2 Hz), -70.83 (d m, J_{HP} = 204.4 Hz), -137.58 (t q, J_{HP(t)} = 197.2 Hz, J_{HP(q)} = 5.8 Hz); ³¹P{¹H} NMR (reaction mixture) δ -23.33 (s), -70.82 (s), -137.57 (s). The flask was again cooled in an ice bath, and another quantity of acrylonitrile (30 mL, 0.46 mol) was added against a nitrogen counter-flow. After stirring for *ca.* 12 hours, the mixture was once again cooled in an ice bath and the

resulting precipitate collected on a medium glass frit in air. Washing the collected solid with MeOH gave a white solid (79 g, 24%). ^1H NMR (CD_3CN) δ 2.54 (d t, $J_{\text{HH(t)}} = 7.8$ Hz, $J_{\text{HP}} = 10.5$ Hz, 6H), 1.83 (t, $J_{\text{HH}} = 7.7$ Hz, 6H); ^{31}P NMR (CD_3CN) δ -22.91 (sept, $J_{\text{HP}} = 10.3$ Hz); $^{31}\text{P}\{^1\text{H}\}$ NMR (CD_3CN) δ -22.91 (s); MS (ESI) Calcd. m/z 194.0842 ($[\text{M}+\text{H}]^+$), found m/z 194.0848.

HIPT(Benzophenoneimine) (54). $\text{Pd}_2(\text{dba})_3$ (489 mg, 0.53 mmol) and *rac*-BINAP (998 mg, 1.60 mmol) were added to a 50 mL round bottom flask followed by toluene (*ca.* 25 mL). The mixture was filtered through celite after stirring for *ca.* 3 hours into 100 mL solvent bomb type flask. $\text{NaO-}t\text{-Bu}$ (2.74 g, 28.5 mmol) and HIPTBr (10.0 g, 17.8 mmol) were added, and the volume wash brought to *ca.* 50 mL. Benzophenone imine (3.1 mL, 18.4 mmol) was added against a counter-flow of nitrogen and the reaction was stirred at *ca.* 80 °C for *ca.* 16 hours. The resulting mixture was filtered through a plug of silica gel and dried *in vacuo*. After trituration in MeOH, **11** (11 g, 93%) was obtained as a microcrystalline yellow/orange powder. ^1H NMR (C_6D_6) δ 7.93-7.87 (m, 2H), 7.18 (s, 4H), 7.11-7.07 (m, 2H), 7.01 (s, 4H), 6.67 (d, $J_{\text{HH}} = 1.4$ Hz, 2H), 6.65 (t, $J_{\text{HH}} = 1.5$ Hz, 1H), 2.96-2.77 (m, 6H), 1.28 (d, $J_{\text{HH}} = 6.9$ Hz, 12H), 1.17 (d, $J_{\text{HH}} = 6.9$ Hz, 12H), 1.16 (d, $J_{\text{HH}} = 6.9$ Hz, 12H); MS (ESI) Calcd. m/z 662.4720 ($[\text{M}+\text{H}]^+$), found m/z 662.4741.

HIPT(NH₂) (55). **11** (5.0 g, 7.55 mmol) was dissolved in wet THF, to which was added conc. HCl (*ca.* 1 mL). The reaction was dried *in vacuo* and redissolved in a 4:1 (by volume) mixture of THF:water. To this, NaBH_4 (343 mg, 9.07 mmol) was added and the reaction allowed to stir for *ca.* 6 hours. The reaction was extracted with methylene chloride and chromatographed on silica gel using toluene as the eluent to give **12** (3.3 g, 88%). ^1H NMR (C_6D_6) δ 7.21 (s, 4H), 6.51 (br s, 1H), 6.30-6.28 (m, 2H), 3.13 (sept, 6.9 Hz, 4H), 2.88 (sept, $J_{\text{HH}} = 6.9$ Hz, 2H), 2.78 (s, 2H), 1.29 (d, $J_{\text{HH}} = 7.0$ Hz, 12H), 1.27 (d, $J_{\text{HH}} = 7.1$ Hz, 12H), 1.24 (d, $J_{\text{HH}} = 7.0$ Hz, 12H); MS (ESI) Calcd. m/z 498.4094 ($[\text{M}+\text{H}]^+$), found m/z 498.4095.

4.7 References

- ¹ Alexander Kolchinski, *unpublished results*.
- ² Greco, G. E.; Schrock, R. R. *Inorg. Chem.* **2001**, *40*, 3850.
- ³ Alvey, L. J.; Rutherford, D.; Juliette, J. J. J.; Gladysz, J. A. *J. Org. Chem.* **1998**, *63*, 6302. and references therein.
- ⁴ Gordon, A. J.; Ford, R. A. *The Chemist's Companion: A Handbook of Practical Data, Techniques, and References*; John Wiley & Sons: New York, 1972.
- ⁵ Kwong, F. Y.; Buchwald, S. L. *Organic Letters* **2003**, *5*, 793.
- ⁶ Tattersall, P. I.; Breslin, D.; Grayson, S. M.; Heath, W. H.; Lou, K.; McAdams, C. L.; McKean, D.; Rathsack, B. M.; Willson, C. G. *Chem. Mater.* **2004**, *16*, 1770.
- ⁷ Williams, G. D.; Pike, R. A.; Wade, C. E.; Wills, M. *Organic Letters* **2003**, *5*, 4227.
- ⁸ Bangerter, B. W.; Beatty, R. P.; Kouba, J. K.; Wreford, S. S. *J. Org. Chem.* **1977**, *42*, 3247.
- ⁹ Vedejs, E.; Stults, J. S. *J. Org. Chem.* **1988**, *53*, 2226.
- ¹⁰ Honaker, M. T.; Sandeful, B. J.; Hargett, J. L.; McDaniel, A. L.; Savatore, R. N. *Tetrahedron Lett.* **2003**, *44*, 8473.
- ¹¹ MacLachlan, E. A.; Fryzuk, M. D. *Organometallics* **2005**, *26*, 1112.
- ¹² Burns, J. A.; Butler, J. C.; Moran, J.; Whitesides, G. M. *J. Org. Chem.* **1991**, *56*, 2648.
- ¹³ George E. Greco, *Ph.D. Thesis*, MIT, **1995**
- ¹⁴ Rauhut, M. M.; Hechenbleikner, I.; Currier, H. A.; Schaefer, F. C.; Wystrach, V. P. *J. Am. Chem. Soc.* **1959**, *81*, 1103.
- ¹⁵ Semenzin, D.; Etemad-Moghadam, G.; Albouy, D.; Koenig, M. *Tetrahedron Lett.* **1994**, *35*, 3297.
- ¹⁶ Wolfe, J. P.; Ahman, J.; Sadighi, J. P.; Singer, R. A.; Buchwald, S. L. *Tetrahedron Lett.* **1997**, *38*, 6367.
- ¹⁷ Huang, X.; Buchwald, S. L. *Organic Letters* **2001**, *3*, 3417.
- ¹⁸ Lee, S.; Jorgensen, M.; Hartwig, J. F. *Organic Letters* **2001**, *3*, 2729.
- ¹⁹ Yandulov, D. V.; Schrock, R. R. *J. Am. Chem. Soc.* **2002**, *124*, 6252.
- ²⁰ Yandulov, D. V.; Schrock, R. R.; Rheingold, A. L.; Ceccarelli, C.; Davis, W. M. *Inorg. Chem.* **2003**, *42*, 796.
- ²¹ Schrock, R. R.; Seidel, S. W.; Schrodi, Y.; Davis, W. M. *Organometallics* **1999**, *18*, 428.
- ²² Yoshihara, M.; Eda, T.; Sakaki, K.; Maeshima, T. *Synthesis* **1980**, 746.

Appendix A

Crystallographic Data

Table A.1: Crystal data and structure refinement for [HIPTN₃N]V(THF) (1).*

Identification code	05099	
Empirical formula	C ₁₃₂ H ₁₉₉ N ₄ OV	
Formula weight	1908.89	
Temperature	100(2) K	
Wavelength	0.71073 Å	
Crystal system	Triclinic	
Space group	P $\bar{1}$	
Unit cell dimensions	a = 17.7727(6) Å	α = 113.9930(10)°
	b = 18.3700(7) Å	β = 99.8920(10)°
	c = 21.2032(9) Å	γ = 96.5660(10)°
Volume	6098.5(4) Å ³	
Z	2	
Density (calculated)	1.040 Mg/m ³	
Absorption coefficient	0.130 mm ⁻¹	
F(000)	2100	
Crystal size	0.20 x 0.20 x 0.08 mm ³	
Theta range for data collection	1.40 to 28.28°	
Index ranges	-23 ≤ h ≤ 23, -24 ≤ k ≤ 24, -28 ≤ l ≤ 27	
Reflections collected	127420	
Independent reflections	30238 [R _{int} = 0.0638]	
Completeness to theta = 28.28°	99.9%	
Absorption correction	Semi-empirical from equivalents	
Max. and min. transmission	0.9897 and 0.9745	
Refinement method	Full-matrix least-squares on F ²	
Data / restraints / parameters	30238 / 397 / 1243	
Goodness-of-fit on F ²	1.043	
Final R indices [I > 2σ(I)]	R ₁ = 0.0696, wR ₂ = 0.1764	
R indices (all data)	R ₁ = 0.1069, wR ₂ = 0.2005	
Largest diff. peak and hole	0.896 and -0.562 eÅ ⁻³	

* Structure solution by Dr. Peter Müller.

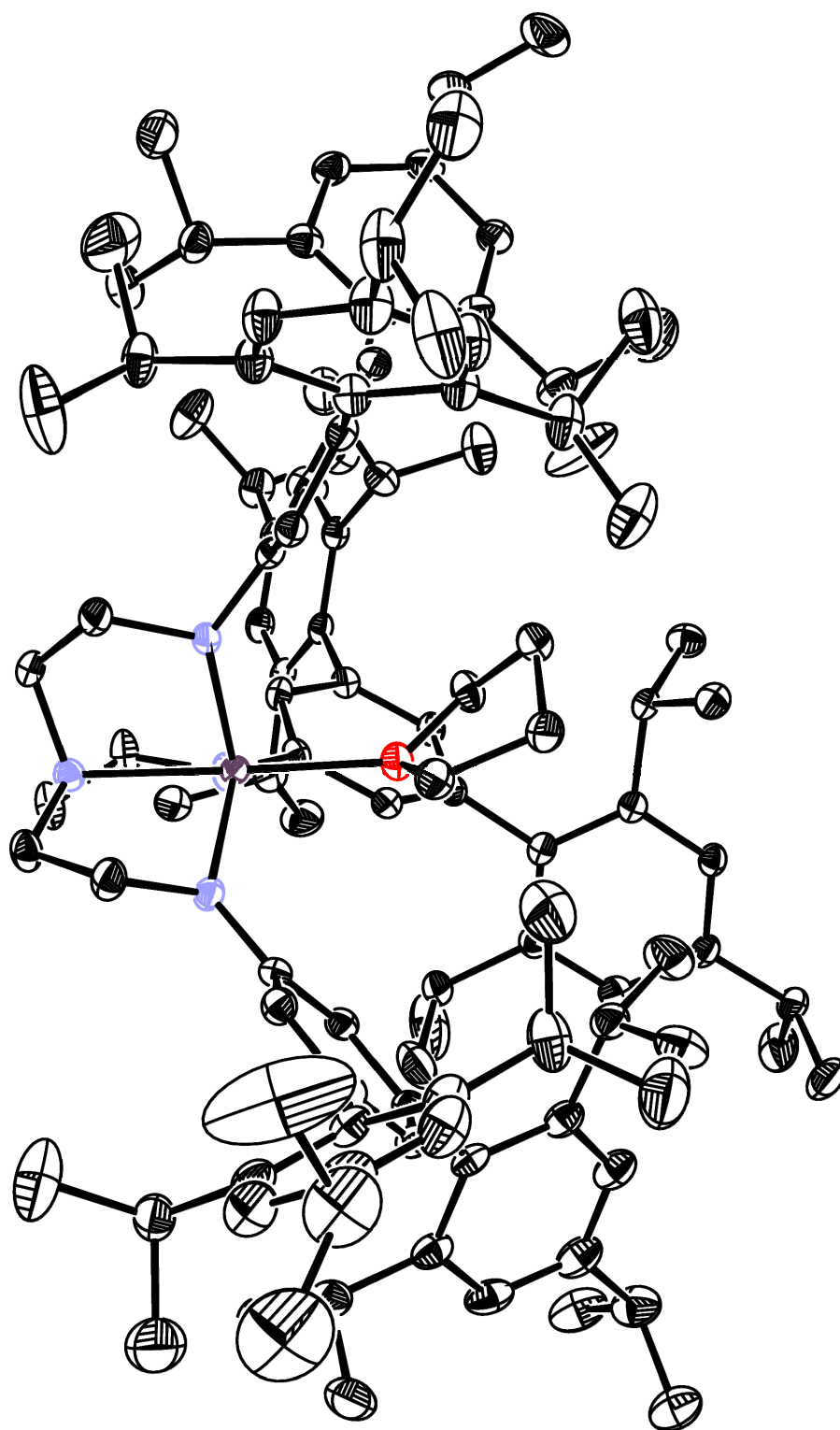


Figure A.1: Full ORTEP diagram of [HIPTN₃N]V(THF) (1). Thermal ellipsoids at 50% probability, hydrogen atoms and solvent omitted.

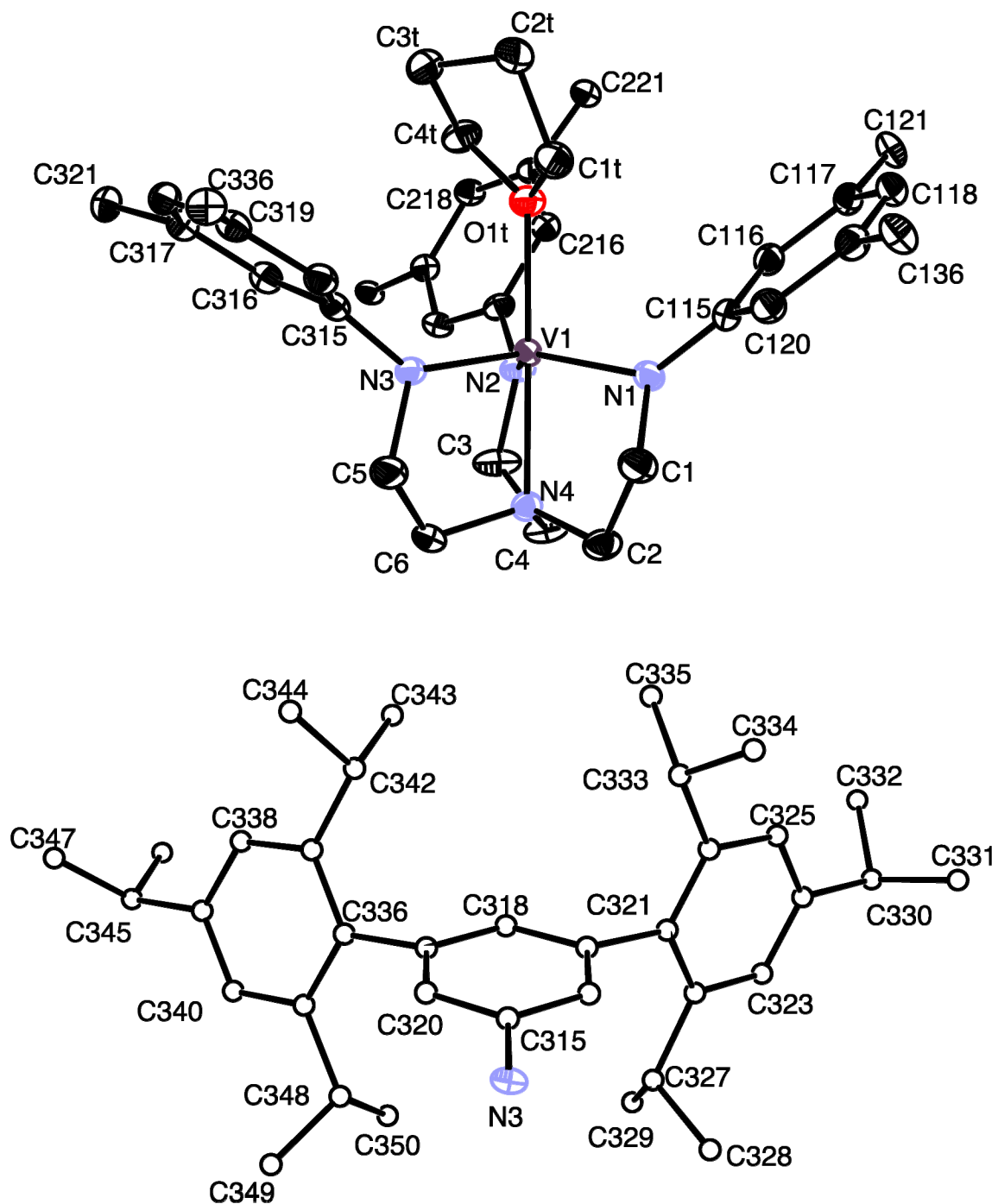


Figure A.2: Labeling scheme for [HIPTN₃N]V(THF) (1).

Table A.2: Atomic coordinates ($\times 10^4$) and equivalent isotropic displacement parameters ($\text{\AA}^2 \times 10^3$) for [HIPTN₃N]V(THF) (**1**, solvent omitted). $U(\text{eq})$ is defined as one third of the trace of the orthogonalized U_{ij} tensor.

	x	y	z	U(eq)
V(1)	-1403(1)	1478(1)	1270(1)	13(1)
O(1T)	-1320(1)	2090(1)	2388(1)	21(1)
C(1T)	-1595(1)	2863(1)	2654(1)	25(1)
C(2T)	-1224(1)	3291(2)	3445(1)	28(1)
C(3T)	-453(1)	3005(1)	3493(1)	26(1)
C(4T)	-696(1)	2119(1)	2951(1)	25(1)
N(1)	-2446(1)	1684(1)	986(1)	18(1)
N(2)	-1196(1)	390(1)	1092(1)	18(1)
N(3)	-551(1)	2253(1)	1315(1)	19(1)
N(4)	-1495(1)	1034(1)	141(1)	17(1)
C(1)	-2453(1)	1918(2)	401(1)	26(1)
C(2)	-2181(1)	1274(2)	-172(1)	23(1)
C(3)	-1056(2)	-57(2)	382(1)	28(1)
C(4)	-1583(2)	138(1)	-143(1)	25(1)
C(5)	-487(1)	2270(2)	636(1)	29(1)
C(6)	-757(1)	1411(2)	57(1)	24(1)
C(115)	-3037(1)	1881(1)	1338(1)	17(1)
C(116)	-3311(1)	1400(1)	1658(1)	18(1)
C(117)	-3914(1)	1563(1)	2004(1)	18(1)
C(118)	-4255(1)	2224(1)	2038(1)	20(1)
C(119)	-3991(1)	2720(1)	1735(1)	20(1)
C(120)	-3387(1)	2543(1)	1391(1)	20(1)
C(121)	-4225(1)	1007(1)	2298(1)	21(1)
C(122)	-3854(1)	1092(1)	2975(1)	24(1)
C(123)	-4157(1)	563(2)	3233(1)	29(1)
C(124)	-4811(2)	-45(2)	2843(2)	32(1)
C(125)	-5172(1)	-125(2)	2174(1)	31(1)
C(126)	-4889(1)	391(1)	1889(1)	26(1)
C(127)	-3153(1)	1776(2)	3438(1)	26(1)
C(128)	-2567(2)	1563(2)	3922(2)	38(1)
C(129)	-3414(2)	2544(2)	3886(2)	36(1)
C(130)	-5127(2)	-603(2)	3149(2)	38(1)
C(131)	-5125(2)	-1487(2)	2699(2)	44(1)
C(132)	-5923(2)	-478(2)	3281(2)	40(1)
C(133)	-5306(1)	294(2)	1161(1)	31(1)
C(134)	-5469(2)	-586(2)	586(2)	48(1)
C(135)	-6061(2)	621(2)	1208(2)	41(1)
C(136)	-4328(1)	3445(1)	1773(1)	23(1)
C(137)	-4766(1)	3437(2)	1149(1)	27(1)
C(138)	-5023(2)	4142(2)	1186(2)	35(1)
C(139)	-4859(2)	4846(2)	1820(2)	39(1)
C(140)	-4439(2)	4837(2)	2429(2)	37(1)
C(141)	-4172(2)	4149(2)	2423(1)	29(1)
C(142)	-4998(1)	2674(2)	442(1)	30(1)

C(143)	-5856(2)	2285(2)	276(2)	61(1)
C(144)	-4810(3)	2816(2)	-174(2)	64(1)
C(145)	-5104(2)	5628(2)	1846(2)	57(1)
C(146)	-4511(3)	6099(3)	1657(4)	131(3)
C(147)	-5921(3)	5485(3)	1408(3)	86(1)
C(148)	-3691(2)	4188(2)	3109(1)	37(1)
C(149)	-4044(2)	4561(2)	3743(2)	61(1)
C(150)	-2851(2)	4630(2)	3272(2)	59(1)
C(215)	-917(1)	84(1)	1575(1)	16(1)
C(216)	-1266(1)	172(1)	2142(1)	16(1)
C(217)	-1026(1)	-166(1)	2605(1)	16(1)
C(218)	-415(1)	-587(1)	2513(1)	17(1)
C(219)	-65(1)	-691(1)	1953(1)	17(1)
C(220)	-313(1)	-354(1)	1492(1)	18(1)
C(221)	-1444(1)	-185(1)	3156(1)	17(1)
C(222)	-2153(1)	-747(1)	2940(1)	19(1)
C(223)	-2497(1)	-831(1)	3457(1)	22(1)
C(224)	-2145(1)	-393(1)	4181(1)	20(1)
C(225)	-1452(1)	162(1)	4380(1)	19(1)
C(226)	-1093(1)	284(1)	3884(1)	17(1)
C(227)	-2545(1)	-1274(1)	2154(1)	26(1)
C(228)	-3256(2)	-966(2)	1923(2)	52(1)
C(229)	-2747(3)	-2171(2)	1985(2)	61(1)
C(230)	-2509(1)	-503(2)	4746(1)	25(1)
C(231)	-2761(2)	-1394(2)	4582(2)	41(1)
C(232)	-3187(2)	-61(2)	4859(2)	38(1)
C(233)	-333(1)	911(1)	4143(1)	17(1)
C(234)	330(1)	681(2)	4539(1)	26(1)
C(235)	-445(1)	1761(1)	4618(1)	24(1)
C(236)	530(1)	-1215(1)	1809(1)	17(1)
C(237)	1334(1)	-868(1)	2076(1)	19(1)
C(238)	1862(1)	-1384(1)	1927(1)	23(1)
C(239)	1625(1)	-2222(1)	1518(1)	22(1)
C(240)	831(1)	-2544(1)	1251(1)	21(1)
C(241)	274(1)	-2060(1)	1399(1)	19(1)
C(242)	1625(1)	37(1)	2546(1)	23(1)
C(243)	2233(2)	420(2)	2274(2)	43(1)
C(244)	1975(2)	200(2)	3311(1)	38(1)
C(245)	2219(1)	-2774(2)	1401(1)	29(1)
C(246)	2801(2)	-2576(2)	1017(2)	43(1)
C(247)	2650(2)	-2739(2)	2108(1)	32(1)
C(248)	-595(1)	-2448(1)	1130(1)	22(1)
C(249)	-794(2)	-3210(2)	1243(2)	37(1)
C(250)	-901(2)	-2630(2)	356(1)	34(1)
C(315)	45(1)	2861(1)	1882(1)	17(1)
C(316)	709(1)	2647(1)	2162(1)	18(1)
C(317)	1350(1)	3241(1)	2648(1)	18(1)
C(318)	1317(1)	4062(1)	2854(1)	18(1)
C(319)	661(1)	4290(1)	2582(1)	18(1)
C(320)	25(1)	3685(1)	2108(1)	18(1)
C(321)	2102(1)	3036(1)	2900(1)	19(1)
C(322)	2665(1)	2938(1)	2497(1)	21(1)
C(323)	3383(1)	2800(1)	2762(1)	24(1)
C(324)	3555(1)	2758(1)	3407(1)	24(1)

C(325)	2985(1)	2845(1)	3791(1)	23(1)
C(326)	2263(1)	2989(1)	3554(1)	21(1)
C(327)	2502(1)	2963(2)	1776(1)	25(1)
C(328)	2340(2)	2101(2)	1174(1)	35(1)
C(329)	3160(2)	3521(2)	1705(1)	36(1)
C(330)	4344(1)	2617(2)	3687(1)	29(1)
C(331)	4277(2)	1751(2)	3614(2)	42(1)
C(332)	4715(2)	3238(2)	4452(2)	42(1)
C(333)	1669(1)	3099(2)	4006(1)	27(1)
C(334)	1414(2)	2325(2)	4077(2)	64(1)
C(335)	1977(2)	3820(2)	4731(2)	62(1)
C(336)	682(1)	5163(1)	2740(1)	21(1)
C(337)	668(1)	5737(1)	3426(1)	23(1)
C(338)	737(2)	6555(1)	3562(1)	28(1)
C(339)	813(2)	6819(1)	3041(1)	30(1)
C(340)	813(2)	6239(1)	2367(1)	28(1)
C(341)	758(1)	5416(1)	2208(1)	23(1)
C(342)	595(2)	5489(1)	4019(1)	28(1)
C(343)	1335(2)	5859(2)	4620(2)	45(1)
C(344)	-122(2)	5713(2)	4310(2)	43(1)
C(345)	928(2)	7721(2)	3211(1)	38(1)
C(346)	1683(2)	8201(2)	3766(2)	45(1)
C(347)	228(2)	8072(2)	3433(2)	47(1)
C(348)	831(2)	4828(1)	1475(1)	28(1)
C(349)	325(2)	4922(2)	871(2)	59(1)
C(350)	1681(2)	4927(2)	1437(2)	54(1)

Table A.3: Crystal data and structure refinement for [HIPTN₃N]VH.*

Identification code	04123	
Empirical formula	C ₁₂₁ H ₁₇₆ N ₄ V	
Formula weight	1737.60	
Temperature	194(2) K	
Wavelength	0.71073 Å	
Crystal system	Rhombohedral	
Space group	R $\bar{3}c$	
Unit cell dimensions	a = 21.0178(7) Å	$\alpha = 90^\circ$
	b = 21.0178(7) Å	$\beta = 90^\circ$
	c = 98.698(6) Å	$\gamma = 120^\circ$
Volume	37758(3) Å ³	
Z	12	
Density (calculated)	0.917 Mg/m ³	
Absorption coefficient	0.120 mm ⁻¹	
F(000)	11436	
Crystal size	0.30 x 0.28 x 0.20 mm ³	
Theta range for data collection	1.19 to 25.03°	
Index ranges	-23 ≤ h ≤ 25, -24 ≤ k ≤ 25, -114 ≤ l ≤ 117	
Reflections collected	64412	
Independent reflections	7400 [R _{int} = 0.0777]	
Completeness to theta = 25.03°	99.6%	
Absorption correction	Semi-empirical from equivalents	
Max. and min. transmission	0.9764 and 0.9649	
Refinement method	Full-matrix least-squares on F ²	
Data / restraints / parameters	7400 / 808 / 524	
Goodness-of-fit on F ²	1.783	
Final R indices [I > 2σ(I)]	R ₁ = 0.0985, wR ₂ = 0.2642	
R indices (all data)	R ₁ = 0.1296, wR ₂ = 0.2771	
Largest diff. peak and hole	2.305 and -0.308 eÅ ⁻³	

* Structure solution by Dr. Peter Müller.

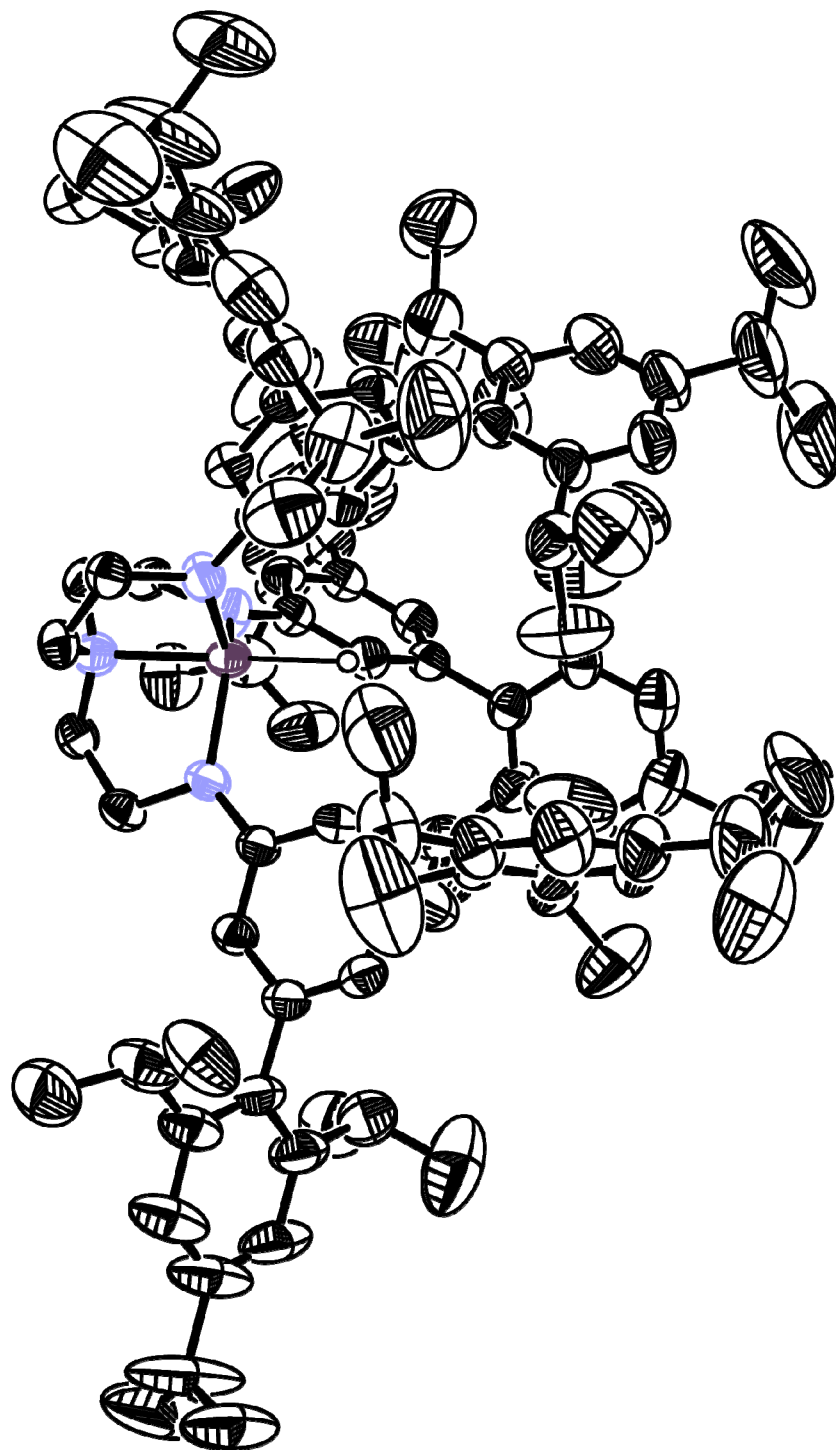


Figure A.3: Full ORTEP diagram of [HIPTN₃N]VH. Thermal ellipsoids at 50% probability, solvent and hydrogen atoms removed (disorder not shown).

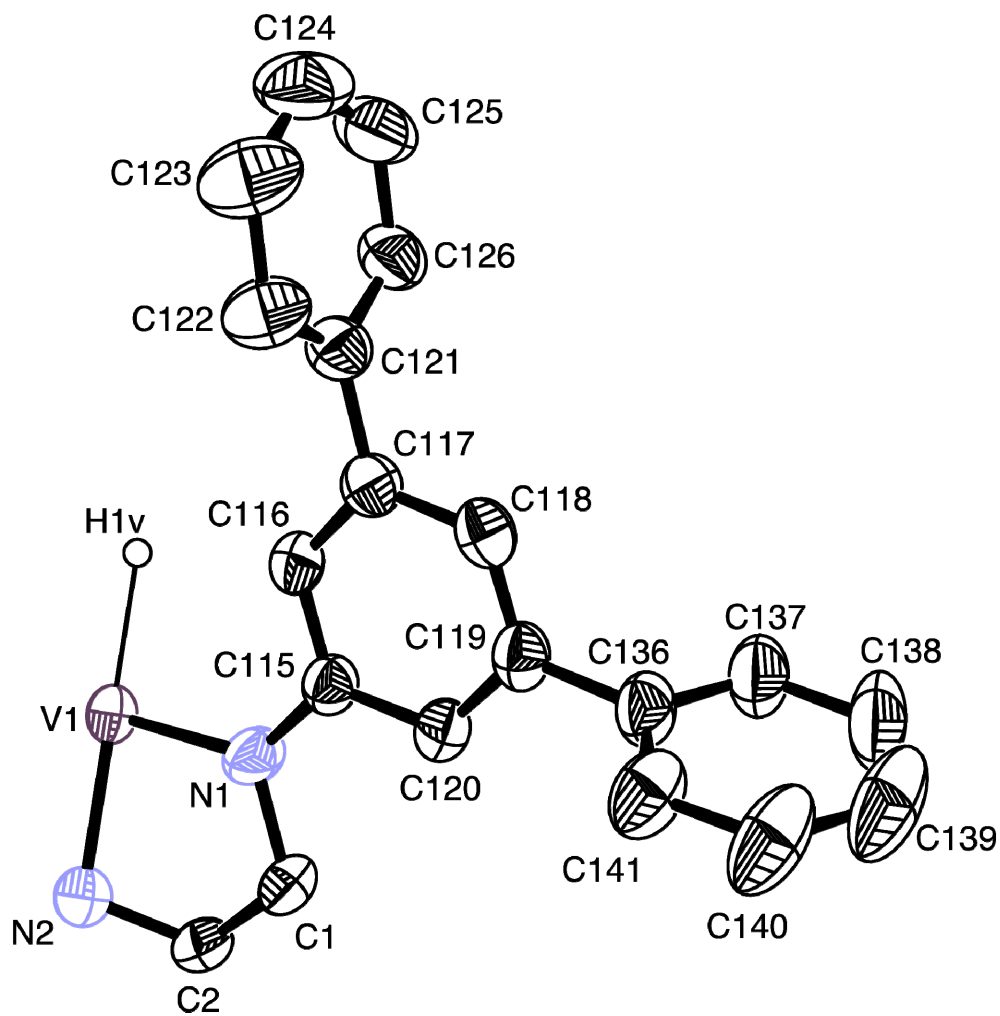


Figure A.4: ORTEP labeling scheme for [HIPTN₃N]VH (disorder not shown).

Table A.4: Atomic coordinates ($\times 10^4$) and equivalent isotropic displacement parameters ($\text{\AA}^2 \times 10^3$) for [HIPTN₃N]VH. $U(\text{eq})$ is defined as one third of the trace of the orthogonalized U_{ij} tensor.

	x	y	z	$U(\text{eq})$
V(1)	3333	6667	139(1)	38(1)
N(1)	3208(2)	7515(2)	116(1)	51(1)
C(1)	2961(4)	7582(3)	-21(1)	46(2)
C(2)	2826(2)	6927(2)	-106(1)	48(2)
N(2)	3333	6667	-72(1)	45(1)
C(115)	3338(2)	8085(2)	206(1)	42(1)
C(116)	3678(2)	8141(2)	331(1)	46(1)
C(117)	3824(2)	8699(2)	421(1)	45(1)
C(118)	3643(2)	9233(2)	385(1)	49(1)
C(119)	3311(2)	9199(2)	263(1)	47(1)
C(120)	3151(2)	8619(2)	174(1)	43(1)
C(121)	4196(2)	8790(2)	556(1)	51(1)
C(122)	4947(2)	9184(2)	568(1)	69(1)
C(123)	5256(3)	9322(3)	697(1)	90(1)
C(124)	4850(3)	9084(3)	812(1)	87(1)
C(125)	4090(3)	8686(3)	798(1)	77(1)
C(126)	3754(2)	8530(2)	673(1)	58(1)
C(127)	5446(2)	9445(3)	444(1)	94(2)
C(128)	5969(4)	10271(4)	448(1)	170(3)
C(129)	5836(4)	9015(5)	428(1)	162(3)
C(130)	5206(5)	9266(5)	955(1)	149(3)
C(131)	4934(12)	8583(8)	1037(1)	207(8)
C(132)	5641(9)	10029(6)	980(1)	180(6)
C(133)	2922(2)	8052(2)	660(1)	67(1)
C(134)	2488(3)	8262(4)	755(1)	129(2)
C(135)	2703(3)	7241(3)	679(1)	123(2)
C(136)	3138(2)	9790(2)	225(1)	56(1)
C(137)	2538(2)	9797(2)	280(1)	72(1)
C(138)	2430(3)	10393(3)	250(1)	91(1)
C(139)	2892(3)	10952(2)	163(1)	99(2)
C(140)	3467(3)	10916(2)	108(1)	89(1)
C(141)	3611(2)	10355(2)	135(1)	68(1)
C(142)	1981(3)	9164(3)	373(1)	89(1)
C(143)	1912(4)	9446(5)	512(1)	168(3)
C(144)	1237(3)	8732(3)	307(1)	110(2)
C(145)	2784(4)	11606(3)	132(1)	169(3)
C(146)	3293(4)	12258(3)	216(1)	135(2)
C(147)	2175(5)	11496(4)	76(1)	196(4)
C(148)	4294(2)	10376(2)	77(1)	82(1)
C(149)	4916(3)	10719(3)	177(1)	106(2)
C(150)	4543(3)	10757(3)	-60(1)	106(2)

Table A.5: Crystal data and structure refinement for [HIPTN₃N]V(NH₃) (5).*

Identification code	03316	
Empirical formula	C ₁₂₁ H ₁₇₈ N ₅ V	
Formula weight	1753.62	
Temperature	193(2) K	
Wavelength	0.71073 Å	
Crystal system	Monoclinic	
Space group	Cc	
Unit cell dimensions	a = 16.1153(4) Å	α = 90°
	b = 39.7548(11) Å	β = 93.0540(10)°
	c = 18.0197(5) Å	γ = 90°
Volume	11528.1(5) Å ³	
Z	4	
Density (calculated)	1.010 Mg/m ³	
Absorption coefficient	0.132 mm ⁻¹	
F(000)	3848	
Crystal size	0.20 x 0.17 x 0.10 mm ³	
Theta range for data collection	1.99 to 25.03°	
Index ranges	-18 ≤ h ≤ 19, -47 ≤ k ≤ 41, -21 ≤ l ≤ 13	
Reflections collected	29563	
Independent reflections	15469 [R _{int} = 0.0305]	
Completeness to theta = 25.03°	99.9%	
Absorption correction	Semi-empirical from equivalents	
Max. and min. transmission	0.9869 and 0.9741	
Refinement method	Full-matrix least-squares on F ²	
Data / restraints / parameters	15469 / 3023 / 1536	
Goodness-of-fit on F ²	1.015	
Final R indices [I > 2σ(I)]	R ₁ = 0.0584, wR ₂ = 0.1452	
R indices (all data)	R ₁ = 0.0766, wR ₂ = 0.1585	
Absolute structure parameter	-0.009(19)	
Largest diff. peak and hole	0.317 and -0.268 eÅ ⁻³	

* Structure solution by Dr. Peter Müller.

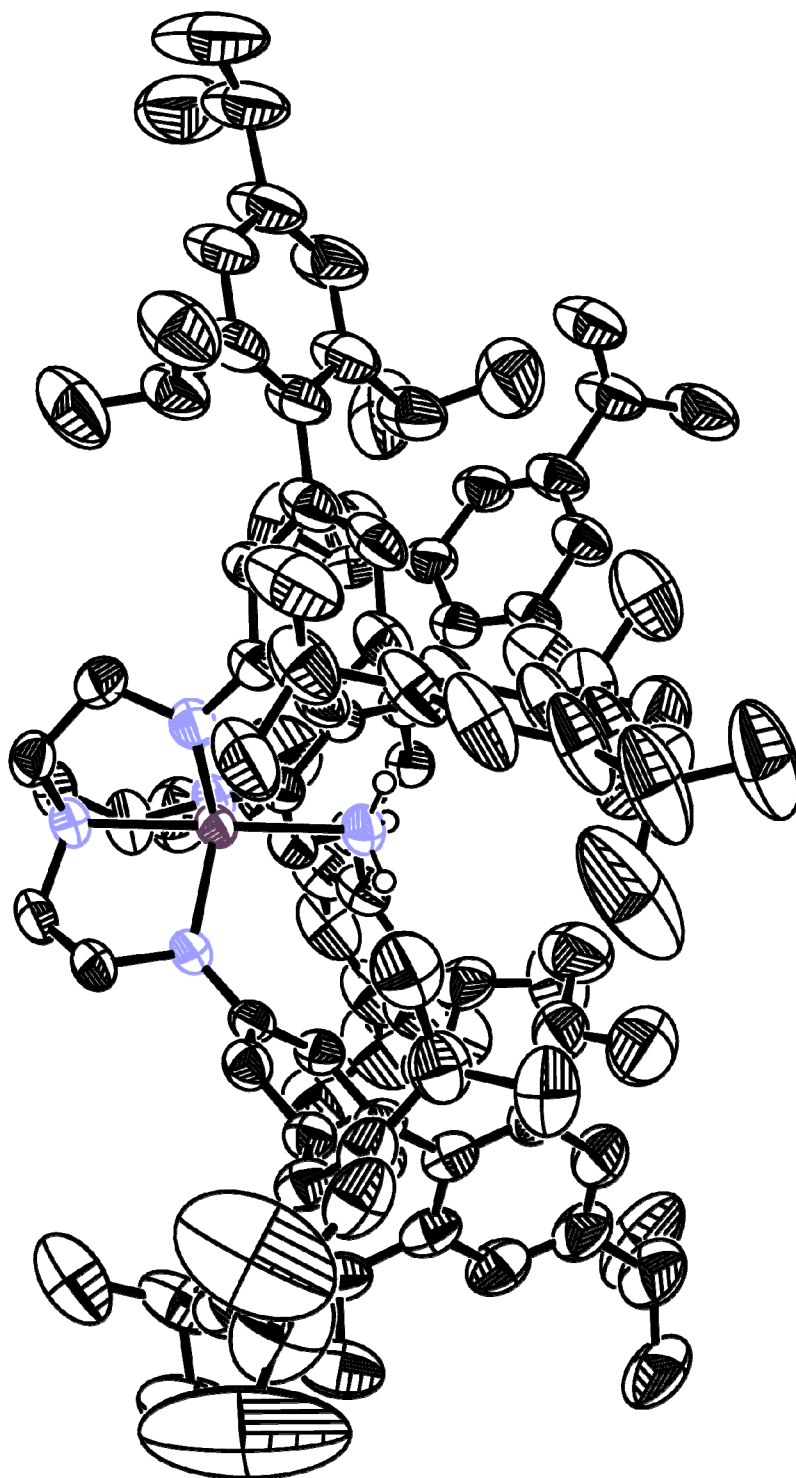


Figure A.5: Full ORTEP of [HIPTN₃N]V(NH₃) (5). Thermal ellipsoids at 50% probability, hydrogen atoms, solvent, and disorder not shown.

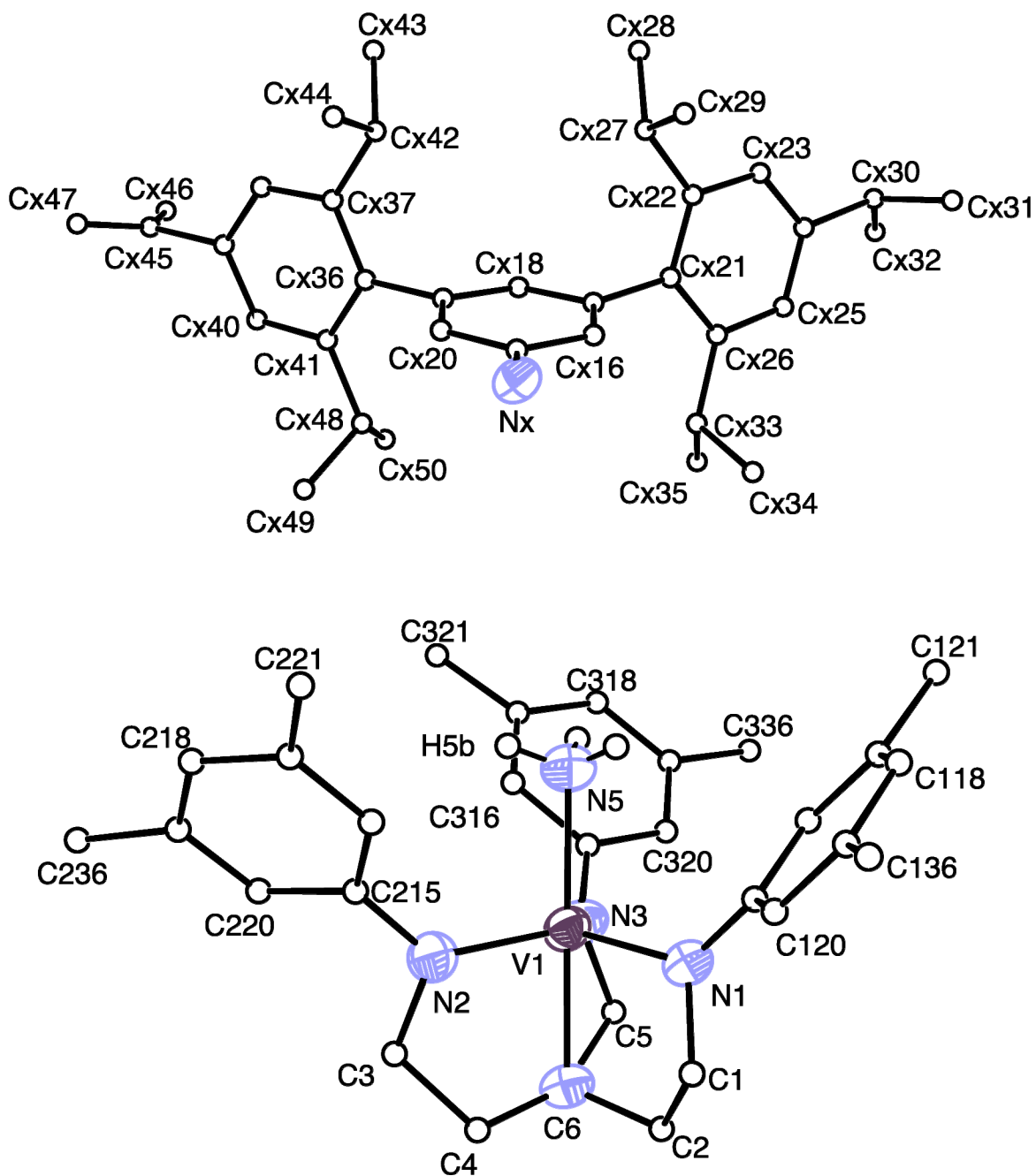


Figure A.6: ORTEP labeling scheme for [HIPTN₃N]V(NH₃) (5). Disorder, non-amine hydrogens, and solvent omitted.

Table A.6: Atomic coordinates ($\times 10^4$) and equivalent isotropic displacement parameters ($\text{\AA}^2 \times 10^3$) for [HIPTN₃N]V(NH₃) (**5**). U(eq) is defined as one third of the trace of the orthogonalized U_{ij} tensor.

	x	y	z	U(eq)
N(4)	7167(1)	5965(1)	6189(1)	45(1)
N(5)	7948(1)	6198(1)	8456(1)	51(1)
V(1)	7557(1)	6079(1)	7320(1)	39(1)
C(1)	8658(1)	6031(1)	6133(1)	56(1)
C(2)	7827(1)	6082(1)	5717(1)	57(1)
C(3)	6749(1)	5472(1)	6865(1)	64(1)
C(4)	7054(1)	5596(1)	6148(1)	58(1)
C(5)	6393(1)	6478(1)	6455(1)	65(1)
C(6)	6377(1)	6148(1)	6031(1)	57(1)
N(1)	8601(1)	6187(1)	6868(1)	44(1)
C(115)	9357(1)	6298(1)	7199(1)	44(1)
C(116)	9394(1)	6608(1)	7578(1)	47(1)
C(117)	10140(1)	6727(1)	7901(1)	53(1)
C(118)	10859(1)	6534(1)	7860(1)	58(1)
C(119)	10835(1)	6229(1)	7480(1)	52(1)
C(120)	10094(1)	6116(1)	7156(1)	50(1)
C(121)	10211(1)	7058(1)	8302(1)	61(1)
C(122)	10474(1)	7343(1)	7923(1)	65(1)
C(123)	10631(1)	7639(1)	8332(1)	81(1)
C(124)	10552(1)	7653(1)	9090(1)	86(1)
C(125)	10268(1)	7372(1)	9440(1)	87(1)
C(126)	10099(1)	7072(1)	9063(1)	71(1)
C(127)	10609(1)	7336(1)	7099(1)	74(1)
C(128)	10192(1)	7634(1)	6686(1)	92(1)
C(129)	11537(1)	7336(1)	6948(1)	110(1)
C(130)	10771(1)	7975(1)	9521(1)	109(1)
C(131)	10064(1)	8203(1)	9473(1)	173(1)
C(132)	11579(1)	8123(1)	9315(1)	123(1)
C(133)	9794(1)	6772(1)	9493(1)	82(1)
C(134)	8941(1)	6833(1)	9774(1)	116(1)
C(135)	10407(1)	6667(1)	10112(1)	134(1)
C(136)	11611(1)	6025(1)	7438(1)	60(1)
C(137)	11852(1)	5808(1)	8024(1)	68(1)
C(138)	12565(1)	5612(1)	7947(1)	90(1)
C(139)	13034(1)	5620(1)	7332(1)	97(1)
C(140)	12791(1)	5845(1)	6778(1)	91(1)
C(141)	12091(1)	6050(1)	6816(1)	74(1)
C(142)	11356(1)	5778(1)	8712(1)	81(1)
C(143)	10858(1)	5455(1)	8720(1)	115(1)
C(144)	11882(1)	5815(1)	9440(1)	136(1)
C(145)	13802(1)	5394(1)	7279(1)	167(1)
C(146)	13637(1)	5036(1)	7331(1)	252(1)
C(147)	14403(1)	5519(1)	6819(2)	361(2)
C(148)	11872(1)	6301(1)	6193(1)	97(1)
C(149)	11557(1)	6126(1)	5486(1)	127(1)
C(150)	12601(1)	6529(1)	6048(1)	162(1)

N(2)	7290(1)	5604(1)	7474(1)	48(1)
C(215)	7290(1)	5413(1)	8123(1)	52(1)
C(216)	8011(1)	5376(1)	8586(1)	55(1)
C(217)	8030(1)	5172(1)	9209(1)	63(1)
C(218)	7307(1)	5002(1)	9387(1)	69(1)
C(219)	6582(1)	5035(1)	8949(1)	67(1)
C(220)	6575(1)	5240(1)	8330(1)	59(1)
C(221)	8832(1)	5094(1)	9647(1)	69(1)
C(222)	9314(1)	4822(1)	9419(1)	83(1)
C(223)	10037(1)	4742(1)	9850(1)	103(1)
C(224)	10275(1)	4912(1)	10484(1)	105(1)
C(225)	9787(1)	5177(1)	10694(1)	95(1)
C(226)	9070(1)	5271(1)	10291(1)	78(1)
C(227)	9094(1)	4620(1)	8722(1)	91(1)
C(228)	9692(1)	4680(1)	8132(1)	108(1)
C(229)	9029(1)	4242(1)	8892(1)	130(1)
C(230)	11089(1)	4820(1)	10923(1)	136(1)
C(231)	11078(1)	4902(1)	11718(1)	155(1)
C(232)	11800(1)	4933(1)	10532(1)	240(1)
C(233)	8536(1)	5550(1)	10574(1)	84(1)
C(234)	9042(1)	5855(1)	10804(1)	148(1)
C(235)	8048(1)	5425(1)	11229(1)	120(1)
C(236)	5804(1)	4842(1)	9096(1)	73(1)
C(237)	5187(1)	4986(1)	9513(1)	89(1)
C(238)	4456(1)	4808(1)	9610(1)	100(1)
C(239)	4328(1)	4493(1)	9300(1)	105(1)
C(240)	4953(1)	4354(1)	8910(1)	92(1)
C(241)	5688(1)	4519(1)	8799(1)	82(1)
C(242)	5308(1)	5339(1)	9855(1)	90(1)
C(243)	5353(1)	5321(1)	10696(1)	123(1)
C(244)	4642(1)	5585(1)	9579(1)	137(1)
C(245)	3482(1)	4318(1)	9373(1)	127(1)
C(246)	2848(1)	4469(1)	8840(1)	178(1)
C(247)	3532(1)	3944(1)	9316(1)	183(1)
C(248)	6327(1)	4362(1)	8317(1)	80(1)
C(249)	6058(1)	4375(1)	7516(1)	119(1)
C(250)	6541(1)	4000(1)	8561(1)	109(1)
N(3)	6646(1)	6402(1)	7229(1)	47(1)
C(315)	6362(1)	6632(1)	7747(1)	46(1)
C(316)	6012(1)	6519(1)	8398(1)	50(1)
C(317)	5685(1)	6741(1)	8899(1)	51(1)
C(318)	5730(1)	7086(1)	8764(1)	54(1)
C(319)	6060(1)	7208(1)	8120(1)	54(1)
C(320)	6378(1)	6981(1)	7623(1)	52(1)
C(321)	5210(1)	6625(1)	9545(1)	56(1)
C(322)	4342(1)	6622(1)	9473(1)	69(1)
C(323)	3901(1)	6532(1)	10097(1)	75(1)
C(324)	4288(1)	6440(1)	10755(1)	74(1)
C(325)	5141(1)	6433(1)	10806(1)	71(1)
C(326)	5623(1)	6528(1)	10217(1)	60(1)
C(327)	3879(1)	6710(1)	8755(1)	86(1)
C(328)	3089(1)	6901(1)	8856(1)	145(1)
C(329)	3701(1)	6392(1)	8290(1)	159(1)
C(330)	3756(1)	6340(1)	11406(1)	90(1)

C(331)	3597(1)	5971(1)	11425(1)	96(1)
C(332)	4024(1)	6491(1)	12117(1)	129(1)
C(333)	6557(1)	6515(1)	10300(1)	67(1)
C(334)	6874(1)	6156(1)	10228(1)	93(1)
C(335)	6938(1)	6676(1)	11007(1)	105(1)
C(336)	6089(1)	7577(1)	7968(1)	63(1)
C(337)	5403(1)	7731(1)	7587(1)	79(1)
C(338)	5459(1)	8077(1)	7450(1)	99(1)
C(339)	6130(1)	8269(1)	7666(1)	108(1)
C(340)	6782(1)	8111(1)	8039(1)	94(1)
C(341)	6782(1)	7768(1)	8205(1)	74(1)
C(342)	4642(1)	7526(1)	7340(1)	98(1)
C(343)	3833(1)	7720(1)	7454(1)	171(1)
C(344)	4674(1)	7429(1)	6523(1)	136(1)
C(345)	6157(2)	8644(1)	7505(1)	157(1)
C(346)	5927(1)	8853(1)	8100(1)	162(1)
C(347)	6340(1)	8742(1)	6807(1)	135(1)
C(348)	7511(1)	7613(1)	8641(1)	83(1)
C(349)	8311(1)	7642(1)	8232(1)	116(1)
C(350)	7629(1)	7759(1)	9414(1)	134(1)

Table A.7: Crystal data and structure refinement for {[NNO]VCl}₂ (32).*

Identification code	04116	
Empirical formula	C _{90.50} H _{132.50} ClN ₃ O _{1.75} Si _{1.50} V	
Formula weight	1419.02	
Temperature	193(2) K	
Wavelength	0.71073 Å	
Crystal system	Triclinic	
Space group	P $\bar{1}$	
Unit cell dimensions	a = 17.0771(12) Å	α = 99.977(2)°
	b = 17.7873(14) Å	β = 98.489(2)°
	c = 32.844(3) Å	γ = 111.530(2)°
Volume	8894.0(12) Å ³	
Z	4	
Density (calculated)	1.060 Mg/m ³	
Absorption coefficient	0.206 mm ⁻¹	
F(000)	3086	
Crystal size	0.05 x 0.10 x 0.13 mm ³	
Theta range for data collection	0.65 to 20.82°	
Index ranges	-17 ≤ h ≤ 16, -17 ≤ k ≤ 17, 0 ≤ l ≤ 32	
Reflections collected	18563	
Independent reflections	18563 [R _{int} = 0.0000]	
Completeness to theta = 20.82°	99.7%	
Absorption correction	None	
Refinement method	Full-matrix least-squares on F ²	
Data / restraints / parameters	18563 / 2425 / 1900	
Goodness-of-fit on F ²	1.010	
Final R indices [I > 2σ(I)]	R ₁ = 0.0625, wR ₂ = 0.1404	
R indices (all data)	R ₁ = 0.1235, wR ₂ = 0.1699	
Largest diff. peak and hole	0.372 and -0.305 eÅ ⁻³	

* Structure solution by Dr. Peter Müller.

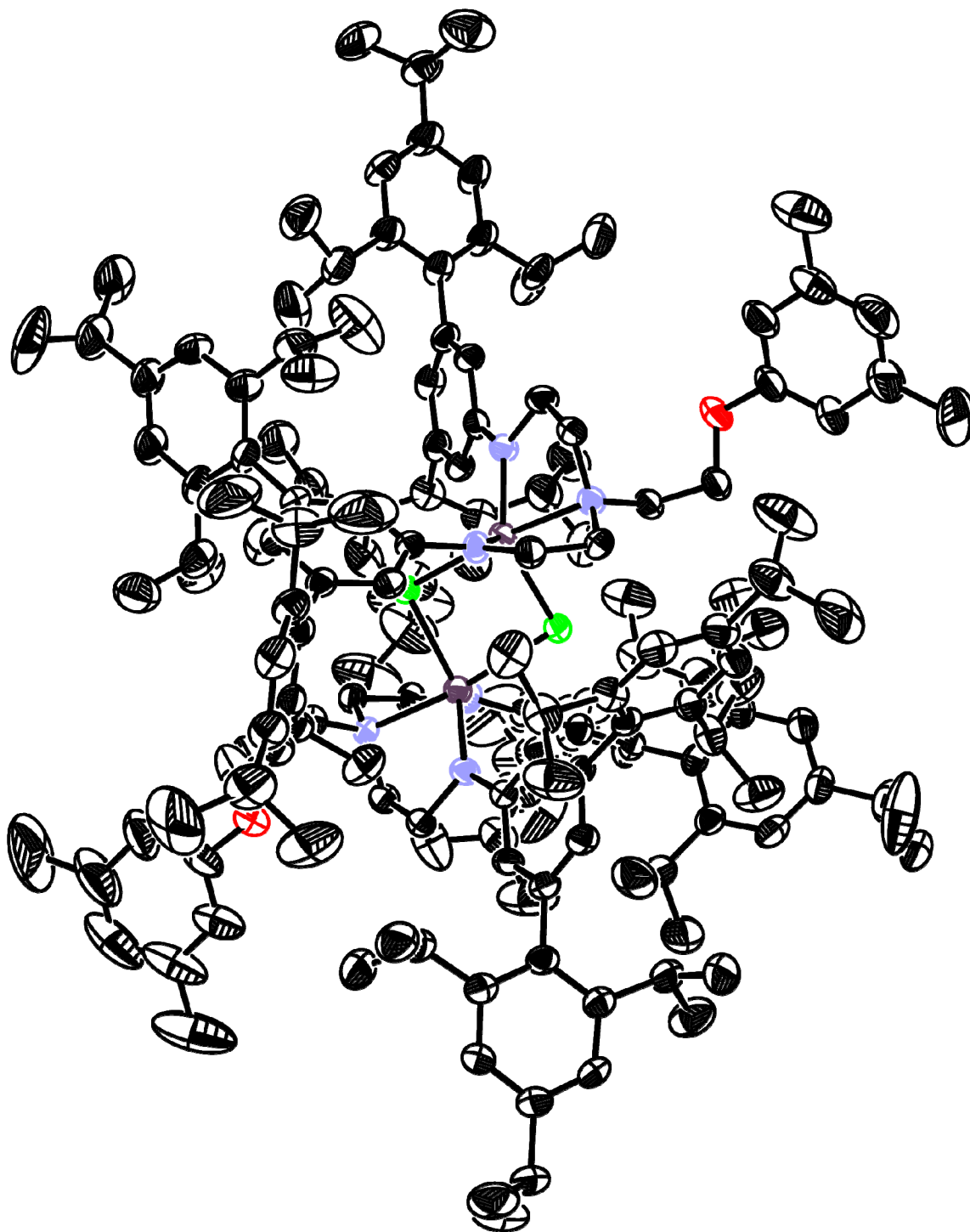


Figure A.7: Full ORTEP of $\{[\text{NNO}]\text{VCl}_2\}_2$ (32). Thermal ellipsoids at 50% probability, hydrogen atoms and solvent omitted.

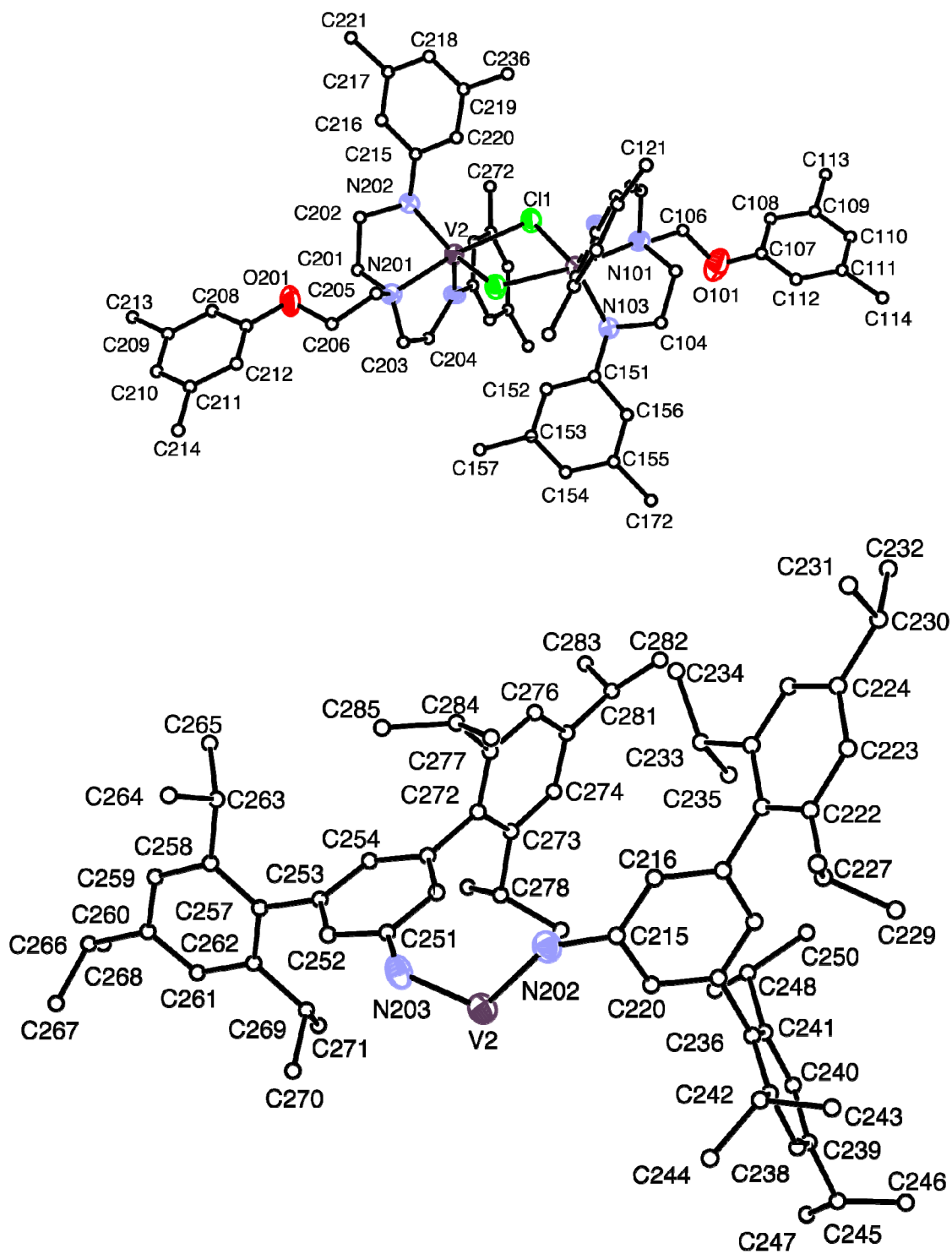


Figure A.8: ORTEP labeling scheme for $\{[NNO]VCl\}_2$ (32, solvent omitted).

Table A.8: Atomic coordinates ($\times 10^4$) and equivalent isotropic displacement parameters ($\text{\AA}^2 \times 10^3$) for $\{[\text{NNO}]\text{VCl}\}_2$ (**32**). $U(\text{eq})$ is defined as one third of the trace of the orthogonalized U_{ij} tensor.

	x	y	z	$U(\text{eq})$
V(1)	17007(1)	7864(1)	7648(1)	32(1)
Cl(1)	16695(1)	7889(1)	6918(1)	38(1)
N(101)	18190(2)	8937(2)	7747(1)	32(1)
N(102)	16704(2)	8669(2)	7980(1)	35(1)
N(103)	17787(2)	7473(2)	7958(1)	35(1)
O(101)	20197(2)	9558(3)	7853(1)	68(1)
C(101)	17880(3)	9605(3)	7717(2)	37(1)
C(102)	17189(3)	9544(3)	7972(2)	40(1)
C(103)	18595(3)	8991(3)	8185(2)	38(1)
C(104)	18594(3)	8156(3)	8218(2)	38(1)
C(105)	18743(3)	8875(3)	7439(2)	40(1)
C(106)	19615(3)	9597(3)	7512(2)	48(2)
C(107)	20969(4)	10264(4)	8026(2)	71(2)
C(108)	21320(4)	10852(5)	7805(2)	100(3)
C(109)	22088(5)	11511(5)	8010(3)	136(3)
C(110)	22478(5)	11596(6)	8427(3)	138(3)
C(111)	22099(5)	11030(6)	8651(3)	108(3)
C(112)	21345(4)	10342(4)	8438(2)	82(2)
C(113)	22496(6)	12178(6)	7776(4)	241(7)
C(114)	22500(5)	11143(6)	9118(3)	166(4)
C(115)	16206(3)	8583(3)	8290(2)	34(1)
C(116)	16044(3)	9249(3)	8505(2)	40(1)
C(117)	15611(3)	9180(3)	8831(2)	41(1)
C(118)	15296(3)	8417(3)	8937(2)	43(1)
C(119)	15404(3)	7732(3)	8719(2)	35(1)
C(120)	15883(3)	7830(3)	8408(2)	36(1)
C(121)	15556(3)	9948(3)	9080(2)	48(1)
C(122)	14766(4)	10029(4)	9053(2)	59(2)
C(123)	14776(4)	10783(4)	9266(2)	82(2)
C(124)	15510(5)	11434(4)	9506(2)	89(2)
C(125)	16276(4)	11333(4)	9537(2)	78(2)
C(126)	16321(3)	10601(3)	9335(2)	55(2)
C(127)	13897(4)	9322(4)	8821(2)	72(2)
C(128)	13413(4)	8946(4)	9148(2)	104(2)
C(129)	13327(4)	9580(5)	8525(2)	97(2)
C(130)	15495(7)	12255(5)	9726(3)	150(4)
C(131)	15804(7)	12521(5)	10158(3)	147(4)
C(132)	15356(8)	12739(5)	9445(3)	179(5)
C(133)	17175(3)	10510(4)	9415(2)	62(2)
C(134)	17409(5)	10472(6)	9874(2)	124(3)
C(135)	17899(4)	11193(4)	9315(3)	117(3)
C(136)	15012(3)	6903(3)	8827(2)	37(1)
C(137)	15488(3)	6648(3)	9114(2)	41(1)
C(138)	15065(4)	5912(3)	9230(2)	50(2)
C(139)	14190(4)	5430(3)	9074(2)	50(2)
C(140)	13739(3)	5674(3)	8780(2)	49(1)
C(141)	14123(3)	6406(3)	8648(2)	41(1)

C(142)	16455(3)	7147(3)	9286(2)	50(2)
C(143)	16955(4)	6737(4)	9047(2)	83(2)
C(144)	16736(4)	7282(5)	9763(2)	93(2)
C(145)	13738(4)	4662(4)	9232(2)	72(2)
C(146)	13976(6)	3991(4)	9096(3)	141(4)
C(147)	13765(4)	4881(4)	9697(2)	72(2)
C(148)	13599(3)	6637(3)	8323(2)	50(2)
C(149)	13260(4)	5993(4)	7900(2)	80(2)
C(150)	12850(4)	6776(5)	8477(2)	90(2)
C(151)	17758(3)	6681(3)	7997(2)	31(1)
C(152)	17142(3)	5938(3)	7714(2)	32(1)
C(153)	17090(3)	5154(3)	7746(2)	32(1)
C(154)	17703(3)	5108(3)	8060(2)	37(1)
C(155)	18345(3)	5823(3)	8338(2)	34(1)
C(156)	18344(3)	6583(3)	8307(2)	35(1)
C(157)	16378(3)	4360(3)	7472(2)	32(1)
C(158)	16494(3)	3879(3)	7119(2)	41(1)
C(159)	15806(3)	3147(3)	6884(2)	46(1)
C(160)	15009(3)	2858(3)	6988(2)	47(2)
C(161)	14914(3)	3335(3)	7340(2)	48(1)
C(162)	15574(3)	4077(3)	7589(2)	40(1)
C(163)	17360(3)	4133(3)	6993(2)	52(2)
C(164)	17289(4)	3904(4)	6514(2)	63(2)
C(165)	17914(4)	3747(5)	7210(2)	89(2)
C(166)	14274(4)	2051(3)	6721(2)	66(2)
C(167)	13490(4)	2188(4)	6541(2)	110(3)
C(168)	14068(4)	1378(4)	6960(2)	104(3)
C(169)	15432(3)	4546(3)	7984(2)	51(2)
C(170)	15524(4)	4141(4)	8349(2)	76(2)
C(171)	14578(4)	4636(4)	7918(2)	72(2)
C(172)	19040(3)	5772(3)	8656(2)	36(1)
C(173)	19894(3)	6078(3)	8604(2)	44(1)
C(174)	20542(3)	6039(3)	8898(2)	47(1)
C(175)	20386(3)	5700(3)	9240(2)	48(1)
C(176)	19546(3)	5403(3)	9286(2)	46(1)
C(177)	18865(3)	5433(3)	9002(2)	39(1)
C(178)	20131(3)	6434(3)	8233(2)	52(2)
C(179)	20791(4)	7334(4)	8366(2)	70(2)
C(180)	20440(4)	5878(4)	7942(2)	71(2)
C(181)	21107(3)	5686(4)	9568(2)	57(2)
C(182)	21719(4)	5392(4)	9372(2)	80(2)
C(183)	21562(4)	6512(4)	9880(2)	93(2)
C(184)	17957(3)	5079(3)	9081(2)	52(2)
C(185)	17930(4)	5447(4)	9533(2)	78(2)
C(186)	17593(4)	4122(4)	8989(2)	78(2)
V(2)	15439(1)	6544(1)	6703(1)	31(1)
Cl(2)	15571(1)	6700(1)	7448(1)	37(1)
N(201)	14467(2)	5307(2)	6565(1)	32(1)
N(202)	14564(2)	6663(2)	6308(1)	32(1)
N(203)	16063(2)	5955(2)	6475(1)	33(1)
O(201)	12547(2)	4126(2)	6348(1)	64(1)
C(201)	14127(3)	5159(3)	6102(2)	36(1)
C(202)	13918(3)	5882(3)	6020(2)	40(1)
C(203)	14963(3)	4803(3)	6655(2)	37(1)

C(204)	15770(3)	5065(3)	6474(2)	39(1)
C(205)	13795(3)	5227(3)	6814(2)	36(1)
C(206)	13100(3)	4365(3)	6757(2)	43(1)
C(207)	11935(3)	3313(3)	6202(2)	51(2)
C(208)	11601(3)	3028(4)	5770(2)	60(2)
C(209)	10994(3)	2222(4)	5600(2)	62(2)
C(210)	10716(4)	1724(4)	5870(2)	84(2)
C(211)	11027(4)	2012(4)	6304(2)	82(2)
C(212)	11658(3)	2820(3)	6475(2)	65(2)
C(213)	10643(4)	1916(5)	5122(2)	97(2)
C(214)	10717(6)	1468(5)	6613(3)	165(4)
C(215)	14420(3)	7380(3)	6264(2)	33(1)
C(216)	13876(3)	7401(3)	5904(2)	37(1)
C(217)	13723(3)	8106(3)	5878(2)	39(1)
C(218)	14104(3)	8803(3)	6221(2)	44(1)
C(219)	14636(3)	8798(3)	6580(2)	39(1)
C(220)	14790(3)	8094(3)	6600(2)	38(1)
C(221)	13138(3)	8096(3)	5488(2)	42(1)
C(222)	12295(3)	8010(3)	5496(2)	49(1)
C(223)	11774(4)	8016(4)	5128(2)	59(2)
C(224)	12047(3)	8097(4)	4758(2)	55(2)
C(225)	12879(3)	8167(3)	4756(2)	52(2)
C(226)	13442(3)	8180(3)	5115(2)	49(1)
C(227)	11919(3)	7886(4)	5880(2)	58(2)
C(228)	11052(4)	7118(4)	5766(2)	90(2)
C(229)	11806(4)	8662(4)	6095(2)	81(2)
C(230)	11415(4)	8051(4)	4364(2)	64(2)
C(231)	10805(5)	7186(4)	4161(2)	105(3)
C(232)	11826(4)	8489(4)	4060(2)	94(2)
C(233)	14356(3)	8261(4)	5099(2)	61(2)
C(234)	14470(4)	8009(4)	4646(2)	85(2)
C(235)	15028(4)	9137(4)	5328(2)	103(3)
C(236)	14982(3)	9509(3)	6976(2)	47(1)
C(237)	14566(3)	9424(3)	7309(2)	53(2)
C(238)	14902(4)	10054(4)	7683(2)	77(2)
C(239)	15632(4)	10780(4)	7726(2)	77(2)
C(240)	16016(4)	10862(3)	7388(2)	68(2)
C(241)	15716(4)	10236(3)	7013(2)	54(2)
C(242)	13744(4)	8663(4)	7277(2)	71(2)
C(243)	12984(4)	8925(5)	7301(2)	96(2)
C(244)	13872(4)	8186(4)	7603(2)	90(2)
C(245)	15977(5)	11457(5)	8151(3)	120(3)
C(246)	15525(7)	11975(6)	8162(3)	192(6)
C(247)	16907(5)	11808(5)	8309(3)	161(4)
C(248)	16176(4)	10355(3)	6654(2)	63(2)
C(249)	17167(4)	10700(5)	6810(2)	107(3)
C(250)	15960(4)	10936(4)	6410(2)	89(2)
C(251)	16740(3)	6236(3)	6261(2)	33(1)
C(252)	17401(3)	5952(3)	6279(2)	36(1)
C(253)	18079(3)	6259(3)	6080(2)	34(1)
C(254)	18072(3)	6838(3)	5848(2)	36(1)
C(255)	17409(3)	7121(3)	5814(2)	35(1)
C(256)	16767(3)	6826(3)	6028(2)	33(1)
C(257)	18808(3)	5981(3)	6141(2)	36(1)

C(258)	18859(3)	5369(3)	5829(2)	44(1)
C(259)	19518(3)	5097(3)	5922(2)	52(2)
C(260)	20116(3)	5404(4)	6305(2)	51(2)
C(261)	20058(3)	6022(3)	6601(2)	47(1)
C(262)	19419(3)	6328(3)	6530(2)	40(1)
C(263)	18219(4)	5004(4)	5397(2)	60(2)
C(264)	17646(5)	4093(4)	5342(2)	138(3)
C(265)	18655(5)	5136(6)	5035(2)	139(4)
C(266)	20828(4)	5093(4)	6395(2)	76(2)
C(267)	20776(5)	4717(5)	6776(2)	100(2)
C(268)	21717(4)	5781(6)	6443(3)	151(4)
C(269)	19419(3)	7026(3)	6868(2)	43(1)
C(270)	19088(4)	6696(4)	7237(2)	65(2)
C(271)	20301(3)	7752(4)	7031(2)	86(2)
C(272)	17414(3)	7725(3)	5547(2)	40(1)
C(273)	17999(3)	8561(3)	5706(2)	47(1)
C(274)	18032(4)	9118(4)	5455(2)	60(2)
C(275)	17523(4)	8889(4)	5054(2)	66(2)
C(276)	16955(3)	8064(4)	4901(2)	62(2)
C(277)	16874(3)	7469(3)	5141(2)	53(2)
C(278)	18583(4)	8875(3)	6149(2)	56(2)
C(279)	18476(4)	9611(4)	6407(2)	81(2)
C(280)	19530(4)	9093(4)	6122(2)	81(2)
C(281)	17610(4)	9515(5)	4783(3)	103(3)
C(282)	16832(4)	9559(4)	4581(2)	98(3)
C(283)	18328(5)	9668(6)	4595(3)	142(4)
C(284)	16201(4)	6576(4)	4937(2)	64(2)
C(285)	16496(4)	5871(4)	4952(2)	82(2)
C(286)	15331(4)	6409(5)	5028(3)	124(3)

Table A.9: Crystal data and structure refinement for the {[NNO]VCl}₂ reduction product (**33**).*

Identification code	04130	
Empirical formula	C ₁₇₉ H ₂₅₄ K ₂ N ₆ O ₂ V ₂	
Formula weight	2701.96	
Temperature	193(2) K	
Wavelength	0.71073 Å	
Crystal system	Monoclinic	
Space group	P2(1)/c	
Unit cell dimensions	a = 18.8649(14) Å	α = 90°
	b = 19.7714(14) Å	β = 96.776(2)°
	c = 26.269(2) Å	γ = 90°
Volume	9729.6(12) Å ³	
Z	2	
Density (calculated)	0.922 Mg/m ³	
Absorption coefficient	0.183 mm ⁻¹	
F(000)	2940	
Crystal size	0.32 x 0.15 x 0.15 mm ³	
Theta range for data collection	1.50 to 23.26°	
Index ranges	-20 ≤ h ≤ 20, -21 ≤ k ≤ 13, -29 ≤ l ≤ 29	
Reflections collected	45358	
Independent reflections	13945 [R _{int} = 0.0681]	
Completeness to theta = 23.26°	99.9%	
Absorption correction	Semi-empirical from equivalents	
Max. and min. transmission	0.9731 and 0.9438	
Refinement method	Full-matrix least-squares on F ²	
Data / restraints / parameters	13945 / 499 / 977	
Goodness-of-fit on F ²	1.088	
Final R indices [I > 2σ(I)]	R ₁ = 0.0736, wR ₂ = 0.2249	
R indices (all data)	R ₁ = 0.1252, wR ₂ = 0.2665	
Largest diff. peak and hole	1.002 and -0.293 eÅ ⁻³	

* Structure solution by Dr. Peter Müller.

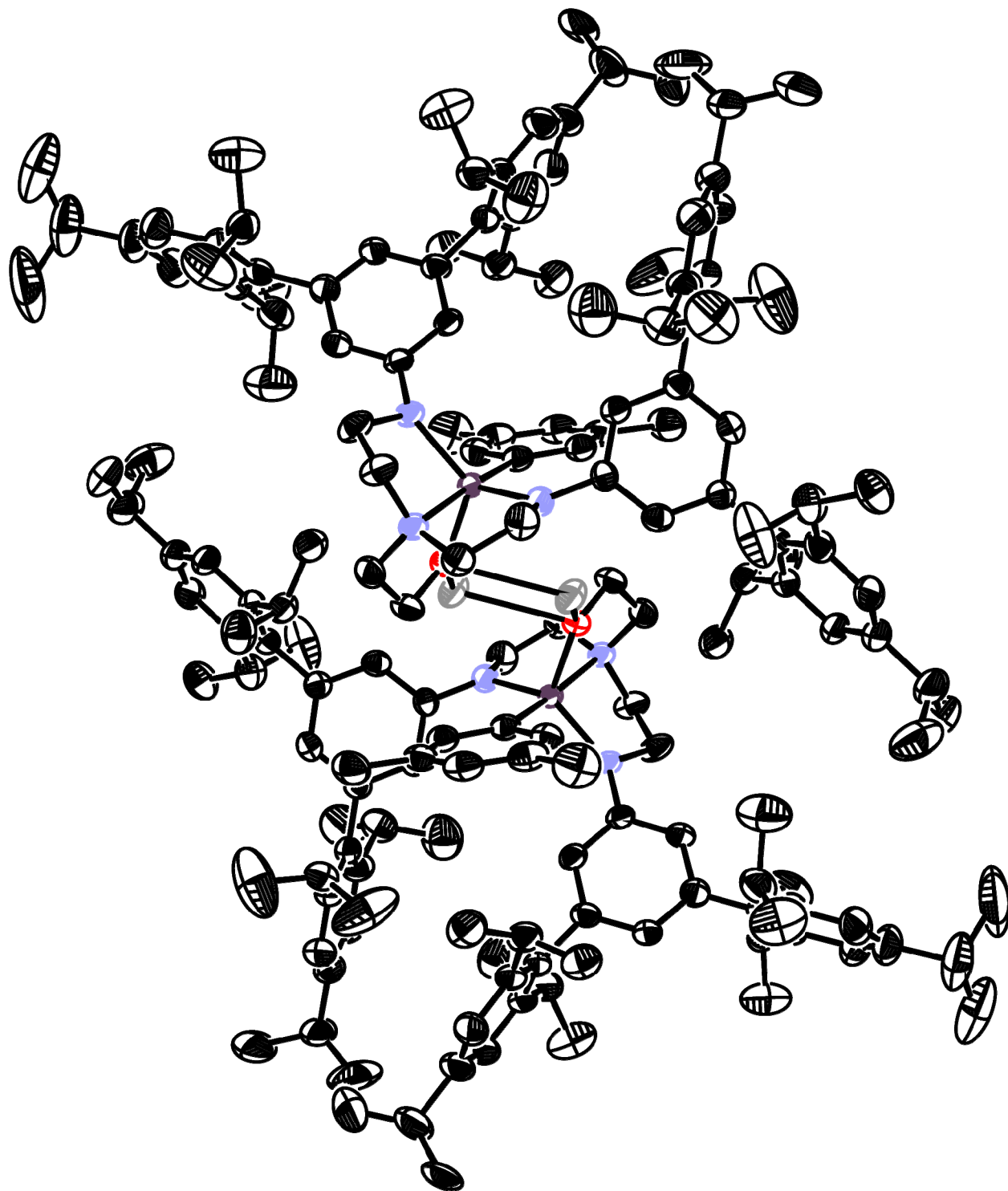


Figure A.9: Full ORTEP of the reduction product of $\{[NNO]VCl\}_2$ (33). Solvent, hydrogen atoms, and disorder omitted.

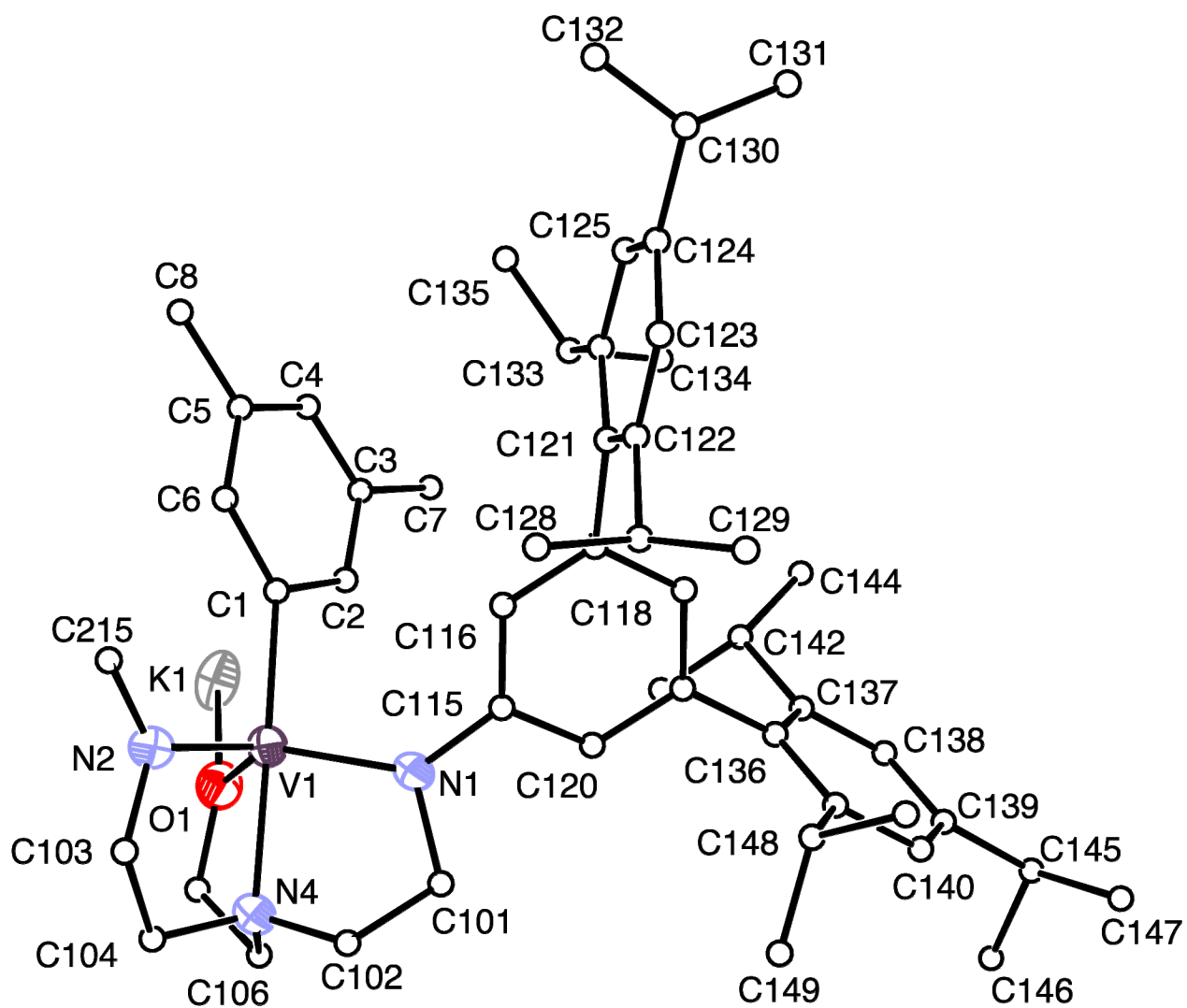


Figure A.10: ORTEP labeling scheme for 33, solvent, disorder, and hydrogen atoms omitted.

Table A.10: Atomic coordinates ($\times 10^4$) and equivalent isotropic displacement parameters ($\text{\AA}^2 \times 10^3$) for **33**. $U(\text{eq})$ is defined as one third of the trace of the orthogonalized $U^{\ddot{J}}$ tensor.

	x	y	z	U(eq)
V(1)	5610(1)	9981(1)	1222(1)	29(1)
K(1)	4128(1)	9679(1)	-31(1)	47(1)
N(1)	5366(2)	9629(2)	1880(1)	34(1)
N(2)	6522(2)	10410(2)	1150(1)	34(1)
N(4)	5436(2)	10953(2)	1580(1)	36(1)
O(1)	4872(2)	10332(2)	718(1)	37(1)
C(101)	5120(3)	10154(2)	2221(2)	52(2)
C(102)	5494(3)	10801(2)	2135(2)	49(1)
C(103)	6678(3)	11062(2)	1420(2)	47(1)
C(104)	5988(3)	11435(2)	1448(2)	44(1)
C(105)	4617(3)	10999(3)	804(2)	48(1)
C(106)	4715(3)	11156(3)	1365(2)	47(1)
C(1)	5618(2)	9062(2)	787(2)	34(1)
C(2)	4962(3)	8710(2)	747(2)	40(1)
C(3)	4828(3)	8111(3)	466(2)	49(1)
C(4)	5371(3)	7843(3)	217(2)	50(1)
C(5)	6029(3)	8152(2)	246(2)	44(1)
C(6)	6136(3)	8745(2)	524(2)	39(1)
C(7)	4107(3)	7767(3)	435(3)	80(2)
C(8)	6600(3)	7852(3)	-39(2)	62(2)
C(115)	5222(2)	8971(2)	2039(2)	33(1)
C(116)	5682(2)	8433(2)	1966(2)	35(1)
C(117)	5580(2)	7798(2)	2177(2)	35(1)
C(118)	5005(2)	7697(2)	2453(2)	40(1)
C(119)	4526(2)	8213(2)	2516(2)	39(1)
C(120)	4639(2)	8843(2)	2305(2)	38(1)
C(121)	6116(2)	7231(2)	2184(2)	40(1)
C(122)	6684(2)	7222(2)	2587(2)	45(1)
C(123)	7139(3)	6667(3)	2630(2)	56(2)
C(124)	7054(3)	6129(3)	2307(3)	60(2)
C(125)	6499(3)	6153(3)	1904(2)	58(2)
C(126)	6028(3)	6697(2)	1836(2)	46(1)
C(127)	6827(3)	7803(3)	2958(2)	52(1)
C(128)	7439(4)	8228(3)	2822(3)	89(2)
C(129)	6941(4)	7581(4)	3511(2)	88(2)
C(130)	7548(3)	5509(3)	2361(3)	85(2)
C(131)	7192(5)	4905(4)	2523(5)	71(3)
C(132)	8068(8)	5485(7)	2022(7)	111(5)
C(31A)	7340(30)	4793(13)	2320(30)	140(20)
C(32A)	8291(10)	5671(19)	2380(30)	76(13)
C(133)	5442(3)	6701(3)	1395(2)	51(1)
C(134)	4768(3)	6353(3)	1532(2)	63(2)
C(135)	5657(3)	6378(3)	904(2)	67(2)
C(136)	3912(2)	8115(2)	2817(2)	41(1)
C(137)	3282(3)	7796(3)	2595(2)	48(1)
C(138)	2721(3)	7727(3)	2892(2)	60(2)
C(139)	2759(3)	7955(3)	3390(2)	66(2)
C(140)	3382(3)	8263(3)	3605(2)	62(2)

C(141)	3966(3)	8344(2)	3324(2)	45(1)
C(142)	3207(3)	7550(3)	2048(2)	59(2)
C(143)	2901(4)	8101(4)	1676(3)	100(2)
C(144)	2783(4)	6893(4)	1964(3)	100(2)
C(145)	2119(4)	7885(4)	3698(3)	105(3)
C(146)	1632(5)	8498(5)	3577(5)	185(6)
C(147)	2330(5)	7789(5)	4269(3)	141(4)
C(148)	4637(3)	8671(3)	3584(2)	50(1)
C(149)	4517(4)	9411(3)	3708(3)	93(2)
C(150)	4941(4)	8290(3)	4062(3)	88(2)
C(215)	7167(2)	10102(2)	1037(2)	33(1)
C(216)	7491(2)	9595(2)	1344(2)	36(1)
C(217)	8139(2)	9316(2)	1250(2)	36(1)
C(218)	8445(2)	9524(2)	819(2)	37(1)
C(219)	8143(2)	10042(2)	508(2)	33(1)
C(220)	7509(2)	10330(2)	626(2)	35(1)
C(221)	8541(2)	8848(2)	1632(2)	40(1)
C(222)	8546(2)	8146(3)	1549(2)	44(1)
C(223)	8937(3)	7735(3)	1912(2)	52(1)
C(224)	9307(3)	7999(3)	2356(2)	55(2)
C(225)	9280(3)	8689(3)	2432(2)	56(2)
C(226)	8904(3)	9126(3)	2076(2)	47(1)
C(227)	8115(3)	7832(3)	1090(2)	51(1)
C(228)	8583(4)	7494(5)	736(3)	138(4)
C(229)	7556(4)	7366(5)	1247(3)	131(4)
C(230)	9736(3)	7540(3)	2744(2)	70(2)
C(231)	9290(4)	7013(5)	2945(4)	143(4)
C(232)	10387(4)	7275(4)	2547(3)	110(3)
C(233)	8893(3)	9869(3)	2193(2)	60(2)
C(234)	8432(4)	10011(4)	2611(3)	97(2)
C(235)	9634(4)	10173(4)	2333(3)	96(2)
C(236)	8487(2)	10312(2)	62(2)	39(1)
C(237)	9141(2)	10671(2)	154(2)	43(1)
C(238)	9423(3)	10943(3)	-267(2)	51(1)
C(239)	9098(3)	10883(3)	-766(2)	54(2)
C(240)	8472(2)	10526(3)	-848(2)	48(1)
C(241)	8160(2)	10234(2)	-441(2)	40(1)
C(242)	9492(2)	10799(3)	692(2)	53(1)
C(243)	9128(3)	11399(4)	923(3)	99(3)
C(244)	10299(3)	10918(3)	733(2)	63(2)
C(245)	9436(3)	11214(4)	-1212(2)	76(2)
C(246)	9393(4)	11987(4)	-1161(3)	98(3)
C(247)	9116(4)	10988(4)	-1735(2)	88(2)
C(248)	7485(2)	9828(2)	-577(2)	42(1)
C(249)	6911(3)	10259(3)	-883(2)	56(2)
C(250)	7629(3)	9190(3)	-864(2)	67(2)

Table A.11: Crystal data and structure refinement for {[NNO]VO}₂ (**34**).*

Identification code	05072	
Empirical formula	C ₁₉₃ H ₂₈₆ N ₆ O ₄ V ₂	
Formula weight	2856.16	
Temperature	100(2) K	
Wavelength	0.71073 Å	
Crystal system	Triclinic	
Space group	P $\bar{1}$	
Unit cell dimensions	a = 16.0895(11) Å	α = 64.742(2)°
	b = 16.4483(12) Å	β = 81.753(2)°
	c = 18.9799(12) Å	γ = 86.920(2)°
Volume	4495.6(5) Å ³	
Z	1	
Density (calculated)	1.055 Mg/m ³	
Absorption coefficient	0.157 mm ⁻¹	
F(000)	1564	
Crystal size	0.25 x 0.20 x 0.15 mm ³	
Theta range for data collection	1.86 to 25.03°	
Index ranges	-19<=h<=19, -19<=k<=19, -22<=l<=22	
Reflections collected	71667	
Independent reflections	15884 [R _{int} = 0.0628]	
Completeness to theta = 25.03°	100.0%	
Absorption correction	Semi-empirical from equivalents	
Max. and min. transmission	0.9769 and 0.9619	
Refinement method	Full-matrix least-squares on F ²	
Data / restraints / parameters	15884 / 913 / 1141	
Goodness-of-fit on F ²	1.027	
Final R indices [I>2sigma(I)]	R ₁ = 0.0735, wR ₂ = 0.1911	
R indices (all data)	R ₁ = 0.1055, wR ₂ = 0.2193	
Largest diff. peak and hole	1.625 and -0.479 eÅ ⁻³	

* Structure solution by Dr. Peter Müller.

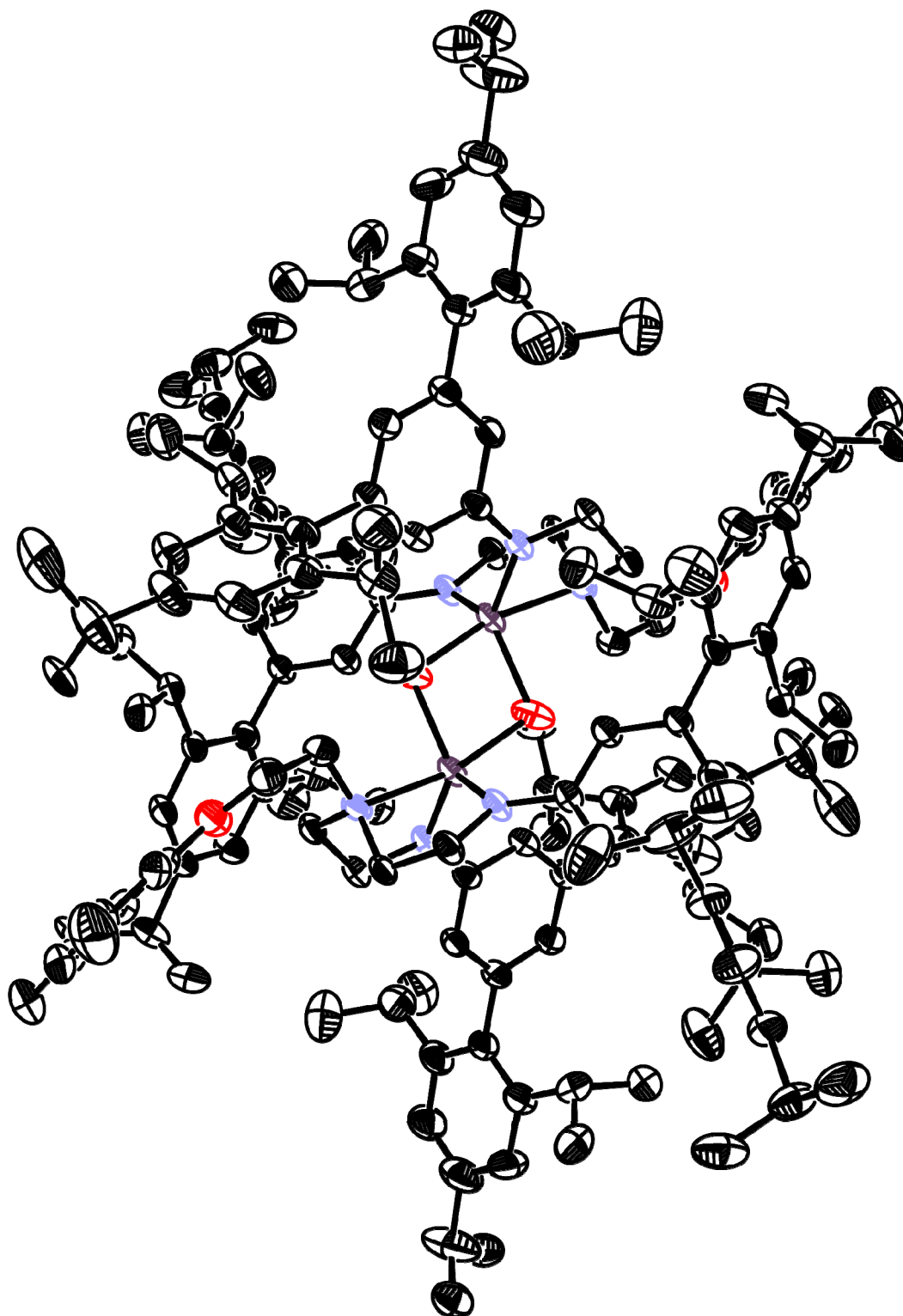


Figure A.11: Full ORTEP of $\{[\text{NNO}]\text{VO}\}_2$ (34). Solvent, disorder and hydrogen atoms omitted.

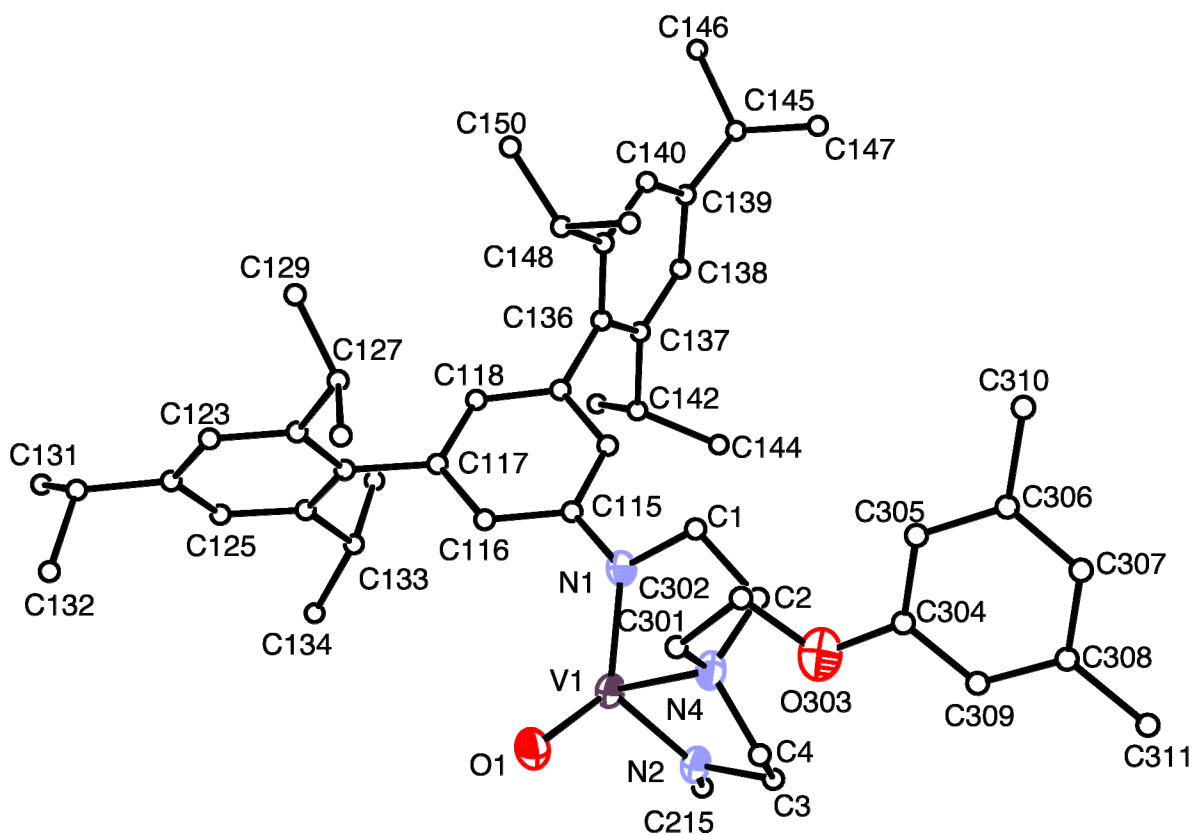


Figure A.12: ORTEP labeling scheme for $\{[NNO]VO\}_2$ (34). Solvent, disorder, and hydrogen atoms omitted.

Table A.12: Atomic coordinates ($\times 10^4$) and equivalent isotropic displacement parameters ($\text{\AA}^2 \times 10^3$) for $\{[\text{NNO}]\text{VO}\}_2$. $U(\text{eq})$ is defined as one third of the trace of the orthogonalized U_{ij} tensor.

	x	y	z	$U(\text{eq})$
V(1)	-1008(1)	19(1)	149(1)	30(1)
O(1)	32(2)	658(2)	173(2)	45(1)
N(1)	-1592(2)	-967(2)	1058(2)	31(1)
N(2)	-1595(2)	659(2)	-774(2)	30(1)
N(4)	-1804(2)	822(2)	602(2)	30(1)
C(1)	-2320(2)	-696(2)	1468(2)	34(1)
C(2)	-2564(2)	246(2)	949(2)	31(1)
C(3)	-2142(2)	1390(2)	-740(2)	34(1)
C(4)	-1929(2)	1653(2)	-117(2)	32(1)
C(115)	-1439(2)	-1904(2)	1393(2)	29(1)
C(116)	-616(2)	-2238(2)	1415(2)	31(1)
C(117)	-459(2)	-3167(2)	1761(2)	31(1)
C(118)	-1128(2)	-3766(2)	2105(2)	33(1)
C(119)	-1951(2)	-3460(2)	2098(2)	31(1)
C(120)	-2097(2)	-2538(2)	1733(2)	31(1)
C(121)	428(2)	-3505(2)	1833(2)	33(1)
C(122)	808(2)	-3542(2)	2465(2)	38(1)
C(123)	1636(2)	-3842(3)	2523(2)	45(1)
C(124)	2086(2)	-4109(3)	1982(3)	45(1)
C(125)	1694(2)	-4093(2)	1373(3)	41(1)
C(126)	864(2)	-3796(2)	1284(2)	35(1)
C(127)	339(2)	-3285(3)	3095(2)	46(1)
C(128)	614(12)	-2347(10)	2930(13)	58(4)
C(129)	436(18)	-3981(16)	3908(11)	71(6)
C(130)	3001(3)	-4382(3)	2052(3)	60(1)
C(131)	3262(13)	-5161(14)	1830(20)	82(6)
C(132)	3575(14)	-3581(11)	1569(13)	66(4)
C(133)	446(2)	-3811(2)	622(2)	39(1)
C(134)	1047(3)	-3710(3)	-111(3)	47(1)
C(135)	-86(3)	-4666(3)	898(3)	50(1)
C(136)	-2682(2)	-4089(2)	2501(2)	33(1)
C(137)	-3171(2)	-4342(2)	2071(2)	34(1)
C(138)	-3881(2)	-4881(2)	2469(2)	39(1)
C(139)	-4124(2)	-5160(3)	3267(2)	43(1)
C(140)	-3624(3)	-4916(3)	3678(2)	50(1)
C(141)	-2906(2)	-4389(3)	3318(2)	45(1)
C(142)	-2940(2)	-4045(2)	1190(2)	38(1)
C(143)	-2736(3)	-4831(3)	985(3)	54(1)
C(144)	-3631(3)	-3477(3)	731(3)	68(1)
C(145)	-4945(3)	-5673(3)	3665(3)	54(1)
C(146)	-4869(3)	-6450(3)	4462(3)	75(2)
C(147)	-5634(3)	-5031(4)	3752(3)	65(1)
C(148)	-2398(3)	-4109(4)	3800(3)	65(1)
C(149)	-2875(5)	-3359(5)	3992(5)	82(2)
C(150)	-2212(5)	-4890(5)	4552(4)	75(2)
C(215)	-1726(2)	391(2)	-1359(2)	30(1)
C(216)	-2461(2)	595(2)	-1724(2)	33(1)

C(217)	-2583(2)	309(2)	-2295(2)	36(1)
C(218)	-1959(2)	-175(2)	-2531(2)	36(1)
C(219)	-1224(2)	-397(2)	-2177(2)	33(1)
C(220)	-1113(2)	-111(2)	-1607(2)	32(1)
C(221)	-3387(2)	506(3)	-2654(3)	44(1)
C(222)	-3496(3)	1344(3)	-3281(3)	53(1)
C(223)	-4233(3)	1503(4)	-3623(3)	64(1)
C(224)	-4850(3)	873(4)	-3372(3)	66(1)
C(225)	-4745(3)	49(4)	-2750(3)	63(1)
C(226)	-4017(3)	-151(3)	-2372(3)	50(1)
C(227)	-2839(3)	2081(3)	-3601(3)	59(1)
C(228)	-2433(4)	2256(4)	-4429(4)	86(2)
C(229)	-3192(4)	2945(3)	-3575(3)	77(2)
C(230)	-5632(3)	1071(6)	-3799(4)	94(2)
C(231)	-6396(5)	734(6)	-3307(5)	57(2)
C(232)	-5471(5)	1015(6)	-4557(5)	55(2)
C(233)	-3918(3)	-1071(3)	-1695(3)	57(1)
C(234)	-4719(3)	-1419(4)	-1117(4)	71(2)
C(235)	-3614(3)	-1764(3)	-2011(4)	69(2)
C(236)	-575(2)	-958(3)	-2418(2)	35(1)
C(237)	-674(2)	-1899(3)	-2067(2)	39(1)
C(238)	-81(3)	-2413(3)	-2309(2)	46(1)
C(239)	588(3)	-2016(3)	-2894(2)	53(1)
C(240)	658(3)	-1091(3)	-3244(2)	48(1)
C(241)	90(2)	-548(3)	-3016(2)	41(1)
C(242)	-1399(3)	-2356(3)	-1421(2)	43(1)
C(243)	-1149(3)	-2568(4)	-621(3)	67(1)
C(244)	-1752(3)	-3184(3)	-1445(3)	65(1)
C(245)	1209(4)	-2598(4)	-3174(3)	75(2)
C(246)	757(10)	-3050(12)	-3570(11)	86(5)
C(247)	1619(9)	-3276(12)	-2493(9)	57(4)
C(248)	174(3)	470(3)	-3443(2)	47(1)
C(249)	1047(3)	808(4)	-3462(3)	69(1)
C(250)	-59(4)	800(3)	-4271(3)	68(1)
C(301)	-1426(2)	1014(3)	1195(2)	40(1)
C(302)	-2024(3)	1268(3)	1752(3)	48(1)
O(303)	-2470(2)	2038(2)	1286(2)	47(1)
C(304)	-3192(5)	2331(6)	1581(6)	44(2)
C(305)	-3506(5)	1981(7)	2372(6)	48(2)
C(306)	-4256(6)	2319(7)	2621(7)	59(3)
C(307)	-4654(6)	3013(7)	2062(9)	58(3)
C(308)	-4342(7)	3375(9)	1264(8)	54(2)
C(309)	-3610(10)	3021(13)	1033(8)	49(3)
C(310)	-4622(8)	1899(7)	3468(7)	89(4)
C(311)	-4796(8)	4115(9)	665(9)	75(3)

Table A.13: Crystal data and structure refinement for **35**.*

Identification code	05085	
Empirical formula	$C_{193}H_{288}Cl_2N_6S_4V_2$	
Formula weight	2993.31	
Temperature	100(2) K	
Wavelength	0.71073 Å	
Crystal system	Triclinic	
Space group	$P\bar{1}$	
Unit cell dimensions	a = 16.1789(14) Å	$\alpha = 99.593(2)^\circ$
	b = 17.5000(14) Å	$\beta = 105.866(2)^\circ$
	c = 17.8993(16) Å	$\gamma = 106.072(2)^\circ$
Volume	4520.4(7) Å ³	
Z	1	
Density (calculated)	1.100 Mg/m ³	
Absorption coefficient	0.230 mm ⁻¹	
F(000)	1632	
Crystal size	0.20 x 0.20 x 0.05 mm ³	
Theta range for data collection	1.87 to 23.26°	
Index ranges	-17<=h<=17, -19<=k<=19, -19<=l<=19	
Reflections collected	59094	
Independent reflections	12956 [$R_{int} = 0.0705$]	
Completeness to theta = 23.26°	100.0%	
Absorption correction	Semi-empirical from equivalents	
Max. and min. transmission	0.9886 and 0.9554	
Refinement method	Full-matrix least-squares on F ²	
Data / restraints / parameters	12956 / 613 / 1005	
Goodness-of-fit on F ²	1.063	
Final R indices [$I > 2\sigma(I)$]	$R_1 = 0.0558$, $wR_2 = 0.1162$	
R indices (all data)	$R_1 = 0.1050$, $wR_2 = 0.1405$	
Largest diff. peak and hole	0.575 and -0.620 eÅ ⁻³	

* Structure solution by Dr. Peter Müller.

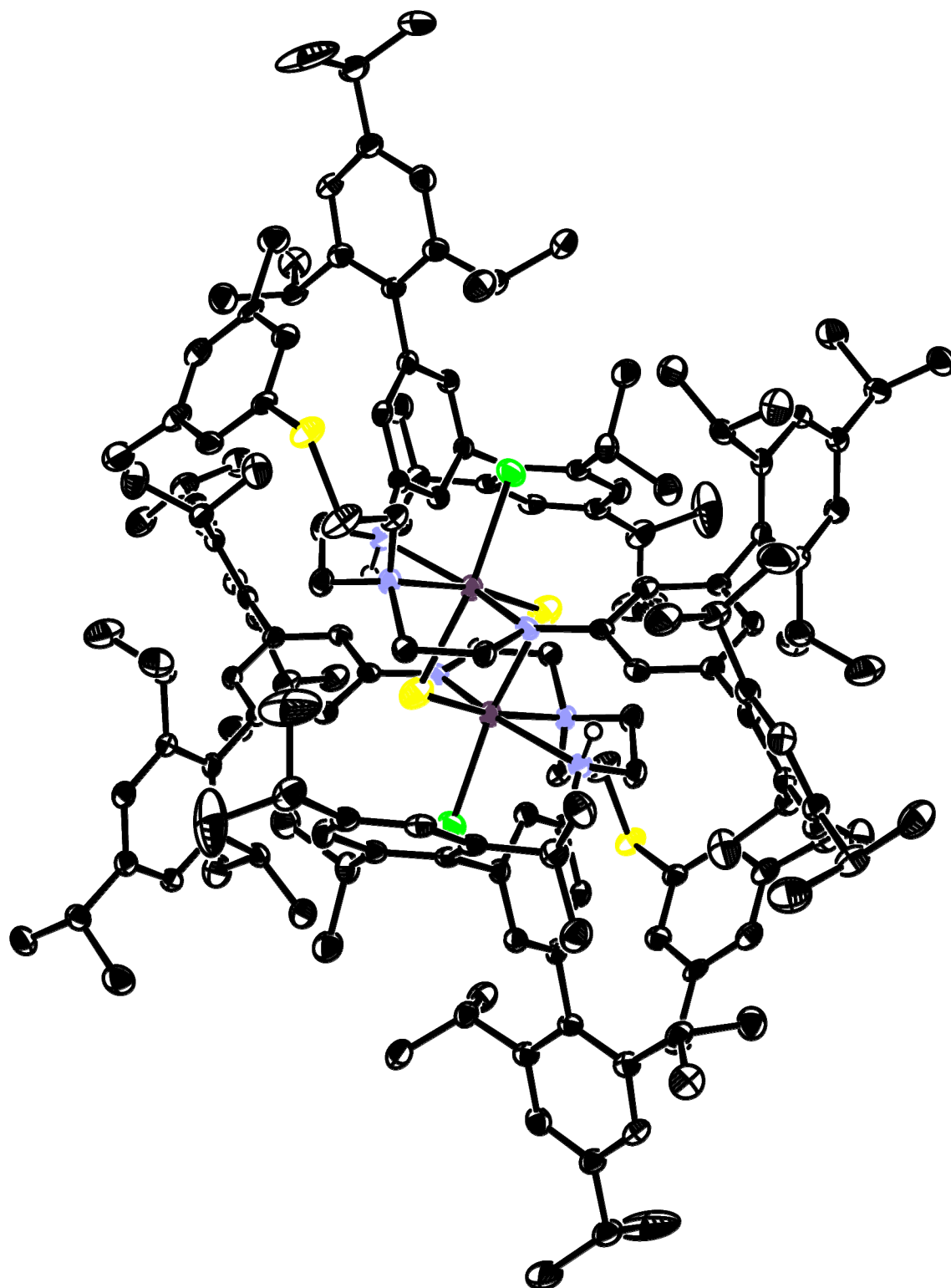


Figure A.13: Full ORTEP of 35. Solvent, disorder, and non-amine hydrogen atoms omitted.

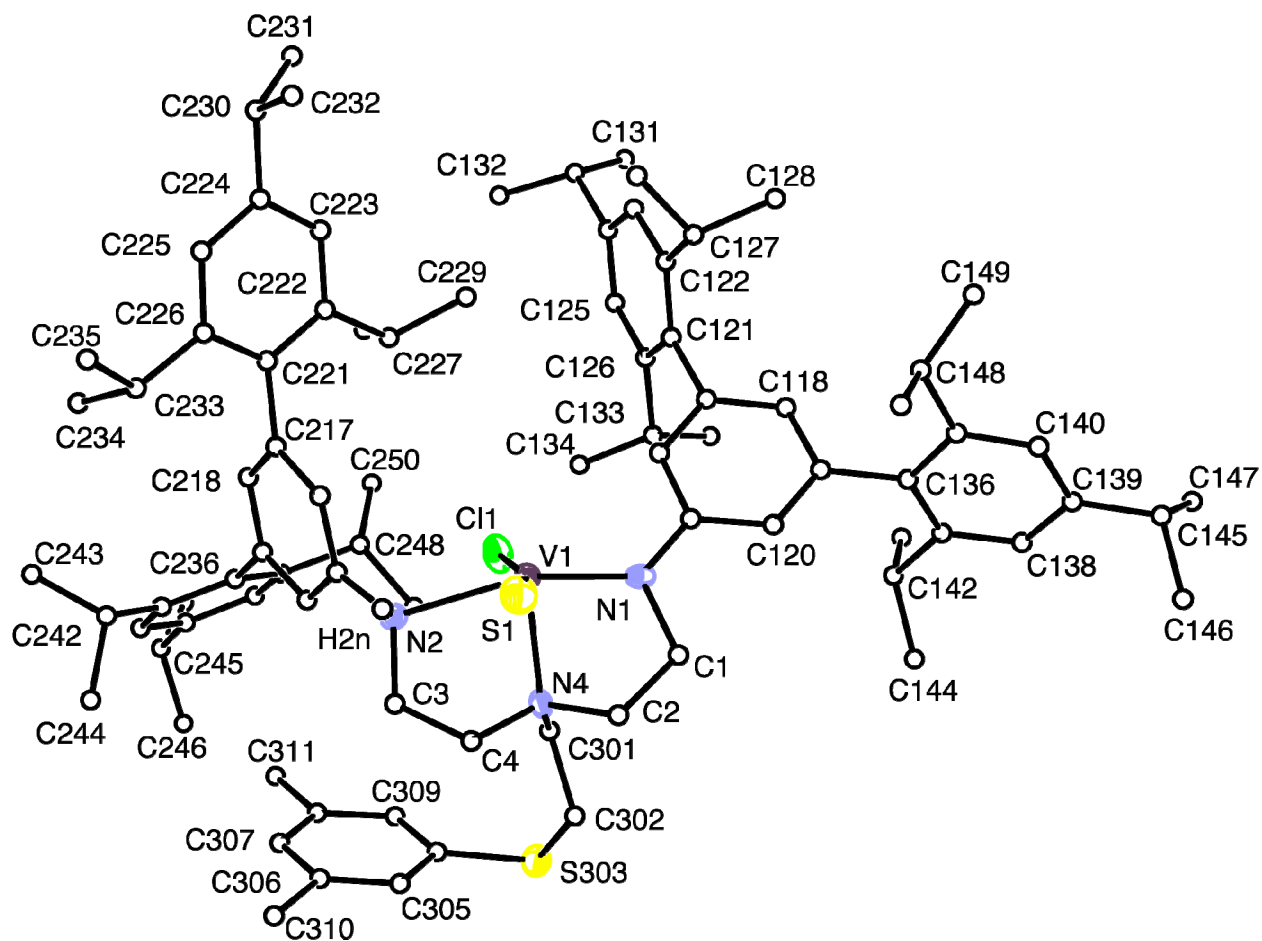


Figure A.14: ORTEP labeling scheme for 35. Solvent, disorder, and non-amine hydrogen atoms omitted.

Table A.14: Atomic coordinates ($\times 10^4$) and equivalent isotropic displacement parameters ($\text{\AA}^2 \times 10^3$) for **35**. $U(\text{eq})$ is defined as one third of the trace of the orthogonalized $U^{\ddot{J}}$ tensor.

	x	y	z	U(eq)
V(1)	46(1)	8975(1)	-346(1)	21(1)
S(1)	864(1)	10414(1)	-211(1)	35(1)
Cl(1)	-551(1)	7716(1)	-81(1)	32(1)
N(1)	-679(2)	8675(2)	-1467(2)	18(1)
N(2)	1241(2)	9243(2)	871(2)	19(1)
N(4)	1044(2)	8651(2)	-810(2)	21(1)
C(1)	-149(2)	8633(2)	-2023(2)	20(1)
C(2)	864(2)	8955(2)	-1553(2)	22(1)
C(3)	1960(2)	9001(2)	632(2)	24(1)
C(4)	1949(2)	9130(2)	-191(2)	24(1)
C(115)	-1634(2)	8372(2)	-1851(2)	18(1)
C(116)	-2220(2)	8131(2)	-1409(2)	20(1)
C(117)	-3163(2)	7787(2)	-1779(2)	18(1)
C(118)	-3550(2)	7686(2)	-2598(2)	20(1)
C(119)	-2998(2)	7934(2)	-3053(2)	18(1)
C(120)	-2055(2)	8271(2)	-2678(2)	18(1)
C(121)	-3762(2)	7449(2)	-1308(2)	19(1)
C(122)	-4270(2)	7888(2)	-1026(2)	22(1)
C(123)	-4816(2)	7538(2)	-600(2)	23(1)
C(124)	-4862(2)	6778(2)	-441(2)	22(1)
C(125)	-4357(2)	6361(2)	-730(2)	21(1)
C(126)	-3802(2)	6678(2)	-1163(2)	20(1)
C(127)	-4234(3)	8732(2)	-1163(2)	29(1)
C(128)	-5047(3)	8659(3)	-1883(3)	44(1)
C(129)	-4189(3)	9347(3)	-420(2)	38(1)
C(130)	-5460(2)	6425(2)	33(2)	23(1)
C(131)	-6283(2)	5681(2)	-505(2)	31(1)
C(132)	-4915(3)	6216(3)	768(2)	33(1)
C(133)	-3297(2)	6160(2)	-1483(2)	23(1)
C(134)	-2700(3)	5907(3)	-813(2)	31(1)
C(135)	-3966(3)	5412(3)	-2159(2)	36(1)
C(136)	-3408(2)	7838(2)	-3938(2)	21(1)
C(137)	-3381(2)	7187(2)	-4500(2)	21(1)
C(138)	-3738(2)	7129(2)	-5314(2)	23(1)
C(139)	-4113(2)	7694(2)	-5596(2)	22(1)
C(140)	-4149(2)	8322(2)	-5032(2)	22(1)
C(141)	-3818(2)	8406(2)	-4206(2)	19(1)
C(142)	-3018(3)	6524(2)	-4231(2)	26(1)
C(143)	-3814(3)	5754(3)	-4346(3)	47(1)
C(144)	-2394(3)	6310(3)	-4672(3)	39(1)
C(145)	-4472(3)	7624(2)	-6492(2)	29(1)
C(146)	-3695(3)	7775(3)	-6841(2)	43(1)
C(147)	-5212(3)	6789(3)	-6946(2)	37(1)
C(148)	-3880(2)	9099(2)	-3615(2)	23(1)
C(149)	-4757(3)	9298(3)	-3911(3)	38(1)
C(150)	-3049(3)	9870(2)	-3388(3)	39(1)
C(215)	1003(2)	8947(2)	1528(2)	16(1)
C(216)	527(2)	9344(2)	1892(2)	19(1)

C(217)	167(2)	9047(2)	2452(2)	17(1)
C(218)	324(2)	8349(2)	2659(2)	18(1)
C(219)	824(2)	7958(2)	2317(2)	19(1)
C(220)	1164(2)	8259(2)	1743(2)	19(1)
C(221)	-447(2)	9430(2)	2760(2)	17(1)
C(222)	-1386(2)	9125(2)	2315(2)	20(1)
C(223)	-1951(2)	9510(2)	2563(2)	24(1)
C(224)	-1613(2)	10186(2)	3227(2)	22(1)
C(225)	-684(2)	10466(2)	3659(2)	22(1)
C(226)	-88(2)	10099(2)	3440(2)	19(1)
C(227)	-1802(2)	8369(2)	1594(2)	24(1)
C(228)	-2112(3)	7579(2)	1863(2)	33(1)
C(229)	-2601(3)	8404(3)	920(2)	31(1)
C(230)	-2211(3)	10645(3)	3480(2)	31(1)
C(231)	-3187(3)	10122(3)	3282(4)	80(2)
C(232)	-2148(5)	11398(4)	3145(4)	85(2)
C(233)	922(2)	10420(2)	3950(2)	24(1)
C(234)	1145(3)	9876(3)	4513(2)	33(1)
C(235)	1278(3)	11314(2)	4445(2)	32(1)
C(236)	948(2)	7190(2)	2536(2)	18(1)
C(237)	1668(2)	7251(2)	3227(2)	21(1)
C(238)	1745(2)	6526(2)	3415(2)	24(1)
C(239)	1147(2)	5751(2)	2962(2)	24(1)
C(240)	444(2)	5707(2)	2287(2)	25(1)
C(241)	330(2)	6409(2)	2066(2)	21(1)
C(242)	2364(2)	8077(2)	3750(2)	23(1)
C(243)	2423(3)	8207(3)	4630(2)	36(1)
C(244)	3308(3)	8181(3)	3681(2)	34(1)
C(245)	1288(3)	4981(2)	3179(2)	30(1)
C(246)	1835(5)	4670(4)	2715(4)	91(2)
C(247)	417(3)	4304(3)	3061(4)	71(2)
C(248)	-459(2)	6300(2)	1311(2)	23(1)
C(249)	-281(3)	5928(3)	558(2)	32(1)
C(250)	-1376(2)	5779(3)	1339(2)	33(1)
C(301)	905(3)	7748(2)	-1031(2)	26(1)
C(302)	1505(3)	7522(3)	-1511(2)	38(1)
S(303)	1845(1)	6661(1)	-1315(1)	28(1)
C(304)	2445(3)	7021(3)	-257(3)	22(1)
C(305)	3198(3)	7743(3)	77(3)	23(1)
C(306)	3678(4)	7992(4)	901(3)	26(1)
C(307)	3401(9)	7493(8)	1378(4)	25(2)
C(308)	2655(4)	6763(4)	1058(3)	23(1)
C(309)	2166(3)	6535(3)	232(3)	23(1)
C(310)	4512(3)	8746(3)	1280(3)	36(1)
C(311)	2346(4)	6213(4)	1577(3)	30(1)

Table A.15: Crystal data and structure refinement for [HIPTN₃N]CrCO (39).*

Identification code	05129	
Empirical formula	C ₁₂₂ H ₁₇₅ CrN ₄ O	
Formula weight	1765.66	
Temperature	100(2) K	
Wavelength	0.71073 Å	
Crystal system	Monoclinic	
Space group	Cc	
Unit cell dimensions	a = 15.7406(14) Å	α = 90°
	b = 39.859(4) Å	β = 95.342(3)°
	c = 17.7657(17) Å	γ = 90°
Volume	11098.0(18) Å ³	
Z	4	
Density (calculated)	1.057 Mg/m ³	
Absorption coefficient	0.151 mm ⁻¹	
F(000)	3868	
Crystal size	0.32 x 0.28 x 0.23 mm ³	
Theta range for data collection	1.54 to 28.70°	
Index ranges	-21 ≤ h ≤ 21, -53 ≤ k ≤ 53, -24 ≤ l ≤ 24	
Reflections collected	110415	
Independent reflections	28448 [R _{int} = 0.0566]	
Completeness to theta = 28.70°	100.0%	
Absorption correction	Semi-empirical from equivalents	
Max. and min. transmission	0.9660 and 0.9531	
Refinement method	Full-matrix least-squares on F ²	
Data / restraints / parameters	28448 / 289 / 1191	
Goodness-of-fit on F ²	1.067	
Final R indices [I > 2σ(I)]	R ₁ = 0.0612, wR ₂ = 0.1465	
R indices (all data)	R ₁ = 0.0825, wR ₂ = 0.1627	
Absolute structure parameter	-0.016(12)	
Largest diff. peak and hole	1.504 and -0.451 eÅ ⁻³	

* Structure solution by Dr. Peter Müller.

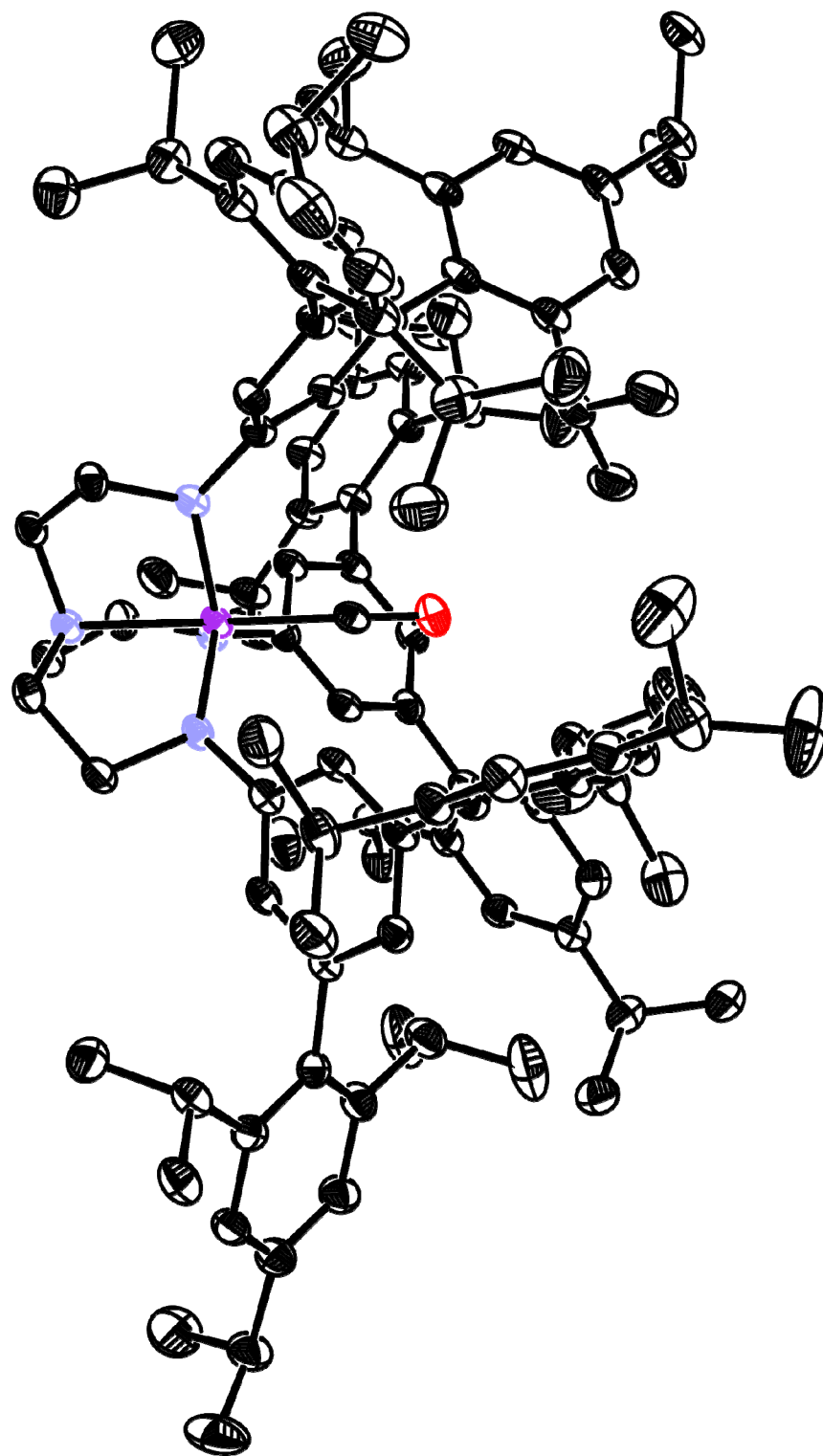


Figure A.15: Full ORTEP of [HIPTN₃N]CrCO (39) with thermal ellipsoids at 50% probability. Solvent and hydrogen atoms omitted.

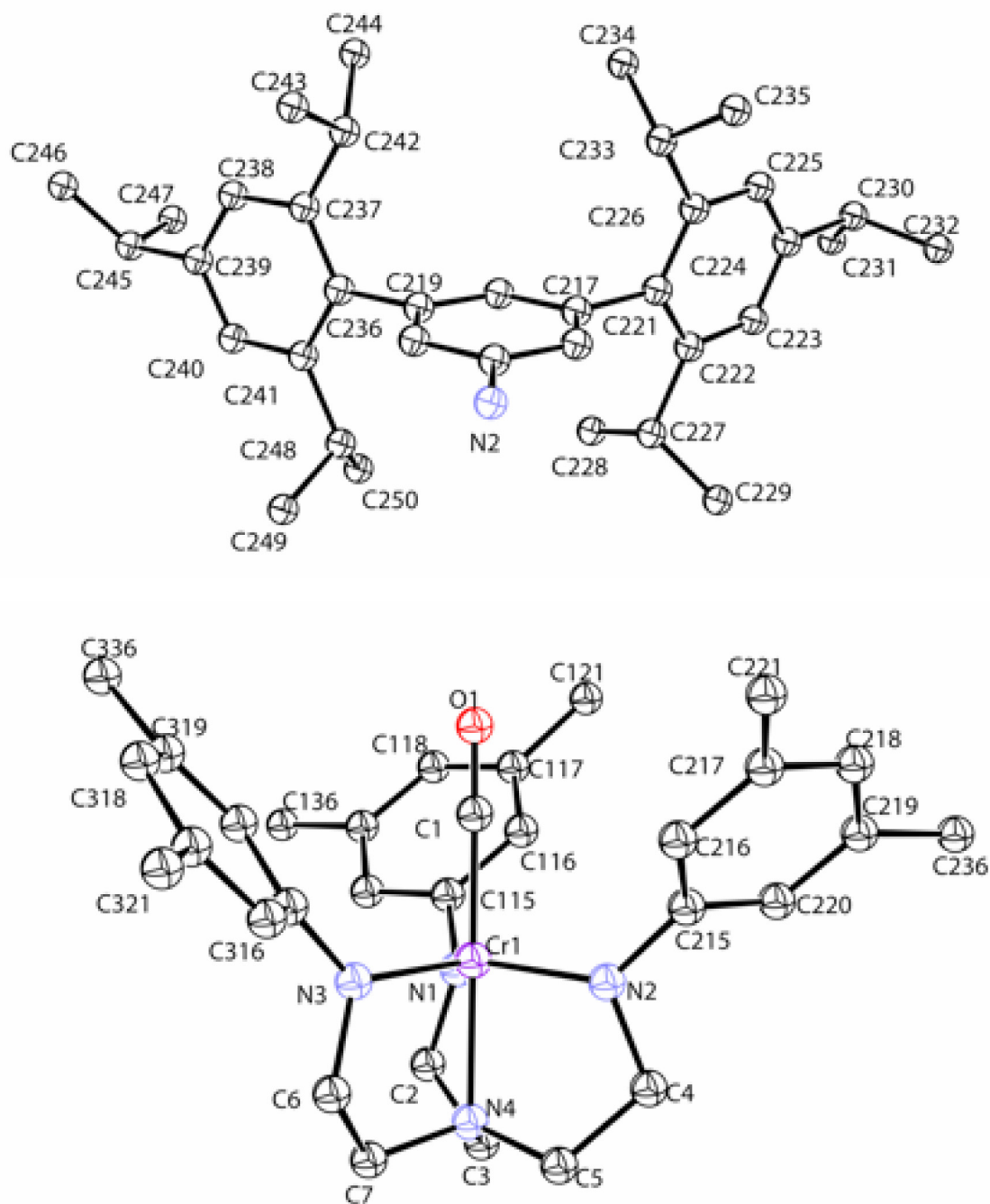


Figure A.16: ORTEP labeling scheme for [HIPTN₃N]CrCO (39). Solvent and hydrogen atoms omitted.

Table A.16: Atomic coordinates ($\times 10^4$) and equivalent isotropic displacement parameters ($\text{\AA}^2 \times 10^3$) for [HIPTN₃N]CrCO (**39**). U(eq) is defined as one third of the trace of the orthogonalized U_{ij} tensor.

	x	y	z	U(eq)
Cr(1)	9877(1)	3952(1)	3160(1)	17(1)
C(1)	10279(2)	3835(1)	4171(1)	21(1)
O(1)	10521(1)	3768(1)	4778(1)	32(1)
C(2)	10936(2)	3961(1)	1949(1)	23(1)
C(3)	10053(2)	3937(1)	1542(1)	21(1)
C(4)	8549(2)	3606(1)	2292(1)	25(1)
C(5)	8572(2)	3939(1)	1882(1)	21(1)
C(6)	9184(2)	4593(1)	2721(1)	24(1)
C(7)	9434(2)	4451(1)	1990(1)	23(1)
N(1)	10872(1)	3833(1)	2716(1)	19(1)
N(2)	8948(1)	3656(1)	3067(1)	19(1)
N(3)	9670(1)	4408(1)	3345(1)	20(1)
N(4)	9445(1)	4082(1)	2039(1)	19(1)
C(115)	11662(2)	3708(1)	3063(1)	20(1)
C(116)	11695(2)	3399(1)	3431(1)	21(1)
C(117)	12474(2)	3267(1)	3731(1)	22(1)
C(118)	13220(2)	3450(1)	3666(2)	24(1)
C(119)	13201(2)	3758(1)	3306(1)	22(1)
C(120)	12420(2)	3888(1)	3002(1)	22(1)
C(121)	12560(2)	2938(1)	4138(2)	24(1)
C(122)	12792(2)	2646(1)	3758(2)	25(1)
C(123)	12977(2)	2355(1)	4180(2)	27(1)
C(124)	12937(2)	2345(1)	4953(2)	28(1)
C(125)	12687(2)	2632(1)	5311(2)	29(1)
C(126)	12494(2)	2928(1)	4917(2)	26(1)
C(127)	12884(2)	2645(1)	2915(2)	28(1)
C(128)	13817(2)	2682(1)	2763(2)	41(1)
C(129)	12515(2)	2329(1)	2520(2)	33(1)
C(130)	13146(2)	2026(1)	5403(2)	32(1)
C(131)	12399(2)	1780(1)	5328(2)	49(1)
C(132)	13957(2)	1859(1)	5183(2)	39(1)
C(133)	12253(2)	3237(1)	5350(2)	28(1)
C(134)	11484(2)	3176(1)	5792(2)	44(1)
C(135)	13016(2)	3359(1)	5883(2)	49(1)
C(136)	14007(2)	3948(1)	3233(2)	23(1)
C(137)	14365(2)	4149(1)	3833(2)	27(1)
C(138)	15121(2)	4322(1)	3738(2)	31(1)
C(139)	15531(2)	4295(1)	3087(2)	29(1)
C(140)	15172(2)	4089(1)	2505(2)	28(1)
C(141)	14419(2)	3913(1)	2572(2)	24(1)
C(142)	13929(2)	4187(1)	4553(2)	33(1)
C(143)	13410(2)	4507(1)	4553(2)	49(1)
C(144)	14551(2)	4164(1)	5268(2)	50(1)
C(145)	16405(2)	4452(1)	3015(2)	35(1)
C(146)	16499(2)	4803(1)	3339(2)	41(1)
C(147)	17082(2)	4206(1)	3379(2)	39(1)
C(148)	14071(2)	3684(1)	1930(2)	29(1)

C(149)	13723(2)	3887(1)	1236(2)	38(1)
C(150)	14742(2)	3429(1)	1728(2)	39(1)
C(215)	8693(1)	3411(1)	3585(1)	21(1)
C(216)	8354(2)	3509(1)	4251(1)	21(1)
C(217)	8044(2)	3269(1)	4733(1)	23(1)
C(218)	8104(2)	2932(1)	4555(1)	23(1)
C(219)	8431(2)	2829(1)	3887(1)	22(1)
C(220)	8726(2)	3071(1)	3413(1)	21(1)
C(221)	7589(2)	3367(1)	5404(1)	23(1)
C(222)	6693(2)	3332(1)	5385(1)	24(1)
C(223)	6289(2)	3427(1)	6013(2)	26(1)
C(224)	6736(2)	3555(1)	6669(2)	26(1)
C(225)	7616(2)	3580(1)	6680(2)	27(1)
C(226)	8051(2)	3484(1)	6070(2)	24(1)
C(227)	6169(2)	3189(1)	4686(2)	29(1)
C(228)	6045(2)	3433(1)	4050(2)	50(1)
C(229)	5303(2)	3040(1)	4859(2)	43(1)
C(230)	6250(2)	3665(1)	7324(2)	31(1)
C(231)	6078(2)	4038(1)	7293(2)	39(1)
C(232)	6685(2)	3564(1)	8094(2)	41(1)
C(233)	9020(2)	3504(1)	6133(2)	28(1)
C(234)	9318(2)	3867(1)	6209(3)	51(1)
C(235)	9409(2)	3292(1)	6791(2)	59(1)
C(236)	8404(2)	2467(1)	3672(1)	22(1)
C(237)	9086(2)	2252(1)	3904(2)	24(1)
C(238)	9026(2)	1916(1)	3704(2)	27(1)
C(239)	8319(2)	1786(1)	3274(2)	28(1)
C(240)	7653(2)	2005(1)	3048(2)	28(1)
C(241)	7676(2)	2342(1)	3246(2)	24(1)
C(242)	9872(2)	2383(1)	4380(2)	29(1)
C(243)	9913(2)	2252(1)	5182(2)	53(1)
C(244)	10693(2)	2298(1)	4024(2)	40(1)
C(245)	8252(2)	1416(1)	3089(2)	35(1)
C(246)	8167(3)	1210(1)	3794(3)	58(1)
C(247)	9007(2)	1289(1)	2688(2)	38(1)
C(248)	6927(2)	2574(1)	3003(2)	30(1)
C(249)	6980(2)	2707(1)	2209(2)	43(1)
C(250)	6065(2)	2412(1)	3063(3)	53(1)
C(315)	9725(2)	4591(1)	4031(1)	20(1)
C(316)	9021(2)	4769(1)	4244(1)	22(1)
C(317)	9069(2)	4969(1)	4880(1)	21(1)
C(318)	9845(2)	4994(1)	5327(1)	23(1)
C(319)	10563(2)	4819(1)	5128(1)	21(1)
C(320)	10498(2)	4615(1)	4492(1)	21(1)
C(321)	8292(2)	5165(1)	5043(1)	23(1)
C(322)	7659(2)	5017(1)	5436(2)	28(1)
C(323)	6908(2)	5196(1)	5519(2)	31(1)
C(324)	6761(2)	5510(1)	5207(2)	30(1)
C(325)	7399(2)	5654(1)	4825(2)	27(1)
C(326)	8169(2)	5489(1)	4743(1)	23(1)
C(327)	7774(2)	4669(1)	5778(2)	34(1)
C(328)	7003(3)	4441(1)	5589(2)	56(1)
C(329)	7969(3)	4684(1)	6625(2)	59(1)
C(330)	5891(2)	5673(1)	5238(2)	36(1)

C(331)	5912(3)	6053(1)	5217(3)	57(1)
C(332)	5266(2)	5537(1)	4604(2)	61(1)
C(333)	8827(2)	5650(1)	4281(2)	27(1)
C(334)	8587(2)	5590(1)	3436(2)	35(1)
C(335)	8943(2)	6024(1)	4429(2)	33(1)
C(336)	11408(2)	4886(1)	5572(1)	21(1)
C(337)	11922(2)	5148(1)	5337(2)	25(1)
C(338)	12687(2)	5219(1)	5767(2)	27(1)
C(339)	12958(2)	5043(1)	6419(2)	26(1)
C(340)	12440(2)	4786(1)	6641(2)	26(1)
C(341)	11667(2)	4703(1)	6226(2)	23(1)
C(342)	11658(2)	5356(1)	4636(2)	29(1)
C(343)	11538(2)	5722(1)	4839(2)	38(1)
C(344)	12289(2)	5318(1)	4046(2)	38(1)
C(345)	13803(2)	5128(1)	6868(2)	33(1)
C(346)	14548(2)	5016(2)	6456(2)	76(2)
C(347)	13889(2)	5001(2)	7667(2)	69(1)
C(348)	11113(2)	4432(1)	6520(2)	29(1)
C(349)	11621(2)	4125(1)	6811(2)	45(1)
C(350)	10601(2)	4572(1)	7138(2)	40(1)

Table A.17: Crystal data and structure refinement for [HIPTN₃N]CrNO (41).*

Identification code	05137	
Empirical formula	C ₁₂₁ H ₁₇₅ CrN ₅ O	
Formula weight	1767.66	
Temperature	100(2) K	
Wavelength	0.71073 Å	
Crystal system	Monoclinic	
Space group	Cc	
Unit cell dimensions	a = 15.7440(6) Å	α = 90°
	b = 39.7549(16) Å	β = 95.2400(10)°
	c = 17.7703(6) Å	γ = 90°
Volume	11076.0(7) Å ³	
Z	4	
Density (calculated)	1.060 Mg/m ³	
Absorption coefficient	0.152 mm ⁻¹	
F(000)	3872	
Crystal size	0.11 x 0.11 x 0.11 mm ³	
Theta range for data collection	1.73 to 29.13°	
Index ranges	-21 ≤ h ≤ 21, -54 ≤ k ≤ 54, -24 ≤ l ≤ 24	
Reflections collected	121078	
Independent reflections	29400 [R _{int} = 0.0450]	
Completeness to theta = 29.13°	100.0%	
Absorption correction	Semi-empirical from equivalents	
Max. and min. transmission	0.9820 and 0.9820	
Refinement method	Full-matrix least-squares on F ²	
Data / restraints / parameters	29400 / 289 / 1191	
Goodness-of-fit on F ²	1.027	
Final R indices [I > 2σ(I)]	R ₁ = 0.0451, wR ₂ = 0.1050	
R indices (all data)	R ₁ = 0.0546, wR ₂ = 0.1104	
Absolute structure parameter	-0.009(8)	
Largest diff. peak and hole	0.499 and -0.214 eÅ ⁻³	

* Structure solution by Dr. Peter Müller.

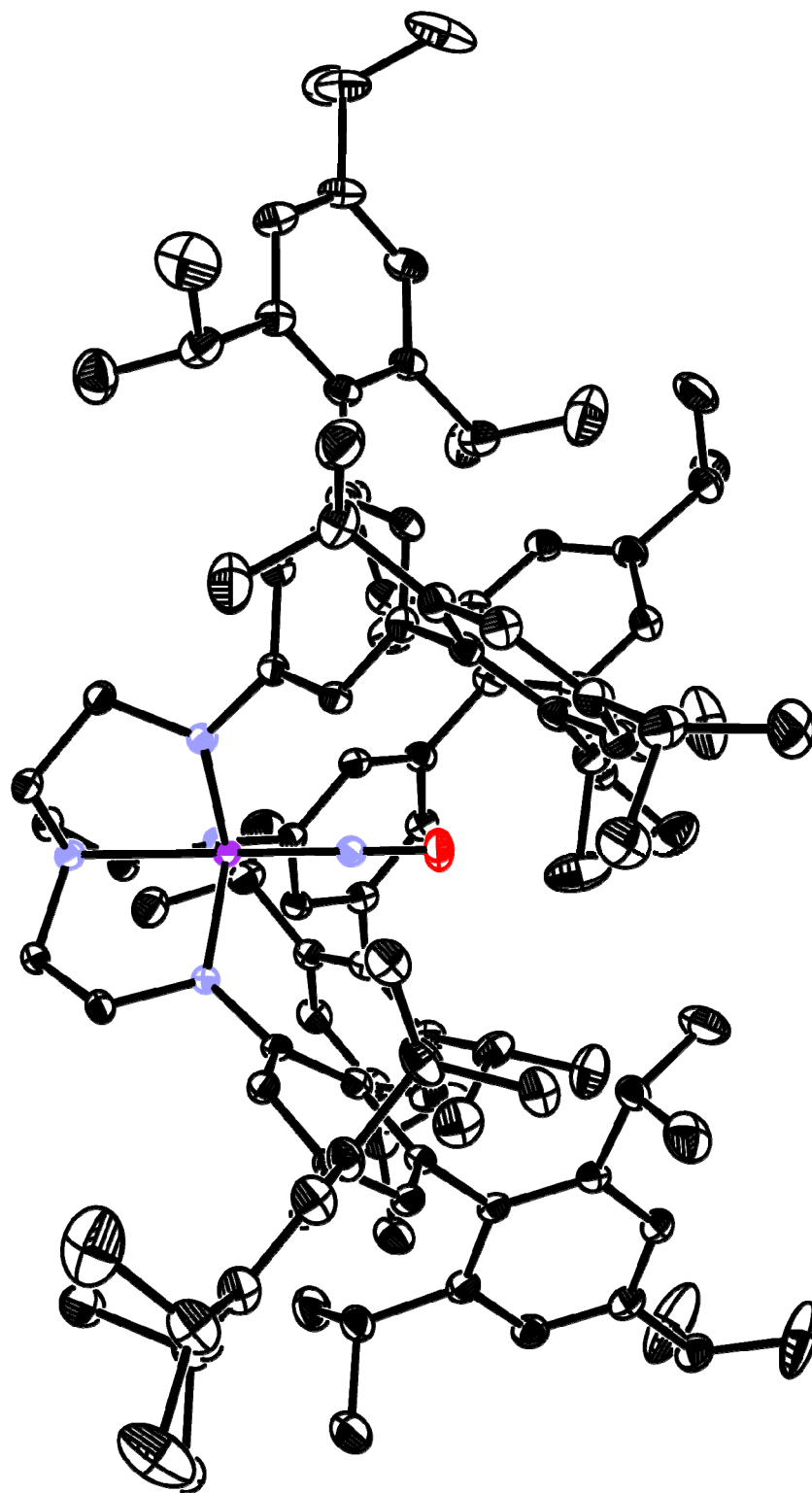


Figure A.17: Full ORTEP of [HIPTN₃N]CrNO (41). Thermal ellipsoids at 50% probability, hydrogen atoms and solvent omitted.

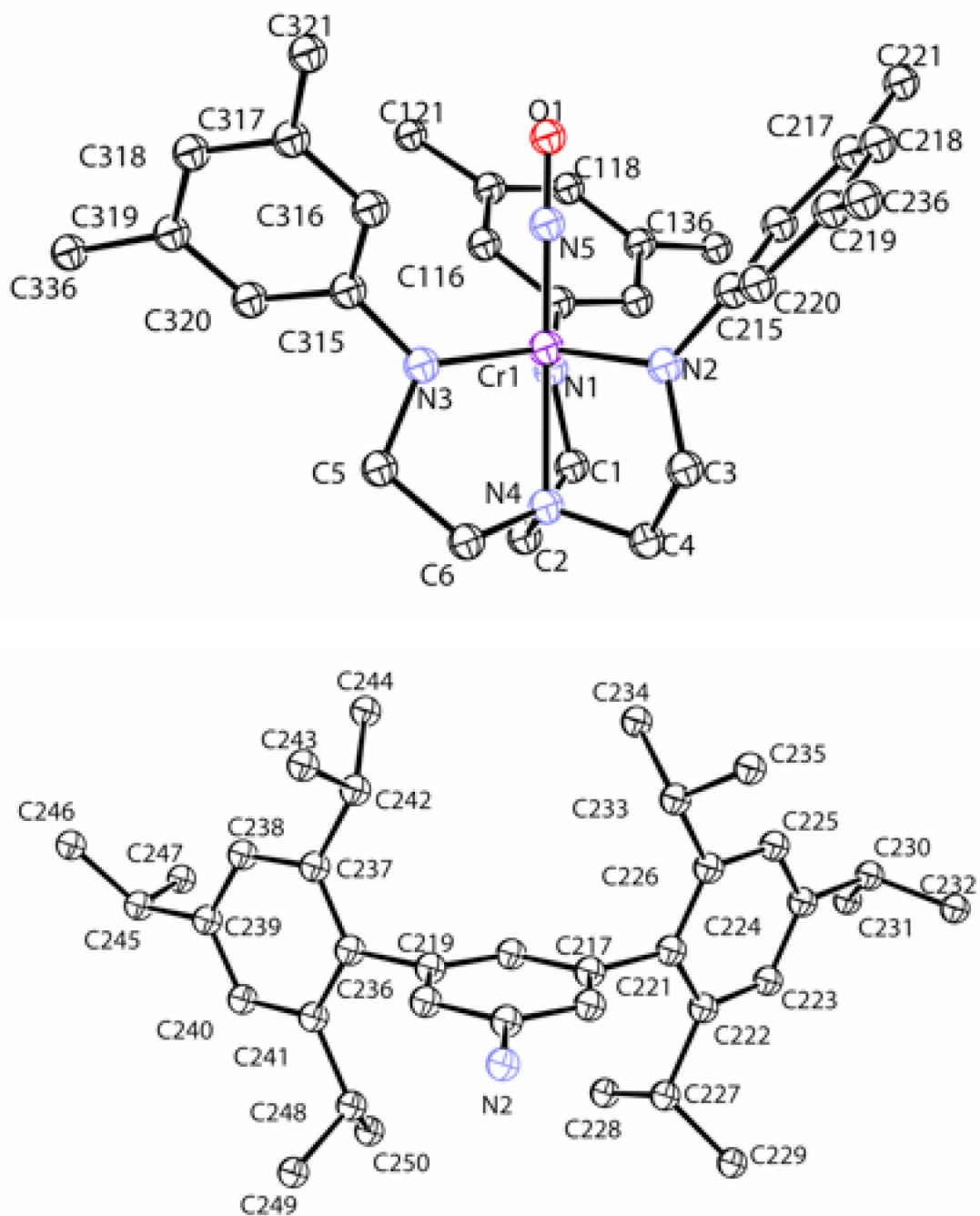


Figure A.18: ORTEP labeling scheme for $[\text{HIPTN}_3\text{N}]\text{CrNO}$ (**41**). Solvent and hydrogen atoms omitted.

Table A.18: Atomic coordinates ($\times 10^4$) and equivalent isotropic displacement parameters ($\text{\AA}^2 \times 10^3$) for [HIPTN₃N]CrNO (**41**). $U(\text{eq})$ is defined as one third of the trace of the orthogonalized $U^{\ddot{J}}$ tensor

	x	y	z	$U(\text{eq})$
Cr(1)	-333(1)	-8950(1)	-2113(1)	12(1)
N(1)	-1262(1)	-8655(1)	-2227(1)	15(1)
N(2)	656(1)	-8837(1)	-2571(1)	15(1)
N(3)	-550(1)	-9407(1)	-1942(1)	14(1)
N(4)	-774(1)	-9082(1)	-3244(1)	15(1)
C(1)	-1666(1)	-8608(1)	-2996(1)	19(1)
C(2)	-1647(1)	-8942(1)	-3402(1)	18(1)
C(3)	713(1)	-8962(1)	-3347(1)	19(1)
C(4)	-168(1)	-8937(1)	-3747(1)	19(1)
C(5)	-1032(1)	-9593(1)	-2560(1)	19(1)
C(6)	-779(1)	-9454(1)	-3296(1)	18(1)
N(5)	17(1)	-8844(1)	-1226(1)	15(1)
O(1)	269(1)	-8769(1)	-601(1)	26(1)
C(115)	-1517(1)	-8409(1)	-1709(1)	16(1)
C(116)	-1857(1)	-8508(1)	-1043(1)	16(1)
C(117)	-2174(1)	-8268(1)	-565(1)	17(1)
C(118)	-2119(1)	-7928(1)	-746(1)	17(1)
C(119)	-1789(1)	-7826(1)	-1409(1)	17(1)
C(120)	-1490(1)	-8067(1)	-1885(1)	17(1)
C(121)	-2627(1)	-8367(1)	109(1)	17(1)
C(122)	-3523(1)	-8332(1)	88(1)	20(1)
C(123)	-3923(1)	-8427(1)	723(1)	22(1)
C(124)	-3479(1)	-8554(1)	1373(1)	21(1)
C(125)	-2598(1)	-8580(1)	1386(1)	22(1)
C(126)	-2163(1)	-8485(1)	768(1)	20(1)
C(127)	-4049(1)	-8187(1)	-603(1)	25(1)
C(128)	-4166(2)	-8431(1)	-1247(1)	42(1)
C(129)	-4924(1)	-8045(1)	-432(1)	35(1)
C(130)	-3961(1)	-8664(1)	2032(1)	26(1)
C(131)	-4137(1)	-9041(1)	1998(1)	34(1)
C(132)	-3524(2)	-8566(1)	2796(1)	38(1)
C(133)	-1195(1)	-8503(1)	833(1)	23(1)
C(134)	-796(2)	-8305(1)	1507(1)	51(1)
C(135)	-896(1)	-8869(1)	860(2)	42(1)
C(136)	-1817(1)	-7462(1)	-1625(1)	18(1)
C(137)	-1134(1)	-7249(1)	-1397(1)	20(1)
C(138)	-1195(1)	-6910(1)	-1600(1)	24(1)
C(139)	-1905(1)	-6782(1)	-2024(1)	24(1)
C(140)	-2570(1)	-7000(1)	-2248(1)	24(1)
C(141)	-2546(1)	-7339(1)	-2048(1)	20(1)
C(142)	-349(1)	-7379(1)	-924(1)	24(1)
C(143)	-314(2)	-7250(1)	-119(1)	49(1)
C(144)	471(1)	-7292(1)	-1275(1)	37(1)
C(145)	-1973(1)	-6410(1)	-2217(1)	32(1)
C(146)	-2047(2)	-6202(1)	-1507(2)	54(1)
C(147)	-1218(1)	-6284(1)	-2620(1)	34(1)
C(148)	-3294(1)	-7571(1)	-2289(1)	26(1)

C(149)	-4159(1)	-7411(1)	-2220(2)	51(1)
C(150)	-3245(2)	-7702(1)	-3085(1)	41(1)
C(215)	1439(1)	-8712(1)	-2231(1)	16(1)
C(216)	1474(1)	-8401(1)	-1860(1)	17(1)
C(217)	2250(1)	-8269(1)	-1565(1)	18(1)
C(218)	2997(1)	-8450(1)	-1633(1)	19(1)
C(219)	2979(1)	-8761(1)	-1993(1)	18(1)
C(220)	2202(1)	-8890(1)	-2291(1)	17(1)
C(221)	2335(1)	-7938(1)	-1158(1)	19(1)
C(222)	2572(1)	-7646(1)	-1535(1)	20(1)
C(223)	2758(1)	-7355(1)	-1114(1)	22(1)
C(224)	2715(1)	-7345(1)	-339(1)	23(1)
C(225)	2455(1)	-7632(1)	17(1)	24(1)
C(226)	2260(1)	-7929(1)	-379(1)	22(1)
C(227)	2669(1)	-7645(1)	-2377(1)	23(1)
C(228)	3605(1)	-7680(1)	-2527(1)	36(1)
C(229)	2298(1)	-7327(1)	-2771(1)	28(1)
C(230)	2922(1)	-7027(1)	116(1)	28(1)
C(231)	3740(1)	-6862(1)	-99(1)	35(1)
C(232)	2181(2)	-6780(1)	36(2)	43(1)
C(233)	2015(1)	-8240(1)	52(1)	25(1)
C(234)	2769(2)	-8360(1)	595(1)	44(1)
C(235)	1223(2)	-8181(1)	466(1)	40(1)
C(236)	3788(1)	-8950(1)	-2061(1)	19(1)
C(237)	4145(1)	-9149(1)	-1462(1)	22(1)
C(238)	4906(1)	-9321(1)	-1552(1)	25(1)
C(239)	5319(1)	-9294(1)	-2208(1)	24(1)
C(240)	4961(1)	-9092(1)	-2787(1)	24(1)
C(241)	4202(1)	-8916(1)	-2727(1)	20(1)
C(242)	3712(1)	-9183(1)	-736(1)	28(1)
C(243)	3190(2)	-9504(1)	-737(1)	45(1)
C(244)	4334(2)	-9157(1)	-28(1)	44(1)
C(245)	6193(1)	-9453(1)	-2276(1)	30(1)
C(246)	6286(1)	-9805(1)	-1951(1)	36(1)
C(247)	6866(1)	-9208(1)	-1912(1)	34(1)
C(248)	3856(1)	-8688(1)	-3367(1)	25(1)
C(249)	3513(1)	-8892(1)	-4059(1)	33(1)
C(250)	4523(1)	-8430(1)	-3571(1)	36(1)
C(315)	-497(1)	-9586(1)	-1250(1)	15(1)
C(316)	273(1)	-9608(1)	-791(1)	17(1)
C(317)	341(1)	-9816(1)	-154(1)	16(1)
C(318)	-378(1)	-9993(1)	37(1)	18(1)
C(319)	-1149(1)	-9970(1)	-403(1)	16(1)
C(320)	-1201(1)	-9766(1)	-1042(1)	17(1)
C(321)	1182(1)	-9883(1)	283(1)	17(1)
C(322)	1700(1)	-10144(1)	50(1)	21(1)
C(323)	2465(1)	-10216(1)	476(1)	23(1)
C(324)	2737(1)	-10039(1)	1130(1)	23(1)
C(325)	2214(1)	-9783(1)	1352(1)	22(1)
C(326)	1443(1)	-9702(1)	943(1)	19(1)
C(327)	1440(1)	-10352(1)	-652(1)	24(1)
C(328)	2069(2)	-10311(1)	-1246(1)	35(1)
C(329)	1317(2)	-10721(1)	-451(1)	34(1)
C(330)	3582(1)	-10126(1)	1576(1)	27(1)

C(331)	3661(2)	-10004(1)	2376(1)	65(1)
C(332)	4324(2)	-10008(1)	1171(2)	74(1)
C(333)	879(1)	-9431(1)	1236(1)	24(1)
C(334)	1382(2)	-9125(1)	1541(2)	40(1)
C(335)	366(1)	-9576(1)	1852(1)	38(1)
C(336)	-1929(1)	-10166(1)	-243(1)	18(1)
C(337)	-2563(1)	-10017(1)	152(1)	23(1)
C(338)	-3314(1)	-10195(1)	232(1)	26(1)
C(339)	-3464(1)	-10512(1)	-86(1)	25(1)
C(340)	-2822(1)	-10656(1)	-468(1)	23(1)
C(341)	-2052(1)	-10491(1)	-548(1)	20(1)
C(342)	-2448(1)	-9669(1)	493(1)	28(1)
C(343)	-3210(2)	-9438(1)	298(2)	51(1)
C(344)	-2261(2)	-9683(1)	1337(1)	54(1)
C(345)	-4335(1)	-10674(1)	-55(1)	31(1)
C(346)	-4958(2)	-10531(1)	-681(2)	57(1)
C(347)	-4318(2)	-11056(1)	-89(2)	52(1)
C(348)	-1394(1)	-10652(1)	-1009(1)	22(1)
C(349)	-1638(1)	-10593(1)	-1852(1)	31(1)
C(350)	-1276(1)	-11028(1)	-861(1)	27(1)

Table A.19: Crystal data and structure refinement for [HIPTN₃N]CrCl (42).*

Identification code	05105	
Empirical formula	C ₁₂₁ H ₁₇₅ ClCrN ₄	
Formula weight	1773.10	
Temperature	100(2) K	
Wavelength	0.71073 Å	
Crystal system	Monoclinic	
Space group	Cc	
Unit cell dimensions	a = 15.7588(8) Å	α = 90°
	b = 39.997(2) Å	β = 95.501(2)°
	c = 17.7963(10) Å	γ = 90°
Volume	11165.5(10) Å ³	
Z	4	
Density (calculated)	1.055 Mg/m ³	
Absorption coefficient	0.173 mm ⁻¹	
F(000)	3880	
Crystal size	0.26 x 0.24 x 0.08 mm ³	
Theta range for data collection	1.54 to 28.70°	
Index ranges	-21 ≤ h ≤ 21, -54 ≤ k ≤ 54, -24 ≤ l ≤ 23	
Reflections collected	106812	
Independent reflections	28684 [R _{int} = 0.0410]	
Completeness to theta = 28.70°	100.0%	
Absorption correction	Semi-empirical from equivalents	
Max. and min. transmission	0.9863 and 0.9580	
Refinement method	Full-matrix least-squares on F ²	
Data / restraints / parameters	28684 / 289 / 1182	
Goodness-of-fit on F ²	1.029	
Final R indices [I > 2σ(I)]	R ₁ = 0.0433, wR ₂ = 0.1008	
R indices (all data)	R ₁ = 0.0545, wR ₂ = 0.1081	
Absolute structure parameter	-0.015(8)	
Largest diff. peak and hole	0.596 and -0.316 eÅ ⁻³	

* Structure solution by Dr. Peter Müller.

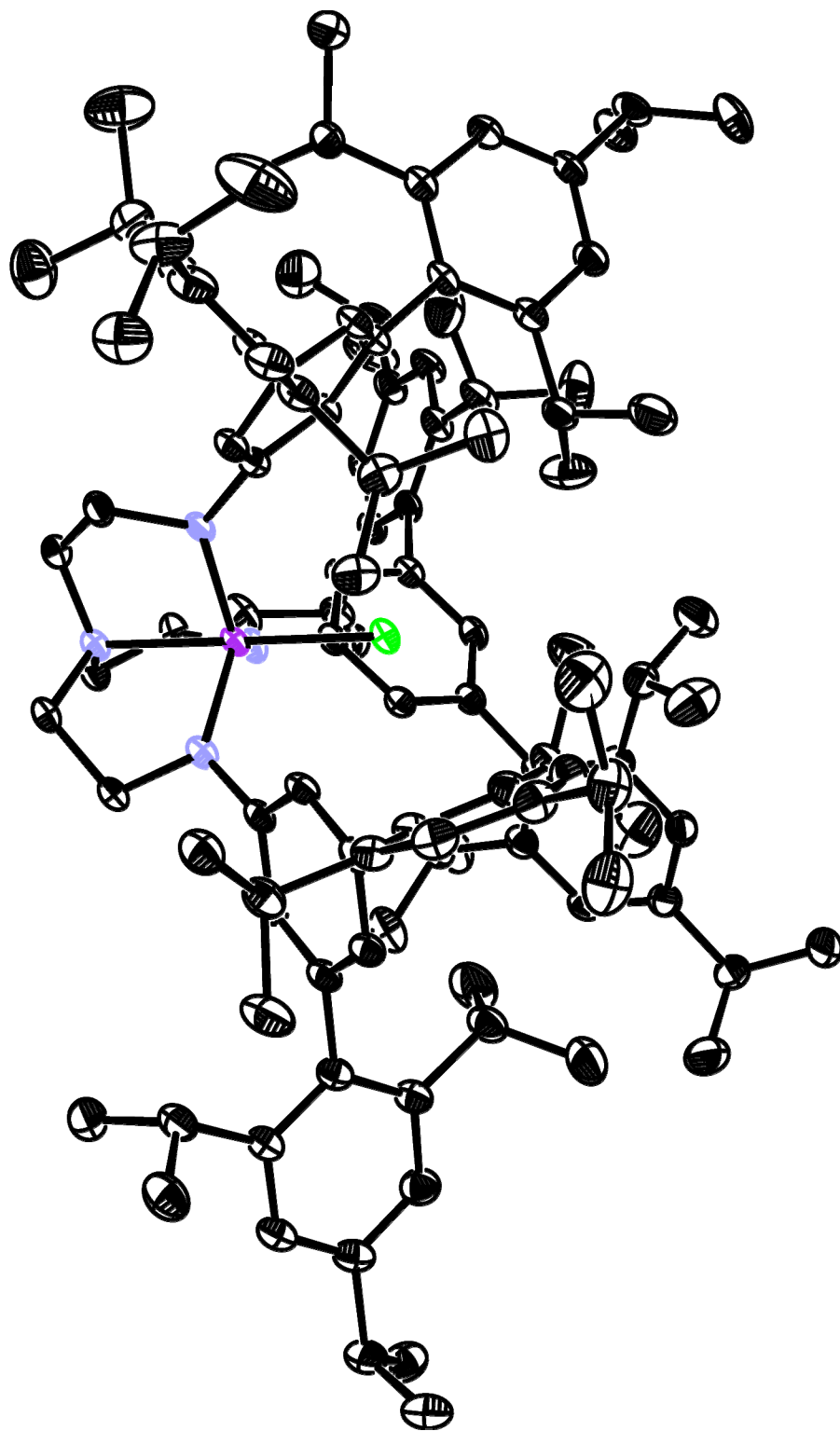


Figure A.19: Full ORTEP of $[\text{HIPTN}_3\text{N}]\text{CrCl}$ (42). Thermal ellipsoids at 50% probability, solvent and hydrogen atoms omitted.

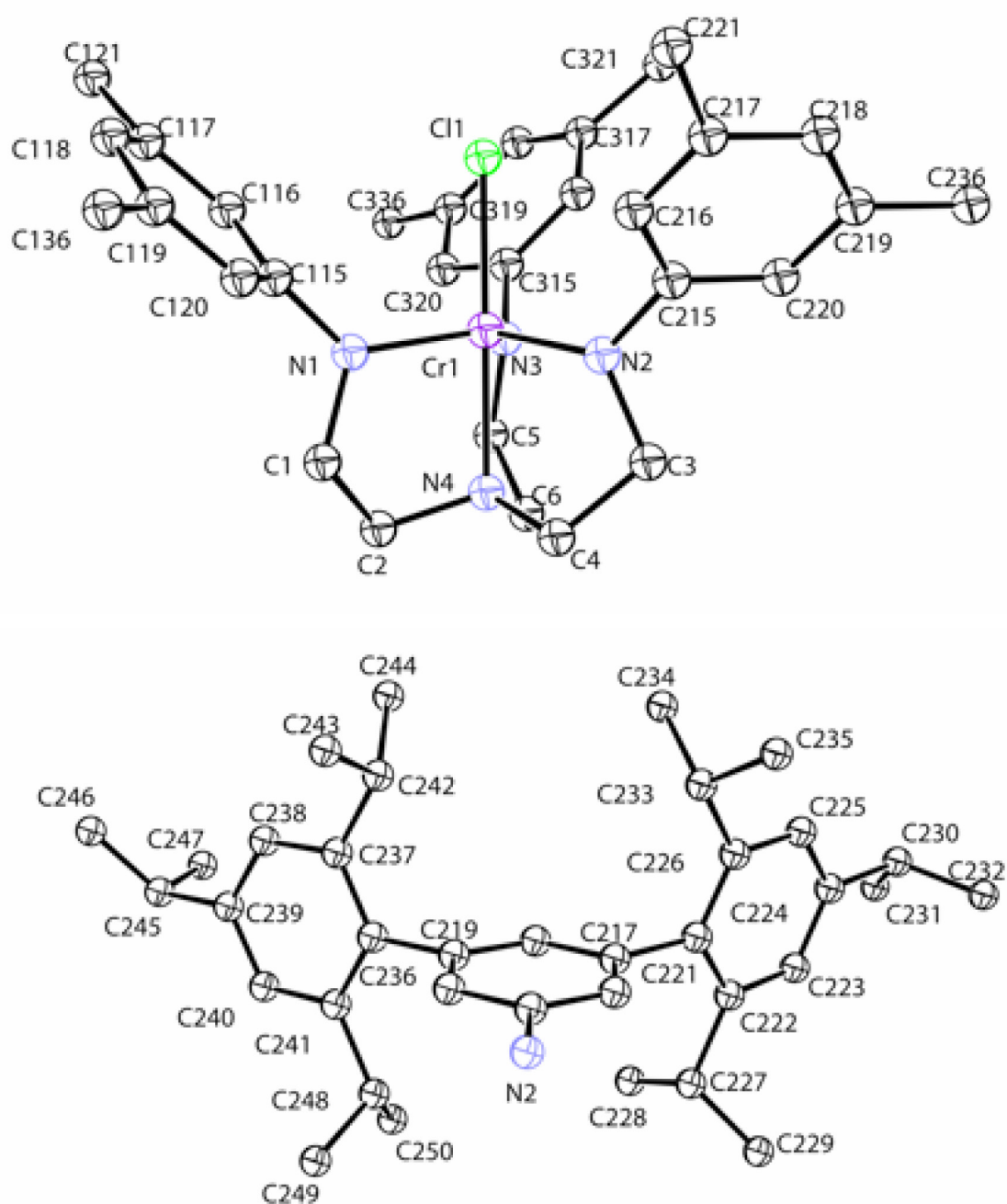


Figure A.20: ORTEP labeling scheme for [HIPTN₃N]CrCl (42). Solvent and hydrogen atoms omitted.

Table A.20: Atomic coordinates ($\times 10^4$) and equivalent isotropic displacement parameters ($\text{\AA}^2 \times 10^3$) for [HIPTN₃N]CrCl (42). U(eq) is defined as one third of the trace of the orthogonalized U_{ij} tensor.

	x	y	z	U(eq)
Cr(1)	338(1)	8950(1)	2112(1)	16(1)
Cl(1)	-125(1)	8805(1)	921(1)	20(1)
N(1)	1278(1)	8660(1)	2214(1)	19(1)
N(2)	-650(1)	8831(1)	2569(1)	20(1)
N(3)	532(1)	9409(1)	1929(1)	19(1)
N(4)	782(1)	9085(1)	3236(1)	18(1)
C(1)	1689(1)	8615(1)	2987(1)	23(1)
C(2)	1658(1)	8948(1)	3391(1)	23(1)
C(3)	-704(1)	8958(1)	3340(1)	24(1)
C(4)	184(1)	8936(1)	3742(1)	22(1)
C(5)	1011(1)	9595(1)	2549(1)	23(1)
C(6)	772(1)	9455(1)	3286(1)	23(1)
C(115)	1536(1)	8412(1)	1700(1)	20(1)
C(116)	1889(1)	8507(1)	1042(1)	20(1)
C(117)	2204(1)	8266(1)	569(1)	20(1)
C(118)	2136(1)	7929(1)	754(1)	22(1)
C(119)	1797(1)	7830(1)	1414(1)	21(1)
C(120)	1492(1)	8073(1)	1882(1)	21(1)
C(121)	2649(1)	8364(1)	-109(1)	21(1)
C(122)	3545(1)	8325(1)	-96(1)	23(1)
C(123)	3936(1)	8423(1)	-734(1)	25(1)
C(124)	3481(1)	8553(1)	-1378(1)	24(1)
C(125)	2604(1)	8581(1)	-1382(1)	26(1)
C(126)	2174(1)	8486(1)	-760(1)	23(1)
C(127)	4076(1)	8181(1)	594(1)	26(1)
C(128)	4200(1)	8429(1)	1240(1)	39(1)
C(129)	4947(1)	8041(1)	419(1)	33(1)
C(130)	3958(1)	8663(1)	-2043(1)	29(1)
C(131)	4140(2)	9038(1)	-2003(1)	37(1)
C(132)	3506(2)	8569(1)	-2812(1)	41(1)
C(133)	1207(1)	8507(1)	-814(1)	25(1)
C(134)	798(2)	8299(1)	-1473(2)	53(1)
C(135)	908(1)	8870(1)	-872(2)	44(1)
C(136)	1820(1)	7468(1)	1634(1)	21(1)
C(137)	1137(1)	7255(1)	1405(1)	24(1)
C(138)	1196(1)	6918(1)	1607(1)	27(1)
C(139)	1908(1)	6790(1)	2039(1)	28(1)
C(140)	2573(1)	7007(1)	2264(1)	28(1)
C(141)	2549(1)	7344(1)	2063(1)	24(1)
C(142)	346(1)	7384(1)	927(1)	29(1)
C(143)	314(2)	7255(1)	119(1)	54(1)
C(144)	-471(1)	7299(1)	1276(1)	39(1)
C(145)	1975(1)	6419(1)	2230(1)	36(1)
C(146)	2047(2)	6211(1)	1523(2)	61(1)
C(147)	1219(1)	6295(1)	2637(1)	39(1)
C(148)	3298(1)	7577(1)	2309(1)	30(1)
C(149)	4161(2)	7420(1)	2233(2)	57(1)

C(150)	3246(2)	7703(1)	3115(1)	48(1)
C(215)	-1440(1)	8704(1)	2232(1)	20(1)
C(216)	-1481(1)	8389(1)	1885(1)	21(1)
C(217)	-2264(1)	8257(1)	1598(1)	22(1)
C(218)	-3006(1)	8442(1)	1655(1)	22(1)
C(219)	-2982(1)	8756(1)	1995(1)	21(1)
C(220)	-2196(1)	8887(1)	2284(1)	21(1)
C(221)	-2350(1)	7929(1)	1188(1)	22(1)
C(222)	-2581(1)	7635(1)	1561(1)	24(1)
C(223)	-2763(1)	7347(1)	1131(1)	27(1)
C(224)	-2720(1)	7340(1)	360(1)	28(1)
C(225)	-2463(1)	7628(1)	6(1)	29(1)
C(226)	-2272(1)	7923(1)	408(1)	25(1)
C(227)	-2670(1)	7632(1)	2410(1)	27(1)
C(228)	-3601(1)	7672(1)	2561(1)	40(1)
C(229)	-2304(1)	7314(1)	2797(1)	32(1)
C(230)	-2928(1)	7023(1)	-102(1)	33(1)
C(231)	-3739(2)	6858(1)	112(1)	42(1)
C(232)	-2180(2)	6780(1)	-30(2)	50(1)
C(233)	-2019(1)	8233(1)	-16(1)	28(1)
C(234)	-2747(2)	8347(1)	-590(1)	46(1)
C(235)	-1199(2)	8175(1)	-394(2)	45(1)
C(236)	-3788(1)	8947(1)	2062(1)	22(1)
C(237)	-4135(1)	9150(1)	1463(1)	25(1)
C(238)	-4890(1)	9323(1)	1547(1)	30(1)
C(239)	-5312(1)	9296(1)	2196(1)	27(1)
C(240)	-4963(1)	9091(1)	2776(1)	27(1)
C(241)	-4209(1)	8913(1)	2722(1)	24(1)
C(242)	-3693(1)	9185(1)	740(1)	32(1)
C(243)	-3200(2)	9510(1)	729(2)	49(1)
C(244)	-4306(2)	9149(1)	26(1)	46(1)
C(245)	-6187(1)	9454(1)	2263(1)	33(1)
C(246)	-6282(1)	9806(1)	1934(1)	39(1)
C(247)	-6863(1)	9210(1)	1895(1)	38(1)
C(248)	-3866(1)	8685(1)	3367(1)	28(1)
C(249)	-3523(1)	8888(1)	4061(1)	37(1)
C(250)	-4539(2)	8431(1)	3568(1)	38(1)
C(315)	476(1)	9590(1)	1235(1)	19(1)
C(316)	-301(1)	9620(1)	785(1)	20(1)
C(317)	-361(1)	9827(1)	147(1)	20(1)
C(318)	362(1)	9998(1)	-45(1)	22(1)
C(319)	1139(1)	9970(1)	393(1)	20(1)
C(320)	1189(1)	9763(1)	1025(1)	21(1)
C(321)	-1203(1)	9893(1)	-298(1)	21(1)
C(322)	-1723(1)	10155(1)	-77(1)	24(1)
C(323)	-2489(1)	10222(1)	-511(1)	26(1)
C(324)	-2758(1)	10041(1)	-1156(1)	25(1)
C(325)	-2239(1)	9783(1)	-1368(1)	26(1)
C(326)	-1463(1)	9705(1)	-947(1)	23(1)
C(327)	-1461(1)	10366(1)	622(1)	28(1)
C(328)	-2091(2)	10327(1)	1214(1)	39(1)
C(329)	-1346(2)	10733(1)	418(1)	38(1)
C(330)	-3610(1)	10123(1)	-1608(1)	30(1)
C(331)	-3699(2)	9984(1)	-2398(1)	63(1)

C(332)	-4350(2)	10016(1)	-1190(2)	69(1)
C(333)	-904(1)	9431(1)	-1225(1)	28(1)
C(334)	-1410(2)	9122(1)	-1502(2)	50(1)
C(335)	-393(2)	9568(1)	-1855(1)	46(1)
C(336)	1920(1)	10165(1)	235(1)	21(1)
C(337)	2557(1)	10016(1)	-157(1)	26(1)
C(338)	3306(1)	10194(1)	-235(1)	29(1)
C(339)	3452(1)	10510(1)	78(1)	28(1)
C(340)	2807(1)	10656(1)	455(1)	26(1)
C(341)	2042(1)	10489(1)	537(1)	24(1)
C(342)	2443(1)	9667(1)	-496(1)	31(1)
C(343)	3222(2)	9443(1)	-318(2)	51(1)
C(344)	2225(2)	9684(1)	-1341(1)	56(1)
C(345)	4322(1)	10674(1)	45(1)	35(1)
C(346)	4947(2)	10535(1)	679(2)	57(1)
C(347)	4299(2)	11055(1)	77(2)	55(1)
C(348)	1379(1)	10649(1)	998(1)	26(1)
C(349)	1622(2)	10585(1)	1844(1)	35(1)
C(350)	1272(1)	11025(1)	861(1)	30(1)

Table A.21: Crystal data and structure refinement for [HIPTN₃N]CrCl (42) / [HIPTN₃N]CrN₃.*

Identification code	05131	
Empirical formula	C ₁₂₁ H ₁₇₅ Cl _{0.66} CrN ₅	
Formula weight	1775.27	
Temperature	100(2) K	
Wavelength	0.71073 Å	
Crystal system	Monoclinic	
Space group	Cc	
Unit cell dimensions	a = 15.7434(6) Å	α = 90°
	b = 39.9919(15) Å	β = 95.2800(10)°
	c = 17.7938(7) Å	γ = 90°
Volume	11155.6(7) Å ³	
Z	4	
Density (calculated)	1.057 Mg/m ³	
Absorption coefficient	0.166 mm ⁻¹	
F(000)	3885	
Crystal size	0.30 x 0.25 x 0.20 mm ³	
Theta range for data collection	1.73 to 29.44°	
Index ranges	-21 ≤ h ≤ 21, -55 ≤ k ≤ 53, -24 ≤ l ≤ 24	
Reflections collected	104056	
Independent reflections	30840 [R _{int} = 0.0673]	
Completeness to theta = 29.44°	100.0%	
Absorption correction	Semi-empirical from equivalents	
Max. and min. transmission	0.9676 and 0.9519	
Refinement method	Full-matrix least-squares on F ²	
Data / restraints / parameters	30840 / 314 / 1210	
Goodness-of-fit on F ²	1.037	
Final R indices [I > 2σ(I)]	R ₁ = 0.0586, wR ₂ = 0.1200	
R indices (all data)	R ₁ = 0.0842, wR ₂ = 0.1313	
Absolute structure parameter	-0.022(11)	
Largest diff. peak and hole	0.728 and -0.327 eÅ ⁻³	

* Structure solution by Dr. Peter Müller.

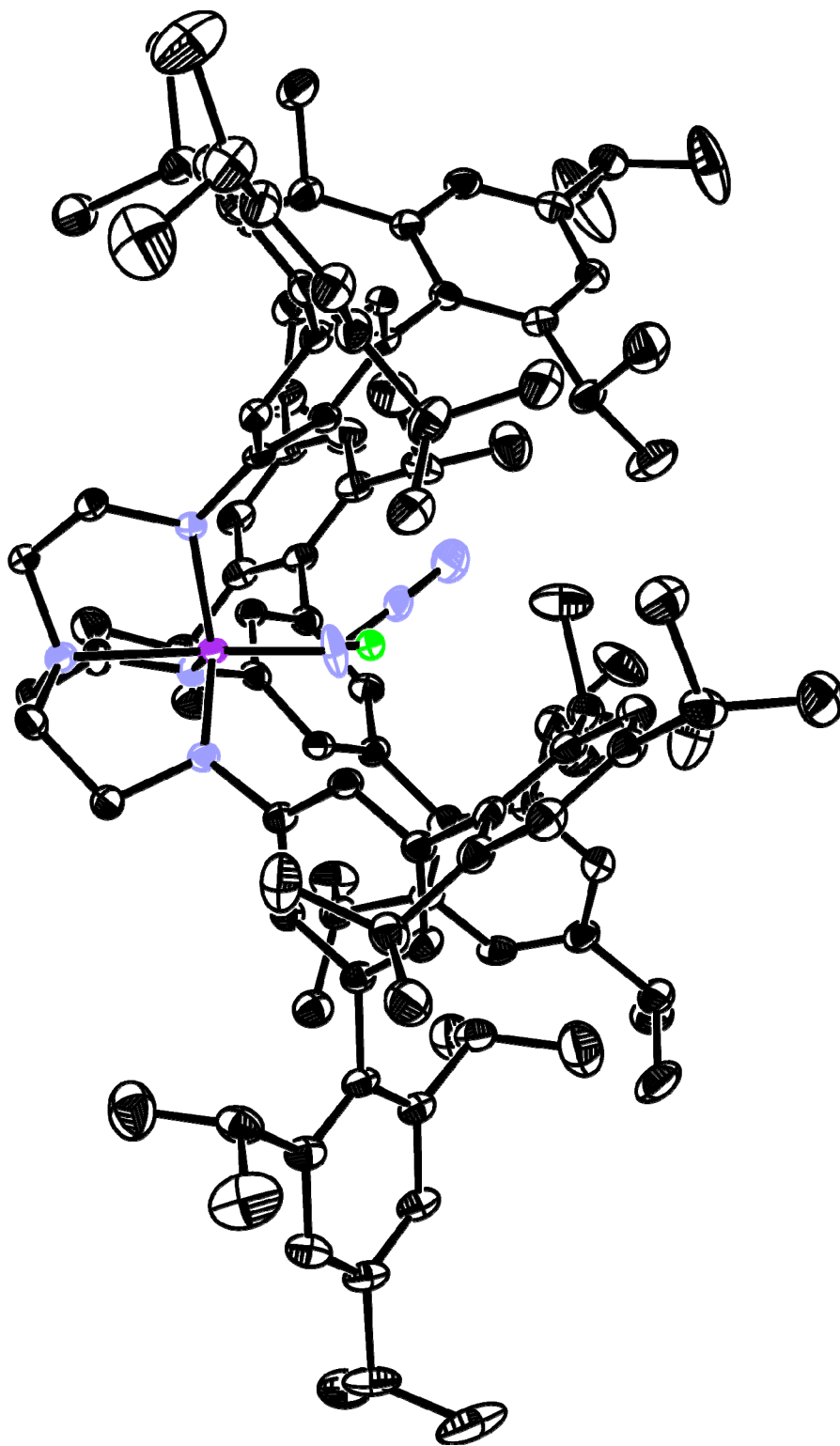


Figure A.21: Full ORTEP of $[\text{HIPTN}_3\text{N}]\text{CrCl}$ (42) / $[\text{HIPTN}_3\text{N}]\text{CrN}_3$. Thermal ellipsoids at 50% probability, solvent and hydrogen atoms omitted.

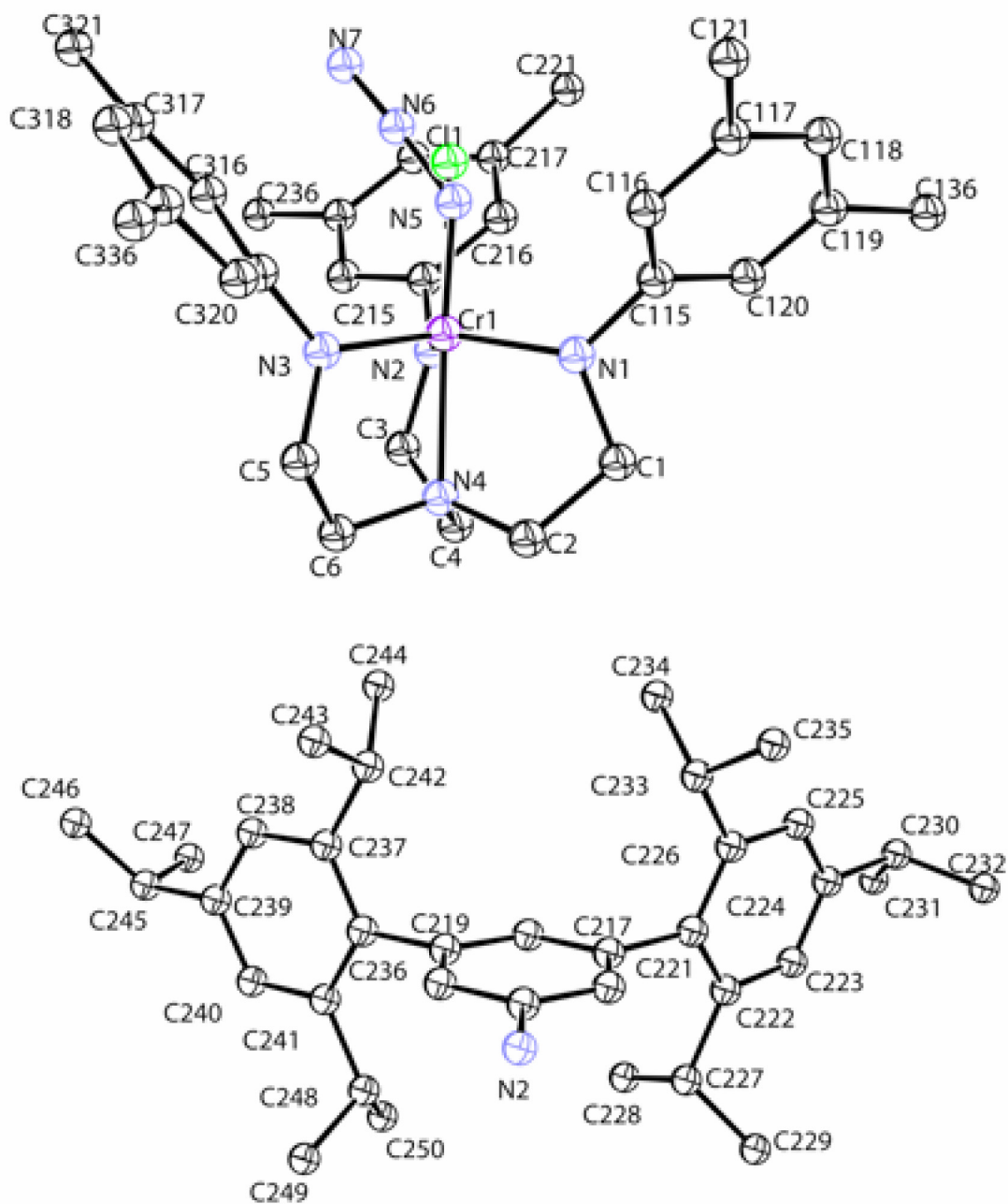


Figure A.22: ORTEP labeling scheme for $[\text{HIPTN}_3\text{N}]\text{CrCl}$ (42) / $[\text{HIPTN}_3\text{N}]\text{CrN}_3$. Solvent and hydrogen atoms omitted.

Table A.22: Atomic coordinates ($\times 10^4$) and equivalent isotropic displacement parameters ($\text{\AA}^2 \times 10^3$) for $[\text{HIPTN}_3\text{N}]\text{CrCl}$ (**42**) / $[\text{HIPTN}_3\text{N}]\text{CrN}_3$. $U(\text{eq})$ is defined as one third of the trace of the orthogonalized U^{ij} tensor.

	x	y	z	$U(\text{eq})$
Cr(1)	333(1)	8947(1)	2113(1)	15(1)
Cl(1)	-117(1)	8804(1)	930(1)	17(1)
N(5)	9(8)	8823(3)	1208(7)	47(3)
N(6)	-664(5)	8889(2)	714(4)	29(2)
N(7)	-1285(5)	8954(2)	306(4)	41(2)
N(1)	1276(1)	8657(1)	2216(1)	17(1)
N(2)	-658(1)	8826(1)	2566(1)	18(1)
N(3)	525(1)	9407(1)	1938(1)	18(1)
N(4)	769(1)	9080(1)	3242(1)	18(1)
C(1)	1673(1)	8610(1)	2988(1)	23(1)
C(2)	1647(1)	8942(1)	3397(1)	21(1)
C(3)	-718(1)	8953(1)	3340(1)	23(1)
C(4)	167(1)	8931(1)	3746(1)	21(1)
C(5)	1009(2)	9591(1)	2558(1)	24(1)
C(6)	767(2)	9452(1)	3294(1)	22(1)
C(115)	1526(1)	8410(1)	1701(1)	18(1)
C(116)	1874(1)	8505(1)	1040(1)	19(1)
C(117)	2187(1)	8266(1)	563(1)	19(1)
C(118)	2124(1)	7928(1)	750(1)	21(1)
C(119)	1788(1)	7828(1)	1410(1)	19(1)
C(120)	1486(1)	8069(1)	1882(1)	20(1)
C(121)	2629(1)	8364(1)	-117(1)	20(1)
C(122)	3530(1)	8327(1)	-103(1)	23(1)
C(123)	3918(1)	8424(1)	-743(1)	25(1)
C(124)	3469(2)	8553(1)	-1382(1)	24(1)
C(125)	2586(2)	8580(1)	-1387(1)	26(1)
C(126)	2157(1)	8484(1)	-763(1)	22(1)
C(127)	4062(1)	8184(1)	586(1)	26(1)
C(128)	4183(2)	8434(1)	1227(2)	40(1)
C(129)	4935(2)	8046(1)	413(2)	34(1)
C(130)	3946(2)	8662(1)	-2049(1)	28(1)
C(131)	4139(2)	9036(1)	-2006(2)	37(1)
C(132)	3494(2)	8571(1)	-2813(2)	42(1)
C(133)	1189(1)	8504(1)	-815(1)	25(1)
C(134)	780(2)	8314(1)	-1500(2)	53(1)
C(135)	889(2)	8867(1)	-824(2)	45(1)
C(136)	1817(1)	7465(1)	1631(1)	21(1)
C(137)	1137(1)	7253(1)	1401(1)	23(1)
C(138)	1200(1)	6915(1)	1605(1)	26(1)
C(139)	1910(2)	6788(1)	2031(2)	27(1)
C(140)	2572(1)	7006(1)	2257(2)	28(1)
C(141)	2547(1)	7344(1)	2056(1)	23(1)
C(142)	343(1)	7379(1)	927(2)	28(1)
C(143)	309(2)	7248(1)	125(2)	53(1)
C(144)	-474(2)	7295(1)	1283(2)	40(1)
C(145)	1977(2)	6417(1)	2225(2)	36(1)
C(146)	2035(3)	6209(1)	1519(2)	63(1)

C(147)	1229(2)	6297(1)	2648(2)	40(1)
C(148)	3291(2)	7576(1)	2303(2)	30(1)
C(149)	4158(2)	7423(1)	2209(3)	60(1)
C(150)	3246(2)	7694(1)	3110(2)	51(1)
C(215)	-1444(1)	8699(1)	2228(1)	18(1)
C(216)	-1480(1)	8384(1)	1881(1)	18(1)
C(217)	-2258(1)	8252(1)	1593(1)	20(1)
C(218)	-3005(1)	8437(1)	1646(1)	22(1)
C(219)	-2984(1)	8751(1)	1987(1)	20(1)
C(220)	-2200(1)	8880(1)	2275(1)	20(1)
C(221)	-2349(1)	7922(1)	1186(1)	21(1)
C(222)	-2582(1)	7630(1)	1568(1)	23(1)
C(223)	-2765(1)	7340(1)	1142(1)	26(1)
C(224)	-2721(1)	7331(1)	370(1)	27(1)
C(225)	-2464(2)	7618(1)	11(2)	28(1)
C(226)	-2270(1)	7913(1)	411(1)	25(1)
C(227)	-2673(2)	7629(1)	2411(1)	26(1)
C(228)	-3605(2)	7672(1)	2567(2)	40(1)
C(229)	-2308(2)	7313(1)	2802(2)	32(1)
C(230)	-2929(2)	7014(1)	-86(2)	34(1)
C(231)	-3751(2)	6850(1)	128(2)	43(1)
C(232)	-2186(2)	6769(1)	-8(2)	50(1)
C(233)	-2016(2)	8222(1)	-18(1)	29(1)
C(234)	-2721(2)	8327(1)	-619(2)	53(1)
C(235)	-1169(2)	8169(1)	-356(2)	50(1)
C(236)	-3790(1)	8942(1)	2046(1)	21(1)
C(237)	-4130(1)	9143(1)	1446(1)	26(1)
C(238)	-4888(2)	9319(1)	1531(2)	31(1)
C(239)	-5310(1)	9294(1)	2179(2)	30(1)
C(240)	-4968(1)	9091(1)	2761(2)	28(1)
C(241)	-4214(1)	8912(1)	2710(1)	25(1)
C(242)	-3684(2)	9177(1)	726(2)	32(1)
C(243)	-3187(2)	9505(1)	717(2)	47(1)
C(244)	-4291(2)	9140(1)	13(2)	48(1)
C(245)	-6183(2)	9458(1)	2248(2)	39(1)
C(246)	-6270(2)	9806(1)	1920(2)	45(1)
C(247)	-6865(2)	9209(1)	1902(2)	44(1)
C(248)	-3875(2)	8685(1)	3355(1)	29(1)
C(249)	-3530(2)	8889(1)	4042(2)	37(1)
C(250)	-4554(2)	8433(1)	3563(2)	40(1)
C(315)	477(1)	9586(1)	1246(1)	18(1)
C(316)	-298(1)	9619(1)	796(1)	19(1)
C(317)	-354(1)	9824(1)	155(1)	18(1)
C(318)	374(1)	9991(1)	-38(1)	20(1)
C(319)	1149(1)	9961(1)	398(1)	19(1)
C(320)	1193(1)	9757(1)	1030(1)	20(1)
C(321)	-1194(1)	9891(1)	-290(1)	19(1)
C(322)	-1715(1)	10153(1)	-62(1)	23(1)
C(323)	-2480(1)	10221(1)	-493(1)	25(1)
C(324)	-2752(1)	10042(1)	-1139(1)	25(1)
C(325)	-2226(1)	9786(1)	-1354(1)	24(1)
C(326)	-1454(1)	9706(1)	-941(1)	22(1)
C(327)	-1455(2)	10363(1)	636(1)	26(1)
C(328)	-2082(2)	10322(1)	1231(2)	39(1)

C(329)	-1340(2)	10730(1)	435(2)	37(1)
C(330)	-3601(2)	10123(1)	-1586(1)	30(1)
C(331)	-3657(2)	10014(1)	-2390(2)	75(1)
C(332)	-4334(2)	9984(2)	-1206(2)	94(2)
C(333)	-890(2)	9434(1)	-1226(1)	26(1)
C(334)	-1398(2)	9128(1)	-1522(2)	46(1)
C(335)	-372(2)	9575(1)	-1847(2)	43(1)
C(336)	1934(1)	10156(1)	239(1)	21(1)
C(337)	2569(2)	10006(1)	-150(1)	26(1)
C(338)	3317(2)	10184(1)	-233(1)	30(1)
C(339)	3467(2)	10500(1)	79(1)	29(1)
C(340)	2825(2)	10644(1)	458(1)	26(1)
C(341)	2053(1)	10479(1)	540(1)	23(1)
C(342)	2455(2)	9657(1)	-490(2)	31(1)
C(343)	3226(2)	9433(1)	-303(2)	52(1)
C(344)	2247(2)	9674(1)	-1335(2)	54(1)
C(345)	4339(2)	10662(1)	42(2)	36(1)
C(346)	4966(2)	10523(1)	666(2)	63(1)
C(347)	4314(2)	11046(1)	81(2)	57(1)
C(348)	1394(2)	10639(1)	1002(1)	26(1)
C(349)	1640(2)	10580(1)	1847(2)	35(1)
C(350)	1280(2)	11015(1)	857(2)	31(1)

Table A.23: Crystal data and structure refinement for [HIPTN₃N]CrN (43) / [HIPTN₃N]CrN₃.*

Identification code	05167	
Empirical formula	C ₁₂₁ H ₁₇₅ CrN _{5,99}	
Formula weight	1765.46	
Temperature	100(2) K	
Wavelength	0.71073 Å	
Crystal system	Monoclinic	
Space group	Cc	
Unit cell dimensions	a = 15.795(2) Å	α = 90°
	b = 39.976(7) Å	β = 94.499(5)°
	c = 17.856(3) Å	γ = 90°
Volume	11240(3) Å ³	
Z	4	
Density (calculated)	1.043 Mg/m ³	
Absorption coefficient	0.149 mm ⁻¹	
F(000)	3868	
Crystal size	0.23 x 0.17 x 0.11 mm ³	
Theta range for data collection	1.73 to 25.03°	
Index ranges	-18 ≤ h ≤ 18, -47 ≤ k ≤ 47, -21 ≤ l ≤ 21	
Reflections collected	86770	
Independent reflections	19766 [R _{int} = 0.0861]	
Completeness to theta = 25.03°	100.0%	
Absorption correction	Semi-empirical from equivalents	
Max. and min. transmission	0.9852 and 0.9679	
Refinement method	Full-matrix least-squares on F ²	
Data / restraints / parameters	19766 / 606 / 1229	
Goodness-of-fit on F ²	1.031	
Final R indices [I > 2σ(I)]	R ₁ = 0.0562, wR ₂ = 0.1286	
R indices (all data)	R ₁ = 0.0714, wR ₂ = 0.1357	
Absolute structure parameter	0.019(15)	
Largest diff. peak and hole	0.355 and -0.267 eÅ ⁻³	

* Structure solution by Dr. Peter Müller.

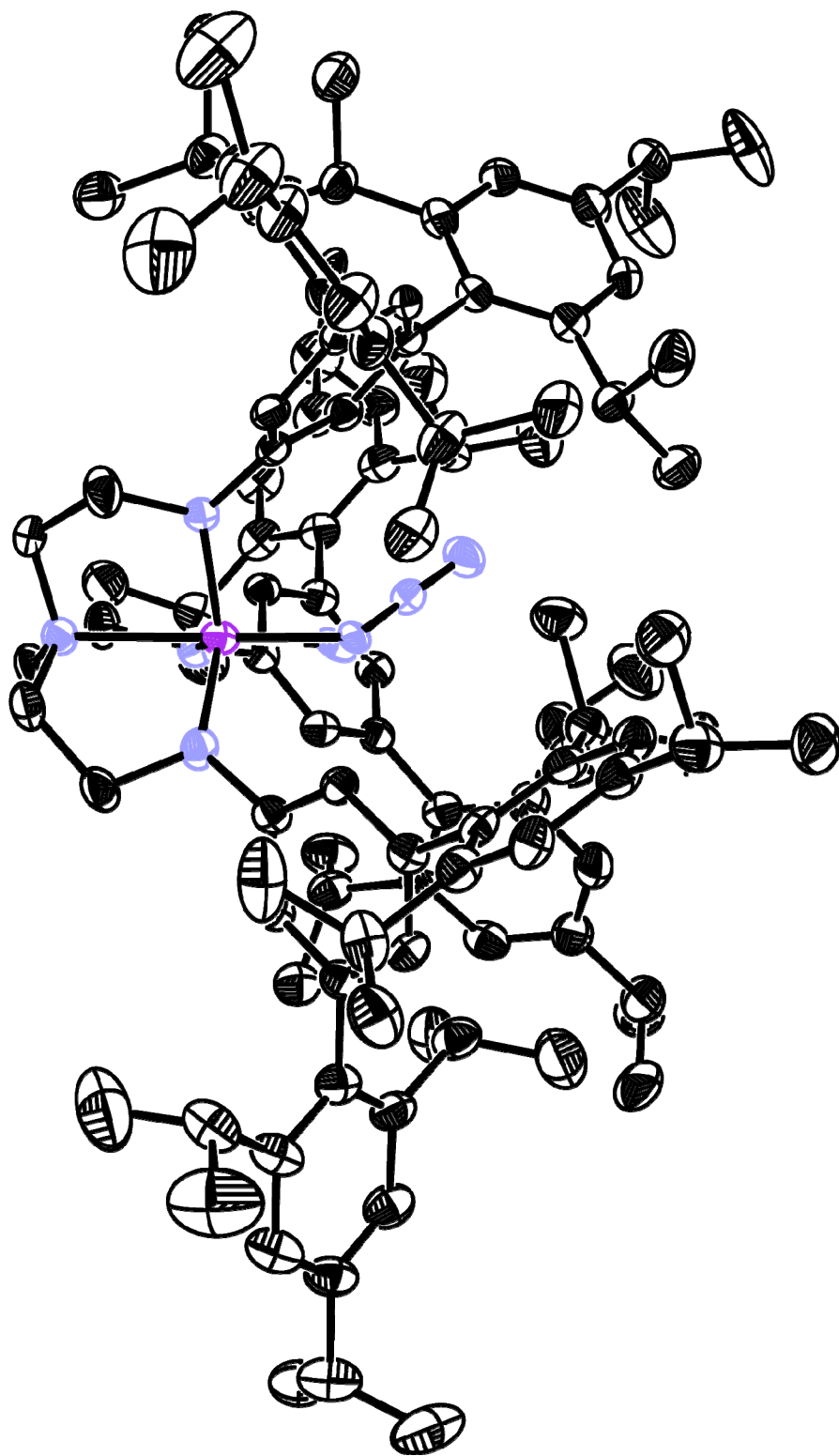


Figure A.23: Full ORTEP of $[\text{HIPTN}_3\text{N}]\text{CrN}$ (43) / $[\text{HIPTN}_3\text{N}]\text{CrN}_3$. Thermal ellipsoids at 50% probability, solvent, hydrogen atoms, and disorder not related to the nitride/azide substituent omitted.

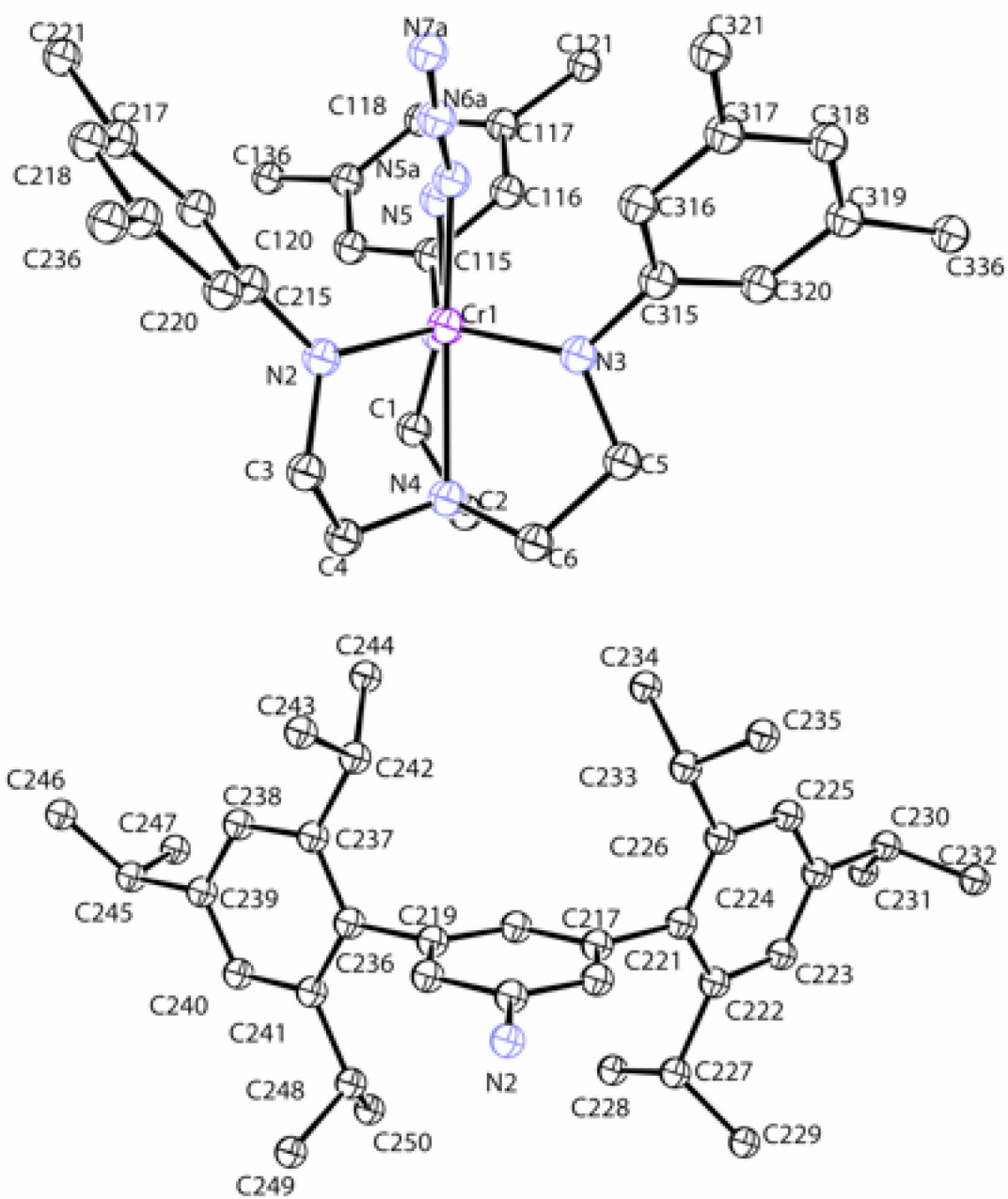


Figure A.24: ORTEP labeling scheme for $[\text{HIPTN}_3\text{N}]\text{CrN}$ (**43**) / $[\text{HIPTN}_3\text{N}]\text{CrN}_3$. Solvent, hydrogen atoms, and disorder not relating to the nitride/azide substituent omitted.

Table A.24: Atomic coordinates ($\times 10^4$) and equivalent isotropic displacement parameters ($\text{\AA}^2 \times 10^3$) for $[\text{HIPTN}_3\text{N}]\text{CrN}$ (**43**) / $[\text{HIPTN}_3\text{N}]\text{CrN}_3$. $U(\text{eq})$ is defined as one third of the trace of the orthogonalized U_{ij} tensor.

	x	y	z	U(eq)
Cr(1)	309(1)	8933(1)	2092(1)	23(1)
N(5)	-33(19)	8812(8)	1247(7)	24(3)
N(5A)	-30(20)	8829(8)	1083(7)	21(3)
N(6A)	-677(4)	8887(1)	715(3)	27(2)
N(7A)	-1281(4)	8949(1)	310(3)	40(2)
N(1)	1235(2)	8636(1)	2226(1)	28(1)
N(2)	-680(2)	8826(1)	2566(1)	24(1)
N(3)	543(2)	9392(1)	1943(1)	26(1)
N(4)	757(2)	9068(1)	3271(1)	26(1)
C(1)	1599(2)	8582(1)	3000(2)	40(1)
C(2)	1613(2)	8913(1)	3415(2)	34(1)
C(3)	-737(2)	8962(1)	3330(2)	34(1)
C(4)	127(2)	8932(1)	3753(2)	30(1)
C(5)	1051(3)	9564(1)	2553(2)	45(1)
C(6)	794(2)	9439(1)	3303(2)	35(1)
C(115)	1497(2)	8393(1)	1706(2)	26(1)
C(116)	1829(2)	8493(1)	1041(2)	26(1)
C(117)	2155(2)	8261(1)	559(2)	26(1)
C(118)	2104(2)	7920(1)	737(2)	28(1)
C(119)	1781(2)	7814(1)	1398(2)	29(1)
C(120)	1474(2)	8053(1)	1875(2)	30(1)
C(121)	2601(2)	8364(1)	-118(2)	28(1)
C(122)	3501(2)	8334(1)	-93(2)	33(1)
C(123)	3899(2)	8429(1)	-738(2)	33(1)
C(124)	3451(2)	8553(1)	-1381(2)	32(1)
C(125)	2563(2)	8574(1)	-1395(2)	32(1)
C(126)	2128(2)	8479(1)	-771(2)	29(1)
C(127)	4026(2)	8201(1)	597(2)	41(1)
C(128)	4134(3)	8460(1)	1214(2)	68(1)
C(129)	4902(3)	8063(1)	436(2)	53(1)
C(130)	3933(2)	8658(1)	-2042(2)	39(1)
C(131)	4145(3)	9028(1)	-2006(2)	45(1)
C(132)	3490(3)	8567(1)	-2805(2)	51(1)
C(133)	1167(2)	8495(1)	-821(2)	30(1)
C(134)	739(3)	8342(1)	-1552(2)	54(1)
C(135)	854(2)	8854(1)	-729(2)	45(1)
C(136)	1806(2)	7449(1)	1609(2)	32(1)
C(137)	1129(2)	7237(1)	1389(2)	36(1)
C(138)	1193(2)	6900(1)	1589(2)	41(1)
C(139)	1911(2)	6774(1)	2005(2)	42(1)
C(140)	2569(2)	6990(1)	2226(2)	47(1)
C(141)	2545(2)	7326(1)	2031(2)	40(1)
C(142)	338(2)	7367(1)	924(2)	41(1)
C(143)	287(3)	7237(1)	128(2)	67(1)
C(144)	-473(2)	7287(1)	1296(2)	54(1)
C(145)	1964(3)	6401(1)	2206(3)	55(1)

C(146)	1998(4)	6188(1)	1503(3)	77(2)
C(147)	1263(3)	6283(1)	2658(2)	55(1)
C(148)	3286(2)	7557(1)	2279(2)	50(1)
C(149)	4145(3)	7414(1)	2143(4)	100(2)
C(150)	3266(4)	7659(2)	3094(3)	94(2)
C(215)	-1457(2)	8700(1)	2228(2)	25(1)
C(216)	-1490(2)	8384(1)	1880(2)	26(1)
C(217)	-2262(2)	8252(1)	1590(2)	27(1)
C(218)	-3003(2)	8436(1)	1644(2)	29(1)
C(219)	-2990(2)	8752(1)	1984(2)	29(1)
C(220)	-2215(2)	8878(1)	2274(2)	26(1)
C(221)	-2349(2)	7918(1)	1192(2)	30(1)
C(222)	-2594(2)	7629(1)	1577(2)	33(1)
C(223)	-2774(2)	7340(1)	1155(2)	39(1)
C(224)	-2720(2)	7326(1)	387(2)	42(1)
C(225)	-2451(3)	7610(1)	27(2)	45(1)
C(226)	-2269(2)	7907(1)	418(2)	39(1)
C(227)	-2700(2)	7633(1)	2417(2)	38(1)
C(228)	-3634(3)	7672(1)	2579(3)	56(1)
C(229)	-2327(2)	7321(1)	2819(2)	44(1)
C(230)	-2927(3)	7005(1)	-60(2)	52(1)
C(231)	-3748(3)	6847(1)	143(3)	64(1)
C(232)	-2194(3)	6763(1)	12(3)	63(1)
C(233)	-1997(3)	8213(1)	-13(2)	43(1)
C(234)	-2658(3)	8306(1)	-657(3)	73(1)
C(235)	-1113(3)	8166(1)	-279(3)	67(1)
C(236)	-3793(2)	8944(1)	2030(2)	31(1)
C(237)	-4126(2)	9143(1)	1430(2)	36(1)
C(238)	-4889(2)	9320(1)	1505(2)	46(1)
C(239)	-5315(2)	9301(1)	2160(2)	44(1)
C(240)	-4980(2)	9101(1)	2741(2)	45(1)
C(241)	-4236(2)	8918(1)	2690(2)	38(1)
C(242)	-3667(2)	9171(1)	711(2)	44(1)
C(243)	-3164(3)	9494(1)	690(2)	59(1)
C(244)	-4271(3)	9130(1)	-1(2)	66(1)
C(245)	-6174(3)	9480(1)	2220(3)	64(1)
C(246)	-6260(9)	9805(2)	1953(6)	56(3)
C(247)	-6885(4)	9202(2)	1909(4)	49(2)
C(248)	-3911(2)	8692(1)	3344(2)	41(1)
C(249)	-3567(3)	8899(1)	4019(2)	53(1)
C(250)	-4596(3)	8447(1)	3567(2)	60(1)
C(315)	503(2)	9574(1)	1254(2)	26(1)
C(316)	-260(2)	9608(1)	805(2)	27(1)
C(317)	-316(2)	9814(1)	169(2)	25(1)
C(318)	411(2)	9979(1)	-19(2)	27(1)
C(319)	1176(2)	9951(1)	411(2)	25(1)
C(320)	1215(2)	9743(1)	1047(2)	26(1)
C(321)	-1153(2)	9885(1)	-271(2)	29(1)
C(322)	-1682(2)	10144(1)	-32(2)	31(1)
C(323)	-2439(2)	10215(1)	-459(2)	36(1)
C(324)	-2713(2)	10039(1)	-1111(2)	36(1)
C(325)	-2178(2)	9786(1)	-1337(2)	35(1)
C(326)	-1414(2)	9707(1)	-936(2)	33(1)
C(327)	-1420(2)	10348(1)	671(2)	35(1)

C(328)	-2052(3)	10300(1)	1265(2)	47(1)
C(329)	-1314(3)	10719(1)	477(2)	47(1)
C(330)	-3562(2)	10122(1)	-1547(2)	42(1)
C(331)	-3497(16)	10102(7)	-2383(6)	79(5)
C(332)	-4232(7)	9868(6)	-1312(10)	75(5)
C(333)	-840(2)	9441(1)	-1237(2)	36(1)
C(334)	-1345(3)	9137(1)	-1552(2)	49(1)
C(335)	-303(3)	9589(1)	-1839(2)	50(1)
C(336)	1963(2)	10141(1)	258(2)	30(1)
C(337)	2601(2)	9988(1)	-135(2)	37(1)
C(338)	3352(2)	10167(1)	-215(2)	44(1)
C(339)	3510(2)	10485(1)	94(2)	41(1)
C(340)	2862(2)	10629(1)	467(2)	38(1)
C(341)	2094(2)	10468(1)	555(2)	32(1)
C(342)	2488(2)	9639(1)	-469(2)	40(1)
C(343)	3212(3)	9404(1)	-236(2)	66(1)
C(344)	2333(3)	9656(1)	-1320(2)	63(1)
C(345)	4384(3)	10648(1)	52(2)	53(1)
C(346)	5013(6)	10508(3)	656(6)	76(2)
C(347)	4355(5)	11034(1)	100(9)	69(3)
C(348)	1432(2)	10630(1)	1017(2)	34(1)
C(349)	1681(3)	10582(1)	1850(2)	45(1)
C(350)	1300(2)	11002(1)	843(2)	42(1)

Acknowledgments

I would like to start by thanking Richard Schrock for taking me into his group and for supporting my efforts during my time here. It has been an invaluable learning experience and he has been a great advisor. I would like to thank my thesis committee, Dan Nocera and committee chair Kit Cummins, for useful input and suggestions. The rest of the inorganic faculty have also been a source of help and encouragement. Gretchen Guidess has been fantastic at keeping all things administrative together.

Peter Müller has been great in the X-ray facility, and is responsible for all of the crystal structures contained herein. Jeff Simpson, Mark Wall, David Bray, Hongjun Pan, and Bob Kennedy kept the DCIF on its feet and showed me how to use the spectrometers. Li Li acquired all of the mass spectrometry data. Walter Weare and Dmitry Yandulov performed the catalytic runs.

In addition to pioneering the molybdenum system, Dmitry Yandulov showed me how to work with the types of compounds in this thesis. Parisa Mehrkhodavandi was also invaluable for her help in getting me started in the lab. Walter Weare, Vincent Ritleng, Matt Byrnes, Xuliang Dai, and Jia Min Chin have been terrific compatriots on the dinitrogen project. There were six of us that joined the Schrock group in late 2001. As well as Walter, Jen Adamchuk, Adam Hock, Lara Pryor, and Amrit Sinha were a good group of people with which to learn and grow. My box-mates Sarah Dolman and Constantin Czekelius deserve recognition for being so willing to alter how they work in a glove-box to accommodate the requirements of my project. Jillian Hafer could always be counted on for amusing reactions to stray pieces of chocolate that somehow found their way onto her desk. Pia Lopez helped to keep the lab less desolate at night. Monica Duval-Lungulescu, Stefan Arndt, Andrea Gabert, Rojendra Singh, and Zachery Tonzetich, who haven't yet been mentioned, also deserve recognition. Many other people in the department have also made my time here a positive experience. I wish good luck to the newest members of the group, Megan Dellinger, Annie Jiang, and Keith Wampler, and to Jia Min Chin and Brian Hanna who are carrying on the torch for the dinitrogen project.

My undergraduate advisor Jeff Long and his group *circa* 1999-2001, especially Laurance Beauvais and Miriam Bennett, are a big reason why I have been able to get to this point. There is a lot to be said for a positive undergraduate research experience.

Specific thanks needs to go to Jia Min Chin, Andrea Gabert, and Walter Weare for taking time to read and comment on this thesis.

Finally, I'd like to thank my parents for their love and support. Even with multiple children in college, they made sure I could concentrate on my education rather than scramble for funds or take on large debts. But, more importantly, they taught me how to live and thrive.

Nathan Smythe

Massachusetts Institute of Technology
Department of Chemistry, 6-427
Cambridge, MA 02139
Tel. (617) 452-2466
Fax. (617) 253-7670

70 Pacific St. Apt. 237B
Cambridge, MA 02139
Tel. (617) 452-2466
email nsmythe@mit.edu

Education

Doctor of Philosophy, Inorganic Chemistry *September 2006*
Massachusetts Institute of Technology, Cambridge, MA, USA
Advisor: Professor Richard R. Schrock
Thesis: "Vanadium and Chromium Complexes Supported by Sterically Demanding Ligands. Studies Relevant to the Reduction of Dinitrogen to Ammonia"

Bachelor of Science, Chemistry *May 2001*
University of California at Berkeley, Berkeley, CA, USA
Advisor: Professor Jeffrey R. Long

Research Experience

Massachusetts Institute of Technology *January 2002-present*
Synthesized vanadium and chromium complexes supported by sterically demanding amide-based ligands and assessed their potential for the reduction of dinitrogen to ammonia. Demonstrated that chromium supported by a triamidoamine ligand is unlikely to convert dinitrogen to ammonia. Demonstrated that vanadium can support various intermediates along a potential catalytic cycle.

University of California, Berkeley *1999-May 2001*
Synthesis and reactivity of heavy-metal clusters obtained through high temperature solid-state reactions.

Teaching Experience

Massachusetts Institute of Technology *September 2001-May 2002*
Recitation teaching assistant for Chemistry 5.112, General Chemistry.
Teaching assistant for Chemistry 5.310, Introductory Laboratory Course.

University of California, Berkeley *January 2001-May 2001*
Teaching assistant for Chemistry 108, Advanced Inorganic Laboratory Course.

Publications

Smythe, N. C.; Schrock, R. R.; Müller, P.; Weare, W. W. "Synthesis of [(HIPTNCH₂CH₂)₃N]V Compounds (HIPT = 3,5-(2,4,6-*i*-Pr₃C₆H₂)₂C₆H₃) and an Evaluation of Vanadium for the Reduction of Dinitrogen to Ammonia" *Inorg. Chem.* Submitted.

Smythe, N. C.; Schrock, R. R.; Müller, P.; Weare, W. W. "Synthesis of [(HIPTNCH₂CH₂)₃N]Cr Compounds (HIPT = 3,5-(2,4,6-*i*-Pr₃C₆H₂)₂C₆H₃) and an Evaluation of Chromium for the Reduction of Dinitrogen to Ammonia" *Inorg. Chem.* In Press.

Affiliations

American Chemical Society, Member